Analysis and simulation of defects of operation for air conditioning audit

Daniela Bory

ED n° 432 : « Sciences des Métiers de l'Ingénieur »

N° attribué par la bibliothèque

|_|_|_|_|_|_|_|_|_|_|_|

T H E S E

pour obtenir le grade de

DOCTEUR DE L'ECOLE NATIONALE SUPERIEURE DES MINES DE PARIS

Spécialité "Energétique"

présentée et soutenue publiquement par
Daniela BORY

le 8 septembre 2008

ANALYSIS AND SIMULATION OF DEFECTS OF OPERATION FOR AIR CONDITIONING AUDIT
(ANALYSE ET SIMULATION DE DEFAUTS DES EQUIPEMENTS DE CLIMATISATION EN VUE D'UN AUDIT ENERGETIQUE)

Directeurs de thèse : Jérôme ADNOT, Dominique MARCHIO

Jury :

M. J. LEBRUN – Université de Liège ..... Président
M. M. MASOERO – Politecnico di Torino ..... Rapporteur
M. J. ADNOT – Mines ParisTech ..... Examinateur
M. D. MARCHIO – Mines ParisTech ..... Examinateur
M. A. TROMBE – INSA Toulouse ..... Rapporteur
M. O. MORISOT - ELYO ..... Examinateur

Acknowledgments

I would like to thank Denis Clodic for having offered to me the possibility to develop my research in the Centre for Energy and Process of the Ecole de Mines of Paris.

I would like to acknowledge the contributions of my supervisors Jérôme Adnot and Dominique Marchio: their comments and guidance were crucial in shaping and leading this dissertation to its end.

Philippe Rivière was a key figure all along my project of research and his advice was always useful and appropriate once decrypted.

This work is born, grown and gone further the AUDITAC project: I really appreciated to work with all the members of the project and to contribute with them to the air conditioning efficiency.

Special thanks to Bruno and Maxime for their help and presence in the shiny and cloudy days.

Thanks to Anne Marie, “Speedy” Aline, Maryvonne and Philippe for their support in all administrative and computer problems.

Thanks to my colleagues, Elias, Laurent, Pascal, Sila and to all the CEP colleagues that I met in these exciting and pleasant years.

Thanks to my family that was always near although far.

Finally, I would like to thank Marwane who was always there, and Maya even though she came a little bit later.

Table of contents

List of figures

List of Tables

Nomenclature

Symbol	Definition	Units
A_c	Heat exchanger cross area	m^2
A_{fin}	Heat exchanger fins area	m^2
A_{tube}	Heat exchanger tubes area	m^2
α	Filter packing	-
β	Compression rate	-
C_C	Cunningham slip factor	-
C_D	Draught coefficient	-
D	Diameter	m
D_C	Collar diameter of tubes	m
Δp	Pressure drop	Pa
D_{t_ext}	Outside diameter of tubes	m
E_a	Annual electricity consumption	kWh
E_c	Annual cooling energy	kWh
EER	Energy efficiency ratio	-
f	friction factor	$kg \cdot m^{-1} \cdot s^{-1}$
G	Air mass flow per unit of cross heat exchanger area	$kg \cdot m^{-2} \cdot s^{-1}$
g	Acceleration due to gravity (9.81)	$m \cdot s^{-2}$
H_{exch}	Heat exchanger height	m
h_f	Fin pitch	m
k_B	Boltzmann constant ($1.38 \cdot 10^{-23}$)	$J \cdot K^{-1}$
Ku	Kuwabara number	-
L_{exch}	Heat exchanger depth	m
$LMTD$	Logarithmic mean temperature difference	K
m	Mass	kg
$\dot{m}$	Mass flow rate	$kg \cdot s^{-1}$
μ	Dynamic viscosity	$kg \cdot m^{-1} \cdot s^{-1}$
ν	Kinematic viscosity	$m^2 \cdot s^{-1}$
N_R	Number of rows of tubes	-
N_F	Number of fins	-
N_T	Number of tubes of the heat exchanger	-
N_{TR}	Number of tubes per row of the heat exchanger	-
P_a	Absorbed power	kW
P_c	Cooling capacity	kW
Pe	Peclet number	-
P_l	Longitudinal tube pitch	m
P_t	Transversal tube pitch	m
ρ	Density	$kg \cdot m^{-3}$
Re	Reynolds number	-
SR	Sensible to total heat transfer ratio	-
Stk	Stokes number	-
T	Temperature	$°C$
t_f	Fin thickness	m
τ	Relaxation time	s
U	Bulk air speed	$m \cdot s^{-1}$
Z	Filter thickness	m
W_{exch}	Heat exchanger width	m

1 Reasons and methods for auditing the air conditioning systems

1.1 The air conditioning market and some aspects of the stock

The research in Energy for buildings in France, characterized by the intense activity of the last years in the development of new technologies for building heating and air-conditioning, is nowadays also oriented to the field of existing buildings. This impulse is motivated by objectives of energy and emissions savings translated in the building sector in two major political constraints:

- The implementation of the European Directive on the energy performance of the buildings [EPBD 2002] including the energy certification of the building performance and the inspection of the equipment of the heating and air conditioning plant
- The respect of the next French regulation for "existing buildings"

In the last twenty years many efforts have been made by manufacturers, installers, operators and all air conditioning professionals to improve the energy efficiency of air-conditioning systems through the technology, the operation scheduling and control strategies development.

Air conditioning (AC) systems constitute a stake for the next years as an opportunity for countries to reduce the CO_2 emissions in order to respect the Kyoto protocol terms.

Since global warming leads to an increased average temperature of the earth and comfort expectations are rising with the welfare, air conditioning becomes more and more necessary in order to protect fragile people in the hot season, to ensure the productivity for specific industrial processes all along the year and to ensure comfort condition for workers during the hottest months of the year. Moreover, in the housing sector, the AC is more and more spread thanks to the reduction of the costs of the products, the increased purchasing power and the due to a mode effect.

As shown in the EECCAC study [ECCAC 2003], in the coming years the European stock of air conditioning equipment will partly become obsolete. Most systems will be renovated for the first time (after 10-15 years of operation) and an opportunity exists to introduce higher efficiency systems. Out of the 2.200 Mm^2 of air-conditioned building area in use in 2010 in Europe (Figure 1), 800 Mm^2 will date by more than 15 years and will need urgent renewal. The study showed an energy saving opportunity of about 50 %.

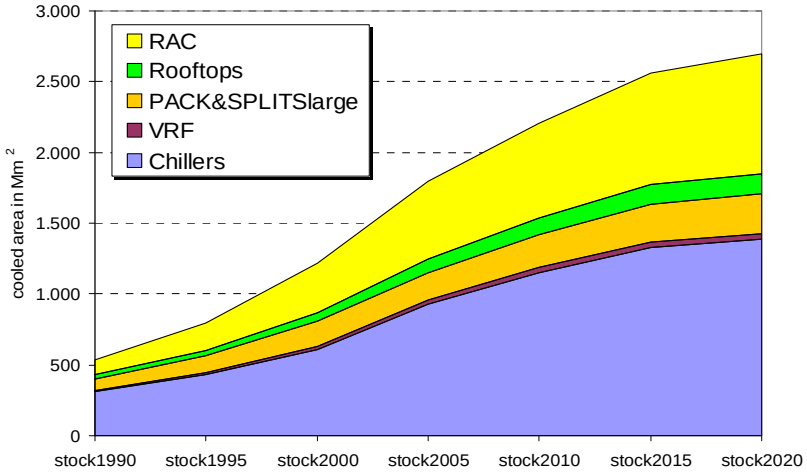

Figure 1: Cooled area (Mm^2) in Europe [EECCAC 2001]

The large market of the AC shows an important increasing trend, it grew strongly in the year 80s and 90s, when it became a consumer product accessible to a large public and being included in most tertiary buildings. The saturation of the market is still far from now and the stock still increases although big efforts have been made in order to reduce the cooling demand in modern construction. New buildings represent just a small part of the cake: the new buildings represents only 1 % of the stock in France while 60 % of the commercial and residential stocks is built before 1975. For the new buildings, the renewables are still uncommon, "passive" buildings are still at the state of demonstration with costs not yet affordable on large scale. Large part of the AC market demand is represented by existing buildings at the time of retrofit or replacement.

The AC market is influenced by several factors in Europe, often contrasting one with another. On one side, in order to reach a better energy efficiency in AC, many efforts have been made to improve the technologies of the EU products with several means. Among them we can mention components standard for components tightness [PrEN 1736], energy labelling and performance certifications (Eurovent Certification programmes), professionals' accreditation programmes (for installers and maintainers etc). Moreover, for the first time, the new energy certification of building stated in the EPDB takes into account all the buildings' points of energy consumption including air conditioning.

On the other hand, the opening of the market to foreign products allows the arrival in the EU of a large number of low cost products coming from Asia. The price seems to be the crucial aspect of the product more than the supplied comfort and the energy aspects, the owner paying attention to the initial investment more than to energy efficiency. Life cycle cost approaches are recently introduced and are more and more integrated starting from the design of the building.

Last but not least, marketing strategies do not target only the main aspect of the product (cooling), but secondary aspects are more highlighted by sellers such as design, noise and filters capabilities etc. The energy efficiency begins to be a feature of interest for labelled products.

Efforts at EU level for air conditioning efficiency

The EU put in place a global policy in order to satisfy the Kyoto objectives strongly oriented to the reduction of the consumption of the building sector representing more than 40 % of the energy consumption in the EU. The objectives deal with all the aspects of the building including all energy consumption points. The European Community pushes the Member States to energy savings, with the Energy Performance of Buildings Directive, strengthening the regulation for the residential and commercial building sectors. The air-conditioning aspect is considered in the article 9 of the Directive through the compulsory **Inspection of air-conditioning systems.**

The article 9 of the EPBD states:

"With regard to reducing energy consumption and limiting carbon dioxide emissions, Member States shall lay down the necessary measures to establish a regular inspection of air conditioning systems of an effective rated output of more than 12 kW.

This inspection shall include an assessment of the air-conditioning efficiency and the sizing compared to the cooling requirements of the building. Appropriate advice shall be provided to the users on possible improvement or replacement of the air-conditioning system and on alternative solutions."

The EPBD considers air conditioning as an important stake about which large opportunity of consumption reductions can be obtained with a set of profitable cost/benefit actions.

The energy savings expected from the inspection would be effective if the inspection is followed by a real energy consumption improvement of the facilities.

The inspection is a quick audit of the installations and, following the text of the Directive, will provide some advice on the possible improvements. To go deeper, this advice should be studied and detailed through a detailed audit of the equipment, which includes an economic analysis of the actions or for equipment replacement. Inspection is a way to motivate the air conditioning owners and operators to take a step forward the improvement of the energy efficiency.

Looking at scientific literature we can notice a lack of methods effective or rather complete, capable to satisfy the requirements of the regulation that is very demanding for air-conditioning especially if compared to the heating one, the knowledge of the last being better and simplified by the small number of system types.

The systems of air-conditioning are more recent (years ' 70) and present a large variety regarding both the cooling plant production and the distribution and terminals. Currently different methods exist and especially for the calculation of the reference values of consumption, often these methods are developed and used by consultancies, they are often arbitrary and result into the application of a number of "generally accepted" measures for energy saving. Few field experiments are referred in scientific literature and rigorous analysis of energy impact remains to be done.

There is a real need for developing methods of audit suitable for air-conditioning by supporting the most effective solutions and validated on the field in order to achieve the expected energy savings that will contribute to respect the Kyoto protocol terms. An essential asset orienting the research is to propose processes applicable in short time making them economically feasible and accessible to the owners.

1.2 Principle of operation of an air conditioning system

The main function of an air conditioning system is to cool a medium, in order to finally cool a room or a limited space.

Although the air conditioning technologies are numerous and based on different energies, we will focus our attention on the most widely spread air conditioners based on the vapour compression technology and with electric input.

In this category all the systems are based on the refrigeration thermodynamic cycle of Figure 2 and uses specific refrigerant fluid which properties allow performing the cycle efficiently using as cold and hot source air or water.

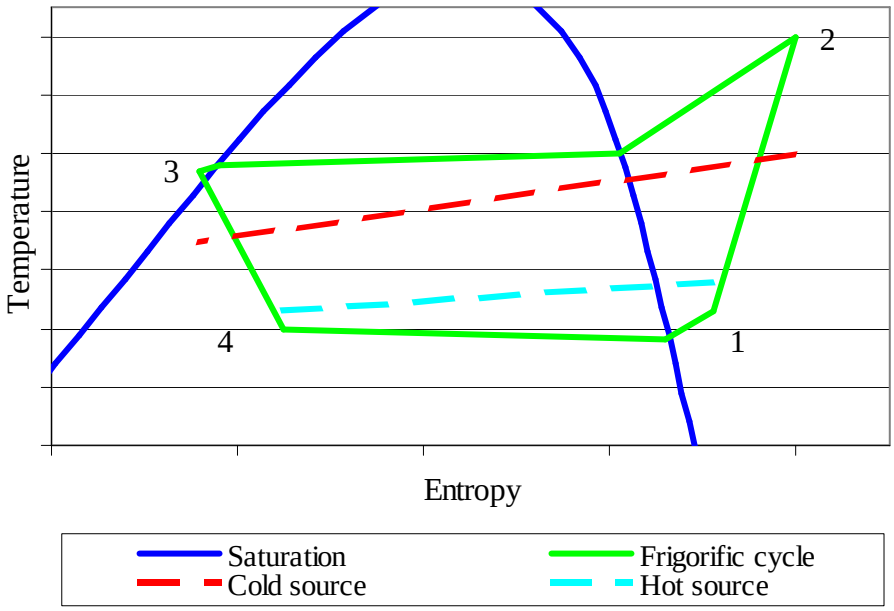

Figure 2: Thermodynamic cycle used on vapour compression systems for air conditioning

The transformations of the cycle are performed by the following components:

- An electrically driven compressor is responsible of the compression (1-2) that increase the refrigerant temperature and pressure, absorbing an amount of electricity that depends on the efficiency of the compressor
- A heat exchanger (condenser) cools the refrigerant (2-3), heating a cold source (red dashed line temperature), the fluid exits as a saturated liquid characterised by a subcooling
- An expansion device expands the fluid reducing its pressure and its temperature (3-4), the expansion is an isenthalpic transformation with no work and no heat transfer
- An heat exchanger (evaporator) cools (4-1) a hot source (blue dashed line temperature) heating the refrigerant, the refrigerant exits as a saturated gas characterised by a superheat

The actual components present several irreversibilities in the cycle: the real compression is a non-isentropic transformation (entropy of the point 2 higher than 1) and the refrigerant flow in the condenser and evaporator is accompanied by a pressure drop due to the friction with the exchanger walls (pressure of 3 lower than 2 and 1 lower than 4).

The subcooling and the superheat are needed for equipment reasons. The subcooled refrigerant at the condenser exit allows increasing and regulating the cooling capacity of the system. The superheat guarantees only gas entering into the compressor, ensuring a longer life of the equipment that can be damaged by the compression of unsaturated vapour.

The system is characterised by its cooling capacity represented by the difference of the enthalpies of the points 3 and 4, and its efficiency is measured by the energy efficiency ratio (*EER*) between the cooling capacity and the compressor absorbed power. The system includes ancillary equipments (pumps, fans, regulators etc.) that also contribute to the global energy consumption.

The systems can operate with different fluids as the hot and cold source: air or water. We can then have four main system typologies.

Table 1: Air conditioners condensing and evaporating source possibilities

Condenser source	Evaporator source
Air	Air
Water	Air
Water	Water
Air	Water

The fluid choice can depend on the local source availability and temperatures, on building constraints and designers' choice.

1.3 General definitions and references about air conditioning audit

To understand the different concepts of audit, pre-audit, inspection etc… we have to refer to the rare publications that try to put order in a domain which has been existing for many years but remains confuse and on which the terminology is still arbitrary and of specific use of firms or countries.

Energy audit refers to the methods used to explain the energy consumption of an existing building and discover what can be improved. This information may then be used to prescribe the introduction of appropriate energy saving technology for a particular building. Such technological installations are referred to as "retrofits".

During recent years much attention has been given on the development of the methods, training and instruments needed for successful energy audits.

The "Guide technique d'audit énergétique des bâtiments" [Krarti 2001] is our reference for the global definition of energy audit for buildings. Four different audit procedures are defined:

1. Energy costs analysis
2. Quick audit with visit
3. Standard energy audit
4. Detailed energy audit

The audits methods are presented in increasing order of complexity and depth of analysis. An entire chapter is dedicated to the air-conditioning audit with the most common improvement solutions.

Moreover this only existing reference can be improved and we have refined the definitions hereunder.

Preliminary definitions
In the following pages one can meet different terms (defect, fault and failure) for which the difference in meaning can be ambiguous and has to be defined. We organised the language used with the following definitions:

- A **fault** is a signal of malfunctioning, either coming from operational error or from some defect
- A **defect** is a hardware imperfection coming either from poor design or poor installation or lack of maintenance
- **Failure** is a state of the system in which the main function is missing, as opposed to a degradated mode of operation of the main function.

Definition of pre Audit
Pre Audit (or Walk-through Audit) leads to the determination of the existence or not of faults or possible improvements within the following limits: 1-2 days, visual verifications, analysis of "as built" records, of system manuals, possible complaints and operating costs (in the sense of the French

audit scheme operates by the ADEME called “pre-diagnosis”). Potentially, short tests of functional performance can be included, but without, or with very limited, additional instrumentation.

Within pre audit, various steps can be defined. Prior to considering possible improvements of the energy system of industrial, commercial or residential sites, it is necessary to realize an inventory of equipment in place and collect information about it. Some building owners or facility managers have a well-documented description of their plants. In other cases, a detailed tour of the building allows to obtain the necessary information about the installation in order to determine the type of equipment in place.

Definition of audit

Audit (also **“General Audit” or “Detailed Audit”**) is the quantitative determination of what can be done to correct the defects or improve the existing plant. Reaching this objective can take some days and be spread out over 1-6 months (in the sense of the French audit scheme operated by the ADEME called “diagnosis”). It is possible to use of continuous monitoring over weeks. This continuous monitoring may include “passive” and/or “active” tests (according to the way of analysing the component behaviour with or without artificial perturbation) of functional performance applied to the whole system or to some selected subsystems and components. Among detailed audits, we can consider the i**nvestment grade audit,** which is a level of audit allowing making the engineering study and the orders for works without turning over on the ground.

AC audit (based on the cooling function) is not a separate action for buildings owners and managers; it is often associated with something else:

- Inspection
- Auditing of AC alone arises sometimes as a specific demand (namely for comfort) without energy consideration;
- Auditing of total building energy use may take place without separating AC;
- Benchmarking of total energy use in comparison with other buildings as well;
- Managing energy use and continuous improvement requires some audit;
- Operating or maintaining AC facility and continuous improvement (continuous commissioning) as well;
- Performance certification requires an audit approach if real consumption is used

The compulsory inspection can be intended as a “pre audit”. It can lead to important savings if followed by more detailed audit and investment-grade audit that lead to a real improvement of the energy efficiency of the systems integrating all the aspects of the air-conditioning system.

Link between inspection and energy audits

The regular inspection is only the first step towards energy efficiency and then energy savings. Indeed, possible actions following the inspection report depend only on the motivation of the building owners. In the best case, they will renovate their installations and will decide voluntarily to have the building audited. Nevertheless, if they decide not to improve their equipment, they will be at least warned about current trouble that occurs on the AC plant. Therefore, they will be able to contract an AC operator (or improve the existing contract with), a maintainer or to simply establish a better internal follow-up. The audit methods have to be tailored to the motivation of the building owners in terms of technical content and cost.

Several factors can lead a building owner to have his/her building audited, especially for AC equipment. First of all, there is the will to decrease the building expenses by trying to reduce the energy bill. Moreover, the building owner can take advantage of financial incentives (ADEME subsidies, 5.5 % VAT on works in France) to invest after an energy audit. However, these subsidies depend directly on the Member State economic conjuncture. Last of all, maybe the building owner needs to improve the image of the firm or local authority. The “political image” is an important parameter as well at the State level but also for its subdivisions (regions, departments or towns for

France) before or during a political mandate. The “economic image” can be improved by actions towards “sustainable development” including Energy Efficiency.

Finally, the most rational incentive is the one that encourages the building owner to reduce the internal costs and so energy consumption. The others are only additional arguments to support the will to reduce internal costs. Nevertheless, the notion of “energy costs” is really relative and depends on the baseline. Indeed, any performance degradation leading to an increase of either the energy bill (efficiency decrease) or O&M costs (breakdown increase) is easily observable by the building owner and then can be corrected without regulatory measures. By opposition, the building owner can hardly detect an installation that operates correctly but with a lower efficiency than present standards of performance. The regular inspection is meant as a vector towards detailed energy audit and more energy efficiency. At the same time, the request that the inspection is independent from installers, operators, etc. in the Directive is not an opening in the direction of “energy services” and will request owners that have already optimised their AC to pay again for something already done.

Energy efficiency in air conditioning

The performances of air conditioning systems should be analysed from several points of view in order to correctly estimate the performance level. A global approach developed in audit procedure will take into account all the aspects related to the system: the building requirement in term of comfort, the thermal aspects related to the air conditioning (such as insulation, solar gains etc.), the systems sizing compared to the cooling demand, the operation of the systems and its maintenance etc. All these aspects can be improved and can lead to better system performances and require different skills to be analysed.

We will focus only on the equipment audit, more in detail on the system components problems that we will call **defects** that are not related with the manufacturing or control of the system but are strictly related with the **operation**, due to poor maintenance or naturally ageing of the system.

The information needed

For the AC systems and their auxiliaries different audit tools exist. The main functions of the system have to be evaluated and, depending on the level of automation of the systems, different possibilities exist. The first approach is the quantitative evaluation of the performance of the system. This evaluation of the results (Energy Efficiency) is often difficult, based on interview with the occupants and staff. Other methods may be used to check part of the means used to reach Energy Efficiency. In the modern system when the level of automation is high, automatic systems for the detection and diagnosis of faults exist and can be embedded in the control or Building Energy Management System. In this case the auditor can access to complex information and his task is one of the task is also to verify the reliability of the monitoring system. When no information is available, the auditor has to build his own system assessment through the observation of the systems and through the measurements he could quickly obtain with a minimum of measurements with portable sensors.

The first information that should be retrieved is the design plans of the system including the further modifications and retrofits. This will inform about the system components, position and installation details and it allows defining the measurements points.

Then the maintenance records should be verified, in order to check the past interventions, their frequencies and to estimate the general status of the system.

When there is a lack of available documents, the auditor should draw the plans by going through the air-conditioned area and technical rooms.

The main information comes from the system plates that report in general: the manufacturer and the name or series number of the machine, the used refrigerant, the nominal performances and the input characteristics. Other information can then come from the manufacturer catalogue although for very old systems it becomes more and more difficult to obtain the catalogue and the reliability of the reported performance should be regarded critically, taking into account the reference test standard. In this sense, Eurovent Certification helps the auditors giving the free access of the certified directories since 1995, directly through the Eurovent Certification website. This will allow auditors to retrieve the

rated performance of old systems, to compare it with the recent performances of air-conditioners of the same manufacturer or with other market products.

In-situ determination of performances of AC systems
Real conditions of operation may be different from test conditions in laboratory used to establish the performances of a system and published on the plates and on the manufacturer documentation Thus difference may be important even if we use seasonal coefficients (i.e. *ESEER)*. So for the auditor it is very important to be able to assess the real performance of the system.

For the evaluation of the real performance, measurements in situ are requested and different methods should be developed for each type of system.

For chillers, J. Phelan et al. [Phelan 1997] have developed a performance testing method for evaluation of annual energy consumption with account of partial load operations. A relationship between energy rate and one or more variables is developed for the equipment and system using a combination of direct measurements, statistical regression analysis and manufacturer's data. They use a model of the chiller where the $1/COP$ ($COP = EER$) and $1/Q_{eva}$ (Q_{eva} is the load at the evaporator) are linearly dependent and four methods of testing: from the simplest to a more complex model Temperature dependent model.

The test methods by Phelan have been validated on two case studies on chillers used in two high schools. For the chillers tested, the results indicate that accurate results can be obtained with relatively small data sets. The results showed that the chiller partial load ratio was the most significant factor affecting the chiller efficiency, with evaporator and condenser temperatures having a secondary effect.

For other types of systems (such as air systems or small split systems) there is no study or method for measurements in the bibliography.

Often, the difficulty to perform the measurements on the field (if there is no place to put the sensors) leads to the impossibility of performances assessment or, in some cases, the weak accuracy of the performances determination (i.e. for measurement on air systems) make the results useless. The determination of the efficiency of the system has to be evaluated in another way.

This kind of assessment is a part of a complete audit and can be performed over some weeks, months or an entire cooling season.

1.4 Methodology of research for air conditioners performance degradation

In this research we want to observe the defect that can occur in an ageing air conditioning system and to take on the auditor point of view in order to know which are the defects that are dangerous, in which conditions, which are the energy performance consequences. We restrained our field of investigation to the "equipment" defects in order to determine the problems that can be easily corrected (through periodic maintenance intervention for energy efficiency) and that can be observed directly by measurements on the site. Design problems that require complete retrofit of the installation (such as incorrect sizing) are out of our scope.

Our objectives can be summarised as follows:

- To apply different methodology of research based on qualitative and quantitative estimation in order to analyse the defects that arise during the lifetime of an air conditioning system
- To define the detection parameters for each defect that could be used on the field with the minimum of tools and information
- To validate experimentally the methodology of research, which uses simulation based on existing models, by comparing the results with the available literature experimental works
- To quantify the defects consequences on the performances on some typical buildings in order to have a seasonal quantitative estimation
- To define some time-related model in order to couple the performance degradation with an optimised frequency of the action for correction taking into account the economic aspect.

The methodology is summarised in the graph below in order to define the main steps that will be developed in the next chapters.

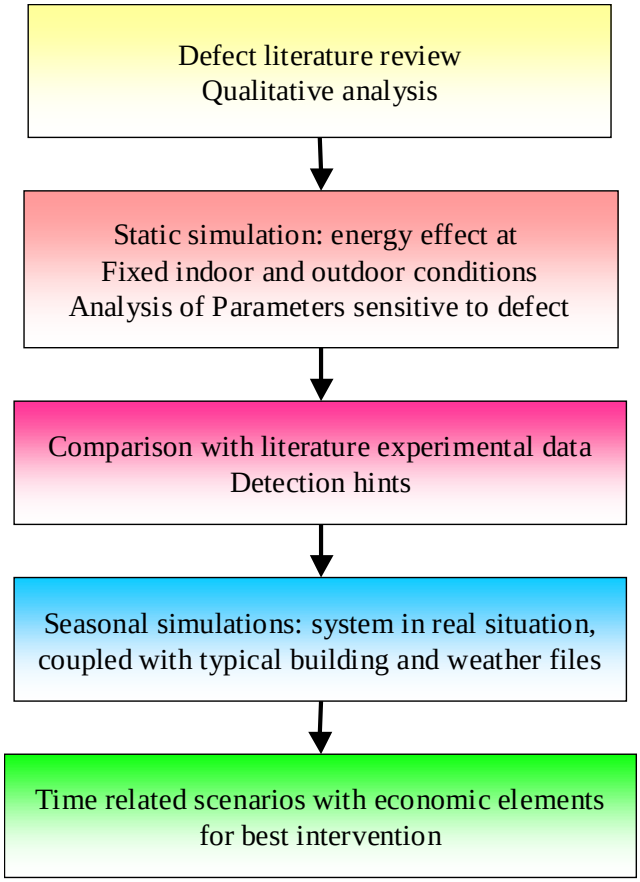

Figure 3: Steps of our methodology of research for air conditioning defect analysis

In order to reach the objectives, the use of a "model" was chosen. Modelling allowed us to perform a research on several defects in very different conditions and to isolate for each defect the consequences. The experimental way would have been too complex and it would have certainly required a lot of time. However, a set of experimental works has been inventoried that we will use all along this work to validate and support the results of the simulations.

The research is applied to two air conditioning system types: the small split air systems and the chillers. The chosen systems are meant to be representative of the most widely spread systems technologies in order not to study a unique case, but to understand if our results are compatible with the largest part of the stock.

All the results of this work have to be considered with the limit of the chosen methodology: the analysis and the results are strictly related to the chosen system. This means that our analysis although applied to systems that are very largely spread on the market would not be applicable for all the systems in the stock. And even more, not only a components similarity is necessary but also a similarity of operation criteria, which would be impossible to verify unless through the perfect knowledge of the components operation characteristic. The manufacturers' choices in terms of components type and sizes and rating operation points are very different from one manufacturer to another.

This analysis allowed us to discover the complexity of the problem and have been useful to give trends and magnitude for the studied systems that if not universal, can be used as example by auditors and inspectors to promote the correction actions and to justify them in front of a doubtful customer.

Focused aspects of the air conditioning

In the following pages the defect analysis will be centred on the energy aspects mainly the energy consumption and the efficiency of the simulated system.

All along the results presentation, the capacity of the system and its sensitivity to the defect will be observed in order to define if the system can still operate for its primary function: to keep the comfort conditions. Although the comfort conditions are very debated and discussed, we will adopt an easy to use comfort assessment criterion linked to the temperature setpoint. We will consider discomfort conditions in the seasonal simulations as the duration of time during which the difference between the temperature setpoint and the room temperature is larger than 1°C. This condition does not take into account strictly the "comfort" concept, this difference would not be perceived by most of the occupants but allowed us to quantify when the system capacity is degradated more than normal fluctuations due to the temperature range of control, the seasonal simulation considering average hourly temperatures.

Other aspects are analysed in order to define detection measurements that an auditor or inspector could perform directly on the field with a minimum of portable measurement equipment. Actually, the auditor should be capable to measure parameter when the system is operating in steady state conditions. The auditor should ensure the operation mode of the system; in some case he/she can force the system to be "on" acting on the set point temperatures and waiting for the steadiness of the operation. Ideally the parameters of "normal" operation should be established from the first operation period of the system with no defects, in the real conditions, at different indoor and outdoor conditions that can differ from the catalogue value because of the conditions of installations (liquid lines length, effective airflow at fans etc.).

2 Analysis of defects occurring during the operation of split systems

2.1 Energy stakes for split systems

Although small systems as room air conditioners (RAC) are not all in the frame of the air conditioning inspection (the inspection is limited to 12 kW of capacity meant as sum of the capacities of the systems present in a building), their importance on the total energy consumption in Europe is large because of their large use in residential and commercial sector. This is true especially for Mediterranean countries that represent the largest part of the split system stock (Spain and Italy representing the 70 % of the total stock) that accounted for more than 7 millions of units in 1996, shared as in the figure below [EERAC 1999].

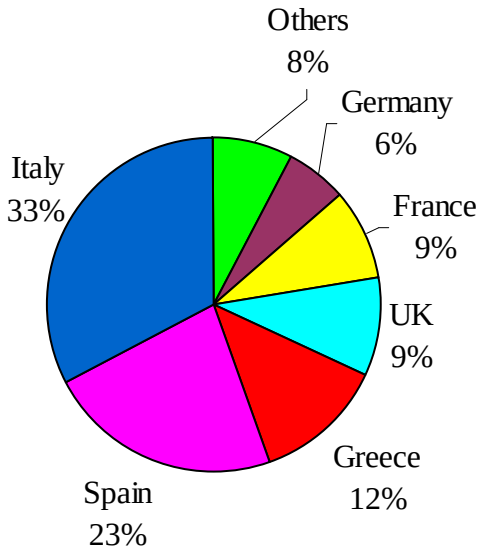

Figure 4: Split stock by country in 1996 (number of units).

The French stock was already important at that time, but its increase has been boosted up after the extremely hot climate in 2003 that led to a quick market increase: +80 % units sold in 2004 [ClimInfo 2005]. Energy savings are important not so much for their single quantity, but for the scale effect due to the large number of units present in the building stock and as result of their ageing state.

The inspector/auditor needs then to be able to target the most important opportunities for energy savings and comfort improvement for this system type, to be able to quickly find out the major problems and estimate the possible improvements subsequent to the correction. For the time being, the audit methods are very scarce and the inspection requires more tools and support to become reproducible. One case of split systems has been studied in order to define the equipment problems that should be investigated by a professional and their effects on comfort and consumption issues. Stress is put on energy consumption and discomfort consequences in relation with the equipment defects arisen during the operation.

2.2 The representative split system chosen

The chosen split has to be representative of the current system in the existing stock. It uses as refrigerant the R22. Although R22 is destined to be phased out by the Montreal protocol and is replaced by new fluids for new systems (mainly R410A), it is still very common and it represents more than 90 % of the fluid demand for the maintenance for air-cooled air conditioners in France in 2005 [Barrault 2007]. The European regulation on certain fluorinated greenhouse gases [F-gas 2006] led to the stop of production of new products using R22 since 2002, but R22 will be still used in maintenance until 2010 as fresh fluid and until 2015 as recycled fluid. After that it will be collected and eventually destroyed. In such systems, R22 is replaced by R407C.

The capacity of the representative split is enough to cool a room of a house or, with several units, a small office building. The system displays the main characteristics of Table 2.

Table 2: Characteristics of the simulated split

Rated Cooling Capacity P_c (kW)	8.69
Rated Compressor and Fans Power P_a (kW)	3.38
Rated *EER*	2.57
Compressor type	Reciprocating
Refrigerant	R22
Expansion device	Capillary tube

A more detailed description of the system is shown in the annex under the form of the input data of Mark V [Annex 1].

The expansion device is a capillary tube as it can be encountered in most split systems [ECODESIGN 2007]. The system uses a reciprocating compressor although the more spread technology for new products nowadays is the scroll technology. Scroll compressors quickly took large market shares since their appearance in 80's for the low capacity systems, however reciprocating are still spread and manufactured thanks to the long experience of the technology.

2.3 The ORNL Heat Pump Model Mark V capabilities

As a first simulation step, we introduced the defects in a thermodynamic model of the system in order to define the effects in the standard conditions at fixed temperatures and full load operation.

The thermodynamic simulation software used is the Oak Ridge National Laboratory (ORNL) heat pump design model - MARK V - version 95d [Fischer 1983, Rice 1991 and 1996]. We validated its using by examining one by one the features that we wanted to represent in our model.

We simulated the base case (new system with no defect) and degradated operation (introduction of defects one by one) for the room air conditioner. The model is capable of defining all the thermal characteristics of the fluids for an air-air heat pump or air conditioner (refrigerant, air status at the condenser and evaporator) based on:

- The air temperature and humidity entering in the heat exchangers
- Blowers characteristics at the rated point
- The geometry parameters of the heat exchangers
- The expansion device characteristics
- The lengths of the links between the components of the system
- The compressor volumetric and isentropic efficiencies expressed in a bi-quadratic law as a function of compressor suction and discharge saturation temperature with six coefficients.

The model allows obtaining all the systems characteristics and all components operation parameters with different convergence criteria: on the subcooling, on the superheat or on the total refrigerant mass. We chose to set the system refrigerant charge, then the condenser exit subcooling and the compressor inlet superheating are computed. The model flowchart is represented in Figure 5.

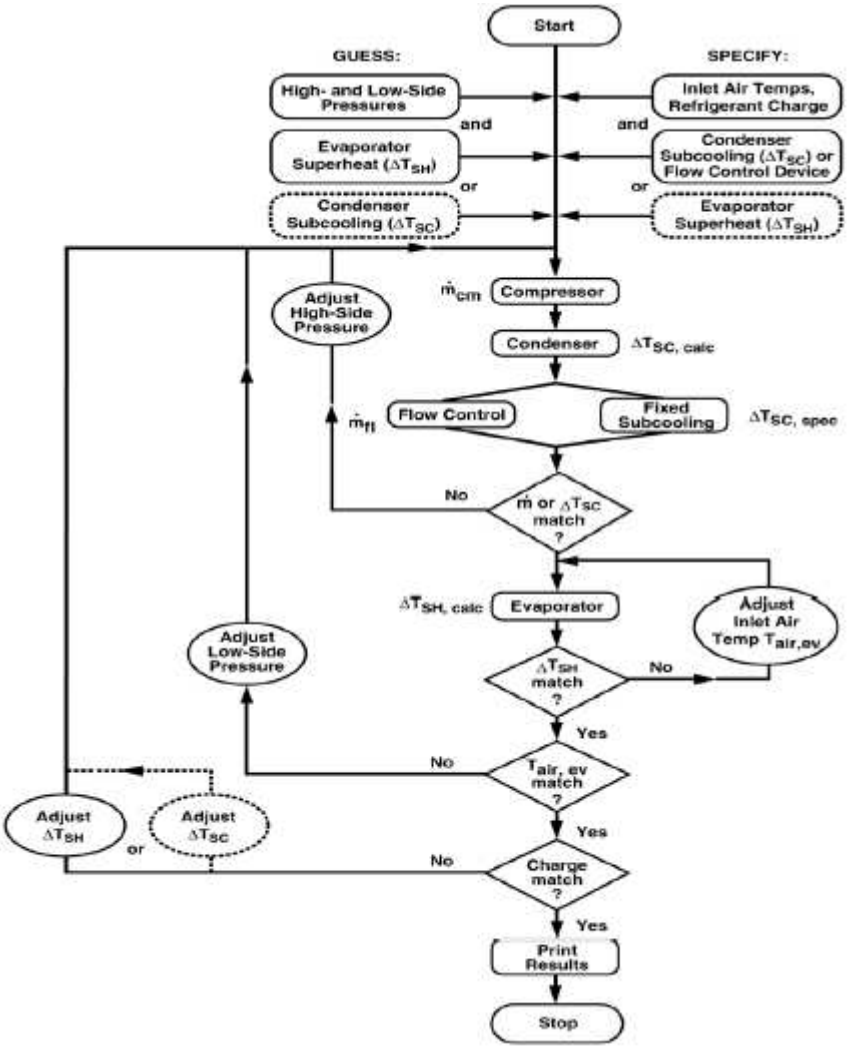

Figure 5: Solution Logic of ORNL Modulating HPDM With Charge-Balancing Option Selected [Rice 1991]

The compressor mass flow and power are represented with six coefficients equations as a function of the condensing and evaporating temperatures. The coefficients could be obtained from a map fit programme that is provided in the stand alone version of the programme introducing the power and refrigerant flow obtained from manufacturer's catalogue tables at different condensing and evaporating temperatures.

In order to simulate a defect, the model allows introducing simply the modifications in the input parameters translating the equipment degradations. For each defect several level of defect are investigated. For each defect, we have observed the modifications of the thermodynamic cycle (condensation pressure, evaporation pressure, some significant temperatures), the variations of the cooling capacity, the power to compressor motor and the energy efficiency ratio in relation with the base case characteristics.

We did not simulate the occurrence of several defects at the same time, our objective was to characterise a single defect and to isolate the defect effects.

2.4 Defects definition and characterisation

The equipment defects that can occur in the lifetime of a packaged air conditioner have been analysed in the work of Chen and Braun at experimental level [Chen 2001]. The main objective of the analysis was to define the impact on measurable parameters in order to develop an automated fault diagnosis and detection system. The detection and diagnosis aspects were developed but their analysis was not focused on the energy aspects. This estimation is crucial in order to quantify the energy savings due to a proper maintenance that corrects the defects, and it can further allow developing an economic assessment of the corrective actions. That is why we have developed thereafter quantification of the energy impact of the defects and provide indicators that can be useful for auditors, inspectors, and energy advisors to promote a better management of room air conditioners.

The defects were identified through analysis of service records by Breuker and Braun [Breuker 1998] for packaged systems and they can be translated for room air conditioner equipment because of the similar structure of the two systems (air to air systems). The following defects were considered:

1. Refrigerant undercharge
2. Condenser fouling
3. Evaporator filter fouling
4. Restriction in the liquid-line
5. Worn compressor

Hereunder a description of each defect follows. It includes a qualitative representation as a tree showing on one side the main effect on energy parameters and on the other side measurable parameters that could be used for detection.

2.4.1 Refrigerant leaks in unitary air conditioners.

The refrigerant leaks can be due to leakage that occurs during operation in correspondence of worn or damaged components (as the joints between different components of the system) for system that operates at pressure higher of the atmosphere pressure. In some cases, the system charge level has been low since the initial operation because the initial charge introduced in the system at the moment of its installation was less than the one recommended by the manufacturer due to a human error. Maintenance operation can also introduce source of leaks. Commonly split system are previously filled in the factory; when liquid lines are longer than previewed, manufacturers suggest for the additional mass to be added to the system for additional liquid line length (as refrigerant mass per liquid line length kg/m). In the first case, a minimum refrigerant mass is the guaranteed. In some other case, the system is fully filled of refrigerant by a professional once installed.

Refrigerant leaks have to be considered carefully in split systems. Generally this kind of system is very sensitive to refrigerant leaks due to the length of the refrigerant lines between the indoor and outdoor unit often exposed to danger and particularly for mobile split systems, for which the periodic displacement of the system induces a more severe deformation on the connecting lines and joints and consequently a greater leakage risk. Refrigerant leaks are dangerous for the system operation but also because the fluids used as refrigerant are very dangerous for the environment since they have high coefficients of ozone depletion and global warming potential.

The European Community took measures about the limitation of refrigerant leaks through the “Regulation on certain fluorinated greenhouse gases” [F-gas 2006] that decided the periodic control of the plants for leaks detection. In France the Directive has been translated in a by-law [Arrêté du 7 mai 2007] and includes annual inspection for all systems with a charge higher than 2 kg, more severe than the EU regulation that puts the limit at 3 kg.

The average annual rate of leakage for small split system (capacity lower than 17.5 kW) has been estimated at 5 % per year for life duration of 15 years [Barrault 2007]. The value takes into account leakage that appears all along the life of the system including a regular maintenance.

The expected effects of the refrigerant leaks are shown in Figure 6.

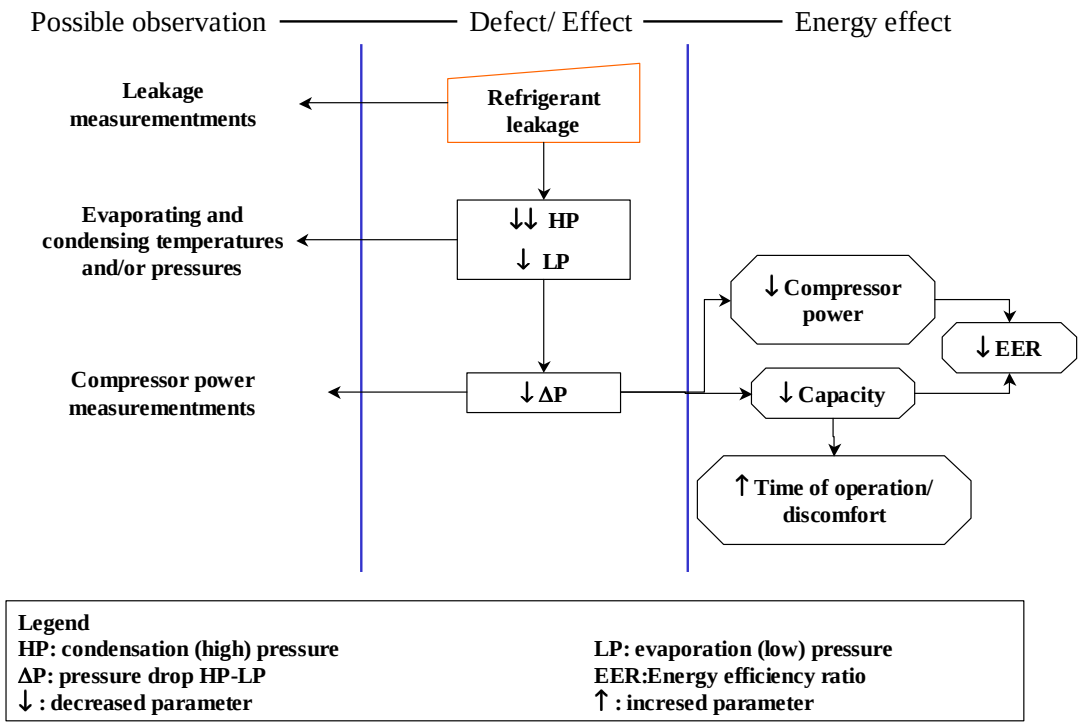

Figure 6: Tree representation of refrigerant leak consequences and possible monitoring parameters

The refrigerant leaks reduce the amount of the refrigerant in the system that cannot consequently keep the same cooling capacity. At the same time the compressor has to compress less mass consuming lower energy. The global effect is anyway a lower efficiency, if the initial charge was optimised.

ORNL model limits for leakage simulation

The ORNL model allows defining the total charge of the system. The tool allows to compute the mass in the different components of the system and to choose different void fraction model for two phase zones in the heat exchangers: the Zivi method was used to calculate the mass [Zivi 1964]. We can easily simulate refrigerant leakage by simulating the system with reduced charges.

The limit of our model occurs for very low values of charge: the expansion model does not allow taking into account unsaturated refrigerant conditions that occur when the higher pressure is lowered (no subcooling at the valve entrance) in case of large leakage. So we could not go over 22 % undercharged system because the model cannot converge anymore in most conditions.

2.4.2 Condenser fouling

The split condenser is a finned heat exchanger. The condenser is part of the outdoor unit and it is exposed to the weather. It is exposed to the environmental conditions and dust. Several authors have studied the mechanisms of the particle deposition on such heat exchanger. A literature review is presented hereunder.

Mechanism of deposition of particles on finned heat exchangers

Deposition mechanisms on finned heat exchangers are associated with the particle inertia (such as impaction and interception on fin edges and refrigerant tubes), gravitational settling of large particles and Brownian diffusion of small particles in the heat exchanger core.

Additional deposition can be caused by turbophoresis, the motion of large particles down a turbulence intensity gradient, in the entry region of the fins. If the heat exchanger is in heating or cooling mode, there can be a change in deposition due to thermal effects (thermophoresis) and humidity concentration gradients (diffusiophoresis), although these effects are typically small compared to other deposition mechanisms.

Condensers heat exchangers are almost always installed with vertical fins to limit gravitational settling, provide for condensation drainage for reversible systems, and to facilitate cleaning.

The most widespread general model for heat exchanger fouling is described by Bott [Bott 1995]. A summary of the predictions of this model appears in Figure 7.

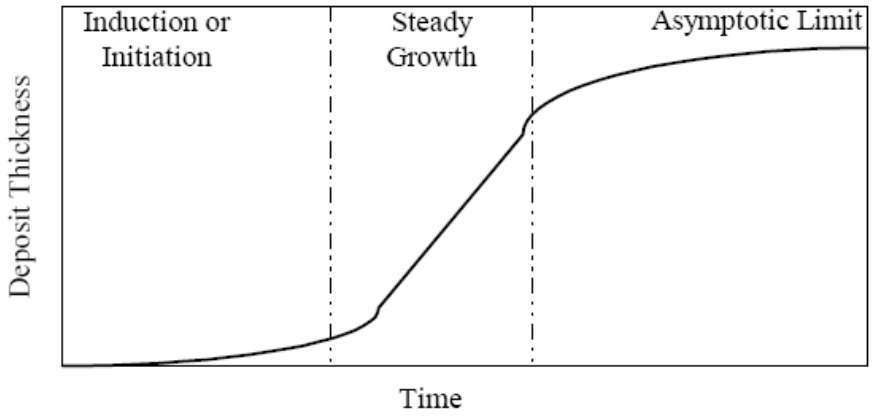

Figure 7: Asymptotic fouling modelled by Bott [Bott 1995]

The amount of deposited material initially remains small during the induction period because adhesive forces are small until sufficient material deposits to condition the surface for future deposition. The length of the induction period can vary greatly for different systems. The steady growth of the layer occurs as surface conditions permit a constant increase in fouling. Finally the deposit layer reaches a maximum and asymptotes. This asymptotic behaviour, although not universal, is caused by a balance between deposition and removal of the fouling agent.

A modelling and experimental work about heat exchanger fouling was developed by Siegel [Siegel 2002]. The author focused on the fouling of indoor heat exchanger for AC systems and determined a deposition model taking into account the different mechanisms. An experimental work was done in order to determine the particle deposition fraction and verify the proposed model. The work focused on ducted indoor units, evaporator heat exchangers and filter efficiencies; the experimental part concerns typical indoor characteristics (i. e. for dust composition). We can observe the values for time of fouling estimated: these are defined as the duration for the fouling to double the initial pressure drop at the heat exchanger for a fixed airflow. The value obtained by the author for the base case is of the magnitude of 4 years.

Pak et al. [Pak 2005] experimentally studied the effect of the fouling and cleaning operation on the performance of several condenser types for fin shape and number of rows. They studied at the same time the additional pressure drop brought by the fouling and the reduction of heat transfer. However the result on the last point do not take into account the reduction of the airflow due to the fouling and the measurements are taken for constant air face velocity. Moreover, the errors on the heat transfer measurement are too large to consider them reliable. About the pressure drop for which the measurement errors were lower (2-4 %), the authors considered the fouling for an equivalent one-year operation of the systems using standard dust. Following the configuration they estimated that the pressure drop increases by 28 to 31 % for one-row heat exchangers and 24 to 38 % for two rows heat exchangers.

More recently, Haghighi et al. [Haghighi 2007] experimentally demonstrated that airside fouling depends on geometrical considerations almost exclusively. They observed that no heat transfer effects have been measured at constant air speed, mainly due to the fact that the fouling remains a “surface” phenomenon and it is caused by the deposit of the particles on the edge of the fins or by the nucleation of smaller particle that enter in the heat exchanger but remain at very low depth and left most of the heat exchanger fin surface available for heat transfer. At constant air speed the heat transfer factor is not affected by the fouling but when the authors simulate a loss of airflow (by a controlled opening in the wind tunnel) the heat transfer is reduced. They do not measure it directly but just observe the reduction of the temperature difference of the water in the coil. The airflow reduction makes the temperature difference decrease: initially it varies from 20 to 25 °C with the air speed and decreases to 10 to 18 °C in the most fouled conditions. The authors determined the critical diameter of particle that

lead to maximum fouling effects on the pressure drop. The particle critical diameter has been estimated as $d_{crit}=0.6D_m$, where D_m is the diameter of the largest sphere that can be inscribed in the inter-fin spacing.

Pressure drop and fan operation characteristic for a fouled condenser

Condenser fouling is due to an accumulation of particles and dust on the face of the condenser coil: on one side it leads to a reduction of heat transfer increasing the overall thermal resistance of the exchanger and on the other side increases the pressure drop reducing the total airflow rate across the circuits of the condenser. The condenser fouling acts on the airflow rate and on the thermal resistance of the coil.

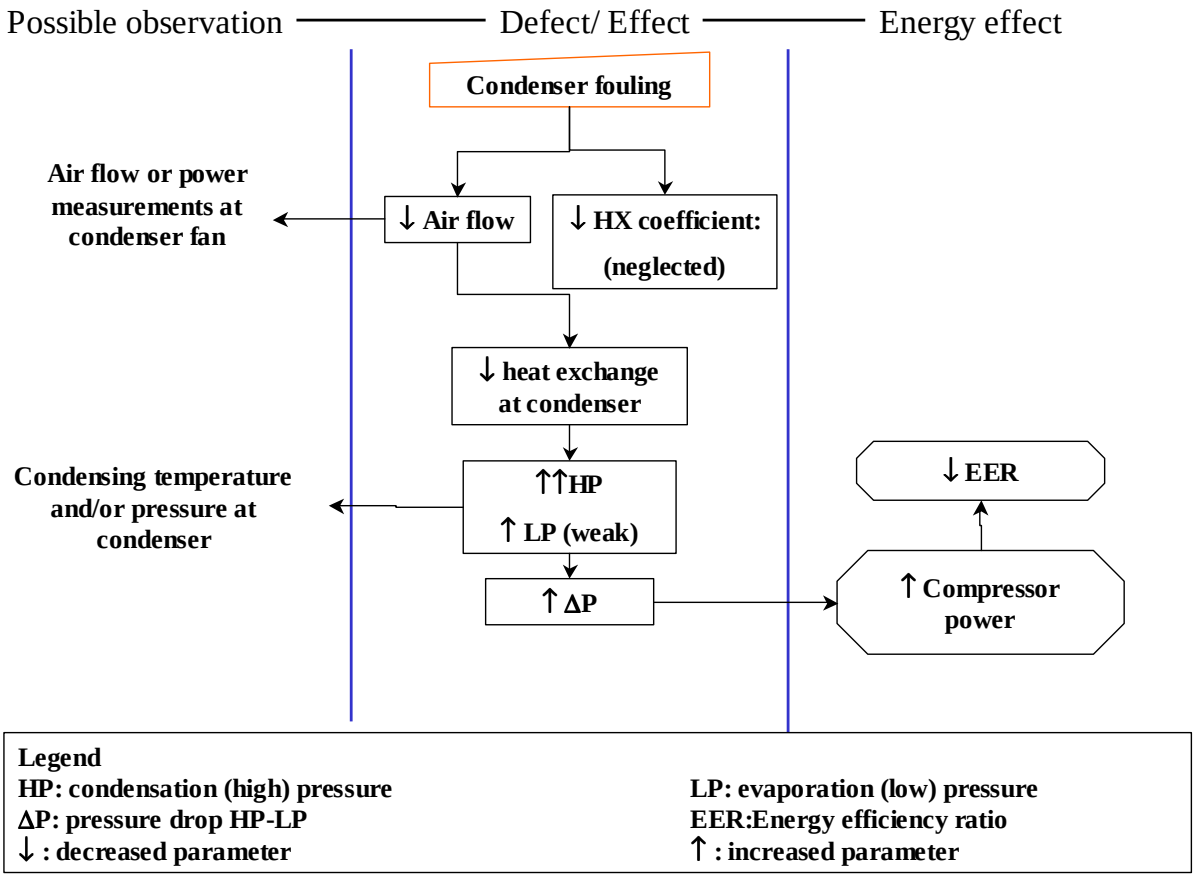

Figure 8: Tree representation of condenser fouling consequences and possible measurement parameters

Following the observations of the previous studies, we considered a fouling effect only on pressure. We kept the Siegel definition, the fouling limit has been considered as the fouling rate that increase the initial pressure drop by 100 % at the initial airflow. The heat transfer reduction is then subsequent to reduction of the airflow and no additional thermal resistance due to the fouling has been considered.

The ORNL computation for pressure drop at the condenser calculation

The pressure drop on the condenser airside estimated by the ORNL model is very low (of the order of 10 Pa). We decided then to estimate separately the pressure drop in order to correct it by the use of the multiplier that the designers added to the program because they were aware of the uncertainty in the correlation used for the pressure drop calculations. Moreover the ORNL model does not allow modelling the fan through its characteristic. For non-rating points we had to introduce manually the parameters of the fan: the airflow, the pressure drop corrected through the use of a multiplier, the fan efficiency and the efficiency of the motor. The two last are both considered constant in the range investigated: the efficiency varies slowly and we have no data to introduce it in the model

(manufacturers rarely give it in catalogues) and the fan works at constant speed, determining a constant motor efficiency.

Once we determined the rated characteristic of the condenser fan, we introduced the fan model allowing representing the fouling through the pressure drop increase and the new points for fouled operation.

The pressure drop at the condenser for the reference case on the airside can be estimated from the literature correlations with the geometrical parameters of the heat exchangers represented in the figure below.

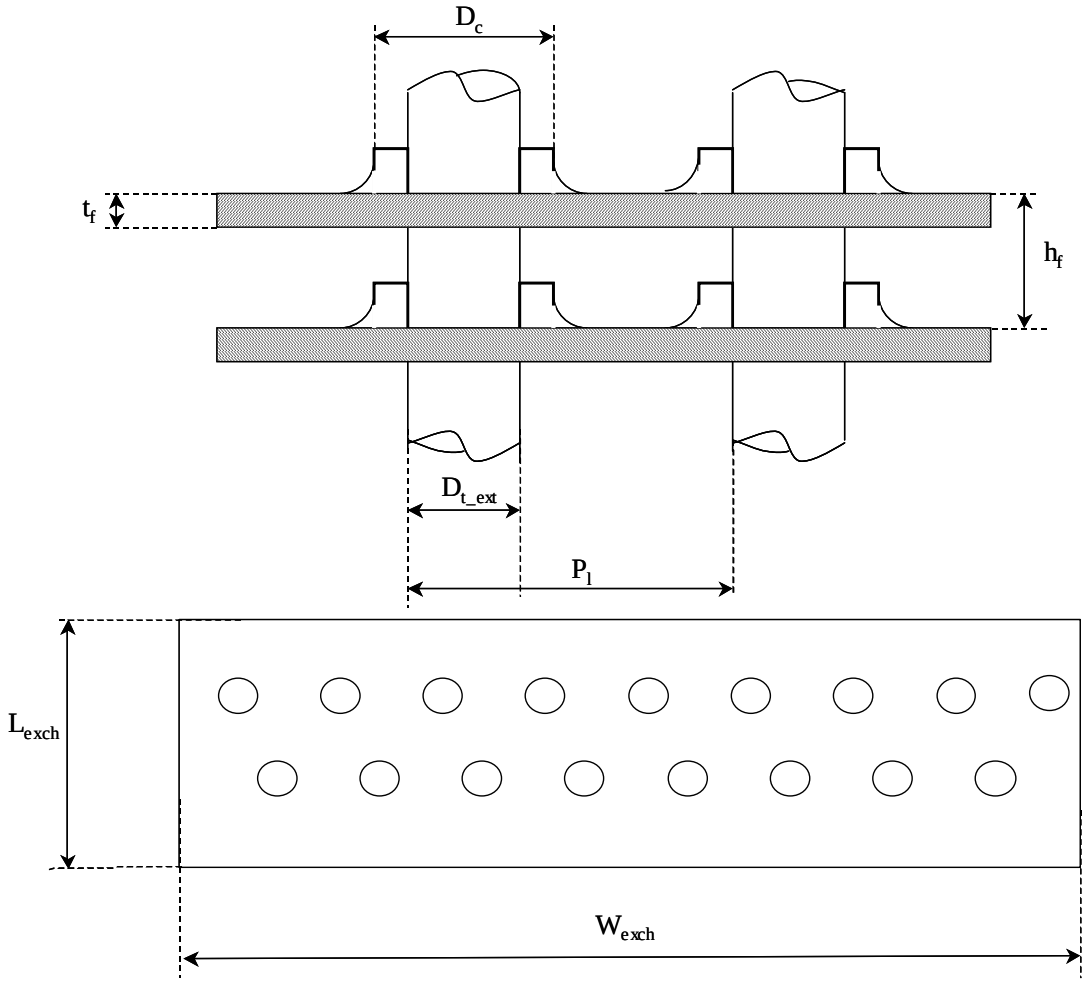

Figure 9: Geometric parameters of the heat exchangers

Based on the cross area A_c and the total area A_{tot}, the pressure drop can be evaluated as:

$$\Delta p = f \cdot \frac{A_{tot}}{A_c} \cdot \frac{G^2}{2\rho} \quad [1]$$

With G the air mass flow per unit of cross heat exchanger area, ρ the air density, f the friction factor.

The cross area and the total area are calculated as:

$$A_{tot} = A_{fin} + A_{tube} \quad [2]$$

$$A_{fin} = 2N_F \cdot (L_{exch.} \cdot W_{exch} - \pi \cdot \frac{D_{t\_ext}^2}{4} \cdot N_T) \quad [3]$$

$$A_{tube} = \pi \cdot D_{t\_ext} \cdot N_T \cdot (H_{exch} - t_f \cdot N_F) \quad [4]$$

$$A_c = (P_l - D_c) \cdot (h_f - t_f) N_F \cdot \cdot N_{TR} \quad [5]$$

With N_F the number of fins, N_T the tubes number of the heat exchanger and N_{TR} the tubes number per row.

D_c, the collar diameter is calculated as:

$$D_c = D_{t\_ext} + 2\,t_f \quad [6]$$

Two different experimental correlation of the literature have been compared.

The friction factor f following the correlation proposed by Kim et al. [Kim 1999] can be calculated:

$$f = f_{fin}\frac{A_{fin}}{A_{tot}} + f_{tube}\left(1-\frac{A_{fin}}{A_{tot}}\right)\left(1-\frac{t_f}{h_f}\right) \quad [7]$$

$$f_{fin} = 1.455 Re_D^{-0.656}\left(\frac{P_t}{P_l}\right)^{-0.347}\left(\frac{s}{D_{t\_ext}}\right)^{-0.134}\left(\frac{P_t}{D_{t\_ext}}\right)^{1.23} \quad [8]$$

$$f_{tube} = \frac{4}{\pi}\left(0.25+\frac{0.118}{\left(\frac{P_t}{D_{t\_ext}}-1\right)^{1.08}}\,Re_D^{-0.16}\right)\left(\frac{P_t}{D_{t\_ext}}-1\right) \quad [9]$$

Where s is the distance between the fins:

$$s = h_f - t_f \quad [10]$$

Re_D the Reynolds number based on the outside tube diameter, defined as:

$$Re_D = \frac{D_{t\_ext}\cdot G}{\nu} \quad [11]$$

Where ν is the kinematic viscosity of the air.

For the correlation proposed by Wang [Wang 1996a] the friction factor f is:

$$f = 1.039 Re D_c^{-0.418}\left(\frac{t_f}{D_c}\right)^{-0.104} N_R^{-0.0935}\left(\frac{h_f}{D_c}\right)^{-0.197} \quad [12]$$

Re_{Dc}, the Reynolds number based on the collar diameter defined as:

$$Re_{Dc} = \frac{D_c\cdot G}{\nu} \quad [13]$$

The table summarize the pressure drops and the friction factor calculated at the rating point:

Table 3: Pressure drop calculations from literature correlations

	Mark V	Kim et al.	Wang et al.
ΔP (Pa)	10	42.9	58.6
f	x	0.73	0.10

The Wang's correlation seems to be more suitable because Kim's correlation was obtained for small tube diameters or large tube pitch respecting the condition:

$0.135 < \frac{t_f}{D_c} < 0.300$

While in our case $\frac{t_f}{D_c}$ =0.012, well under the validity field.

The real case is probably worst than in the calculation due to the presence of security grille to avoid any contact with the fins and the losses due to the recirculation in the case of the condenser. We estimated this initial pressure drop as 60 Pa.

Once we know the pressure drop at rating condition (pressure drop and airflow) we can draw the curve of the pressure drop as a quadratic function of the airflow, passing through the origin with an equation of type:

$$y=k\cdot x^2 \qquad [14]$$

With k= 93.7.

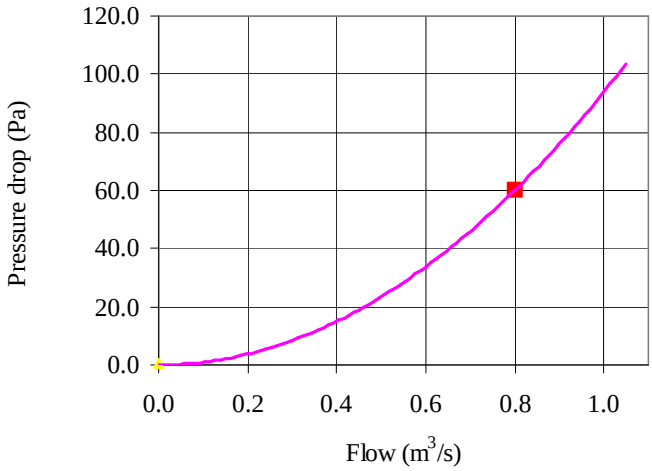

Figure 10: Pressure drop at the condenser fan and nominal operation point (red dot)

Then, we can consider that the increased pressure drop due to fouling leads to a new curve of the circuit:

$$y=k'\cdot x^2 \qquad [15]$$

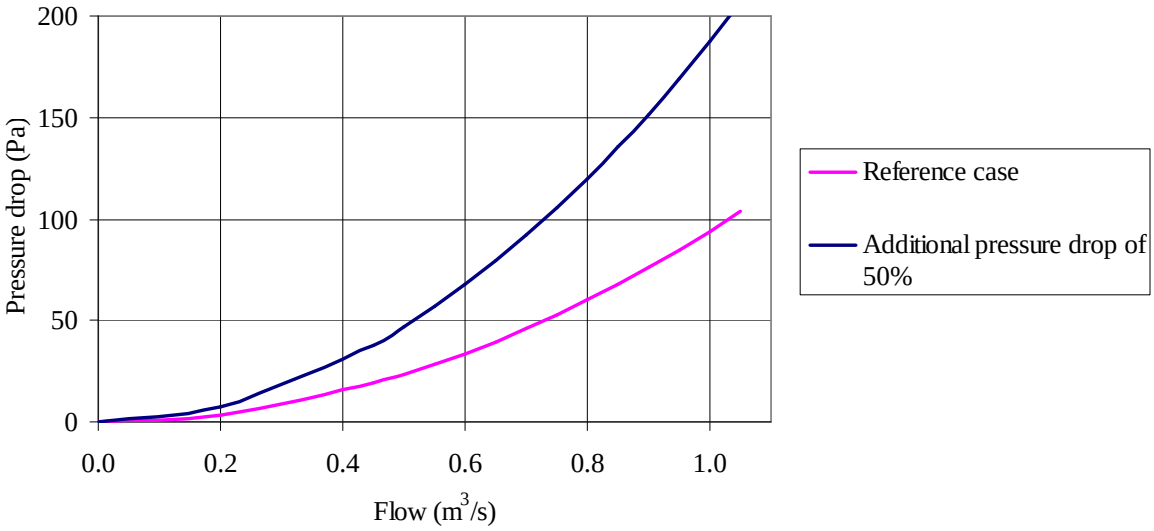

Figure 11: Pressure drop at the condenser fan at reference operation (pink) and for fouled operation (blue)

In this case we have considered an increase of 50 % of the pressure drop and *k'= 140.6*.

We can find the new point of operation considering the intersection point of the load curve and the fan characteristic. The fan characteristic has been calculated from the known rating point (red dot in the Figure 10) and creating a fan curve similar to a fan curve retrieved form a manufacturer catalogue. However because of the uncertainty about the fan curves we will consider the fan consumption constant.

This assumption introduces an under-estimation of the power for the considered airflow range. The power being a decreasing function of the airflow for axial fans, we considered this variation negligible on the global performance of the system. Considering the variation observed in the manufacturers' catalogue and in order to respect the overall consumption of the system, the fan power for an airflow decrease of 20 % is between +10 and +15 %. In power terms, the fan overconsumption would be

between 10 and 30 W for an overall (compressor plus fans) electric consumption of 3.3 kW at rating conditions. In the worst case the consumption would be underestimated by less than 1 %.

The motor characteristic is assumed constant.

The fan characteristic is fitted by a quadratic curve of equation of the type:

$$y=a\cdot x^2+b\cdot x+c \qquad [16]$$

a= -28.2
b= -28.7
c= 101.0

Both the equations representing the load and the characteristic allowed us to calculate the new airflow corresponding to each increased pressure drop as the cross point of the two curves represented as:

$$x'=\frac{-b+\sqrt{b^2-4c(a-k')}}{2(a-k')} \qquad [17]$$

Where *k'* is the coefficient of the pressure drop curve from [15].

For example, for an increased pressure drop of 100 % at rating point *k'=187.5* (Figure 12). The real pressure drop met by the fan is only 20 % larger while the airflow is reduced by 32 %.

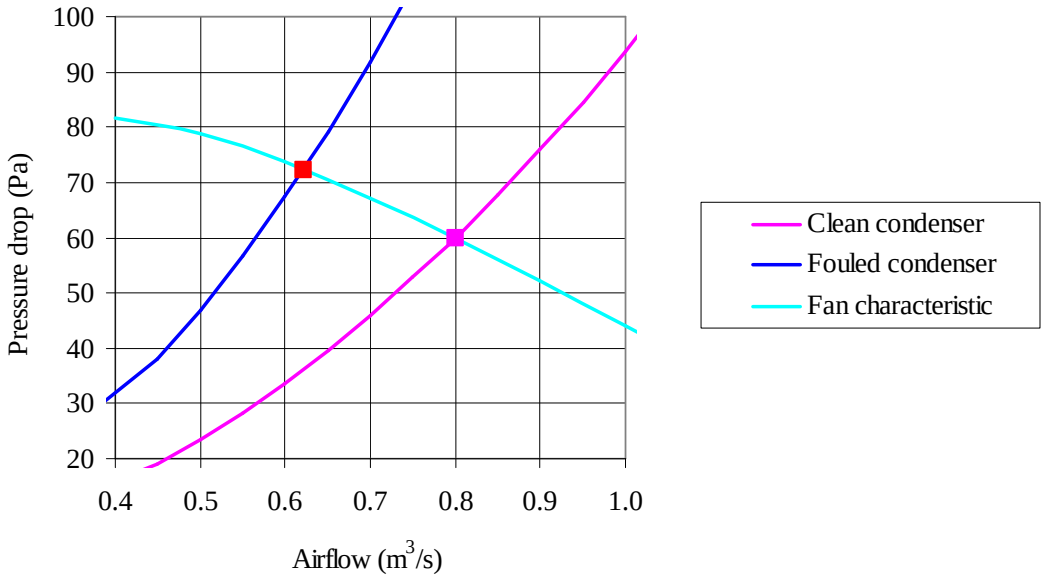

Figure 12: Fan characteristic (cyan) and pressure drop for rating operation (pink) and increased pressure drop by 100 % (blue)

We obtained the values in the table and the multipliers required by the model to obtain the effective pressure drop for the base case and several fouling levels.

Table 4: Condenser parameters for fouled conditions for Mark V input

Increased pressure drop	Pressure drop at rating point	Operating Airflow (m^3/s)	Operating Pressure Drop (Pa)	Pressure Drop Multiplier
0 %	60	0.80	60	6.2
10 %	66	0.77	62	6.5
20 %	72	0.75	64	7.2
30 %	78	0.73	65	7.6
40 %	84	0.71	66	8.2
50 %	90	0.69	68	8.6
100 %	120	0.62	72	11.0

We can observe that the pressure drop increased and the airflow decreased by the quantities in the following table below.

Table 5: Condenser fan airflow and pressure variations for fouled conditions

Increased pressure drop	Airflow (%) Rating Airflow	Pressure drop (%) Rating pressure drop
0 %	0 %	0 %
10 %	3 %	-3 %
20 %	6 %	-6 %
30 %	9 %	-8 %
40 %	11 %	-11 %
50 %	13 %	-13 %
100 %	22 %	-21 %

2.4.3 Air filtration for room air conditioners

Filtration in air conditioning is needed to hold the air particles in order to guarantee a better indoor air quality and a protection from dust of the air conditioning components for a longer duration of the systems.

The air contains a large number of particles of very different size. Particles can have different origins (biological, pollution etc.) with diameters that vary from submicron to hundreds of micrometers. The total amount of particles in a cubic meter of air can vary depending on the location: in high density cities this value can be estimated between 0.10 and 0.15 mg/m^3, it increases in industrial zones where the pollution sources are higher, and decreases in countryside zones.

The main filter function is to remove the particles from the air and this performance is measured by standardised procedures [EN 779:2002] and translated into filtration classes. Two filter characteristics can be defined: the efficiency and the arrestance. The efficiency describes how well an air filter removes microscopic particles such as dust, dust mites, pollen, mold, bacteria, and smoke. The arrestance describes how well an air filter removes larger particles such as dirt, lint, hair, and dust. The efficiency and arrestance are measured in standard conditions in correspondence of an airflow rate specified by the manufacturer or at 0.944 m^3/s (3 400 m^3/h) if the manufacturer does not specify it, using a standard contaminant dust composition[1].

Nine filter classes exist following the efficiency or arrestance and the method used for the determination is different for the two parameters. The class characteristics are summarized in Table 6. Classification of "*F*" filters is based on performance with respect to 0,4 µm particles. Filters found to have an average efficiency value of less then 40 % will be allocated to group "*G*" and the efficiency reported as "<40 %". The classification on "*G*" filters is based on their average arrestance with the loading dust.

[1] The standard synthetic arrestance dust used in the experiment meets specifications set forth in ASHRAE 52.1. The compounded dust consists by weight of:

- 72 % of standardized air cleaner test dust. It is predominantly silica and has a mass-mean diameter of approximately 7.7 µm.
- 23 % of powdered carbon
- 5 % of cotton linter

Table 6: Filter class characteristics

Filter class	Final Pressure Drop (Pa)	Average arrestance (A_m) of synthetic dust %	Average efficiency (E_m) of 0,4 μm particles
G1	250	$A_m < 65$	-
G2	250	$65 \leq A_m < 80$	-
G3	250	$80 \leq A_m < 90$	-
G4	250	$90 \leq A_m$	-
F5	450	-	$40 \leq E_m < 60$
F6	450	-	$60 \leq E_m < 80$
F7	450	-	$80 \leq E_m < 90$
F8	450	-	$90 \leq E_m < 95$
F9	450	-	$95 \leq E_m$

Usually, filters used in room air conditioners and split-systems are coarse filters of low efficiency of classes from *G2* to *G4*. In our case we considered the split systems equipped with a *G2* class filter.

Initial resistance of these filters varies following the air speed, the media used and the thickness of the filters. Media such as fibreglass, polyester or foam are most used. The average values obtained from manufacturers catalogues attest that initial resistance could be considered as 20 Pa at 1.5 m/s air speed for such filters.

More recent room air conditioners can contain several types of filters with different functions (dust removing, deodorizing, anti mould etc.) since the filtration aspect become more and more an issue important for marketing. In all the systems however, an air-filter is present, with the primary function to catch coarse dust. The air filters used for this type of air conditioners are plate filter of arrestance of *G2-G4* class according to the standard**.**

The evaporator filter fouling leads as first consequence to the increase of the pressure drop at the evaporator that leads to a reduction of the air flow following the fan characteristic curve (Figure 13). The lower airflow reduces the heat exchange at the evaporator while reducing the capacity of the system. Because of the pressure difference is lower the compression power is lower. The global effect is a decrease of the *EER*. The split unit capacity being reduced, the system has to work longer to supply the cooling energy demanded.

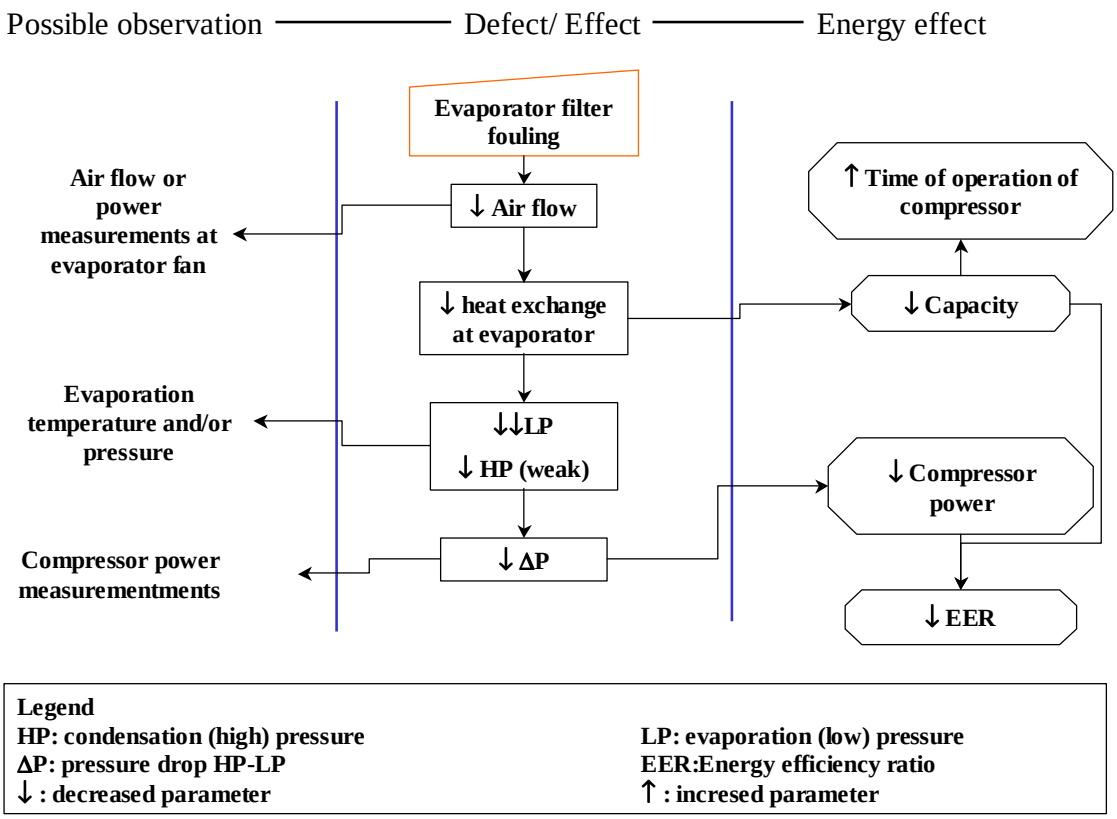

Figure 13: Tree representation of evaporator filter fouling consequences and possible measurement parameters

Calculation of pressure drop at the evaporator in ORNL model

The reference pressure drop at the evaporator airside estimated by the ORNL model is very low (of the order of 40 Pa). We decided then to estimate separately the pressure drop in order to correct it by the use of multiplier available in the program that the designers added to take into account the uncertainty about the correlation used for the pressure drop calculations. Moreover the ORNL model does not allow modelling the fan through its characteristic. For non-rating points we had to introduce manually the parameters of the fan: the airflow, the pressure drop corrected through the multiplier, the fan efficiency and the efficiency of the motor. The fan efficiency varies but we could not find data about its evolution, we built the fan characteristic from manufacturer's catalogue curve. The power decreases generally with the airflow for centrifugal fans; from some manufacturers catalogue values, the global power decreases for an airflow decrease by -20 % between -5 and -25 %. We considered this variation negligible compared with the overall consumption of the system: -10 to -25 W for an overall (compressor plus fans) electric consumption of 3.3 kW at rating conditions. This leads to an overestimation of the absorbed power by -1 %.

The fan works at constant speed, determining a constant motor efficiency.

Once we have determined the rated characteristic of the evaporator fan operation, we introduce a model allowing us to represent filter fouling through the pressure drop increase and compute the new points of fouled operation.

The pressure drop at the evaporator airside for the base case can be estimated by the correlations with the geometrical parameters of the heat exchanger (same parameter of Figure 9). It can be considered as the sum of the filter resistance and the pressure drop across the evaporator heat exchanger.

The last pressure drop, based on the cross area A_c and the total area A_{tot}, can be evaluated as:

$$\Delta p = f \frac{A_{tot}}{A_c} \cdot \frac{G^2}{2\rho} \qquad [18]$$

Where the parameters are the same defined in the formula [1].

The cross area and the total area are:

$$A_{tot} = A_{fin} + A_{tube} \quad [19]$$

$$A_{fin} = 2N_F \cdot (L_{exch} . W_{exch} - \pi D_{t\_ext}^{\ 2} N_T / 4) \quad [20]$$

$$A_{tube} = \pi D_{t\_ext} \cdot N_T \, (H_{ech} - t_f \cdot N_F) \quad [21]$$

$$A_c = (P_l - D_c) \cdot (h_f - t_f) \, N_f \cdot N_{TR} \quad [22]$$

With N_F the number of fins, N_T the tubes number of the heat exchanger and N_{TR} the tubes number per row.

D_c, collar diameter, is calculated as: $D_c = D_{t\_ext} + 2\, t_f$.

The friction factor *f*, following the correlation proposed by Wang et al. [Wang 1996b] for louvered fins, can be calculated:

$$f = 2.486 \cdot Re_{Dc}^{-0.461} \left(\frac{A_{fin}}{A_{tot}}\right)^{-0.06} \left(\frac{h_f}{D_c}\right)^{-0.0798} \quad [23]$$

Re_{Dc} the Reynolds number based on the collar diameter defined as:

$$Re_{Dc} = \frac{D_c \, G}{\nu} \quad [24]$$

The table summarizes the pressure drops calculated at the rating point.

Table 7: Pressure drop at condenser comparison between Mark V and Wang correlation

	Mark V	Wang et al.
ΔP (Pa)	40	67.3

The Wang correlation describes cases respecting the conditions:

$1.27 < h_f < 2.54$

$2 < N < 4$

Our exchanger has the following values: h_f=1.8 and N=2.

We have to add to the heat exchanger calculated pressure drop the initial pressure drop for the filter. The considered filter is a *G2* class filter so that following the value observed for this type of filters on the manufacturers catalogues, we have estimated the initial pressure drop as 20 Pa.

Like in the case of condenser fouling we can define the curve of operation of the fan and the modified points of operations due to the filter fouling.

The fan characteristic has been calculated from the known rating point (red dot in the figure below) and applying a similarity with catalogues curves for similar fans. The motor characteristic is assumed constant.

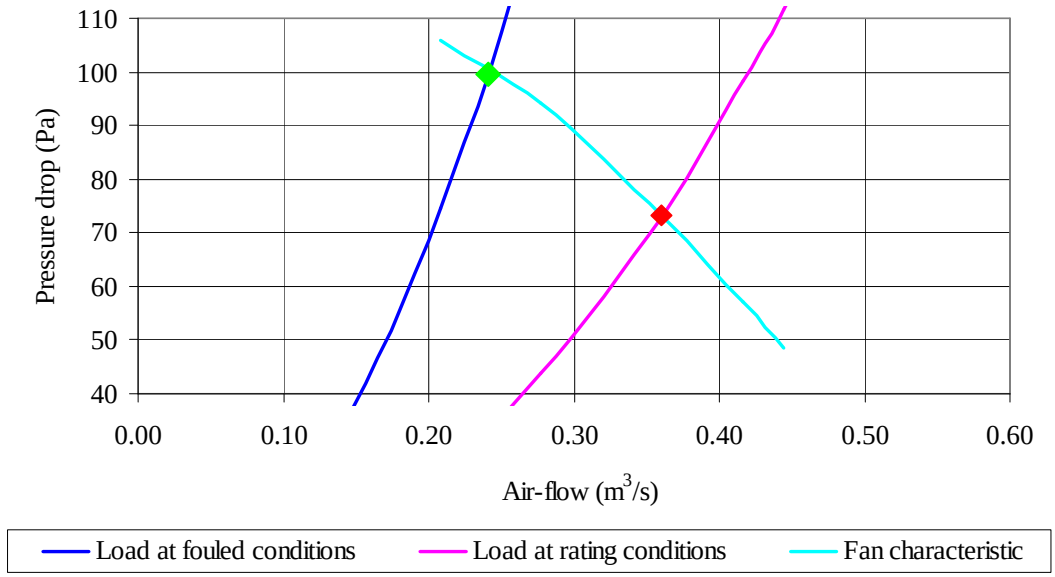

Figure 14: Fan characteristic and pressure drop for rating and fouled conditions at the evaporator

The level of evaporator filter fouling is simulated by reducing the airflow rate across the evaporator, initially set at 1 269 m^3/h. The limit for fouling could be the limit pressure drop stated at 250 Pa in the manufacturers recommendations, but these are meant for low efficiency filter used as pre-filters in the air handling units where the fans have a large range of airflows and the pressure drop of the pre-filter is low compared to the global pressure drop of the network. In small air conditioners, the filter is an important part of the pressure drop of the fan, and the range of operation of the fans used in the indoor units is smaller. As we will see later, the limit will be decided by the simulation convergence limit.

As an initial value for the limit the 250 Pa is kept. Several tests of the model gave the values in the table and the multiplier required by the ORNL model that allows correcting the pressure drop calculation to obtain the actual pressure drop for several fouling level.

Table 8: Evaporator fan operating points for fouled conditions

Pressure drop across the filter at rated airflow (Pa)	Pressure drop at rated point (Pa)	Operating Airflow (m^3/s)	Operating Pressure Drop (Pa)	Pressure Drop Multiplier
20	87	0.36	90	5
66	133	0.32	101	8.0
112	179	0.29	108	11.5
158	224	0.26	113	14.2
204	270	0.25	117	17.2
250	315	0.23	119	20.3

We can observe that the pressure drop increases and the airflow decreases of the quantities in table below.

Table 9: Evaporator fan airflow and pressure drop rates for fouled conditions

Pressure drop across the filter at rated airflow (Pa)	Airflow (%) Rated Airflow	Pressure drop (%) Rated pressure drop
20	0%	0%
66	-11%	13%
112	-20%	21%
158	-26%	26%
204	-32%	30%
250	-36%	33%

The fan consumption has been considered constant in the Mark V fan model.

2.4.4 Additional pressure drop in the liquid line

A liquid-line restriction can be caused by the accumulation of debris in the expansion device. Debris can come for example as result of a poor welding. The liquid line restriction leads the refrigerant to expand before the valve (also named pre-expansion) and to enter in the evaporator at lower temperature and higher quality, the circulating refrigerant flow being reduced and the cooling capacity subsequently. The pressure difference between the low and high side of the cycle is increased thus increasing the absorbed power.

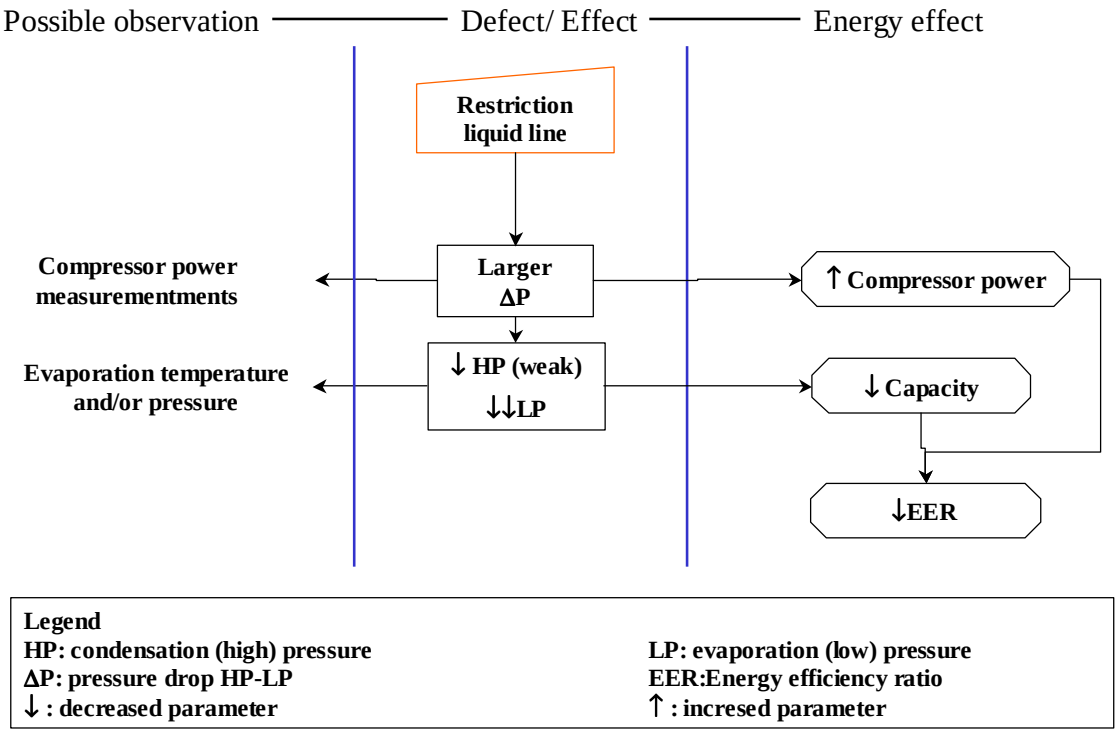

Figure 15: Tree representation of restriction in the liquid line consequences and possible measurement parameters

The ORNL calculation for additional pressure drop in the liquid line

This fault is simulated by an additional pressure drop in the liquid line through the ORNL coefficient added for this purpose in the input file. The pressure drop is represented as a % of the total pressure difference between the high and low pressure at rating conditions for the base case. We varied the value from zero to 30 %.

2.4.5 Compressor efficiency reduction

The compressor is very sensitive to maintenance and lubrication and can be very sensitive to the operation conditions. The most sensitive parts of the reciprocating compressors are the valves that wear quickly.

The presence of other defects of operation can induce the compressor to work at higher pressures and temperatures and to stop before the detection of the real problem. The compressor is then one of the most sensitive components of the system and its failure is often a symptom for other defects.

From the discussion with manufacturers, the compressor failure can be due mainly to bad lubrication or when extreme operation conditions change the oil composition: the oil is burnt in correspondence of the higher temperature zones (especially outlet valve) and separates in smaller molecules that deposit on the components, reducing the lubrication and the sealing and then reduce the volumetric efficiency of the compressor until a quick failure. During this damaged operation the valves do not guarantee anymore the compressor sealing: the high pressure refrigerant in the compressor cylinder

leaks back into the suction line across the suction valve, or the discharged gas leaks back into the cylinder across the discharge valve. This leakage across the compressor valves generates the reduction of the compressor volumetric efficiency.

The reduction of the recirculation of the refrigerant flow in the compressor reduces in turn the circulating refrigerant in the system and its capacity. The absorbed power is constant and the global efficiency reduced.

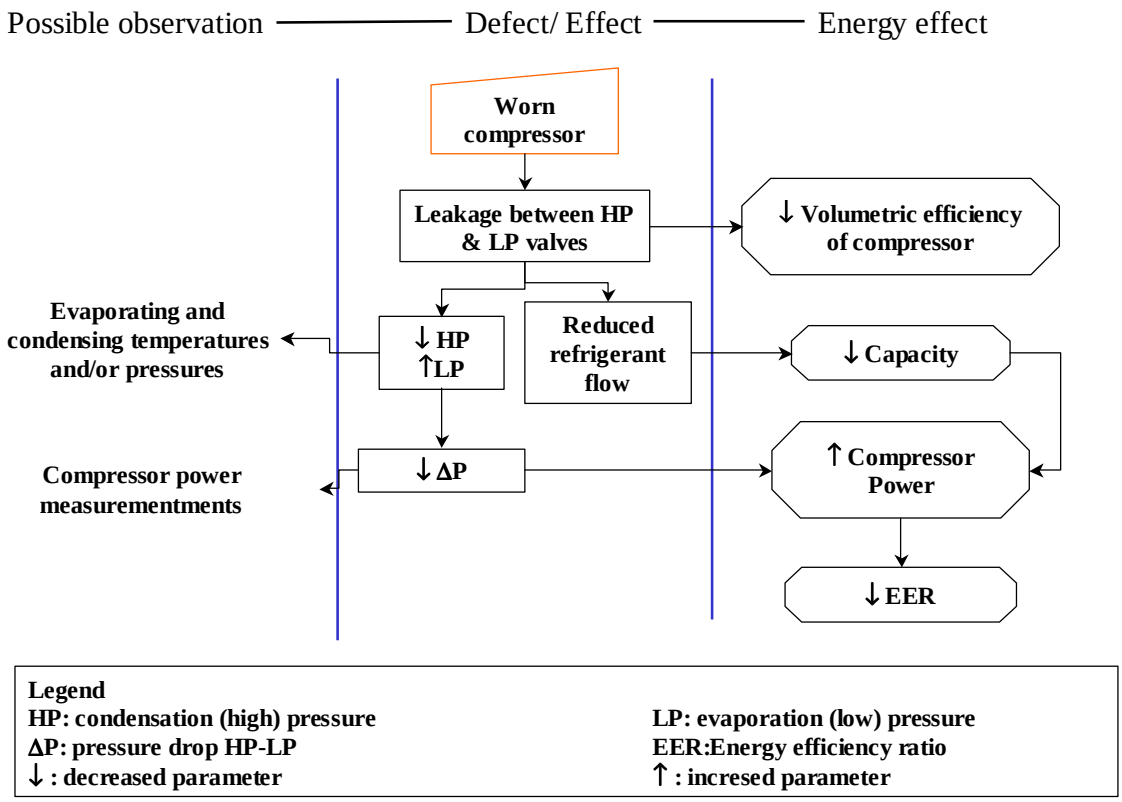

Figure 16: Tree representation of compressor wearing consequences and possible measurement parameters

Compressor characterisation by ORNL

The ORNL model allows introducing the compressor performances based on a map fitting. Once the compressor performance data are available in tabular form, a short computer program is provided that uses a least squares algorithm to compute a six-term polynomial equation similar for both mass flow rate and power consumption. The defect has been introduced by lowering the mass flow rate data and obtaining a new degradated volumetric efficiency curve.

The compressor valve leakage has been simulated by reducing the compressor volumetric efficiency, more precisely by lowering the curve of the volumetric efficiency from 0.0 % to 34.4 %.

2.5 Degradated behaviour at maximum load and fixed conditions

The simulation campaign with Mark V is developed simulating several fixed temperature conditions. The behaviour of the degradated split has been defined for different indoor and outdoor air conditions:

T1: 35 °C condenser inlet, and 27 °C evaporator inlet

T2: 27 °C condenser inlet, and 21 °C evaporator inlet

T12: 35 °C condenser inlet, and 21 °C evaporator inlet

T21: 27 °C condenser inlet, and 27 °C evaporator inlet

The *T1* and *T2* correspond to the standard test conditions [EN 14511], *T1* tested values are displayed by manufacturers; *T12* and *T21* are a combination of the *T1* and *T2* conditions.

2.5.1 Mark V results for refrigerant leaks

The **undercharged** system begins to show large degradation of performances only for values higher than 10 %, this can be due to an intentional overcharge of the system by the manufacturer in prevision of the unavoidable leaks that occurs during operation. This is confirmed by the charge calculation performed by the programme for which the optimal calculated charge is 2.4 kg versus the 2.8 kg from the manufacturer, 15 % less.

In Figure 17, we represent the refrigerant thermodynamic cycle in a pressure-enthalpy plan for the reference case (1-2-3-4) and undercharged system (1'-2'-3'-4') in order to highlight the cycle modifications: the condensing pressure is lowered, the subcooling reduced (tends to zero), the superheating increased.

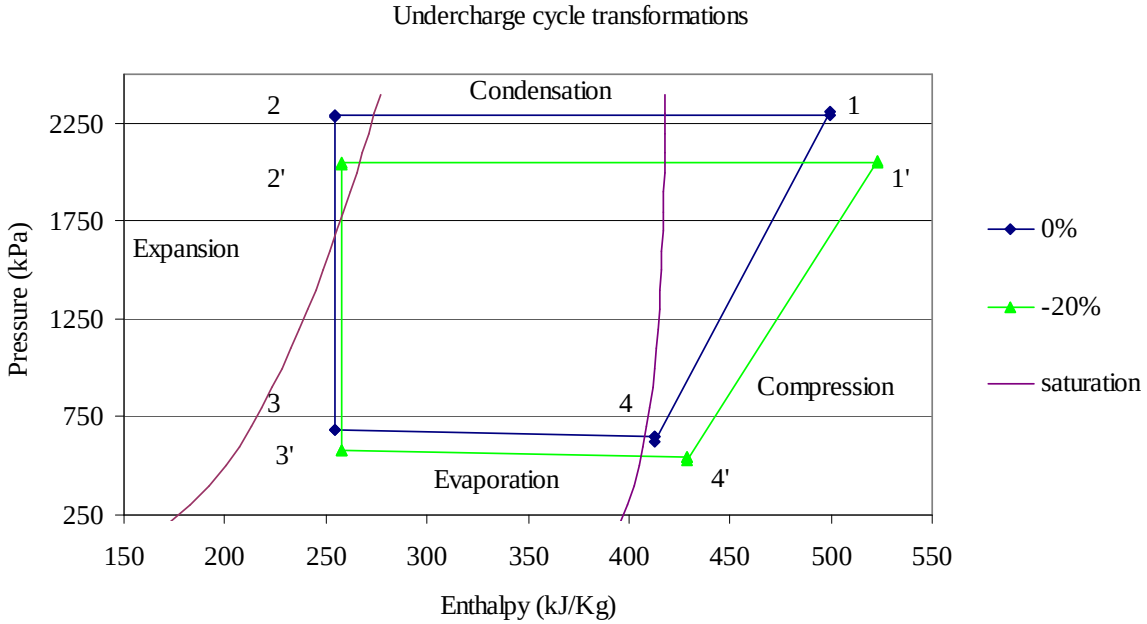

Figure 17: Thermodynamic R22 cycle modification for undercharged system

The lack of refrigerant brings a reduction of the system capacity but at the same time a reduction of the power absorbed at the compressor: the global effect is anyway a reduction of the *EER* (Figure 18).

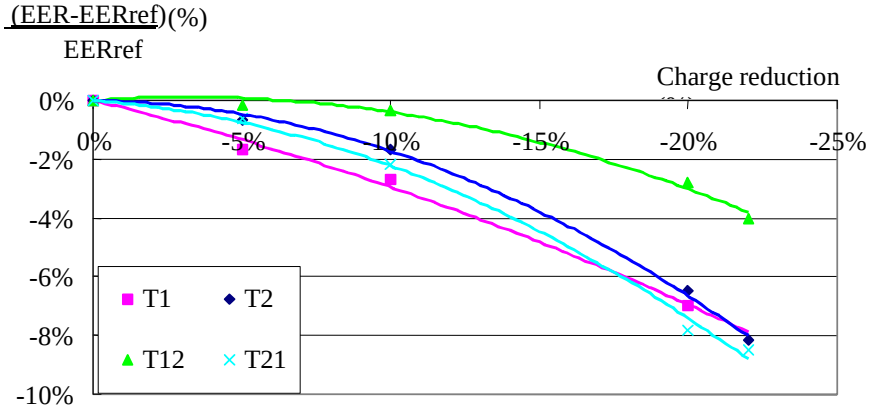

Figure 18: Effect of the lack of refrigerant on the EER.

Moreover, the reduced evaporation temperature increases the latent removal, reducing the amount of cooling energy dedicated for the air temperature lowering.

The sensible to total heat transfer ratio (*SR*) indicates the amount of the cooling power that is devoted to lower the air temperature (P_{c_s}) on the total cooling power (P_{c_t}):

$$SR=\frac{P_{c\_s}}{P_{c\_t}}=\frac{P_{c\_s}}{P_{c\_s}+P_{c\_l}} \quad [25]$$

P_{c_l} is the amount of the power that is used to condense the humidity of the air.

The *SR* is decreasing with increasing refrigerant losses (Figure 19) with a lowered evaporating temperature.

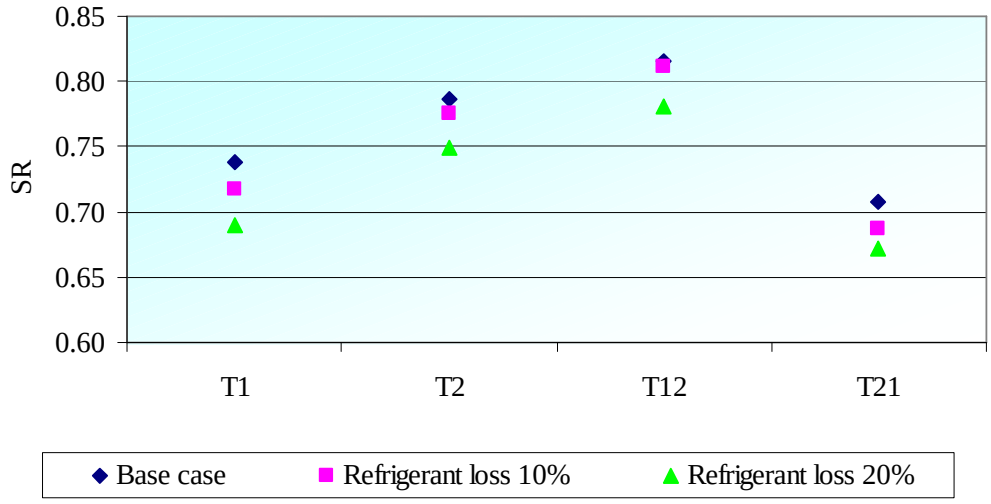

Figure 19: Sensible to total heat transfer ratio for the base case and for refrigerant leaks

This means that not only cooling capacity is decreased, but it is also degradated in the sense that it is used more and more to dehumidify the air and less and less to cool the air: the system will have to operate longer than before in order to reach the temperature setpoint.

Hitherto we did not approach the diagnosis aspect of the defect. If we look at the figure below we can observe the effect of the reduced charge on the main parameters of the systems (pressures, temperatures, energy). The blue values show that the defect increases the parameter shown, the pink value that it decreases it. Refrigerant leak increases significantly superheat that is more than doubled for 20 % of refrigerant loss. Also the air temperature at the evaporator exit is a good indicator, showing important increase. The last can be moreover a source of discomfort because of the feeling of cold air by occupants close to the evaporator.

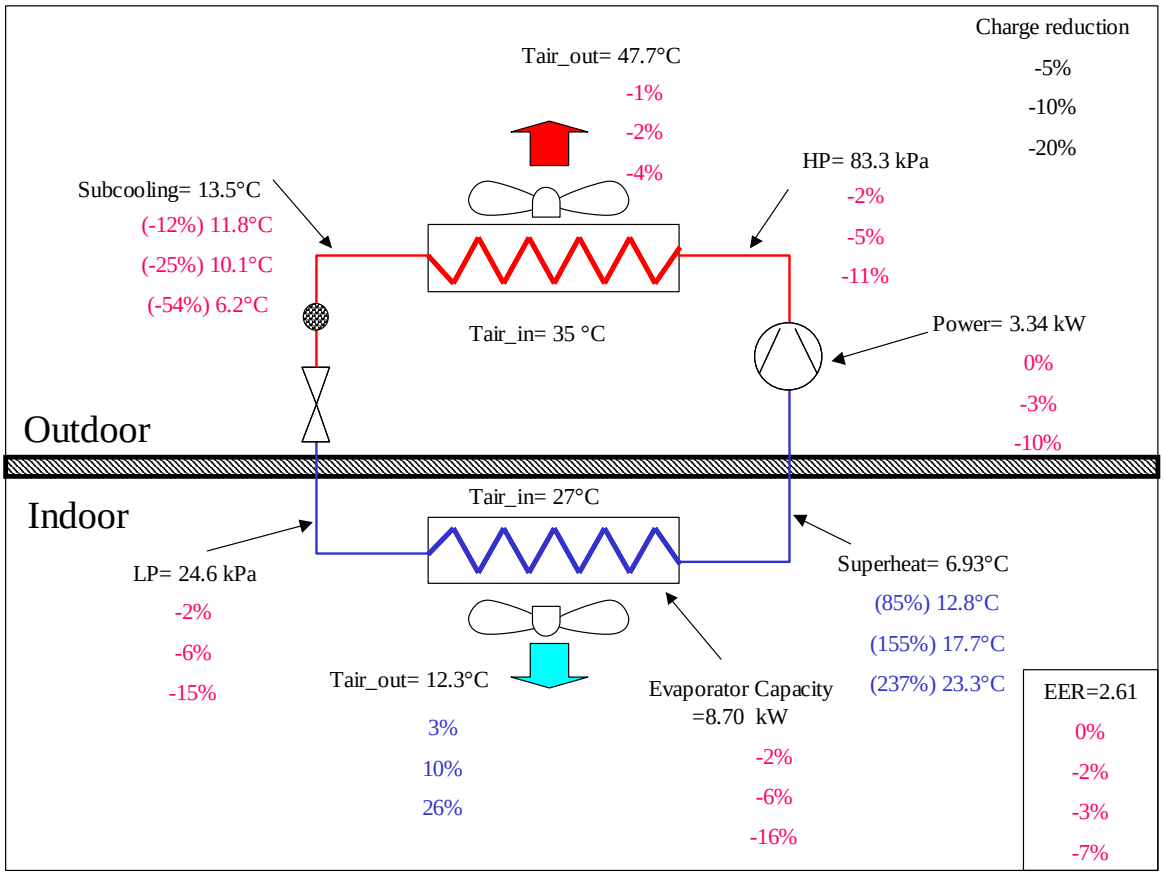

Figure 20: Effect of the lack of refrigerant on the split main parameters at 35 °C outdoor and 27 °C indoor

Measurement techniques for refrigerant leaks are numerous and well developed due to the regulations about refrigerant leaks control and include among others the use of halide torch, soap solutions or electronic detectors. Moreover, the charge losses can be detected by a superheat measurement jointly with a high and low pressures measurement.

Superheat can be easier measured than subcooling in a split system measuring by measuring the low pressure (and obtaining the evaporating temperatures from fluid tables) and the surface temperature at the outdoor unit inlet.

2.5.2 Mark V results for fouled condenser

C**ondenser fouling** shows an important effect on efficiency: capacity is reduced while the absorbed power is increased in a stronger manner than the capacity reduction. The high pressure is increased, while the low pressure remains constant.

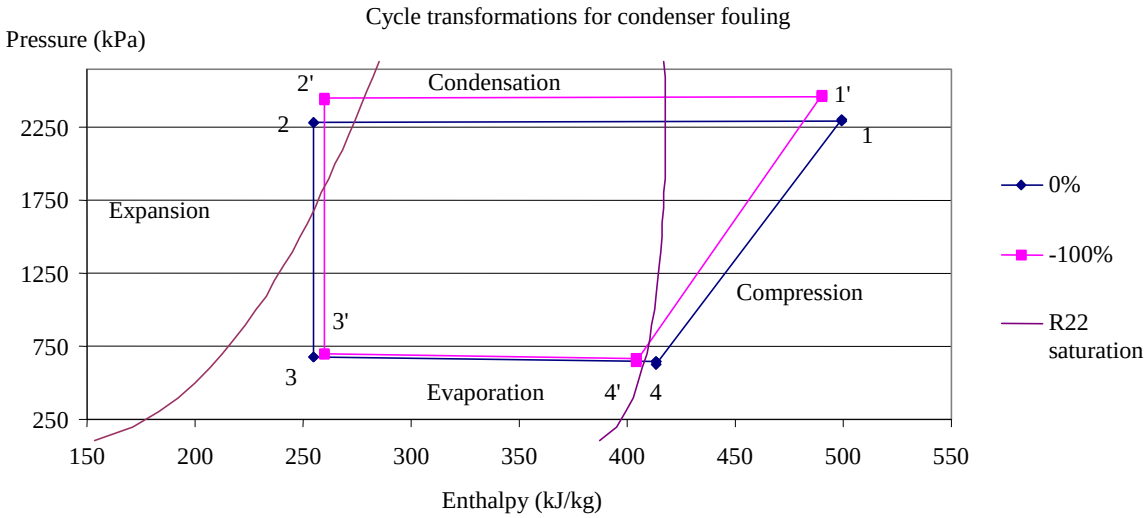

Figure 21: Thermodynamic R22 cycle modification for increased pressure drop at condenser

It should be noted that actually decreasing the heat exchange coefficient at the condenser increases the condensing pressure and the temperature at the outlet of the compressor until a point where the compressor stops due to the thermal protection intervention. The indoor and outdoor conditions do not influence the loss of performance. The *EER* is penalised in the same amount for the *T2*, *T21*, *T12* conditions, but more seriously for *T1* conditions.

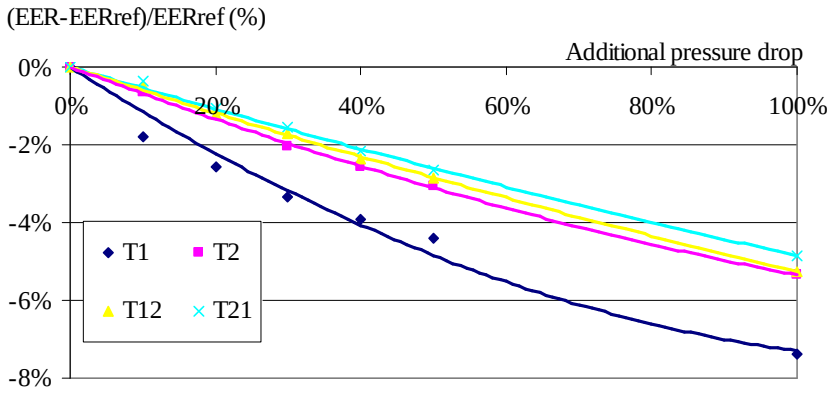

Figure 22: Effect of the condenser fouling on the EER.

On the detection side, the main parameters influenced by the condenser fouling are superheat (strongly reduced), increased compressor power, condensing pressure and the air temperature at the condenser outlet.

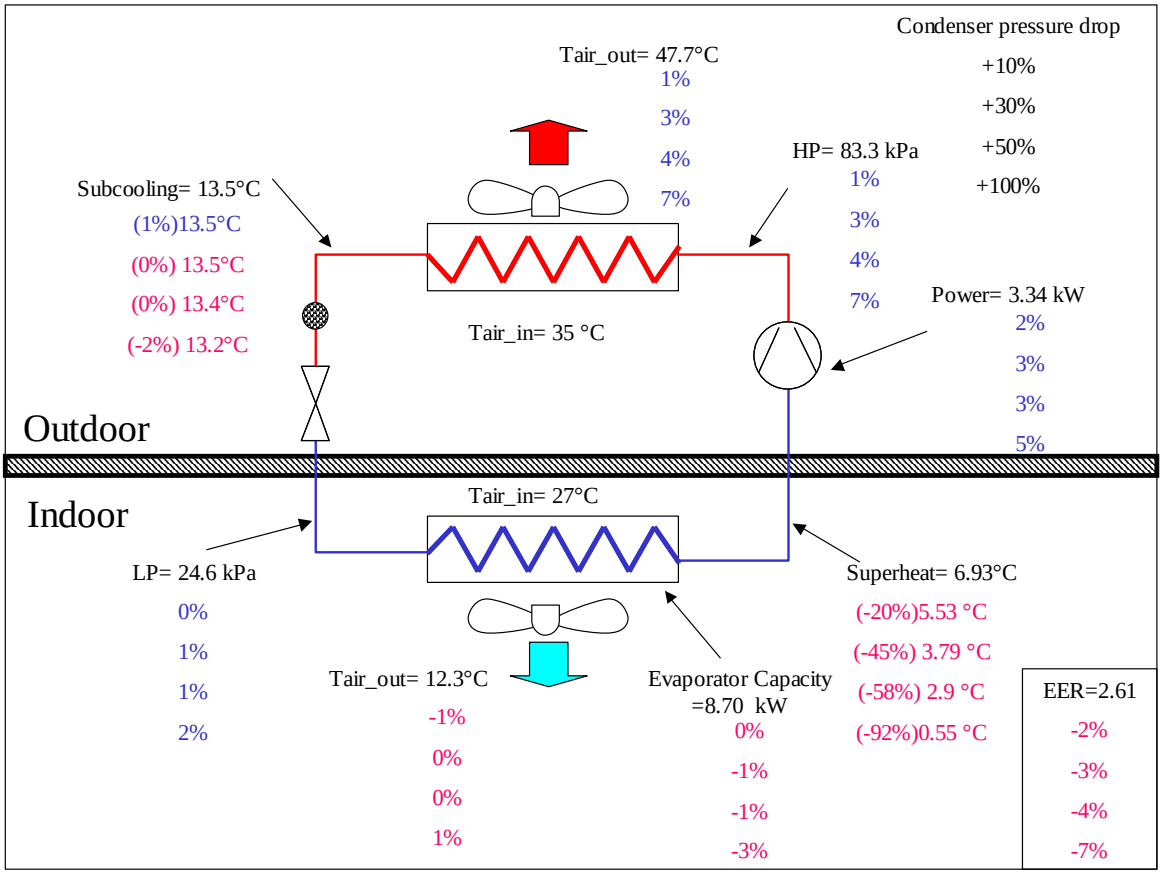

Figure 23: Effect of the condenser fouling on the split main parameters at 35 °C outdoor and 27 °C indoor

One parameter that can be also used as a measurement is the airflow at the condenser fan. We developed a short measurement technique in order to follow the evolution of condenser fouling.

Initially we intended to use the power measurements of the fan, but the in situ measurements of the fan power are difficult because the fan input cable is not easily accessible, all the input cable being linked in a single set with the others. At the fan, airflow and pressure vary by the same amount, the fan characteristic being quite linear for axial fans. But while pressure measurements are quite difficult, we were able to perform airflow speed measurements with a hot wire gauge in order to measure the airflow. We measured the velocities profile of the fan on several points on the x-y axis of the fan, we obtained two different profiles that fit by a bi-quadratic law.

$$\frac{V}{V_{max}}\left(\frac{D}{D_{max}}\right)=a\left(\frac{D}{D_{max}}\right)^4+b\left(\frac{D}{D_{max}}\right)^3+c\left(\frac{D}{D_{max}}\right)^2+d\left(\frac{D}{D_{max}}\right)+e \qquad [26]$$

The global profile results from the fit of the two "*x*" and "*y*" profiles by the shape of Figure 24. The axes have been referred to the fan radius.

Because of the symmetry of the measured curves, the condition:

$$\frac{V}{V_{max}}\left(\frac{D}{D_{max}}\right)=\frac{V}{V_{max}}\left(-\frac{D}{D_{max}}\right) \qquad [27]$$

Leads to consider the coefficients *b* and *c* zero.

$$\frac{V}{V_{max}}\left(\frac{D}{D_{max}}\right)=a\left(\frac{D}{D_{max}}\right)^4+c\left(\frac{D}{D_{max}}\right)^2+e \qquad [28]$$

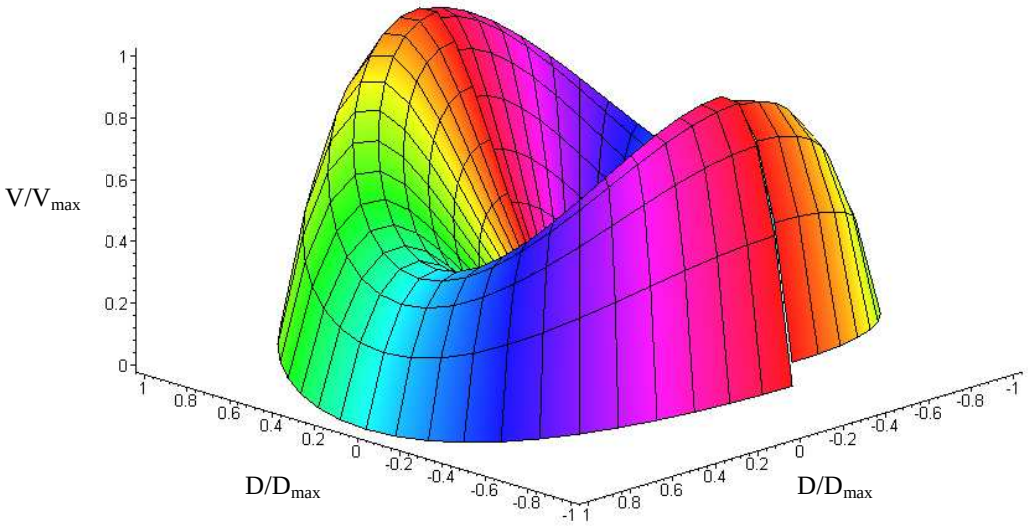

Figure 24: Normalised condenser fan airflow velocity profile

It is important to underline that the simple hot wire gauge measures the intensity of the velocity and not its direction, then the profile does not correspond to the real shape of the airflow (in that case we could observe an expansion of the airflow). The profile is not the same on the two axes because of the rectangular shape of the inlet that allows higher velocities on the horizontal axis "*x*" than on the vertical. From the velocity profile we were able to calculate the total airflow, integrating on the surface of the outlet.

In an audit procedure, we simplified the number of measurements that an auditor can do in order to quantify the airflow modifications. We decide then to specify three points of measurement corresponding to the maximum velocity on the two axes and to the velocity in the centre of the fan. The speed at the centre is different from zero because the point corresponds to a certain distance from the fan (velocities measured after the protection grill) where the profile is developed enough to be different from zero.

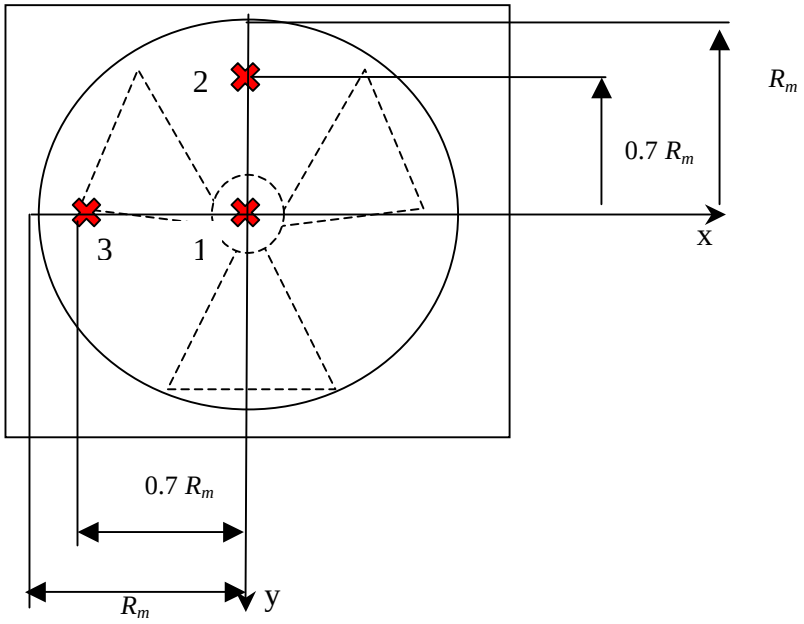

Figure 25: Points of measurements for airflow measurements at the condenser

We approximated the velocity at the extreme of the profile as the velocity at centre. The three points are enough to define the bi-quadratic laws of the profile and to calculate the crossing airflow with the conditions:

$$\frac{V}{V_{max}}(0.7)=1$$

$$\frac{V}{V_{max}}(-0.7)=1$$

$$\frac{V}{V_{max}}(0)=\frac{V}{V_{max}}(1)$$

2.5.3 Mark V results for fouled filter

The **filter fouling** reduces the airflow that crosses the evaporator and consequently the heat exchange, reducing thus the capacity of the system and reducing the evaporation pressure. The condensing and evaporating pressure differences remain constant but since compression from a lower pressure the work demanded to the compressor is lowered and so the absorbed power. The subcooling remains quite constant while the superheat strongly decreases (Figure 26).

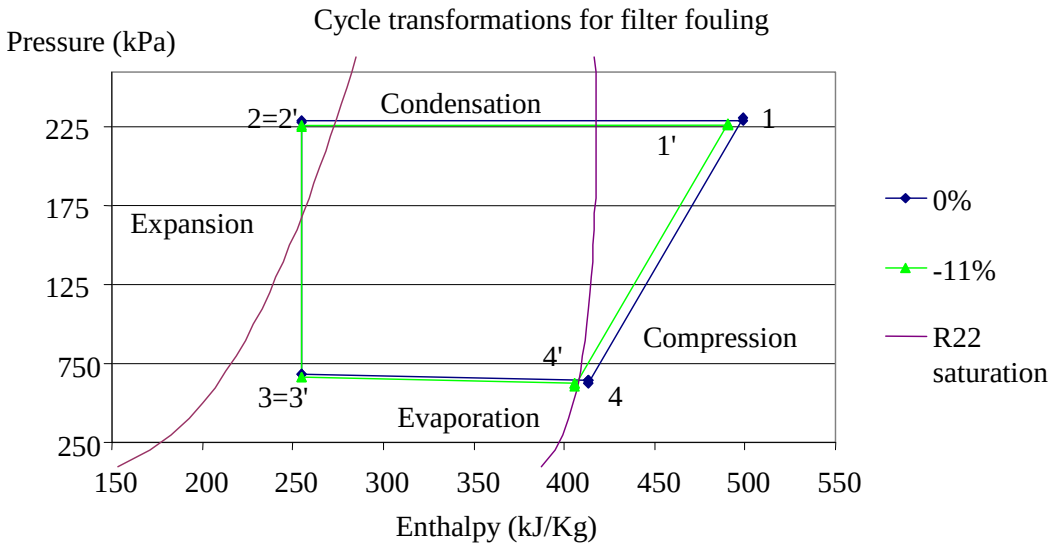

Figure 26: Thermodynamic R22 cycle modification for reduced airflow at evaporator

The global effect is a global reduction of efficiency that remains in most cases small: in all simulated conditions the worst efficiency reduction was -3.5 % for *T1* conditions (Figure 27).

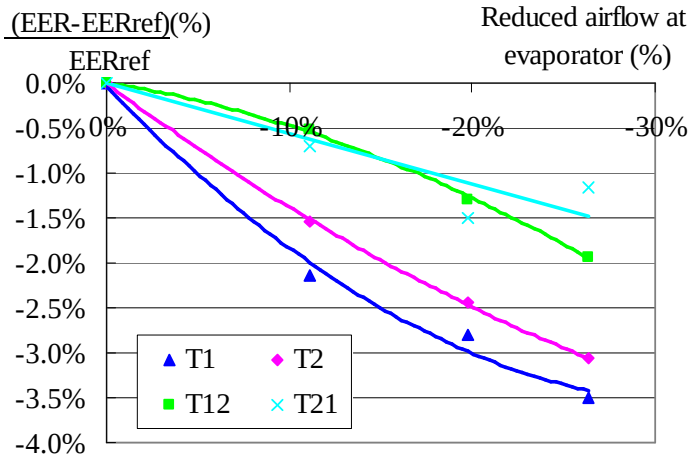

Figure 27: Effect of the filter fouling on the EER.

Filter fouling, although not having strong impact on the efficiency, leads to a decrease of the superheat that can be very dangerous for the compressor: the superheat becomes smaller and for the lowest airflow it becomes zero in most of the simulated conditions. Some liquid enters then in the compressor that can fail early.

Moreover the reduced airflow leads to a reduction of the evaporator temperatures increasing the latent part of the heat transfer used to condensate air moisture. The evaporation temperature decreases until the condensed water forms an ice layer on the heat exchanger: this reduces strongly the efficiency of the split. In conditions studied refrigerant evaporation temperature became of 1.5 °C in the worst case (27 °C-21 °C).

The sensible to total heat transfer ratio *SR* defined in equation [25] decreases with the reduced airflow in the evaporator (Figure 30).

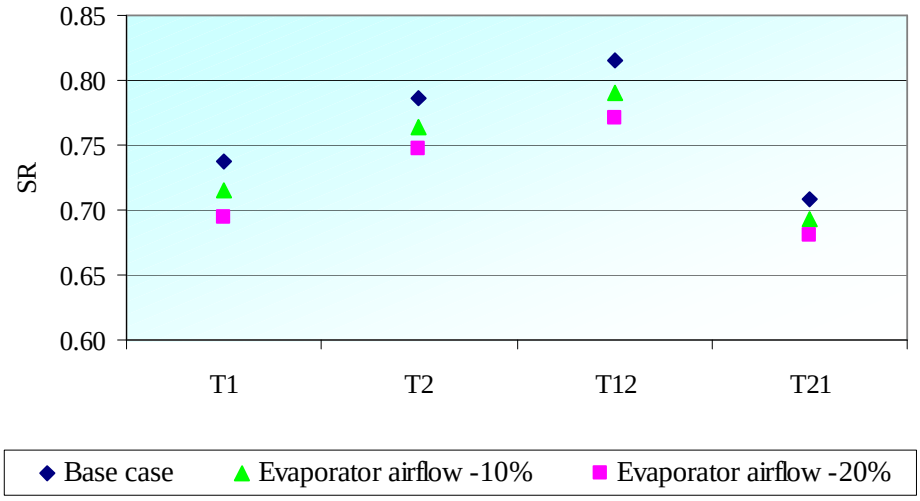

Figure 28: Sensible to total heat transfer ratio for the base case and for fouled filter conditions

The reduction of the airflow at the evaporator due to filter fouling leads to a decrease in the supplied air temperature that can be source of discomfort when an occupant is in the proximity of the unit (feeling of too cold airflow).

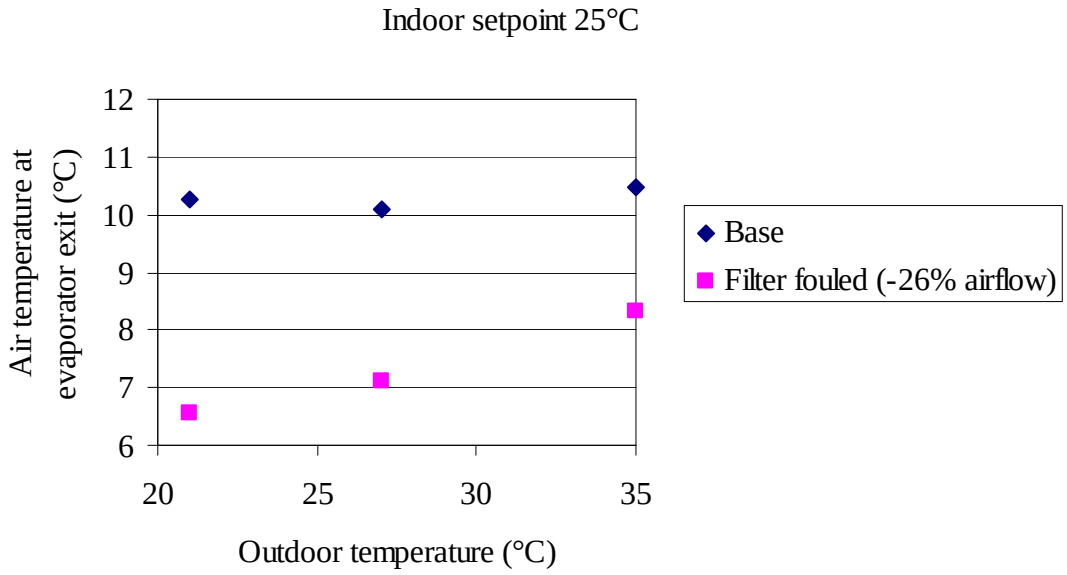

Figure 29: Air temperature at the evaporator exit with clean and fouled filter.

As already noted in the case of the refrigerant leaks, here cooling capacity is also lowered but devoted more to dehumidifying the air than to lower its temperature: the system will work longer than in the base case.

For filter fouling all the parameter are decreased: the superheat is a good indicator plus the pressure measurements.

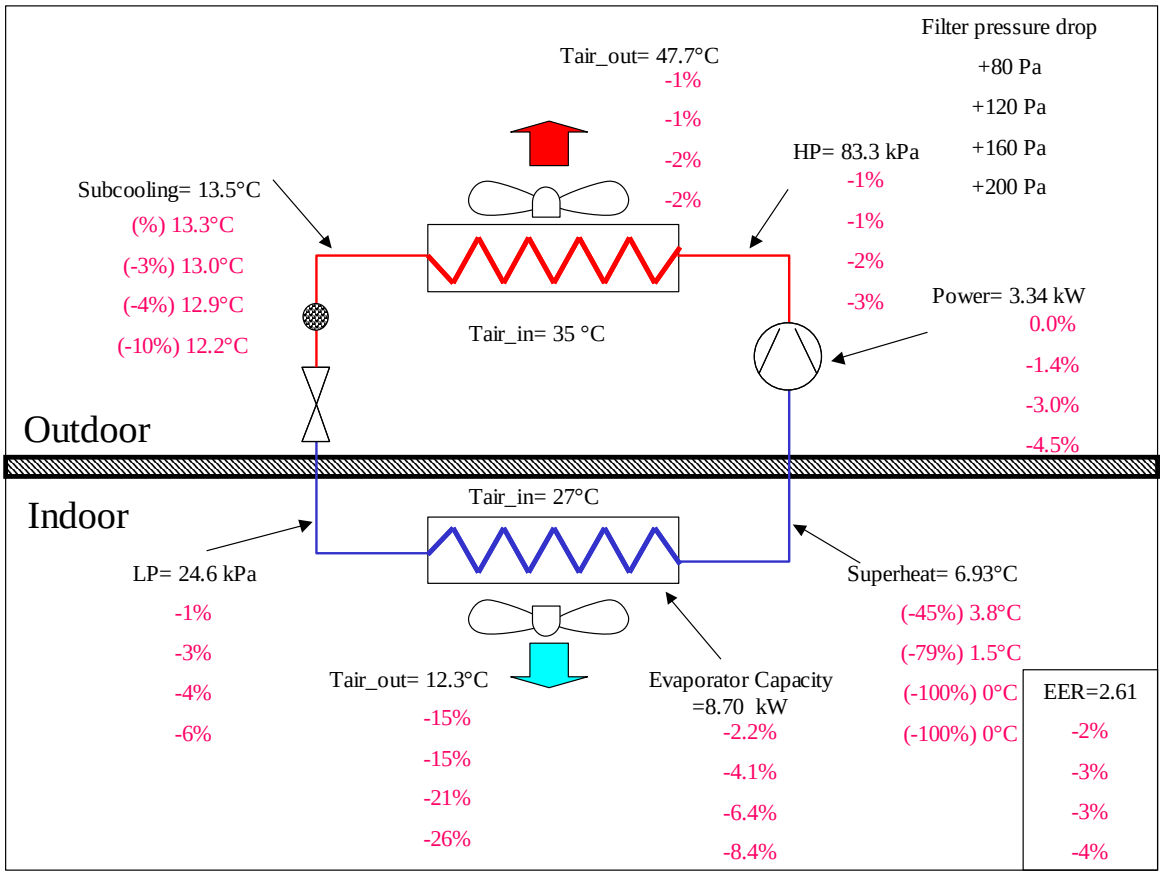

Figure 30: Effect of the filter fouling on the split main parameters at 35 °C outdoor and 27 °C indoor.

The filter can be inspected visually in order to observe its level of fouling.

2.5.4 Mark V results for worn compressor

The reduction of the compressor volumetric efficiency leads to a decrease of both high and low pressures and to a lower superheat.

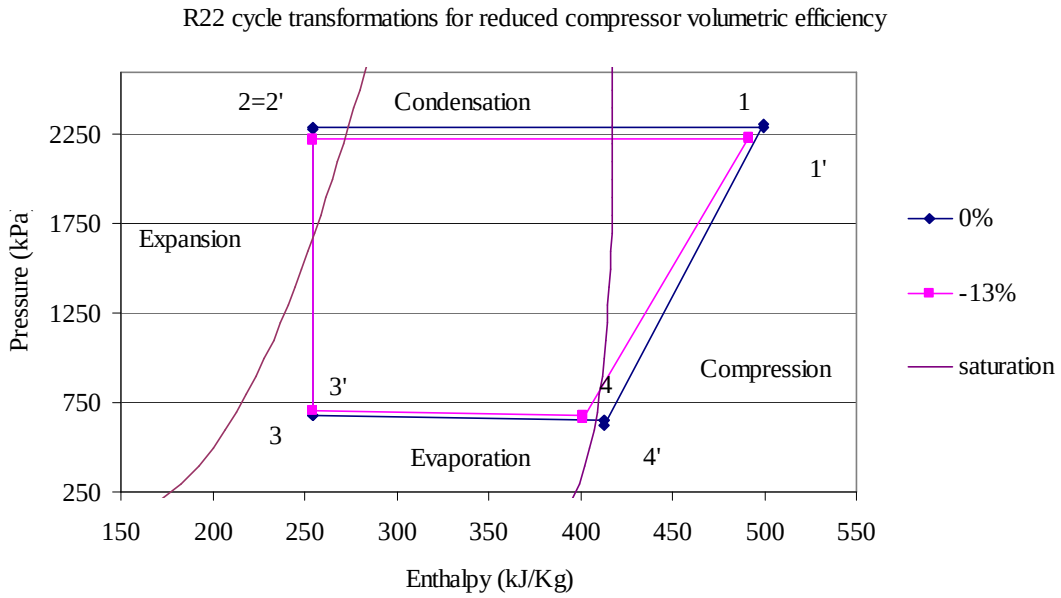

Figure 31: Thermodynamic R22 cycle modification for reduced compressor volumetric efficiency.

The reduction of the compressor volumetric efficiency shows a linear reduction in efficiency (Figure 32), mainly due to a strong reduction of the system capacity, the absorbed power being quite constant. The indoor and outdoor conditions have a small influence on performance.

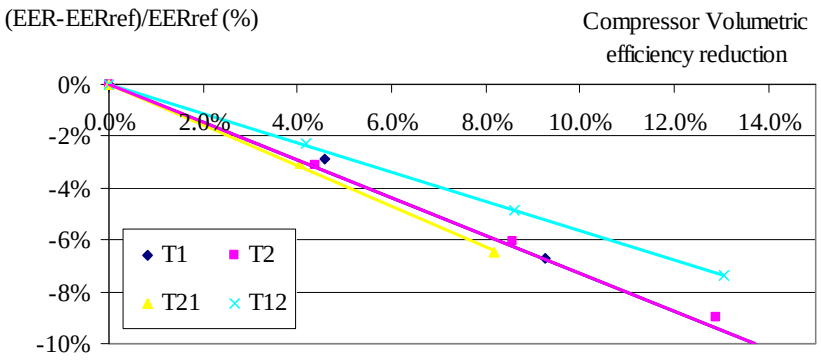

Figure 32: Effect of reduction of the compressor volumetric efficiency on the EER

The split parameters changes are shown in Figure 33.

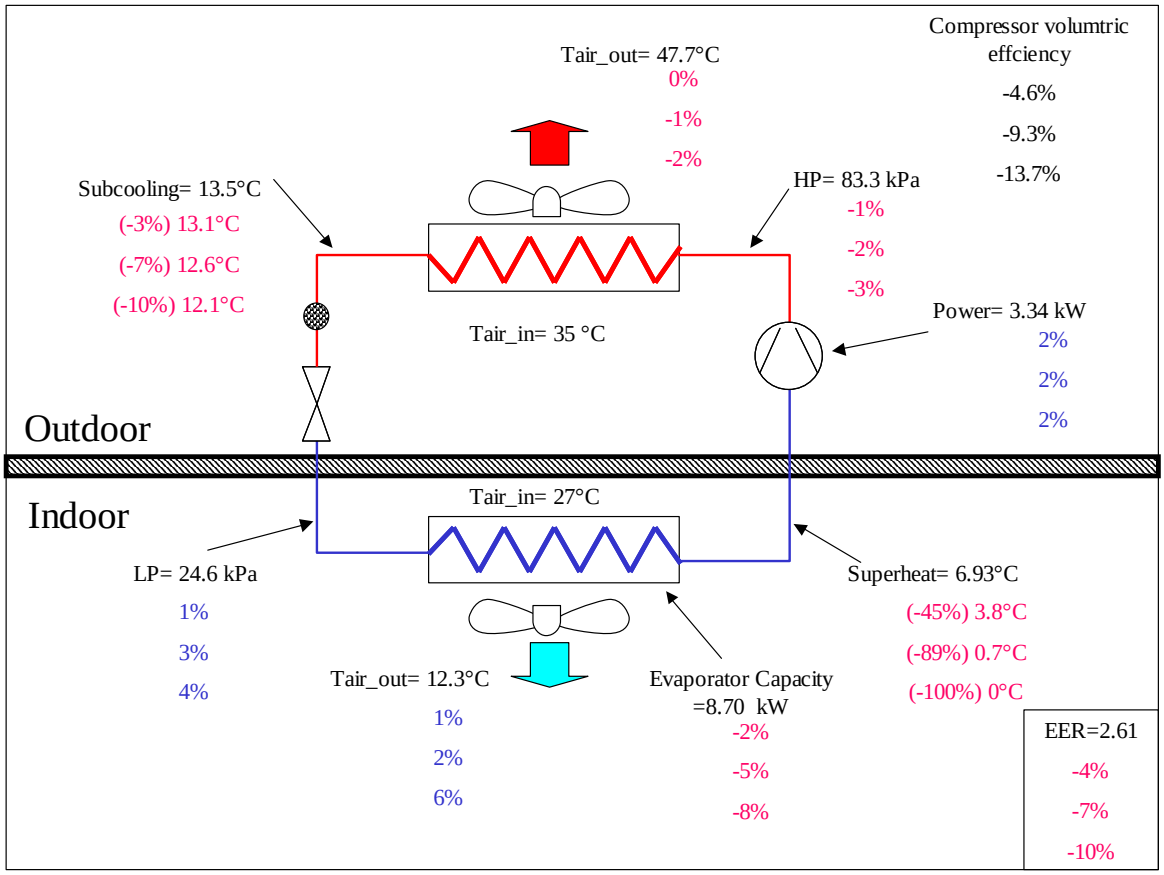

Figure 33: Effect of the compressor efficiency reduction on the split main parameters at 35 °C outdoor and 27 °C indoor.

2.5.5 Mark V results for additional pressure drop in the liquid line

Adding more pressure drop in the liquid line influences the operation of the system for all conditions except for the *T21* condition (35 °C-21 °C).

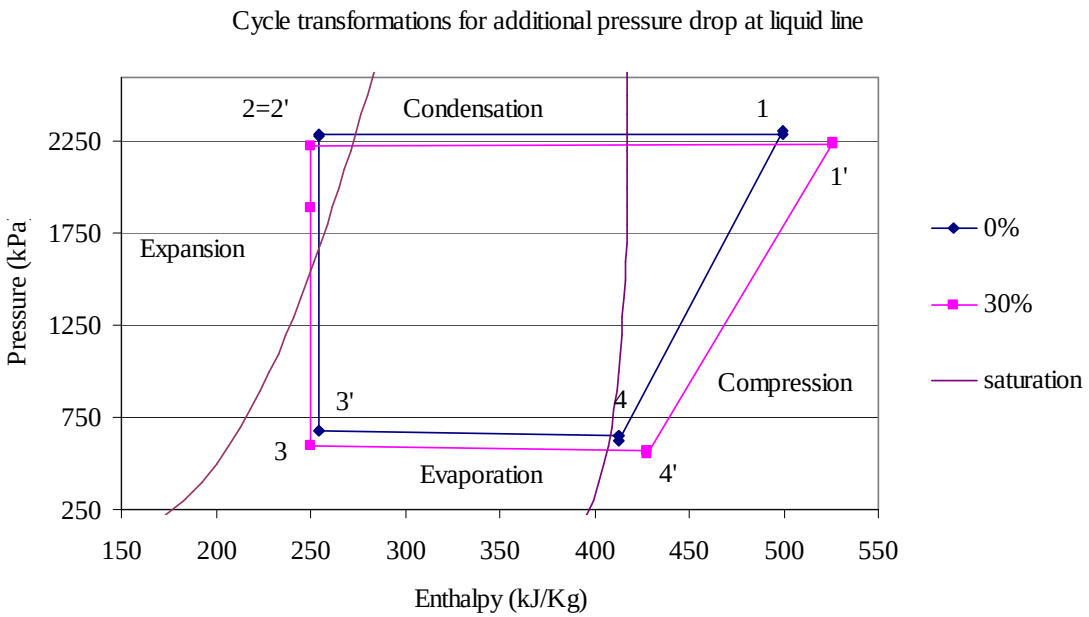

Figure 34: Thermodynamic R22 cycle modification for liquid line restriction..

The refrigerant is throttled more than necessary, the refrigerant flow is decreased and then the system capacity. The compressor also has less mass to compress, with less work. Both the capacity and the absorbed power are decreased but the global system efficiency is reduced (Figure 35).

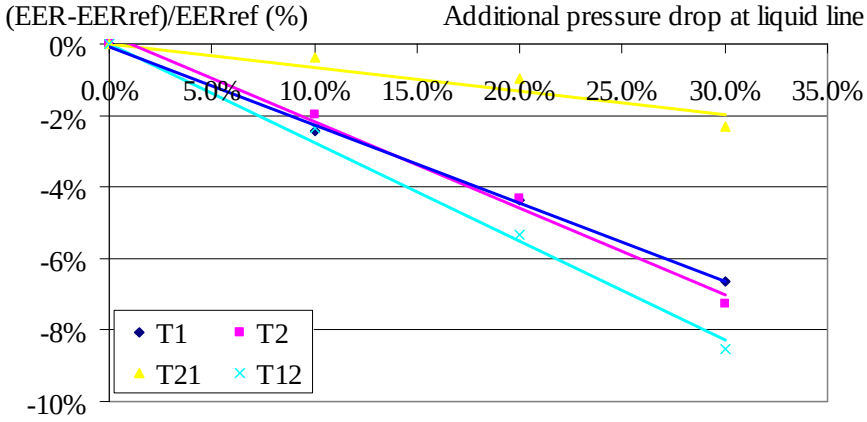

Figure 35: Effect of additional pressure drop in the liquid line on the EER.

The defect is more sensitive at lower compression ratios; lower is the pressure difference, larger is the impact on efficiency.

Similarly to what was found with the previous defects that also lower the low pressure, while reducing the evaporating temperature, also in this case the sensible to total heat transfer ratio *SR* is lowered with consequences on the comfort and on the operation time of the system.

A lack of refrigerant charge would produce exactly the same symptoms as the additional pressure drop in the liquid line except for one aspect; if there is a lack of refrigerant in the system, there will also be a shortage of refrigerant in the condenser, and the subcooling will be smaller. On the contrary, if the capillary is blocked, the refrigerant missing in the evaporator will be in the condenser, and the subcooling will be normal or increased in some case (Figure 36).

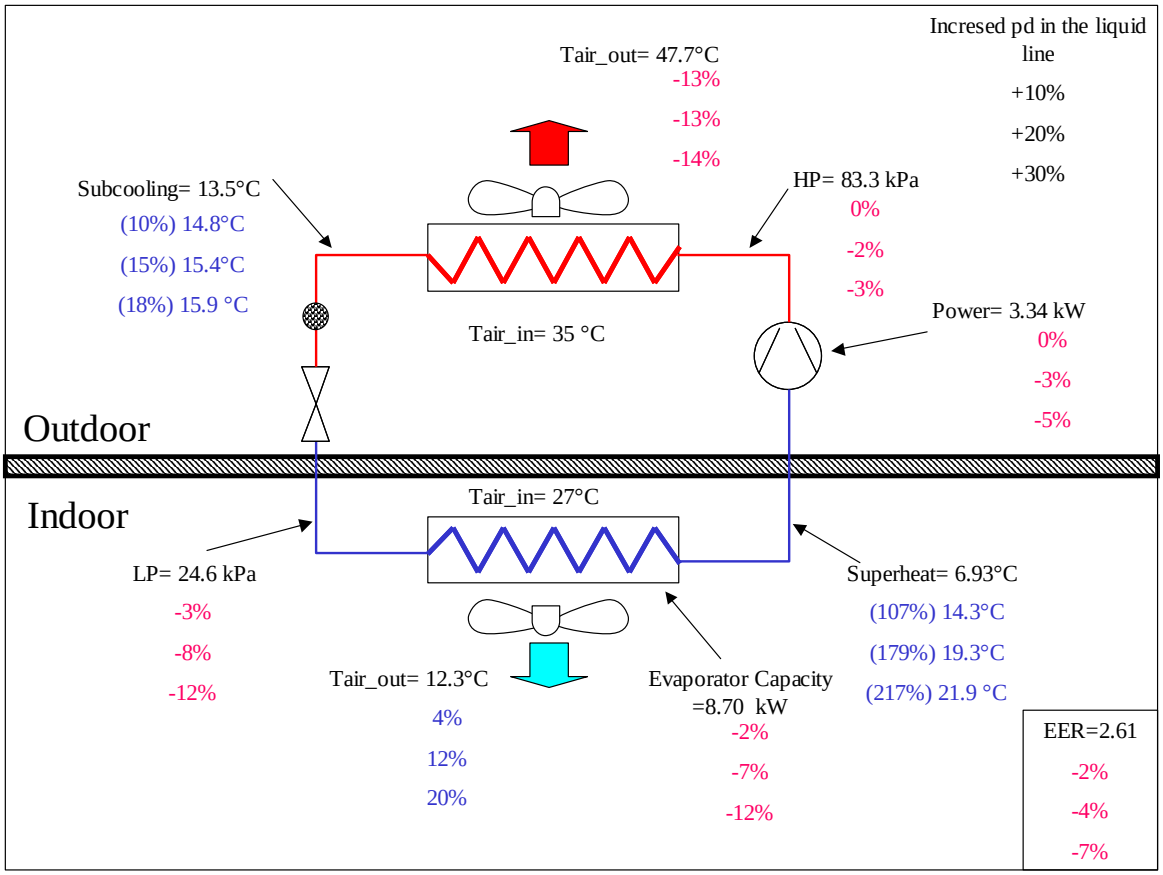

Figure 36: Effect of the additional pressure drop in the liquid line on the split main parameters at 35 °C outdoor and 27 °C indoor.

There is another extremely valuable index that can be used to diagnose a blocked capillary with certainty. If the compressor stops, the pressures will quickly equalise. If the capillary is completely blocked, this equalisation of the pressures will not occur. If there is a partial obstruction then the worse the blockage, the longer this equalisation takes to occur.

2.6 Comparison with literature experimental data

Table 10 summarizes the effects on cooling capacity, on the power of compressor and fans and on the global energy efficiency ratio (*EER*) and on the cycle parameters (condensation and evaporation pressures, superheat and subcooling) for all the defects considered. In the same table in the brackets are shown the trends obtained from Breuker and Braun from experimental test on a rooftop [Breuker 1998]. The tested machine is a 10 kW packaged rooftop unit equipped with a constant speed, hermetically-sealed, reciprocating compressor with on/off control and used fixed-orifice type expansion devices for refrigerant flow control.

Table 10: Impact on system parameters of the reviewed defects and comparison with the Breuker experimental data

Symbol legend: ↑ Increase ↓ Decrease ~ Stable	Cooling Capacity	Compressor Power	*EER*	HP	LP	Subcooling	Superheat
Refrigerant Leaks	↓(↓)	↓	↓ (↓)	↓ (↓)	↓(↓)	↓(↓)	↑ (↑)
Condenser Fouling	↓ (↓)	↑	↓ (↓)	↑ (↑)	~ (↑)	↓ (↓)	↓ (↓)
Evaporator Filter Fouling	↓ (↓)	↓	↓ (↓)	↓ (↓)	↓ (↓)	~ (↓)	↓ (↓)
Compressor Valve Leaks	↓(↓)	↓~	↓(↓)	↓ (↓)	↑ (↑)	↓ (↓)	↓ (↓)
Liquid-Line Restriction	↓(↓)	~↑	↓(↓)	↓ (↓)	↓ (↓)	↑ (↑)	↑ (↑)

There is a general agreement between the experimental and the modelled defects. The magnitudes of variation of the parameters are the same. Unfortunately the condenser fouling was translated in the test experiment by a partial block of the condenser area, this prevented us to make quantitative comparison between the results.

If we consider just as an example, a case were all defects occur at the same time at the lowest simulated level we have the result of the Table 11 with the comparison with the base case values.

Table 11: Impact on system parameters when all defects occur simultaneously

	P_c (kW)	P_a (kW)	*HP* (bar)	*BP* (bar)	Refrigerant flow (kg/s)	*EER*	Subcooling (°C)	Superheat (°C)
Rating conditions	8.7	3.3	23.1	6.8	0.055	2.6	13.5	6.9
Fully degradated	7.6	3.2	21.7	6.2	0.046	2.4	10.3	18.3

It should be noticed that the global effect is worst than the single defects but not simply their sum: the defect effects can compensate or prevail, in such a case detection is too difficult if it is only based on the observation of the parameters. Other criteria of detection and diagnosis should be considered.

The defects will be studied more in detail using dynamic simulations that allow observing the effects of the partial load behaviour of the degradated system and the seasonal defect performance.

2.7 Model for seasonal simulations

The ORNL programme allows us to describe the system at fixed outdoor and indoor conditions but does not allow performing dynamic simulation that can include other aspects such as control, cooling load and occupants or weather data. The programme Consoclim [Consoclim 2002] has been used in order to couple the defects to a dynamic operation in a complex approach: it gathers building model, cold generation and distribution models and allows annual simulation with defined weather data and occupation scheduling.

The cooling capacity and power at different indoor and outdoor conditions are taken into account in Consoclim using the following relation for cooling capacity (P_{c_fl}) and absorbed power (P_{a_fl}) at non rating conditions, full load:

$$P_{c\_fl} = P_{c_{rated}}.(1+D_1.(T_{i\_con}-T_{i\_con_{rated}})+D_2.(T_{i\_eva}-T_{i\_eva_{rated}})) \qquad [29]$$

$$P_{a\_fl} = \frac{P_c}{EER_{rated}}.(1+C_1.DT+C_2.DT^2) \quad [30]$$

$$EER_{fl} = \frac{P_{c\_fl}}{P_{a\_fl}} \quad [31]$$

$$DT=(\frac{T_{i\_con}}{T_{i\_con_{rated}}})-(\frac{T_{i\_eva}}{T_{i\_eva_{rated}}}) \quad [32]$$

Where:

T_{i_con}=inlet temperature at the condenser (K)

T_{i_eva}=inlet temperature at the evaporator (K)

C_1, C_2, D_1 and D_2 constants

_rated = index for parameters defined or calculated at rated conditions

The partial load behaviour of the air conditioner is taken into account and is characterized by a model load (shown in Figure 37) of the type:

$$\frac{EER_{pl}}{EER_{fl}} = \frac{Load}{Load+k} \quad [33]$$

With k=0.1 and 0<*Load*<100 % [Dougherty 2002].

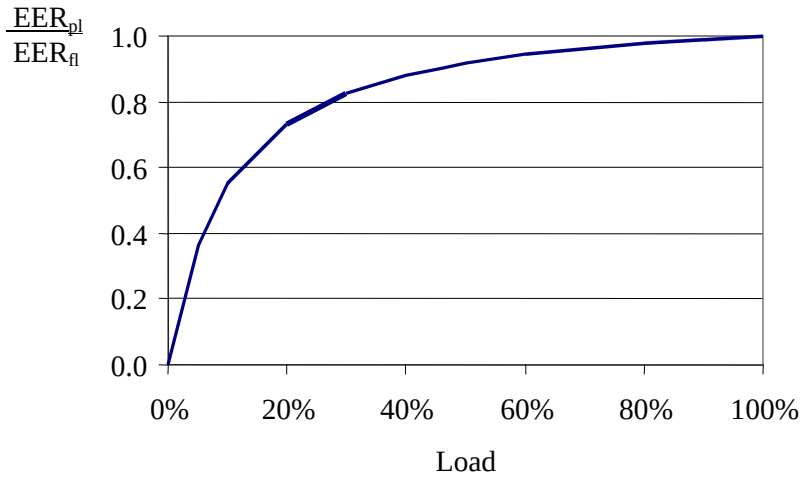

Figure 37: Partial load efficiency in function of the load

The previous Mark V simulation campaign has been used to define the parameters D_1, D_2, C_1 and C_2 which are different for each defect and these have been determined for the reference and degradated system using the least square method. Nine points have been obtained with the program in the range of temperatures *T1-T2* (Table 12).

Table 12: Indoor and outdoor temperature combinations

Indoor temperature (°C) → / Outdoor temperature (°C) ↓	21	25	27
21	21-21	25-21	21-27
27	27-21 (*T2*)	27-25	27-27 (*T2*)
35	35-21 (*T12*)	35-25	35-27 (*T1*)

The use of nine points seems to be accurate enough to define the equipment characteristics. Adding more points seems not to improve significantly the model: one more point improves slightly the capacity model and does not improve significantly the power model, increasing on the other hand significantly the number of simulations.

The capacity and absorbed power are thus defined as a function of the indoor and outdoor temperature. The models obtained with the coefficients for two different cases (base, filter fouled) are shown on Figure 38.

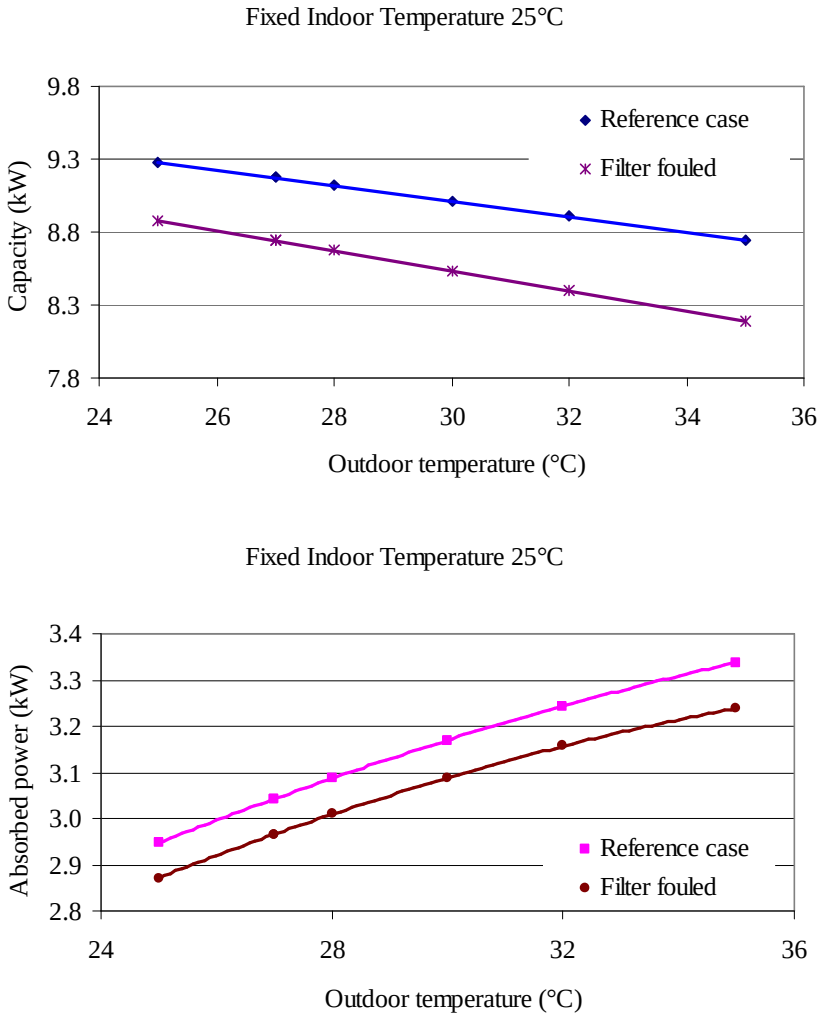

Figure 38: Capacity and absorbed power versus outdoor temperature for reference and filter fouled cases

The table below shows the main results of the linear regression model for capacity for the reference case with the coefficient D_1 and D_2 that have been determined, all other cases with defects being treated in the same way.

Table 13: Regression parameters for capacity for the reference case

Outdoor Temperature (°C)	Indoor Temperature (°C)	P_{c1} from Mark V (kW)	P_{c2} from the equation [29] (kW)	Residuals P_{c1}-P_{c2} (kW)	Quadratic Error $(P_{c1}-P_{c2})^2$ (kW²)
35	27	8.697	8.70	0.0000	0.0000
27	21	8.188	8.09	0.0976	0.0001
35	21	7.345	7.66	-0.3181	0.0102
27	27	9.159	9.12	0.0360	0.0000
21	27	9.268	9.44	-0.1752	0.0009
35	25	8.697	8.36	0.3332	0.0123
27	25	8.894	8.79	0.1036	0.0001
21	25	9.047	9.11	-0.0594	0.0000
21	21	8.509	8.41	0.0991	0.0001

The coefficient of determination R^2 for the capacity is 90 %; the model is considered adapted. For the absorbed power the error is slightly higher because of the sum of the errors on the absorbed power and on the capacity (as shown in the formula [30]). The residuals of the power and of the capacity are shown in Figure 39: the error is never higher than a few percent and no systematic tendency appears.

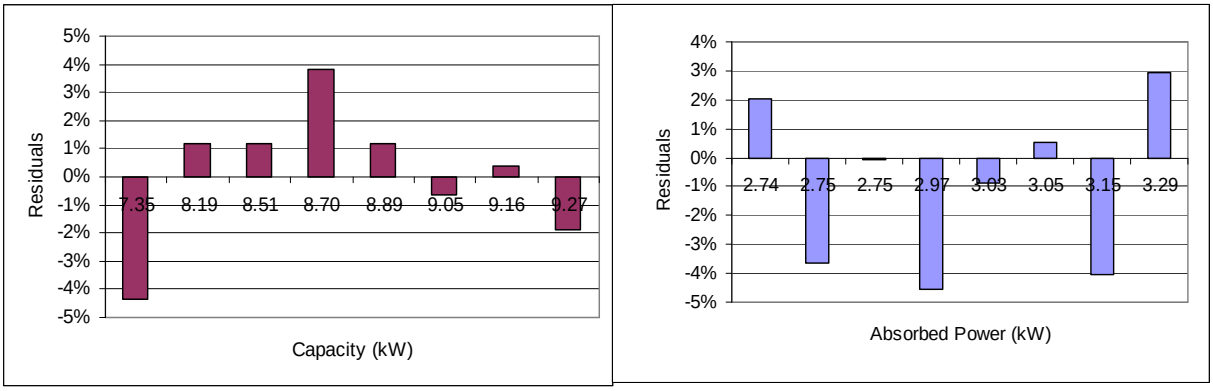

Figure 39: Residuals of the regression for the capacity and the absorbed power of the modelled the reference case.

2.8 Reference buildings characteristics

The characterizations of the degradated operation of the split unit are used for further dynamic simulations linking degradated systems with the operational conditions in typical French office and residential buildings. Office buildings are characterised by internal load very similar in general and no specific use that can strongly differentiate the buildings in the stock. For each building, two French climates are considered representative of two different French weather conditions: Trappes as the typical North continental climate and Nice as the typical temperate Mediterranean climate. The weather files those of the French thermal regulation of 2000. The buildings are made to be representative of existing building with an envelope thermal resistance respecting the French thermal regulation of 1988. An extended description of the simulated buildings is given in annex 2.

Table 14: Installed split unit cooling capacity for the simulated buildings

Office Building					
	Number of Splits	Unitary rated capacity (kW)	Installed capacity (kW)	Area (m²)	Sizing ratio (W/m²)
Trappes	18	8.7	157	762	205
Nice	24	8.7	209	762	274
House					
	Number of Splits	Unitary rated capacity (kW)	Installed capacity	Area (m²)	Sizing ratio (W/m²)
Trappes	1	3.3	3.3	51	65
Nice	2	8.7	17	85	205

The reference consumption for the two building types takes into account the different zone consumptions and a small oversizing factor is applied as it can be easily encountered in the reality: in the office building this capacity considered is about the 30 % higher of the needs calculated with the sizing method suggested by the AICVF [AIC 1996]. For the house this value reaches 50 %.

The use of air conditioning in the living rooms in the case of the less hot weather is not justified, the demand being too small.

The annual consumption due to the air conditioning for the base case for the two buildings in the two separate climates is shown in the Table 15 as a ratio related to the air-conditioned area.

Table 15: Annual Consumptions ratios for an office and a house for two climates.

	House: annual electrical consumption for AC (kWh/m²)	
	Trappes	Nice
Bedrooms	5.2	19.5
Living rooms	x	3.3
Total	5.2	9.1
	Office: annual electrical consumption for AC (kWh/m²)	
	Trappes	Nice
Office A	13.6	35.9
Office B	16.4	37.6
Meeting rooms	2.6	12.0
Total	12.5	31.1

2.9 Buildings seasonal performance with degradated split

The following analysis allows estimating the effects of the defects for different defect intensity and try to find laws that could be easily applied in an audit procedure to quantify first savings due to correction of the defects, improvement of maintenance without major intervention on the system.

In the following figures, E_{a_ref} and E_{c_ref} indicate the annual energy consumption and the total cooling energy for the reference case while E_a and E_c indicate the annual energy consumption and the total cooling energy for the case of the defect in consideration.

All the simulated defects and building results are gathered in the annex 3, in this part we will show for each defect only some results in order to make the explanation lighter.

2.9.1 Building with refrigerant leaks

As it has been seen in the case of previous static model, the loss of efficiency due to refrigerant leaks are significant for leaks over 10 % of the initial charge. This defect does not increase the overall consumption; it can decrease or increase following the case.

In the hotter simulated climate, the overconsumption is decreased but there are large period of discomfort that can reach 16 % and 20 % of the total occupation period respectively for the office building and for the house.

In Trappes, the consequences are less important: the reduction of efficiency leads to a light over-consumption that decreases with a small cooling energy reduction (99 % and 97 % for the office building and for the house for a charge reduction of 20 %) with very low impact on the comfort (discomfort less than 2 %).

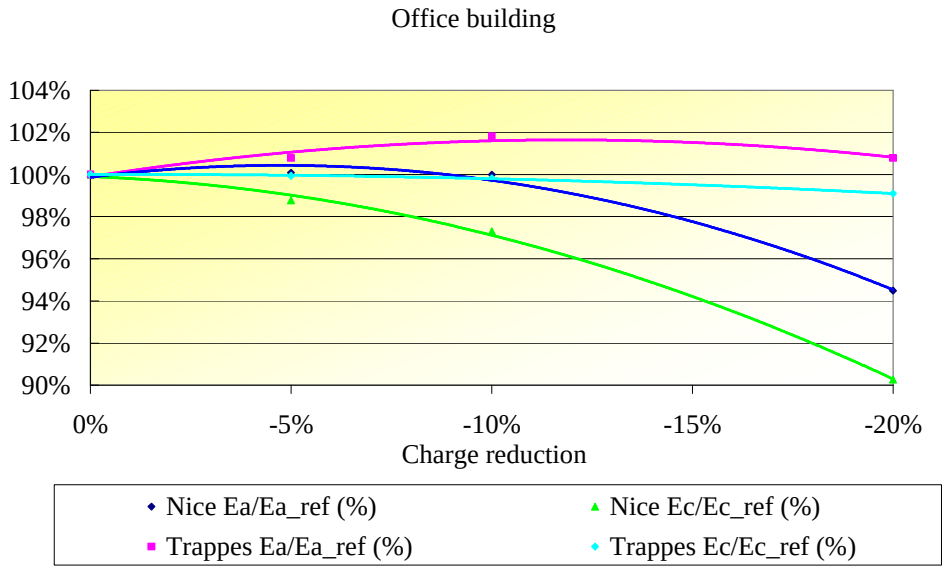

Figure 40: Effect on the annual cooling energy and the energy consumption for an office building in Nice and Trappes for reduced refrigerant charges.

In this case, it is more an issue at comfort level, the capacity being reduced, discomfort periods (considered for indoor temperatures higher of the set point of more than 1 °C) become significant reaching 15 % of the occupation cooling time in Nice for the offices oriented to South (Figure 41).

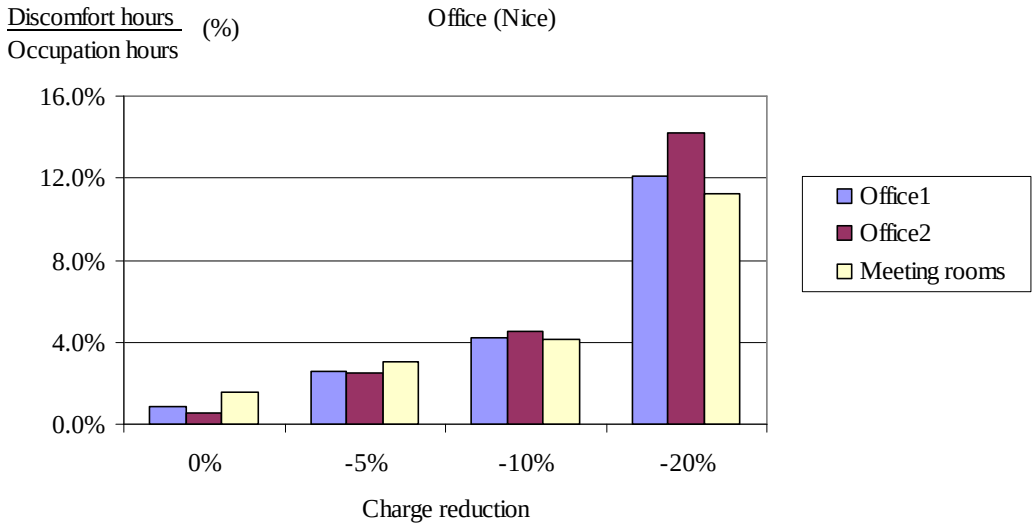

Figure 41: Subsequent discomfort for reduced refrigerant charges for an office building in Nice

We have to highlight that the seasonal performances are overestimated by the model in all the simulated cases because they do not include the effect due to the increased latent part of the cooling capacity that would reduce further the cooling energy used to lower the air temperature, increase the operation time of the system and probably increase furthermore the discomfort rates.

2.9.2 Building with condenser fouling

The fouling of the condenser, since it has no impact on the cooling capacity of the system but only on the electrical consumption, allows always respecting the temperature setpoints but increases the annual energy consumption. The relation between the over-consumption and the reduction due to fouling is linear (R^2>0.95 for all the simulated buildings) and quite independent from the climate. It has very similar impact for Trappes and Nice in both cases of house and office (Figure 42).

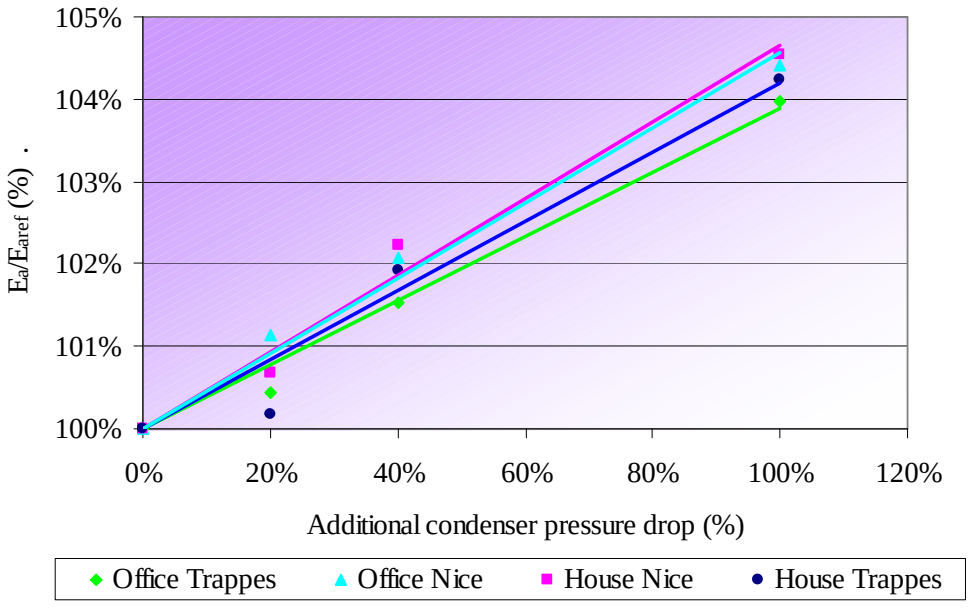

Figure 42: Effect on the annua energy consumption for the office and house buildings with fouled condenser.

2.9.3 Building with fouled evaporator filter

The fouling of the evaporator filter has an effect similar to the refrigerant leaks: the cooling capacity is reduced and the sensitive to total cooling capacity ratio is lowered. This time, the model allows partially taking into account this effect in the calculations through the reduced evaporator airflow.

As a consequence, in all simulated buildings, a light over-consumption has been observed, while higher cooling energy is produced to compensate the higher latent heat removal (Figure 43).

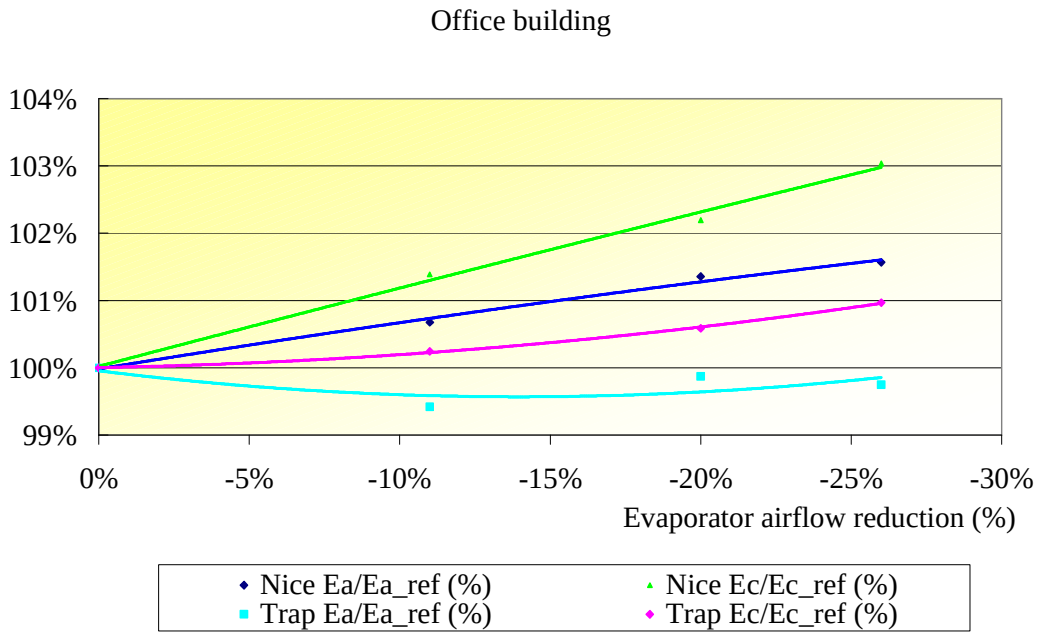

Figure 43: Effect on the annual cooling energy and the energy consumption for an office building for filter fouling.

When the filter is fouled, the systems work with higher load rates (Figure 44) and for a longer time (increased operation times on average by 10 %), improving slightly the efficiency following the part load behaviour defined in Figure 37 and in some cases improving seasonal efficiency.

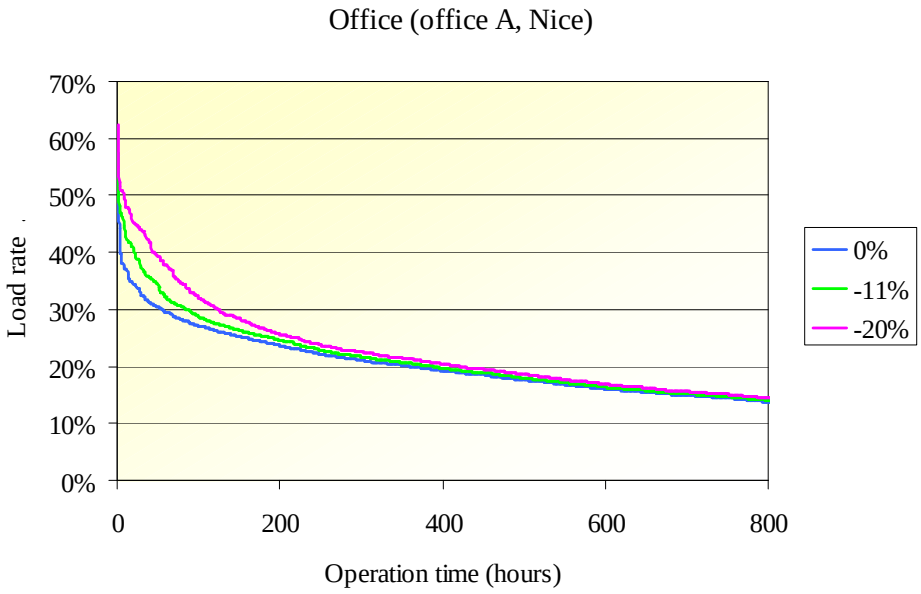

Figure 44: Yearly cooling load curves for office for different filter fouled conditions

2.9.4 Building with worn compressor

The leaks between the valves of the compressor lead to over consumption but influence also the cooling capacity of the system, leading to some comfort problems in the hottest climate. The effect is quite the same for Trappes as for Nice, as we have noticed in the paragraph 2.5.4, since the defect is not dependent on the outdoor temperatures.

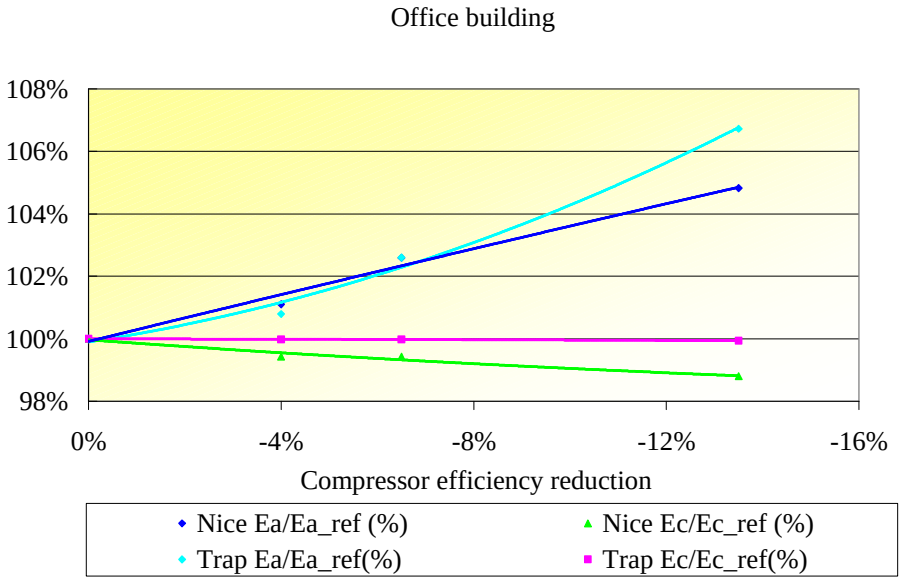

Figure 45: Effect on the annual cooling energy and the energy for an office building with a system with reduced volumetric efficiency of the compressor.

The consumption increases while the discomfort hours grow on average by only 3 % for the office in Nice and there is no discomfort in Trappes, as we saw that the capacity remains quite the same.

2.9.5 Building with additional pressure drop in the liquid line

The restriction of the liquid line can have a different impact on the system seasonal performance depending on the climate and the building type. For all the simulated cases, the lower system capacity leads to an increased loss of comfort and to an increased annual time of operation. The system can work up to 20 % longer for an additional pressure drop of 30 % for the office building in Trappes.

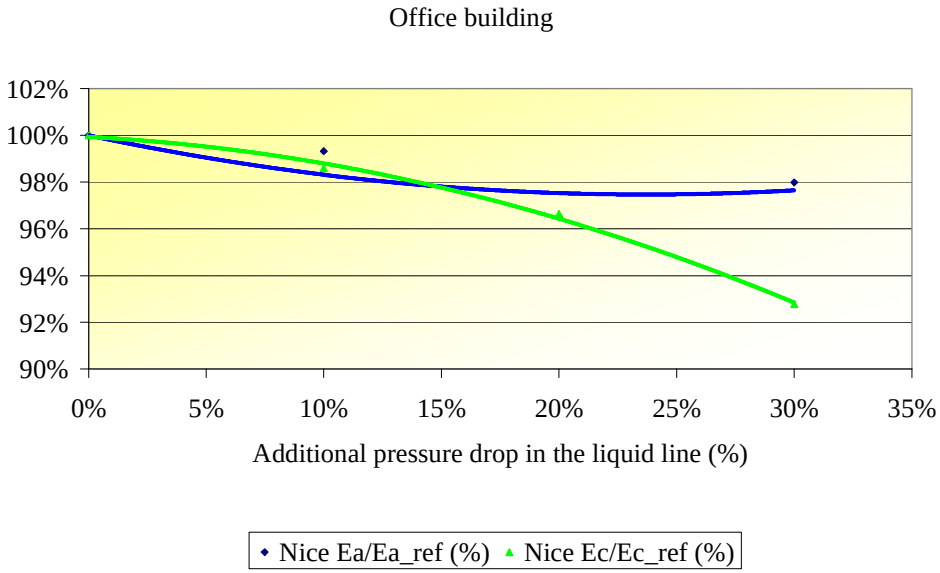

Figure 46: Effect on the annual cooling energy and the energy for an office building with a system with additional pressure drop in the liquid line.

The seasonal performances are over-estimated by the model in all the simulated cases because they do not include the effect due to the increased latent part of the cooling capacity that would reduce further the cooling energy used to lower the air temperature, increase the operation time of the system and probably increase furthermore the discomfort rates.

2.10 Conclusions of analysis of the split units defects

Once we identified a set of frequent defects that occur during the normal operation for split systems, their impact on the performance has been defined using a thermodynamic model. The degradation of the system has been introduced in dynamic simulation in order to investigate the effect on the seasonal energy consumption and on the comfort of occupants in two typical French buildings (a small office building and a house) for two different climates.

The following defects have been considered: fouled condenser, refrigerant charge leaks, reduced compressor volumetric performances, filter fouling and additional pressure drop in liquid line. All the defects have shown important impacts on the cooling capacity and/or on the system consumption.

The defects kept can be sorted into two types of defects: defects that can be mainly source of over-consumption as condenser fouling and defects that have their main effects on the cooling capacity and comfort aspect (while the annual consumption can be found reduced or not depending on the case) as filter fouling, compressor leaks, refrigerant leaks and liquid line restriction.

Several observations have been possible on the calculated annual energy consumption and temperatures. The oversizing factors applied in the common sizing process allows guaranteeing comfort in many cases of defects, and discomfort period becomes very long only for extreme conditions.

General trends can be found in many cases to model the discomfort and the over consumption effects. Starting from the nominal operation characteristic of the system (from design and manufacturer data) the inspector should be able to estimate the intensity of the defect and from the curves presented to estimate the consequences in terms of consumption and discomfort. He/she can also forecast the future behaviour of the system.

Refrigerant leaks check should be a priority for the auditor: for the energy and comfort considerations but also in order to limit the atmosphere contamination with the refrigerant with high global warming potential.

The condenser should then be inspected with care because it has the most important impact at the consumption level: the inspector can estimate visually the fouling (amount of debris and dust on the fins) or measures the airflow with the technique suggested.

The filter fouling leads the system to operate longer and in dangerous conditions (with lower superheat). The status of the filter can be visually checked or estimated by asking to the owner the summary of maintenance operations.

Compressor problems are more difficult to detect and require the catalogue values (often supplied by manufacturers for several outdoor and indoor conditions) as reference consumption, the absorbed power being easily measured. However the compressor defect degradated quickly to compressor failure and if detected should be immediately repaired in order to avoid the failure and the replacement of the compressor that is the most costly part of the system.

Additional pressure drop in the liquid line lead the refrigerant to pre-expand and lower the system performance and the cooling capacity. It can be easily repaired at low cost (replacement of the line).

For the defect detection and diagnosis the characteristic effects are showed in the figure below on the thermodynamic cycle of the R22: the parameters condensing pressure, evaporating pressure subcooling and superheat are useful to detect the defect and distinguish each defect from the others.

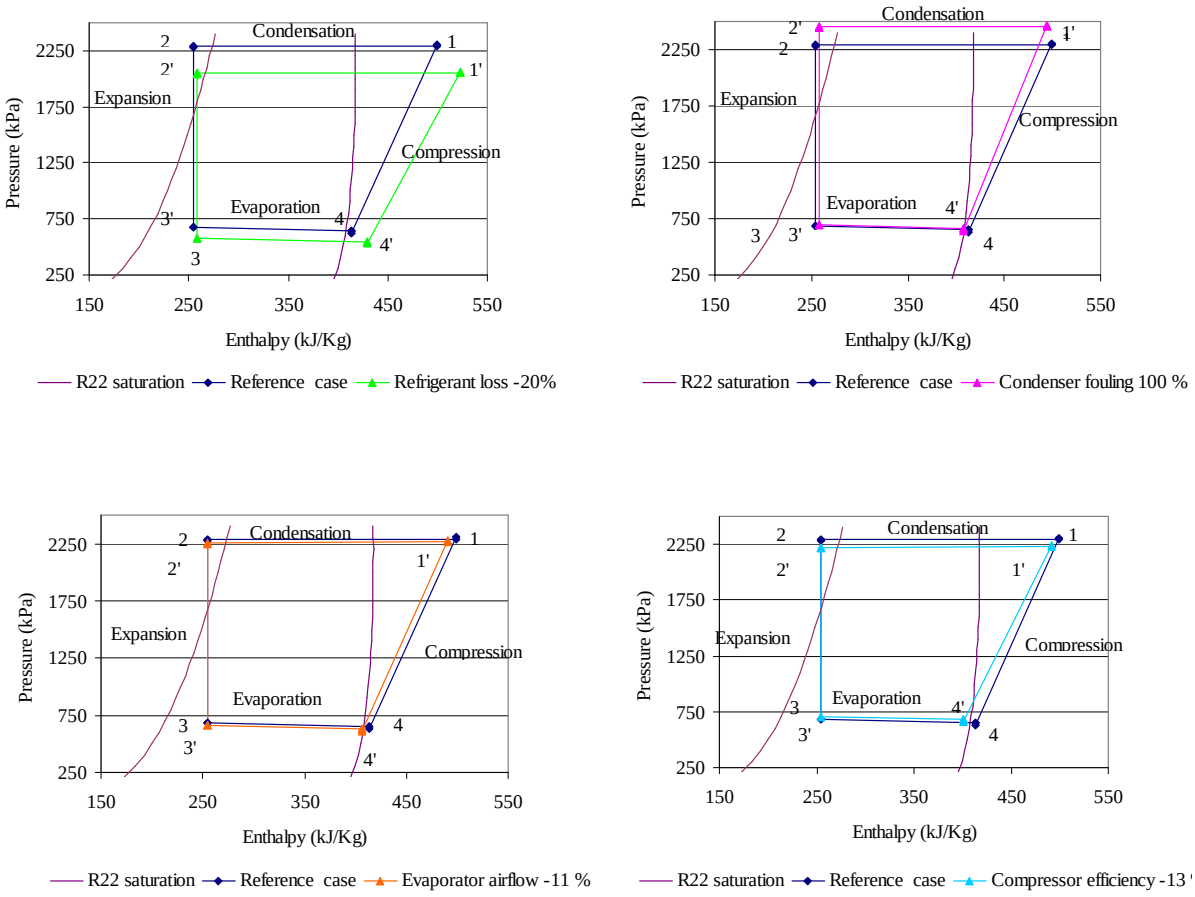

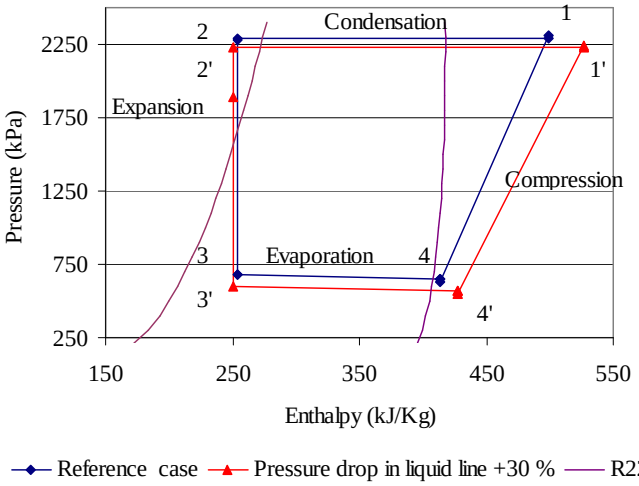

Figure 47: R22 cycle modifications for the analysed defects

The thermodynamic cycle does not allow representing the effects on the performance, on the capacity and on the absorbed energy. We summarise these effects in the Table 16 with further detection hints that can be used for the defect detection.

Table 16: Defects characterisation with parameters sensitivity and detection hints

Symbol legend: ↑ Increase ↓ Decrease ~ Stable	P_c	P_a	*EER*	Other detection hints
Refrigerant Leaks	↓	↓	↓	Oil marks, leaks techniques
Condenser Fouling	~↓	↑	↓	Condenser airflow measurements
Evaporator Filter Fouling	↓	↓	↓	Evaporator airflow and supplied air temperature measurements
Compressor Valve Leaks	↓	~	↓	
Liquid-Line Restriction	↓	~↑	↓	Large temperature difference in the liquid line, when the system is put off slow equalisation of pressures

Refrigerant leaks can be distinguished by evaporator fouling and additional pressure drop in the liquid line that if all lower the operation pressures, the subcooling effect are different: it is lowered for refrigerant leaks, it is unchanged for the filter fouling and increased in the case of liquid line restriction. The condenser fouling result to be the only defect that raises the high pressure, while the compressor loss of efficiency is the only one that increases the lower pressure.

At building level, on the seasonal performance of the simulated buildings, the observation of the parameters for each defect are summarised in Table 17. The effects are shown for unitary defect level, with the assumption of linear dependence although this is true only for condenser fouling. The table put in evidence the defects that lead to discomfort, to overconsumption and those that increase the operation time of the systems.

Table 17: Defect effect on the seasonal performance for the simulated buildings.

			Effect for 1% refrigerant charge	Effect for 1% increased condenser pressure drop	Effect for 1% reduction of evaporator airflow	Effect for 1% loss of volumetric efficiency	Effect for 1% pressure drop in liquid line
Office	Trappes	Discomfort	0.10%				0.03%
		Consumption		0.04%		0.21%	0.07%
		Operation duration	1.20%	-0.02%	0.38%	0.12%	0.60%
		Loss of Seasonal EER	-0.10%	-0.04%		-0.18%	-0.10%
	Nice	Discomfort	0.65%			0.09%	0.33%
		Consumption		0.04%	0.06%	0.15%	
		Operation duration	0.65%	-0.02%	0.38%	0.12%	0.60%
		Loss of Seasonal EER	-0.20%	-0.04%		-0.18%	-0.17%
House	Trappes	Discomfort	0.10%			0.06%	0.33%
		Consumption	-0.25%	0.04%		0.13%	-0.07%
		Operation duration	0.20%	-0.02%	0.12%	0.09%	0.43%
		Loss of Seasonal EER	-0.10%	-0.04%		-0.15%	-0.23%
	Nice	Discomfort	-1.00%			-0.09%	0.53%
		Consumption		0.05%		0.13%	-0.10%
		Operation duration	0.95%	-0.02%	0.27%	-0.18%	0.60%
		Loss of Seasonal EER	-0.30%	-0.04%		-0.21%	-0.07%

3 Analysis of defects occurring during the operation of chiller systems

3.1 Stock of chillers and determination of related energy stakes

Chillers represent one of the wide spread air conditioning technologies in Europe for centralised air conditioning systems. They are used in air conditioning coupled with different types of terminal units such as air handling units, fancoils, chilled beams etc. Moreover they can differ by refrigerant fluid, compressor technology and condensing fluid (air or water). Capacities can go from some kW to several hundreds.

In 2003 chillers represented the largest share of the air conditioning stock as reported in the EECCAC study [EECCAC 2003]: 62 % of the units as in the figure below.

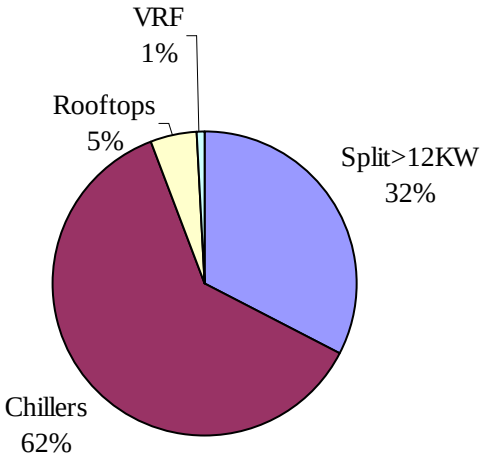

Figure 48: Air conditioning stock (number of units) for system type in 2003 for France [EECCAC]

In France the chiller air conditioned area (all technologies mixed) amounted to 77 *Mm²* in 2003, and its growth forecasted in EECCAC has been confirmed by the recent market data.

Thus the chiller stock is important but it is difficult to know its status and age: no extensive study exists about the service life of a chiller and the replacement rate. The value of 15 years as chiller lifetime is globally accepted, confirmed by the ASHRAE project about operating cost [ASHRAE 2005] that reported for all technologies an average of 15 years on a sample of 270 chillers, but the variation of that the sample goes from 0 (chillers that failed in less than one year) to 35 years. Most of the chillers reported are still in operation. More certain data are on rotary chillers were on a sample of 37 replaced chillers, the mean life was 27 years with a low value of 7 years and a maximum value of 52.

Chillers are used in different building sectors (mainly in commercial sector) and can be also used for refrigeration (with cold temperatures below 0 °C). Most of them are regularly maintained (maintenance for availability).

They enter in the frame of the inspection for refrigerant leaks stated by the European Community for systems with refrigerant charge higher than 3 kg. They would be probably one of the most frequent systems subject to the inspection stated by the Energy Performance Building Directive. For all these reasons, the inspector or auditor can meet many different scenarios.

In this work we imagine the most common scenario that an inspector could meet and we tried to understand which are the problems he/she should look for. We analyse then the more common defects for a common chiller machine in a common context.

Particularly, we developed two main aspects of a degradated operation of a chiller due to equipment defects:

- The impact on the energy aspect namely on the efficiency and capacity
- The definition of detectable parameters that characterise it

The first aspect will allow us to develop quantitative energy indicators for the consequences of a defect in typical situations.

The second aspect will allow us to define “on field” measurements for defect detection with the minimum measurement tools possible or to interpret the logged measurements of an Energy Management System, when available, that can give information on the past operation of the system.

These results could be used to enhance audit and inspection procedures for defect detection and the energy parameters would allow economical analysis and feasibility for repair or renovation. To do this, we followed the methodology explained in the first chapter. A high level view of the methodology is shown in the Figure 49.

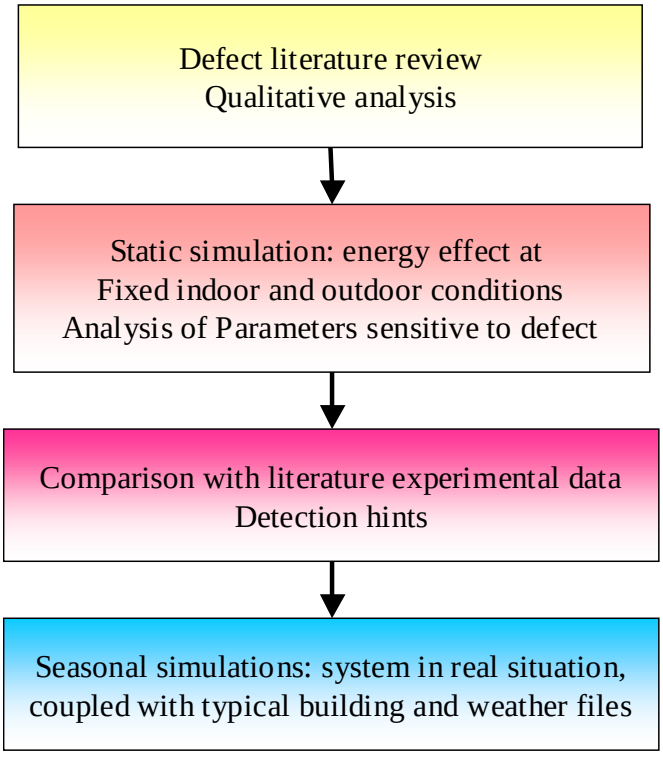

Figure 49: Steps of the methodology developed for the defects analysis

3.2 The representative chiller chosen

The study needs to target a chiller spread on the stock. Being the most present in the 2005 stock, an air-cooled chiller was chosen as reference as shown in the Figure 50.

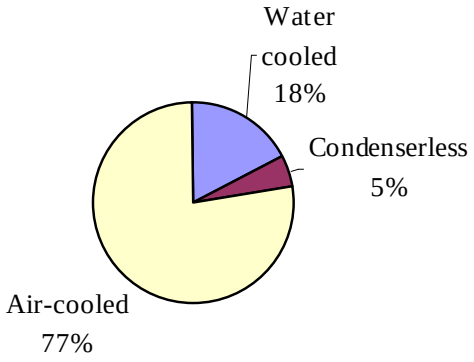

Figure 50: Chillers condensing technology for 2005 market in terms of number of units [Eurovent 2005]

The representative chiller rated *EER* has to be of Class "D" following the Eurovent classification (2.5<*EER*<2.7) product, in order to avoid targeting a top runner chiller and neither a too poor performance chiller technology. Scroll compression technology is the most widely used [EECCAC 2001] for middle chiller capacity (<750 kW).

The chiller with the targeted characteristic was available from the work of Rivière [Rivière 2004]: we could retrieve for the chiller all the system characteristics and the performance obtained for several experimental points. The representative chiller is 150 kW of rated capacity and rated *EER* of 2.63. The chiller presents four capacity stages with two screw compressors tandem that can be used for four different load conditions: 100 %, 75 %, 50 % and 25 % (Figure 51).

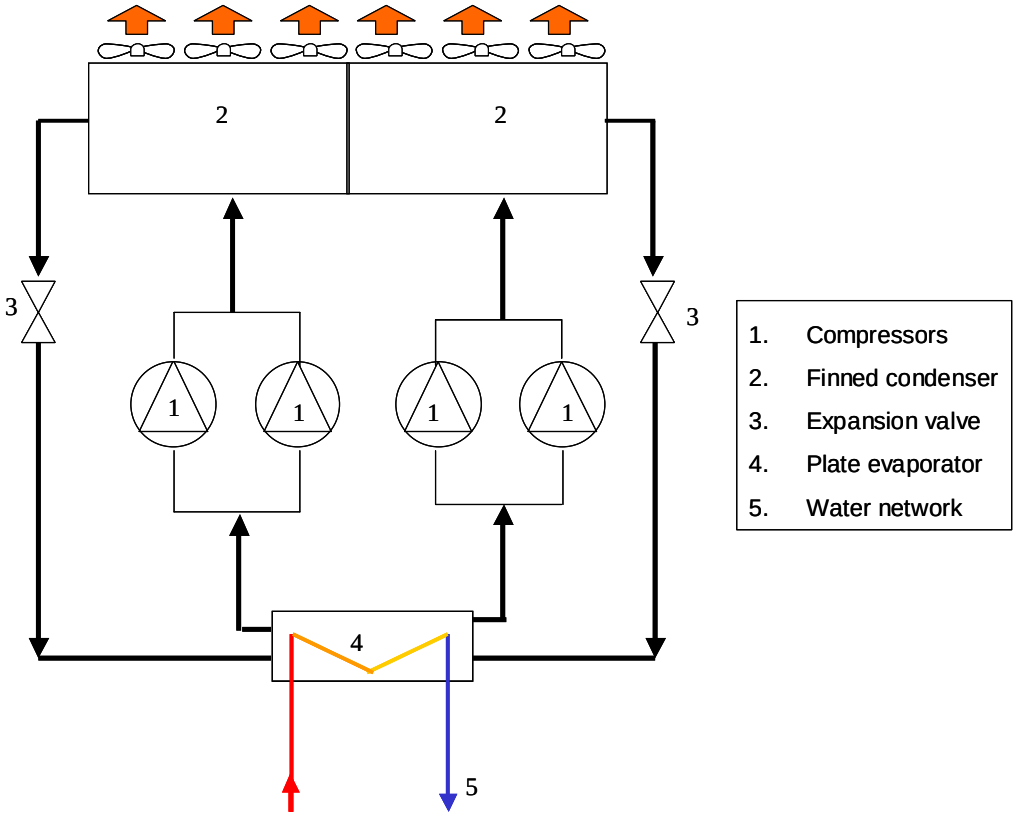

Figure 51: Scheme of components of the original chiller

The two parallel compressors in a tandem are on the same refrigerant network. We consider in our model just half of the system (Figure 52): two compressors working on the same refrigerant network. The behaviour of the global machine is the result of two identical machines. In this way we can consider the several capacities of system: the lowest charge level has a capacity of 40 kW with one operating compressor, the tandem has a capacity of 75 kW, while the global system reaches a cooling capacity of 150 kW.

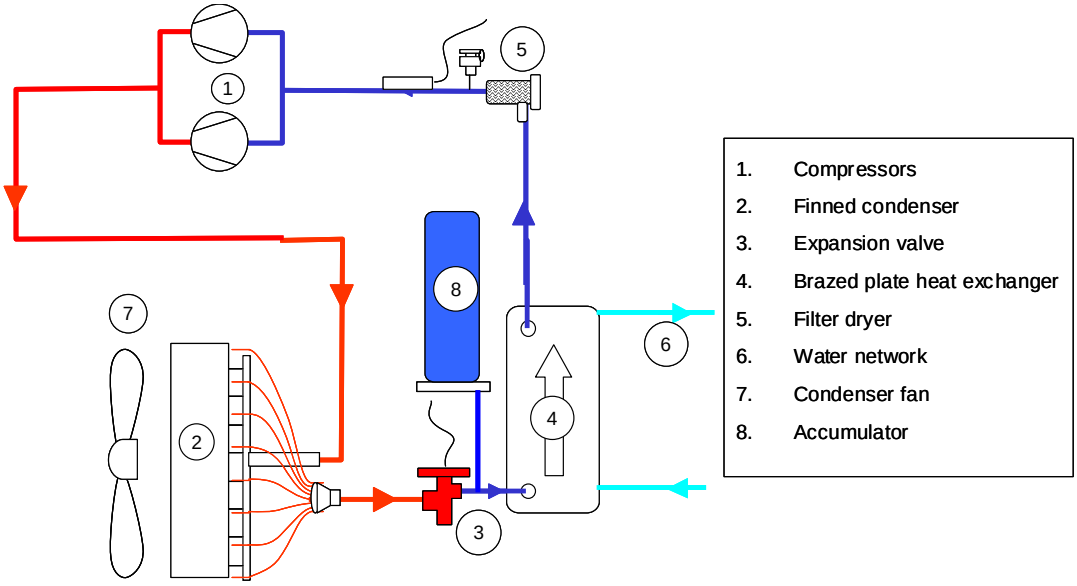

Figure 52: Air-cooled chiller components

The condensers, two finned tubes condensers, are equipped with six fans with a nominal airflow of 48 000 m^3/hour (8 000 m^3/hour per fan).

The evaporator is a brazed plate heat exchanger; the rated water flow is 7.4 m^3/h.

The system uses as refrigerant R407C. Although R22 is still the most widely spread fluid both for chillers and for splits (from the maintenance fluid data of the "Inventory of refrigerant fluid" [Barrault 2007] we preferred examine a chiller using R407C for two main reasons.

Firstly, R407C is the most commonly used refrigerant in new equipment and it is used for R22 drop in: it represents 56 % for new equipment and retrofit while other fluids are R410A (17 %) and R134A (25 %).

R407C gave us the opportunity to observe the effect of defects of operation for refrigerant with temperature glide in unsaturated vapour region.

Moreover, as a difference with the first part of this work, we can believe that while for small split system, the phase out of R22 would be slower because of the low maintenance level of this system type, for chillers the drop in would be faster and the situation presented in the maintenance data will be dominated in some year by R407C.

3.3 Review of the literature about chillers defects

The chiller problems in operation have been studied by several authors, mainly through experimental work and most for automated FDD (Fault detection and diagnosis) development. Some reference works are detailed hereunder.

The first reference of performance monitoring and fault detection can be found in 1996 in the work of Stylianou et al. [Stylianou 1996] for four faults in water-water reciprocating chillers: refrigerant leak, refrigerant line flow restriction, condenser water side flow resistance and evaporator water side flow resistance were tested.

Several authors studied purposely the effect of the refrigerant charge on the chiller performance: Grace et al [Grace 2004] observed experimentally the sensitivity of the performance to charge level for a small (4 kW) water-to-water reciprocating chiller equipped with a thermostatic expansion valve.

Choi et al. [Choi 2004] investigated the effects of the expansion device on the performance of a water-to-water heat pump using R407C and compared R22 and R407C performance for several conditions of charge using capillary tube and electronic expansion valve.

Bailey [Bailey 1998] presents a study involving the operation of a 250 kW helical rotary, dual-circuit, air-cooled chiller while three independent variables are experimentally altered: refrigerant charge level within the chiller plant, outdoor air temperature, and percentage nominal chiller load. The chiller consists of one direct expansion evaporator with a dual-circuit configuration and two independent refrigerant circuits, each including a screw compressor with an electronic expansion valve.

McIntosh et al. [McIntosh 1998] developed a detailed model based on a centrifugal chiller for FDD, it studied the detection of: condenser water flow reduction, evaporator tube fouling, condenser tube fouling, compressor internal faults, motor/transmission faults.

With a particular interest Comstock et al. [Comsotck 2001] presented the results of a fault survey that was conducted among the major American chiller manufacturers in order to identify the most common and expensive faults that occur in chillers. The fault data are presented in terms of frequency of occurrence and relative cost to repair for different chiller types.

Comstock et al. [Comsotck 2002] also presented experimental data from laboratory and results that provide a basis for development of fully automated FDD applied to a centrifugal chiller (316 kW) based on the previous defect review. They investigated eight defects: reduced condenser water flow, reduced evaporator water flow, refrigerant leak/undercharge, refrigerant overcharge, excess oil, condenser fouling, non-condensables in the refrigerant, defective expansion valve.

From the literature review and considering our methodology of research, we could target our analysis on the following defects:

- Fouling of the condenser on the airside
- Refrigerant leaks
- Non-condensable presence in the condenser
- Clogged expansion device
- Compressor faults
- Evaporator fouling on the waterside

Some defects are not taken in consideration because too much difficult to include in the model such as excess of oil because of the neglected oil presence in the model or the refrigerant overcharge due to the model limitations.

3.3.1 Refrigerant leaks

All refrigeration systems can potentially leak because the pressures in the system are usually many times higher than atmospheric. Refrigerant losses contribute to the reduction of the efficiency of the system, leading to increased power consumption (due to the lack of capacity and the longer times of operation of the system) greenhouse gas emissions, higher maintenance costs and eventual system failure.

A low refrigerant charge can be caused by leakages during the refrigerant recharge activities, a wrong fill at the start up, leakages in the damaged joints and bad sealing. Chillers are more subjected to refrigerant leaks than split system, this because they are more often assembled on place and they can be more subject to vibrations. Moreover, when not well performed, the interventions for maintenance can also be source of leaks.

The leaks bring to a global lower pressure level of the system reducing at the same time the capacity and the absorbed power (Figure 53). If the initial charge of the system is correct, its reduction will bring to a lower efficiency.

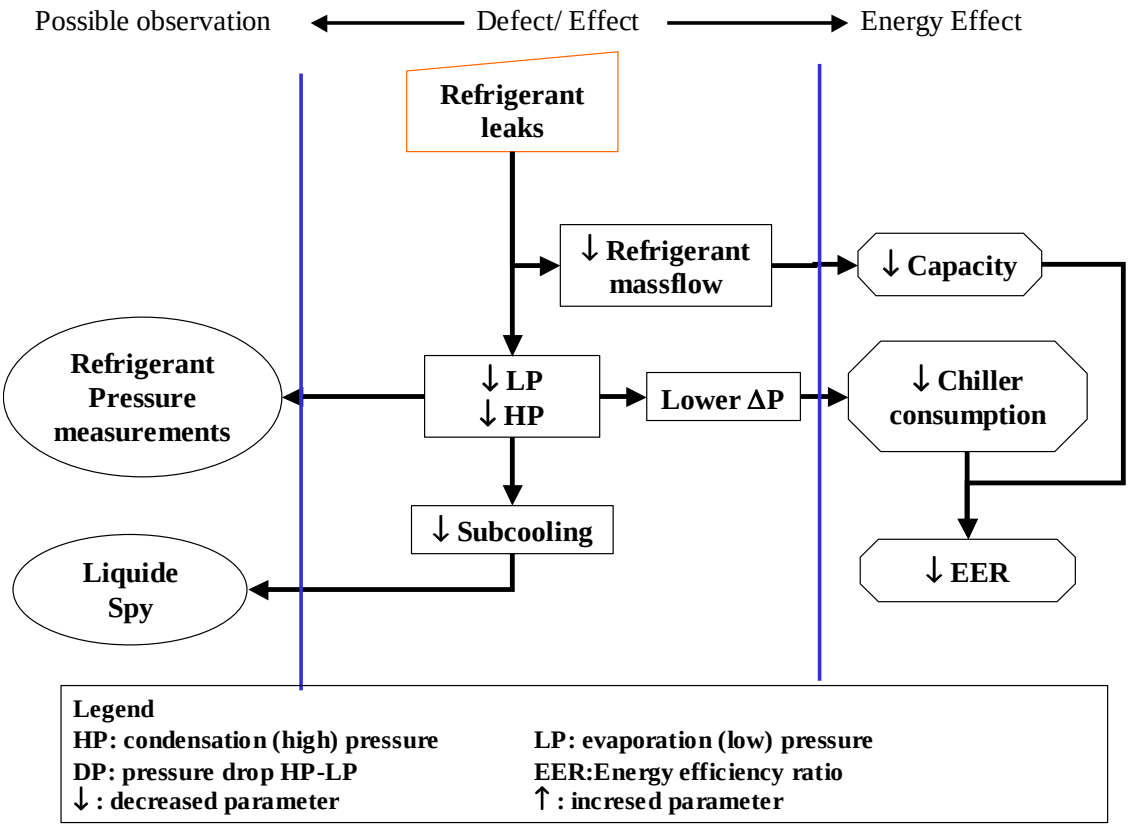

Figure 53: Defect tree for refrigerant leaks

One of the consequences of the refrigerant leaks is to change the mole fraction composition of the refrigerant and changing also its properties. Moreover this composition change is different following the leak its in correspondence of a vapour or liquid state [Johansson 2001]. The change in composition will be neglected in our analysis.

3.3.2 Condenser fouling on the air side

The condenser is a finned tube heat exchanger. This type of fouling is representative of a build-up of debris on the face of the condenser coil, it causes an additional heat transfer resistance and reduces the total flow rate of air across the coil. Many studies exist on the modelling of the mechanism of fouling for this type of heat exchangers as already presented in the part about splits [chapter 2.4.2].

The effect of this defect is more relevant for the reduction of the airflow induced by the increased pressure drop following the characteristic of operation of the condenser fan than the reduction of the heat transfer due to the additional thermal resistance of the dust deposited [Haghigi 2007].

The heat transfer reduction at the condenser side makes the high pressure increase with consequent higher compression power required, the low pressure side remaining the same (Figure 54).

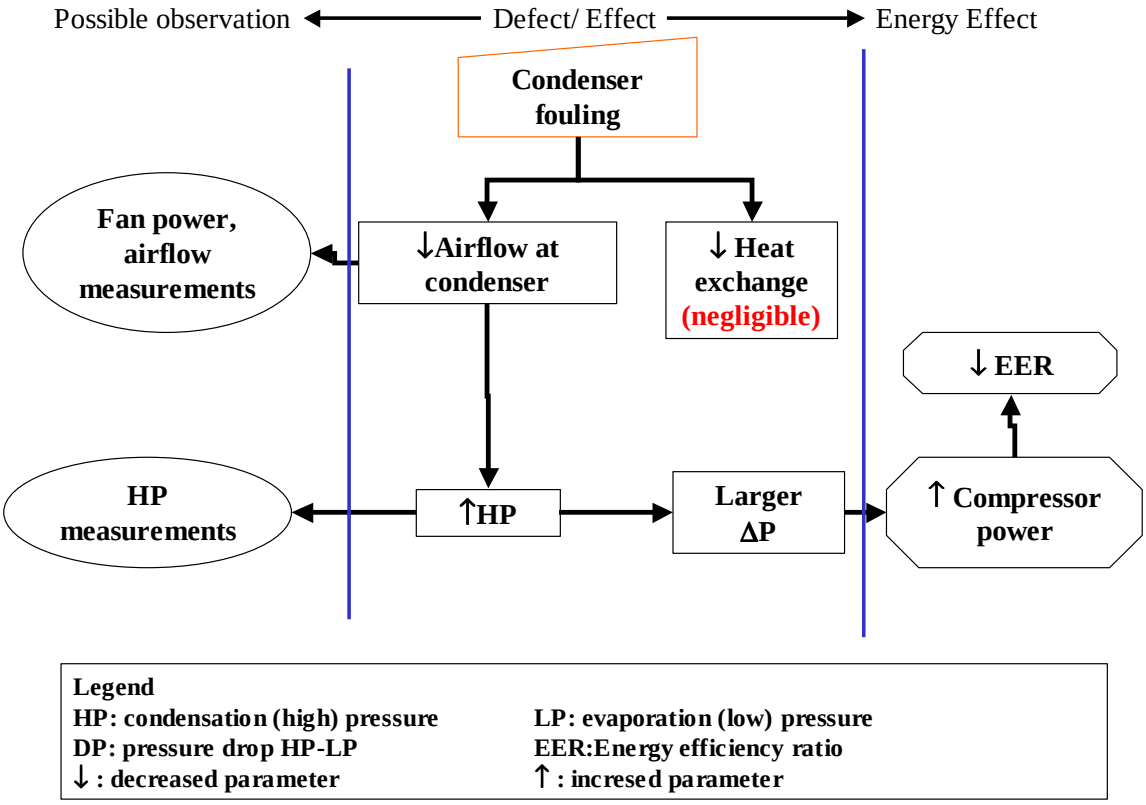

Figure 54: Defect tree for condenser fouling

3.3.3 Presence of non-condensable gazes

When first put into operation, most refrigeration systems can contain gases other than refrigerant that have different condensing temperatures and can remain in vapour state all along the operation of the system. These gases may also accumulate in the system during the operation. They are commonly referred as non-condensable. Non-condensable gases can be a mixture of nitrogen, hydrogen, oxygen, chlorine and other gases. The undesirable gases came from outside the system and are drawn into the compressor along with oil and through leaks in joints, stuffing boxes and the like when the system is operated under a vacuum. They can also enter inside the system by improper evacuation before charging (when the system is temporarily filled with nitrogen), through the lubricant if under the heat of compression various chemical reactions happen within the system and in contamination of the refrigerant supply.

When present, non-condensable gases collect on the high side of the condenser and along the wall (Figure 55) resulting in a higher condensing pressure. These gases form a resistance film over some of the condensing surface, thus simultaneously lowering the heat transfer coefficient. The resistance is very high compared to the other thermal resistances that we can consider it neutralises a portion of the exchange area (Figure 56). Non-condensable gases can be eliminated to a large degree by purging devices[2] that should be used properly in order to avoid refrigerant leaks.

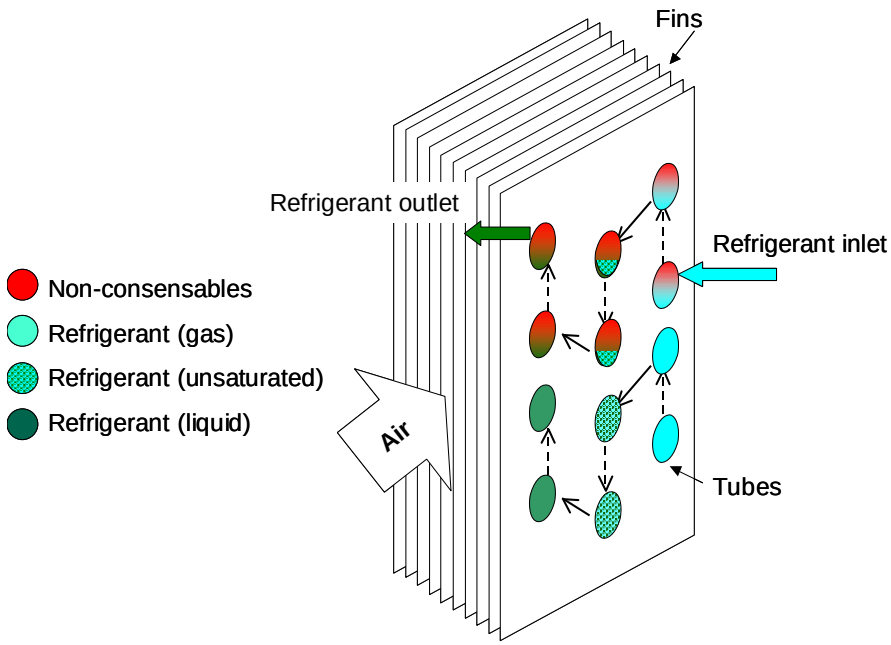

Figure 55: Non-condensable gases accumulation in the condenser

[2] ASHRAE handbook equipment, ARI Standard 580 "Non-Condensable gas purge equipment for use with low pressure centrifugal liquid chillers".

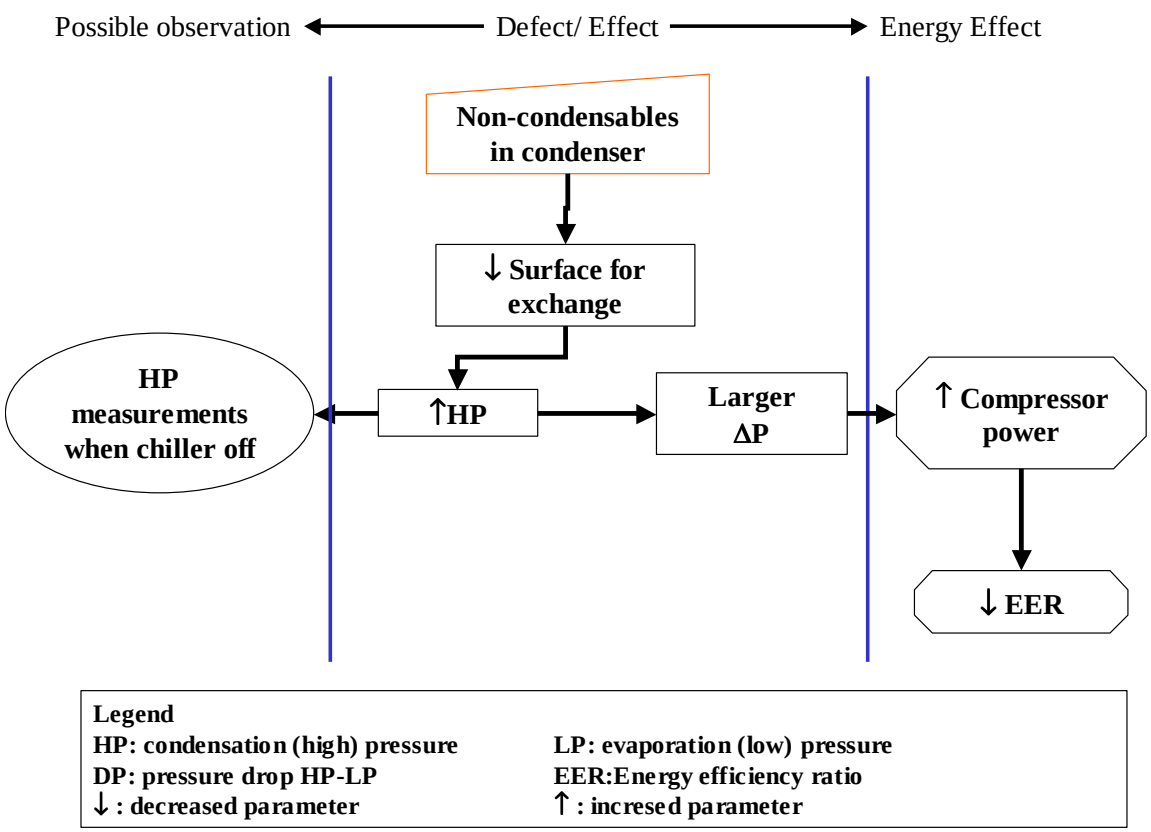

Figure 56: Defect tree for non-condensable gases in the refrigerant loop

3.3.4 Valve defects

Expansion valves may fail in these ways:

- Clogging or blockage
- Sticking either open or closed, or partially open or closed
- Loss of proper metering ability due to wear, or an internal failure

Any of the above conditions could cause the wrong amount of refrigerant to be introduced into the evaporator, which could lead to improper system operation. Any of these problems will require replacement of the expansion valve. The most encountered problem is the clog of the valve by debris introduced in the refrigerant loop and it will be the only one taken into account in this study.

Once debris are stuck in the valve, the reduction of the cross section of the valve reduces the amount of circulating refrigerant flow reducing the heat exchanges: the capacity is lowered, at the same time the compressor would compress a lower mass, the absorbed power would be lowered too. The global effect is anyway an efficiency reduction (Figure 57).

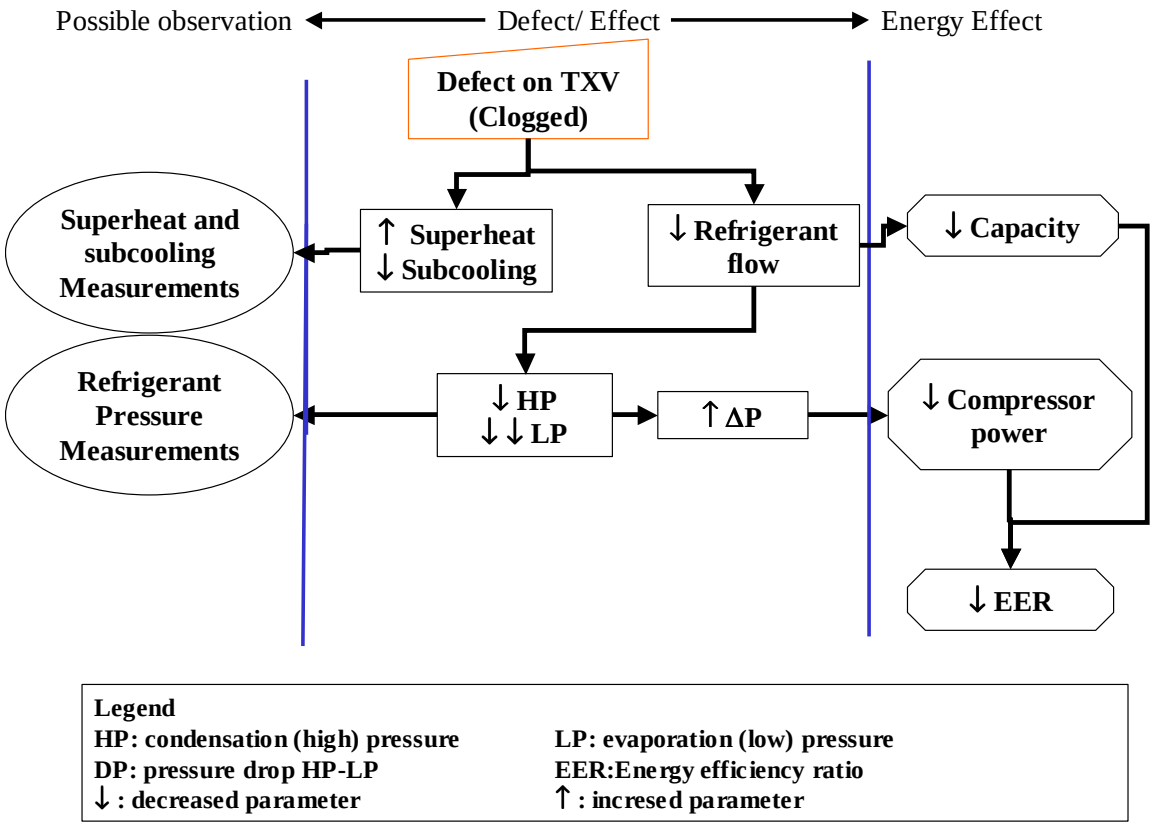

Figure 57: Defect tree for clogged valve

3.3.5 Compressor faults

Scroll compressors represent nowadays one of the best technologies on the market for their robustness. They display a certain number of advantages compared with other compression technologies such as reciprocating compressors. Large suction and discharge ports reduce pressure losses incurred in the suction and discharge processes. Also, physical separation of these processes reduces heat transfer to the suction gas. The absence of valves and re-expansion volumes and the continuous flow process result in high volumetric efficiency over a wide range of operating conditions. Scroll compressors offer a flatter capacity versus outdoor ambient curve than reciprocating products, which means that they can more closely approach indoor requirements at high demand conditions. It includes a minimal number of moving parts compared to other compressor technologies. Since scroll compression requires no valves, impact noise and vibration are completely eliminated.

Defects can occur at the internal level (for example when lubrication is not proper) and have direct impact on the compression and on the isentropic efficiency (Figure 58), or at the external level on the motor or transmission with an impact on the absorbed power of the compressor. Only the first type of defect will be considered. The second is an external loss of performance and have as effect only the increase of the absorbed power; it will not be analysed more in detail.

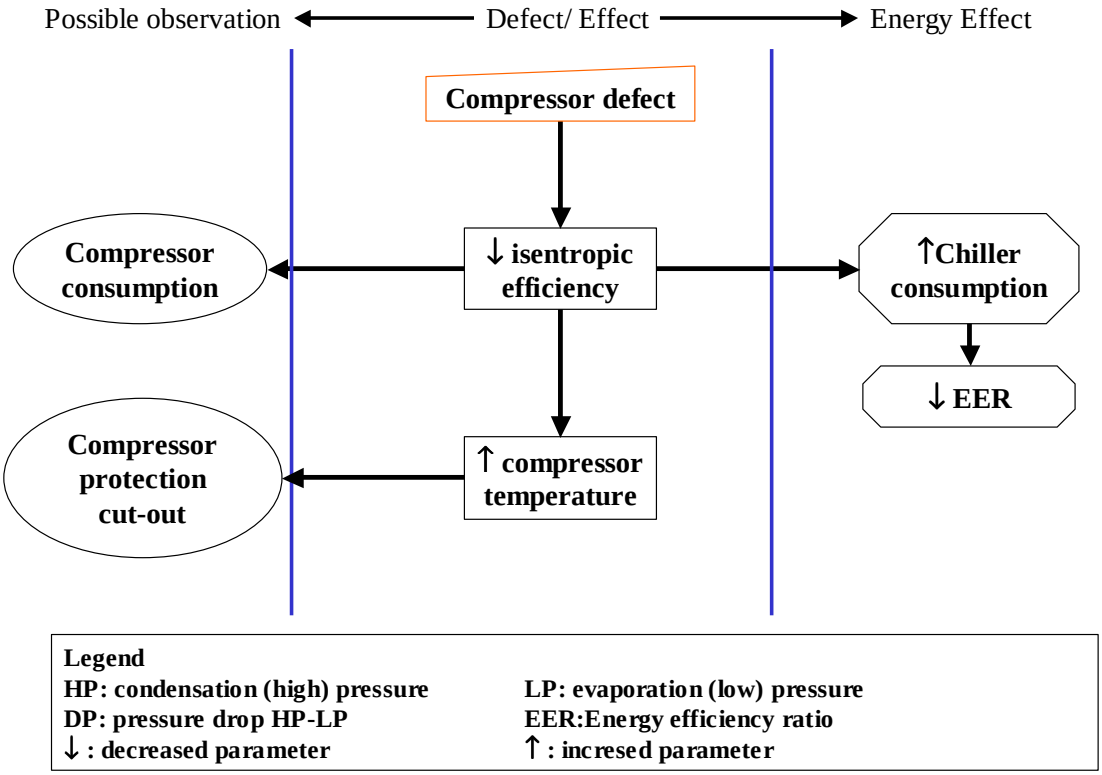

Figure 58: Defect tree for compressor problems

3.3.6 Evaporator fouling or corrosion on chilled water side

The evaporator is a chevron brazed plate heat exchanger. Plate and frame heat exchangers, more commonly known simply as plate heat exchangers (PHEs) owe their higher efficiency in heat transfer to their plate design that features the presence of corrugations or "chevron" (Figure 59). These corrugations force the flow in the plate channels to experience a continuous change in direction and cross-sectional flow area.

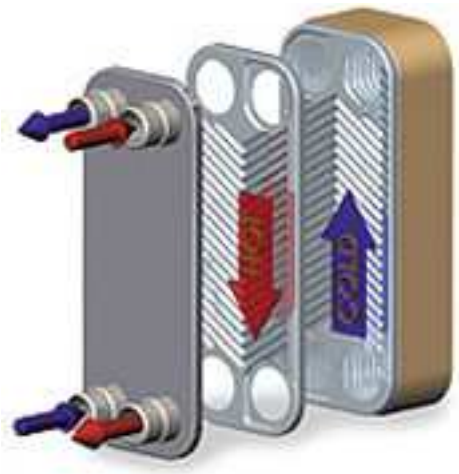

Figure 59: Plate heat exchanger

As a result, turbulence normally expected at higher flow velocities is induced at lower flow velocities. A higher level of turbulence leads to higher heat transfer coefficients and, consequently to a lower heat transfer area requirement for plate heat exchangers. For the same heat load, the heat transfer area

required in plate heat exchangers is considerably lower than that required in shell and tube heat exchangers. Moreover the cost of the heat exchanger is reduced thanks to the use of less material.

Despite their obvious potential for cost and energy savings, plate heat exchangers are not as widely used in the chemical and process industry as other more conventional heat exchangers such as the shell and tube. One of the main reasons behind this lies in the uncertainty of the performance and reliability of plate heat exchangers when fouling is present. Scarce scientific research works have been found on the fouling mechanism for this kind of heat exchangers. This is due essentially to scaling, the chemical deposit layers such as calcium carbonate or magnesium carbonate. The main effects are the reduction of the heat exchanger coefficient and a reduction of the efficiency of the global heat transfer [Bansal 2000].

Some reasons of having deposits specific to plate heat exchangers are:

- The plate heat exchanger inlet dimension is big compared to the inlet between the plates, which leaves a volume area for sedimentation of calcium and other impurities.
- Larger substances like pebbles in the supply water and free rust after dissolving of limestone in the pipelines, which cannot pass between the plates and are deposited in the inlet.
- Impurities of various sizes, which can fasten somewhere between the plates, causing turbulent flow and dead zones, subject to deposits (lime scale).

The global effect of the fouling is contrasted and depends on the localisation of the fouling particles: local deposit formation near the exit would have a significant effect on the pressure drop, while its effect on the heat transfer performance of the entire plate would be considerably less. At the same time, partial blockage of the flow width in the heat transfer section increases the local flow velocities and hence the film heat transfer coefficients, which partly compensate for the additional fouling resistance.

We develop our interest only on the second type of fouling, the first one generally being solved by the use of simple filters in the water loop.

The existing literature concentrates on the scaling of calcium carbonates, as it is the most common scale compound. The main parameters influencing the scaling are the water temperature, the flow velocity and the concentration of the particles. The chemical phenomena are complex and their explanation is out of subject of this dissertation. We will then focus only on the main results of the literature.

We can resume the effect of scaling on the following effects: it adds a fouling heat transfer resistance while the deposition layer reduces the cross section of the heat exchanger and introduces an additional pressure drop. It has been observed that scaling for chevron PHE impacts more on region where the flow is lower; the share effect due to the high flow velocities leads to a lower scale in zones near the diagonal (Figure 60).

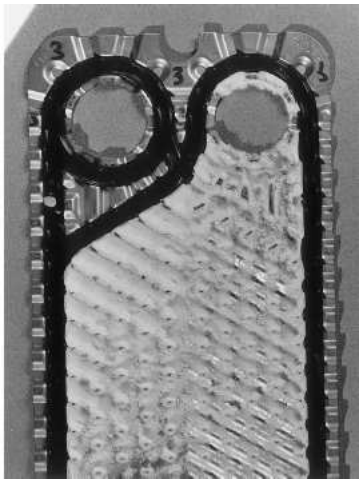

Figure 60: Picture of typical fouled plate from Bansal [Bansal 2000]

Although in the literature results the scaling is uniform on the plates, it is also highlighted that the experimental samples use in general a limited number of plates (often four) and for larger numbers of plates (>20 as in our case) maldistribution is always observed.

Little do we know about the global effect on the performances: the plate heat exchangers scaling contrasting effects are difficult to estimate qualitatively and they are greatly influenced by the relative magnitude of the heat transfer coefficient on the two sides of the plate (water and refrigerant) which are difficult to estimate without enter into quantitative evaluations (Figure 61).

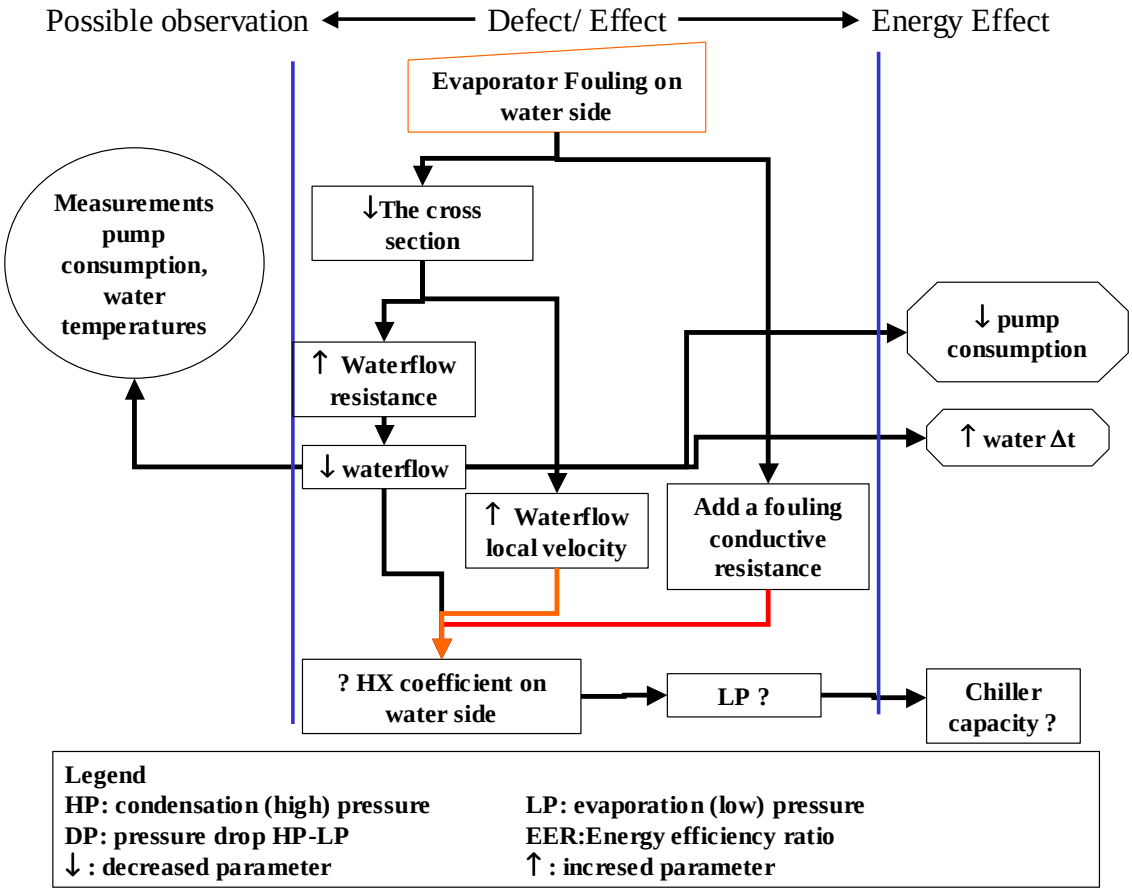

Figure 61: Defect tree for evaporator fouling

3.4 Definition of the chiller model and its validation

3.4.1 Model component and structure

The model used to simulate the chiller in reference conditions has been created by the Ecole des Mines [Kinab 2007] under the C++ environment.

The global model consists in several sub-models of the main components called objects: the compressor, the condenser, the thermostatic expansion valve, the accumulator and the evaporator. The different objects are linked through the refrigerant network: the refrigerant characteristics output of a component is the input of the following one. A set of function is capable of calculating the thermodynamic characteristics of the fluid at each point.

3.4.2 Components model details

The heat exchangers have been subdivided in discrete zones corresponding to the different phases of the refrigerant (liquid, unsaturated, vapour). Both, evaporator and condenser are approximated in counter flow. To calculate the heat exchange (the capacity and the condensing heat), the model uses the approach based on the logarithmic mean temperature differences (*LMTD*):

$$Q = UA \cdot LMTD \quad [34]$$

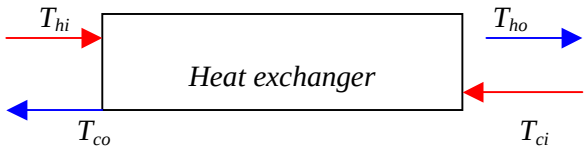

Figure 62: Heat exchanger hot and cold fluids scheme

$$LMTD = \frac{(T_{hi} - T_{co}) - (T_{ho} - T_{ci})}{\log \frac{(T_{hi} - T_{co})}{(T_{ho} - T_{ci})}} \quad [35]$$

Where *h* is for the hot fluid, *c* for the cold fluid, *i* and *o* for inlet and outlet.

UA is the global heat transfer coefficient (W/K), obtained from the experimental correlations applied on both sides of the heat exchange process (*RF* stands for refrigerant). For the condenser:

$$(UA)_{condenser} = \frac{1}{\frac{1}{h_{RF}} \cdot \frac{A_{Air}}{A_{RF}} + \frac{1}{h_{Air}}} \cdot A_{Air} \quad [36]$$

For the evaporator the two exchange areas are identical and the global coefficient is:

$$(UA)_{evaporator} = \frac{1}{\frac{1}{h_{RF}} + \frac{1}{h_{water}}} \cdot A_{plates} \quad [37]$$

The compressor operation is translated through its isentropic and volumetric efficiencies as a function of the compression rate β (Figure 63).

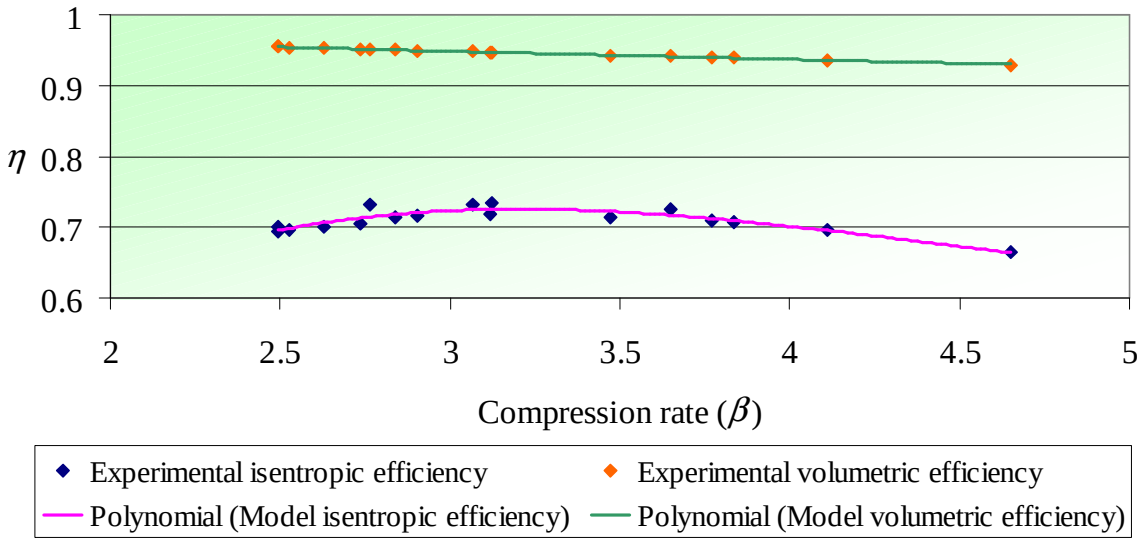

Figure 63: Compressor model and experimental characteristics as a function of the compression rate

The volumetric efficiency can be represented in good approximation by a linear relationship:

$$\eta_{vol} = a_0 + a_1 \cdot \beta \quad [38]$$

The isentropic efficiency relationship has been represented in the form developed by Dehausse [Dehausse 1974] that allows accurately representing the shape of the curve as:

$$\eta_{isen}=k_1+k_2\cdot(\beta-r_1)^2+\frac{k_3}{\beta-r_2} \quad [39]$$

The coefficients have been obtained by a set of experimental data:

a_1=0.983
a_0=-0.0116
k_1=0.935
k_2=-0.00895
k_3=-0.188
r_1=-0.230
r_2=1.41

The expansion is assumed to be a process without heat exchange neither work drawn or produced, thus it is an isenthalpic expansion. In the chiller model, a thermostatic valve is used as flow control device: a bulb is placed at the exit of the evaporator which feeds back the superheat, and adjusts the mass flow to the evaporator in order to maintain a constant superheat, it guaranties the steadiness of the capacity and prevents liquid refrigerant from entering the compressor. Inputs of the model are the inlet enthalpy and pressure, the outlet pressure and the superheat.

The valve mass flow rate model depends on the pressure difference between the condenser and the evaporator, and on the superheat (*SH*):

$$\dot{m}=k\cdot SH\sqrt{\frac{(p_i-p_o)}{\rho_i}} \quad [40]$$

Where k is a coefficient specific to the expansion valve considered that has been modelled as a quadratic function of the SH:

$$k=a\cdot SH^2+b\cdot SH+c \quad [41]$$

The coefficients have been obtained by a set of experimental data, and are different depending on the operation with two or one compressor:

Two operating compressors:

$a = 2.56\cdot10^{-08}$

$b=-6.25\cdot10^{-07}$

$c=5.40\cdot10^{-06}$

One operating compressor:

$a = 4.23\cdot10^{-08}$

$b=-6.91\cdot10^{-07}$

$c=4.12\cdot10^{-06}$

An accumulator is also present in the real system and is added to the model as a neutral element where the fluid is collected with no transformation or transfer.

3.4.3 Model convergence criteria

The model was initially designed in order to calculate the system properties for fixed subcooling conditions. The model flowchart is shown in Figure 64.

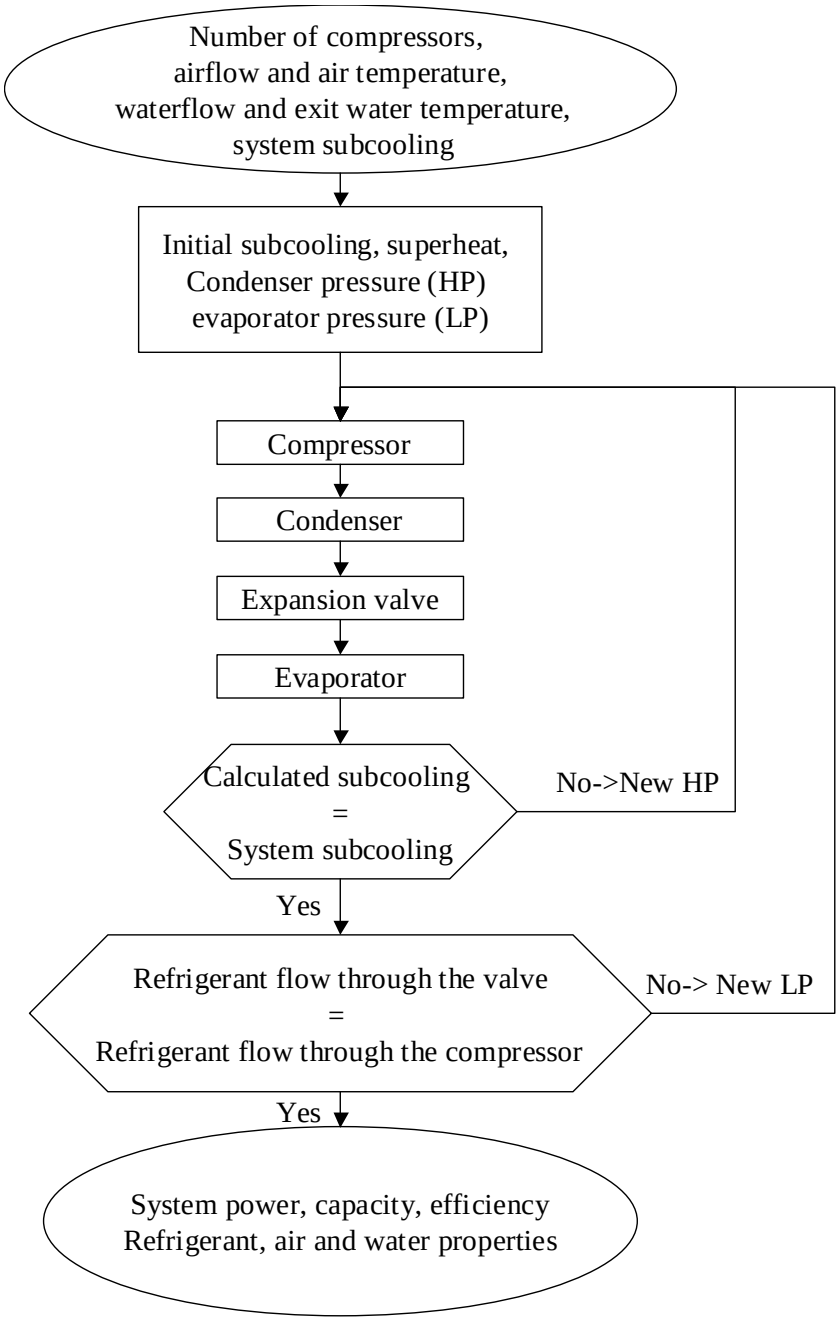

Figure 64: Model scheme for convergence on subcooling

Nevertheless, the defects have a great impact on the subcooling as we have already seen for the split system case; we developed a second version of the model that takes into account the charge as a condition of convergence as in the flowchart below.

The charge is calculated as the sum of the charge contained in every components: after the first simulations we could observe that only the heat exchangers, the accumulator, and the liquid line include fluid masses that are significant. The compressor fluid mass can be then neglected. A major difficulty in charge inventory analysis is proper prediction of the refrigerant mass in the two-phase regions of the condenser and the evaporator. This is because of two basic uncertainties: the degree of vapour-to-liquid slip at each cross section in the two-phase region, and the variation of refrigerant quality with length through the two-phase region. In this case the mass is calculated as:

$$m = m_g + m_l = \rho_g \cdot A_c \int_0^L \alpha \cdot dl + \rho_l \cdot A_c \int_0^L (1-\alpha) \cdot dl \qquad [42]$$

Where α, void fraction, is defined as the ratio between the section occupied by the gas and the total cross section:

$$\alpha = \frac{A_g}{A_c} \qquad [43]$$

Several models exist nowadays that allow estimating the void fraction coefficient. In our model, the mass inventory for the heat exchangers takes into account the density in the two-phase regions of the condenser and evaporator using the Zivi void fraction correlation [Zivi 1964]. This correlation has been chosen for its simplicity, α being:

$$\alpha = \frac{1}{1+\left(\frac{1-x}{x}\right)\left(\frac{\rho_g}{\rho_l}\right)^{2/3}} \qquad [44]$$

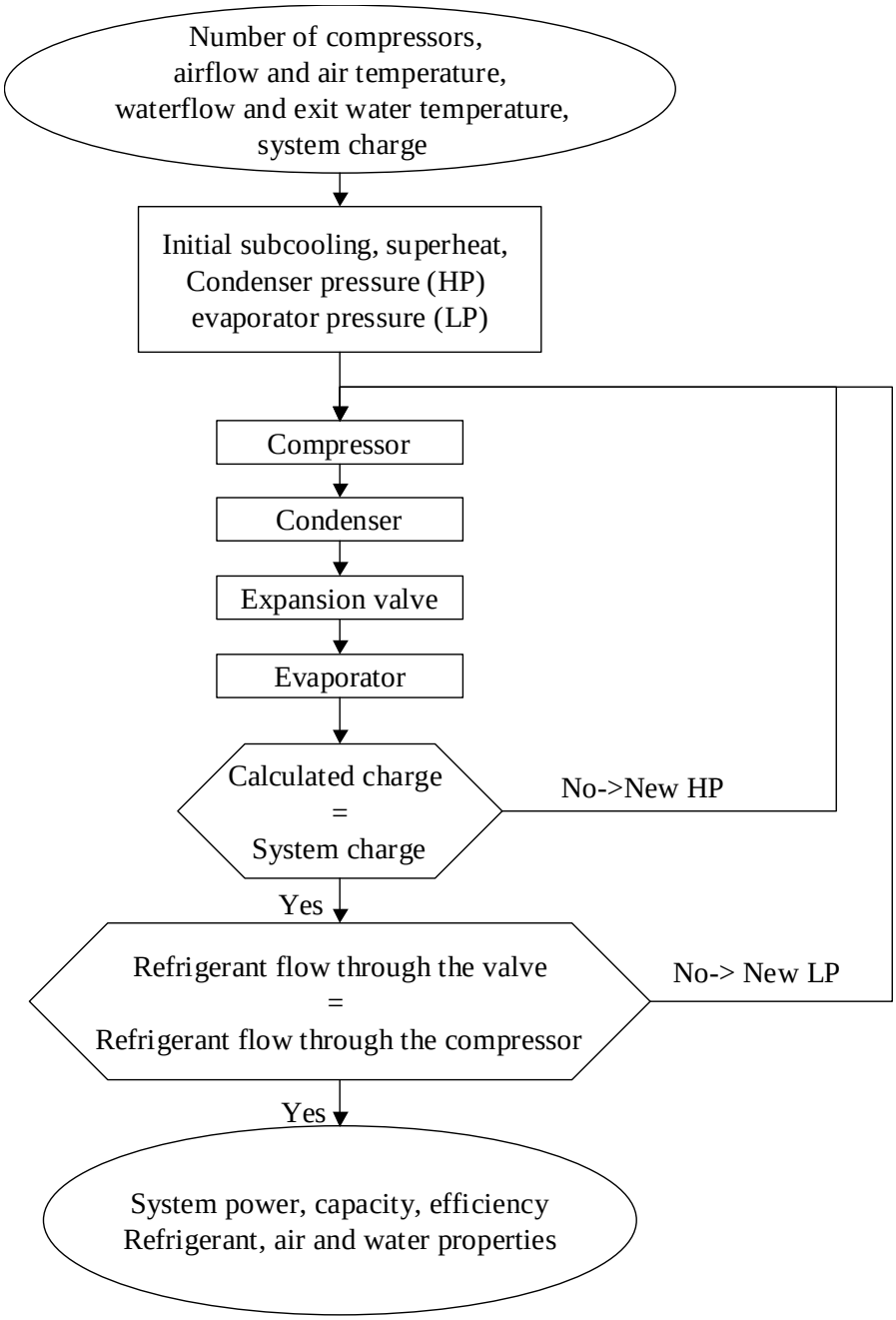

Figure 65: Model scheme for convergence on refrigerant charge

The first model is used in order to estimate the refrigerant charge in the system that is introduced in the second. We obtained it for several points for a fixed subcooling of 5 °C. For fixed subcooling, the charge varies slowly but is in general in good agreement with the experimental mass (22 kg) as shown in the table below.

Table 18: Model calculated mass for different outdoor temperatures at 7 °C outlet water temperature for a fixed subcooling (5 °C)

Calculated mass (kg)		Air inlet temperature (°C)
2 compressors	1 compressor	
20.8	20.5	35
21.3	20.4	30
22.1	21.3	25
22.5	22.3	20

The version with convergence on the mass is more accurate than the first one because it takes into account the real behaviour of the machine that shows variable subcooling at different temperatures conditions. On the other hand the model is more sensitive to the initial parameters and appears to have more convergence problems.

3.4.4 Model adaptation and comparison with actual performance

The model was initially designed to represent a heat pump with R410A fluid. The properties of the R407C have been entered in the model starting from correlations from the CBAT software [CBAT 2000].

R407C is a ternary fluid, its components and their amounts are:

- R 32 (23 %)
- R 125 (25 %)
- R 134A (52 %)

A particular feature is its behaviour during phase change: the temperature does not remain constant while condensing or evaporating, the temperature glide varies with the pressure and is quite important: of ~6 °C at the condensing pressure values normally used in the chillers.

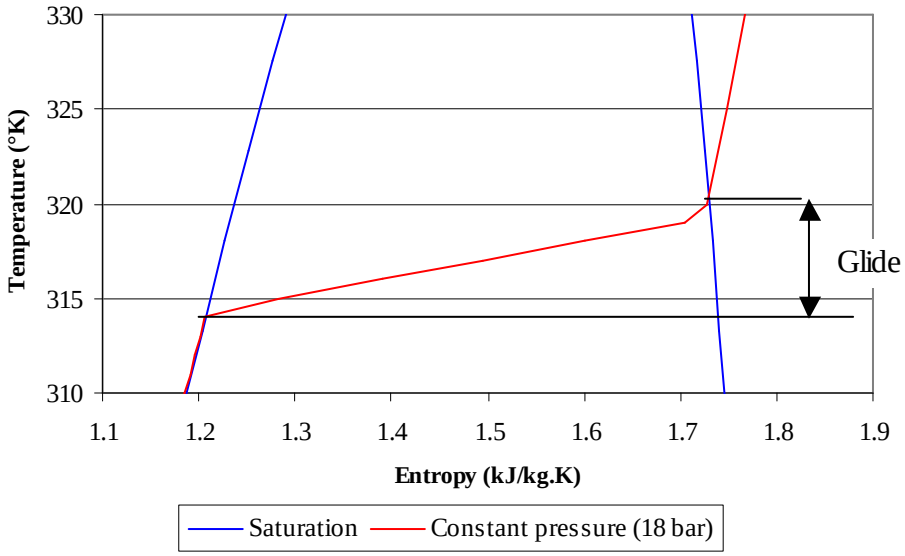

Figure 66: Temperature glide during evaporation at constant pressure for R407C [REFPROP7]

A set of new variables has been entered in the model in order to take account of this phenomenon and of the variation of the properties of the fluid due to the temperature glide: the saturation temperature has been separated in two variables, the dew (saturated vapour) and the bubble (saturated liquid) temperatures at constant pressure.

3.4.5 Hypotheses, simplifications and uncertainties

The main simplifications that have been applied to the model are:

- The pressure drops in the heat exchangers are neglected
- The refrigerant fluid properties in the two-phase region are considered as an average of the properties at vapour and liquid saturation conditions at the same pressure weighted by the quality of vapour.
- The oil presence was neglected

The first approximation leads to an overestimation of the performance of the system: the compressor meets no network resistance and provides only the energy needed to have enough refrigerant to satisfy the cooling need.

The second approximation is needed in order to determine the mass included in the accumulator where the fluid is in the two phases region and we considered the element as a static element in equilibrium.

The third one is often made in heat pump models: the behaviour of the refrigerant and oil mix is not enough well known to be modelled.

The chiller being constituted of two twin circuits, we consider just half of the system, including two compressors that can be started separately. We can obtain the global performance as a sum of the performance of the subsystems. The load level of 75 % is composed coupling the operation of two compressors together plus the single compressor operation; the 100 % is the double of the two compressors operation.

The results of the model for the two and single operating compressors have been compared to several experimental points. The model for the two operating compressors has shown to initially fit poorly with the real chiller with errors magnitudes greater than 10 % with large errors on the cooling capacity. Fit coefficients have been introduced to improve it. The coefficients have been applied to the valve and compressor refrigerant flow models in order to increase the refrigerant flow and to reduce the error. The model sensitivities to the correction factors are shown in the figure below for the efficiency and the cooling capacity, the errors are the averages on the several available experimental points.

Figure 67: Model sensitivity to the valve and compressor flow correction factors

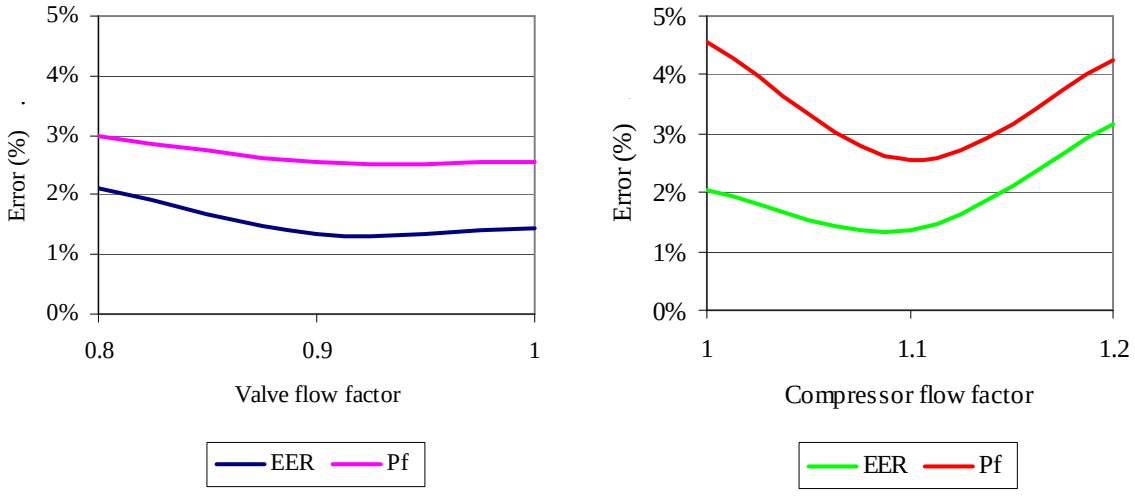

The correction has a great influence on the superheat and the subcooling also. The results obtained for the corrected model for a water temperature set to 7 °C and outdoor air to 35 °C are showed in Table 19.

Table 19: Comparisons between model and experimental data for water temperature of 7 °C and air temperature of 35 °C.

2 compressors	*Pc* (kW)	*Pa* (kW)	*HP* (bar)	*BP* (bar)	Refrigerant flow (kg/s)	*EER*	Subccoling *(°C)*	Superheat *(°C)*
Experimental data	76.8	28.9	22.7	5.5	0.52	2.66	5.0	5.7
Model data	81.5	29.6	20.6	5.1	0.53	2.76	7.7	5.4
Δ(%)	5.8%	2.3%	-9.8%	-7.7%	1.9%	3.5%	x	x
1 compressors								
Experimental data	39.1	12.0	18.5	5.8	0.28	3.25	0.5	3.7
Model data	42.1	12.5	16.9	5.2	0.3	3.4	1.4	3.9
Δ(%)	7.1%	3.8%	-9.7%	-11.9%	-2.4%	3.4%	x	x

The model is in quite good agreement with the experimental data after the application of the correction factors except for the pressures that are always underestimated by the model: this because of the neglected pressure drops in the heat exchangers.

If we consider the comparison with other experimental points, the efficiency is well modelled with errors always lower than 10 % (Figure 69).

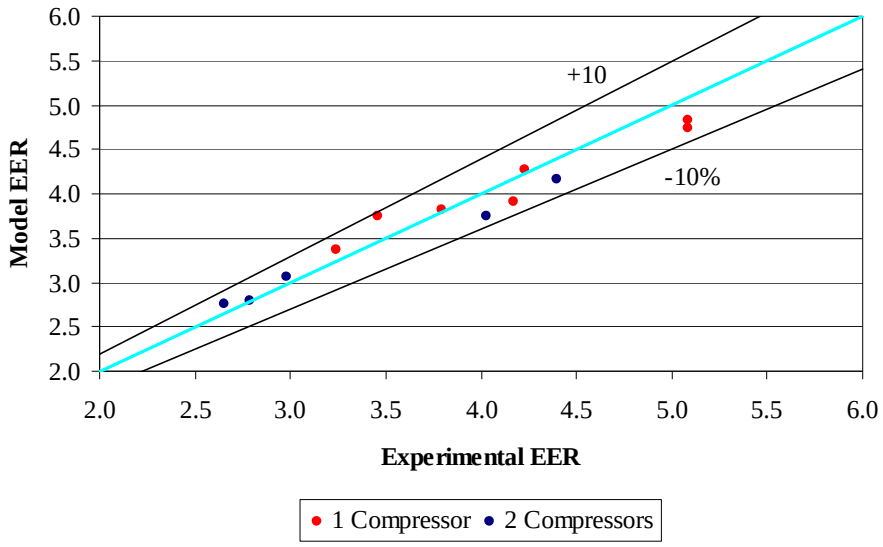

Figure 68: Comparison between experimental and model EER for different air and water temperatures

The model errors on the efficiency are slightly higher for the single compressor than for the tandem operation.

The errors on the other parameters are shown in Figure 69. Errors are in general higher for the point were the compression rate is lower because the model is more uncertain for the extreme values of the compression rate.

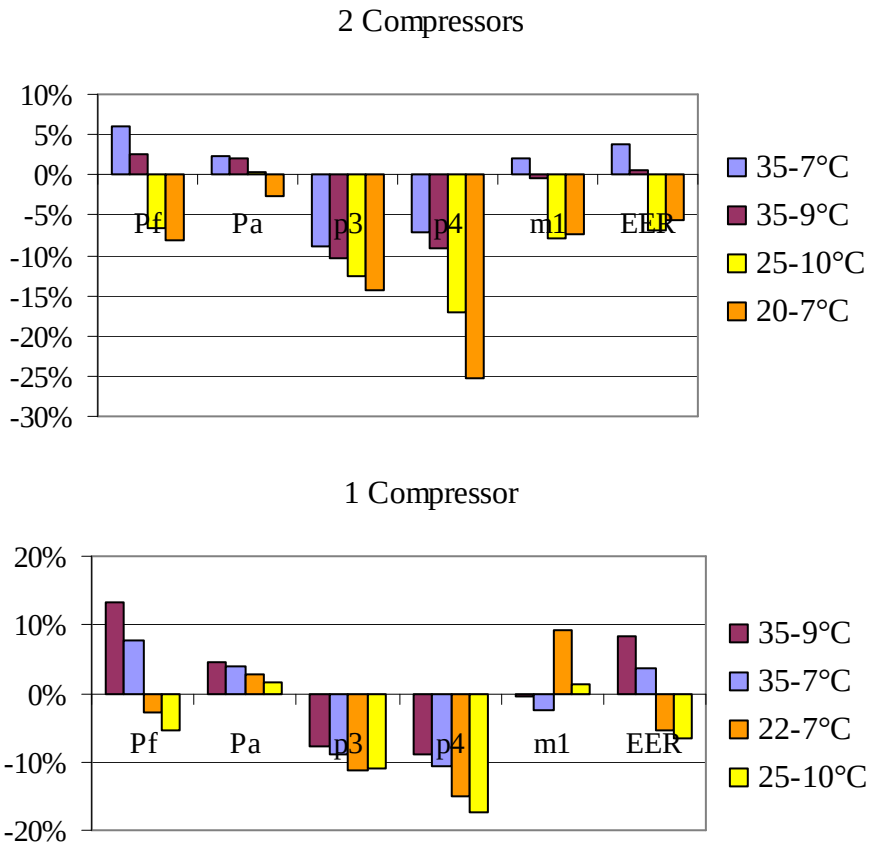

Figure 69: Errors of the model for one and two operating compressors comparing to experimental data

3.5 Results about defects

Preliminary indication about results

Before going deeper in the analysis of the effects on the system of the several defects, we have to point out that some defects have a negligible impact on the operation with one compressor. This is mainly due to the oversized heat exchanger for the single compressor operation. That is why we will not present in the following section the results for one operating compressor except for cases where the impact is significant: in that case the results will be displayed. It is important then to observe that having several capacity stages allows having chillers not only more efficient at partial load conditions but also less sensitive to the defect than one staged chillers.

Because of the uncertainty of the fans consumption and model, the *EER* ratios shown from now on do not take into account the fans consumption and are simply considered as the ratio between the capacity (P_c) and the absorbed power at the compressor (P_a):

$$EER=\frac{P_c}{P_a} \qquad [45]$$

3.5.1 Refrigerant leaks

Although the chiller model allows theoretically simulating different charge levels, in reality the charge reduction cases that we could simulate were few. The reduced charge in the condenser, makes the subcooling decrease until it becomes zero. When no subcooling occurs the equations of the valve are not valid anymore and the model is not appropriate. We could then only simulate fully a loss of charge of 10 % and 15 %.

For refrigerant charge reduced by 20 %, only the simulations at higher outdoor temperatures (35 °C and 30 °C) did converge. In these cases we can observe subcooling values of 0.001 °C (Figure 70).

For lower outdoor temperatures the subcooling would probably be negative, the refrigerant exit from the condenser in two-phase and flow into the valve.

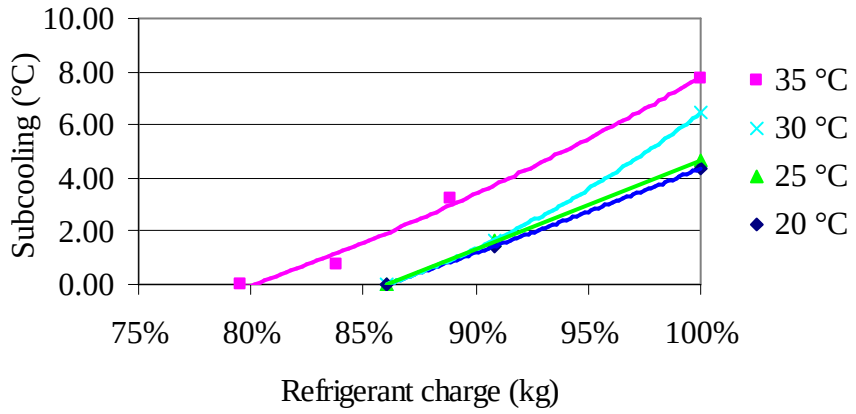

Figure 70: Subcooling as a function of the refrigerant charge

In reality, the expansion model of equation [40] is valid only for saturated refrigerant, for unsaturated condition the refrigerant density changes quickly and the model is not appropriate anymore. The valve position is set in a section that is suitable for liquid refrigerant, but the unsaturated refrigerant has a density lower than liquid, reducing the refrigerant flow.

The effect of the refrigerant leak is a loss of capacity and a simultaneous reduction of the absorbed power. If the chiller has an optimised initial charge, the charge reduction leads to a global reduction of the efficiency. The effect is more noticeable for higher temperatures.

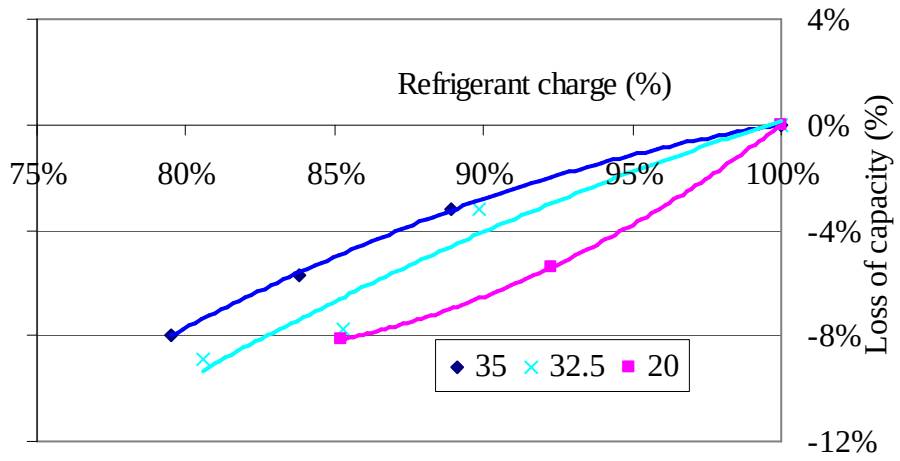

Figure 71: Capacity losses for different refrigerant charge levels

We could thus only fully develop the 10 % leak for the range of temperatures 20-35 °*C (*Figure 72). For lower temperatures the effect of the charge reduction is stronger on the capacity but also on the absorbed power. Globally for this level of defect the impact is small: the efficiency reduction is less than 3 % and the capacity in the worst condition is lowered by 4%.

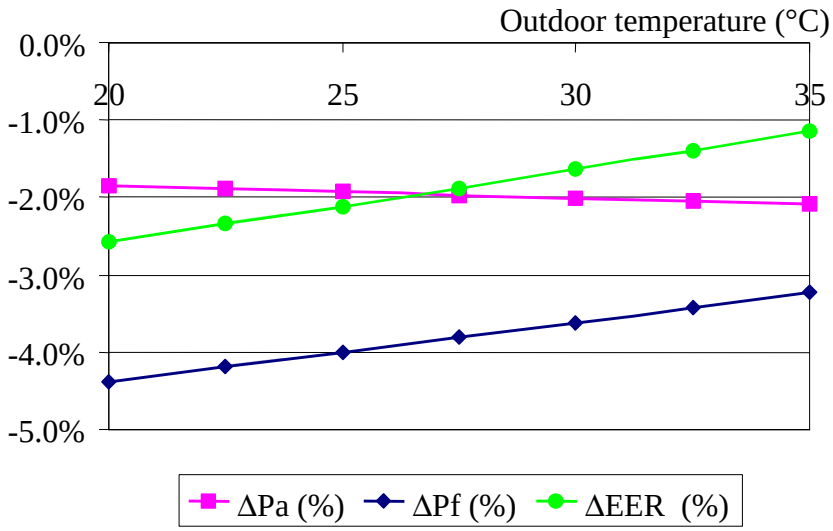

Figure 72: Performance effect of 10 % refrigerant leak (two compressors)

The consequence on the subcooling of the refrigerant leaks forced us to limit our investigation to 10% leaks. Although the model still converges for several conditions for refrigerant charge reduction by 15 %, the subcooling being lower than zero in most of the calculated points, the model mathematically converges, but loose its physical meaning, the behaviour being abnormal.

The loss of charge also influences the one compressor operation, but because of the low initial subcooling for the one compressor operation (~1 °C) only few points at lower charge and high temperatures were available.

In order to validate our results, we can compare the behaviour of the chiller with the results obtained for the refrigerant leaks in the case of the split system (Figure 73). In the chiller case, the refrigerant leaks are compensated by the operation of the valve that reduces by half the impact on the loss of capacity compared to the split case. At the same time, this kind of operation allows leaks to pass unnoticed longer than in the case of a capillary device. That is why systems equipped with thermostatic valves should be object of leaks inspection more frequently than those equipped with a capillary. It also means that before an inspector could be able to detect the refrigerant leak through the visual signal of the liquid spy before the expansion valve (bubbles due to gas entering the valve), the system would have probably lost more than 15 % of its charge.

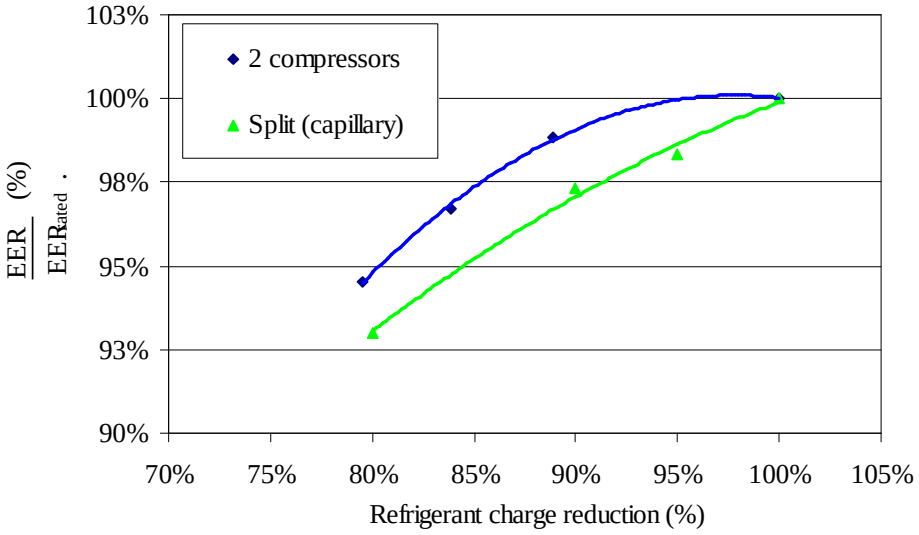

Figure 73: Comparison of the losses of rating efficiency between the chiller and split models

If we look at the literature values [Grace 2000 and California 2005], it seems important to notice that both references showed that refrigerant loses between 20 and 25 % determine an elbow in the performance curve: after this limit, the system losses quickly its efficiency and capacity. In our case this limit is more likely around the 15 % of the charge, value where the subcooling becomes zero for a large range of outdoor temperatures. This value is strongly related to the initial charge level and to the operation range of valve.

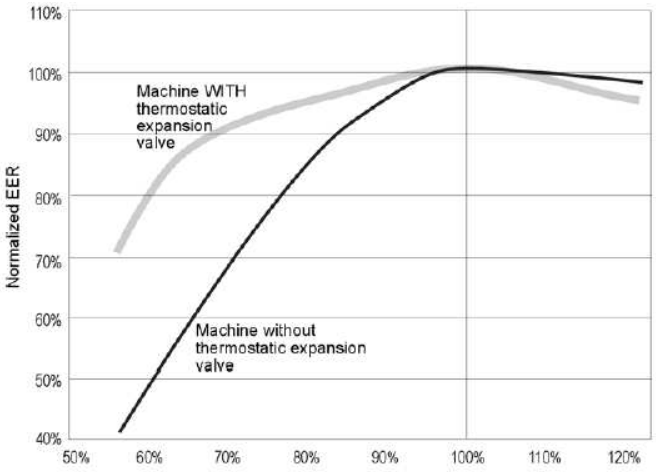

Figure 74: Normalized EER ($EER_{x\%}/EER_{100\%}$) for split systems for several charge levels [California 2005]

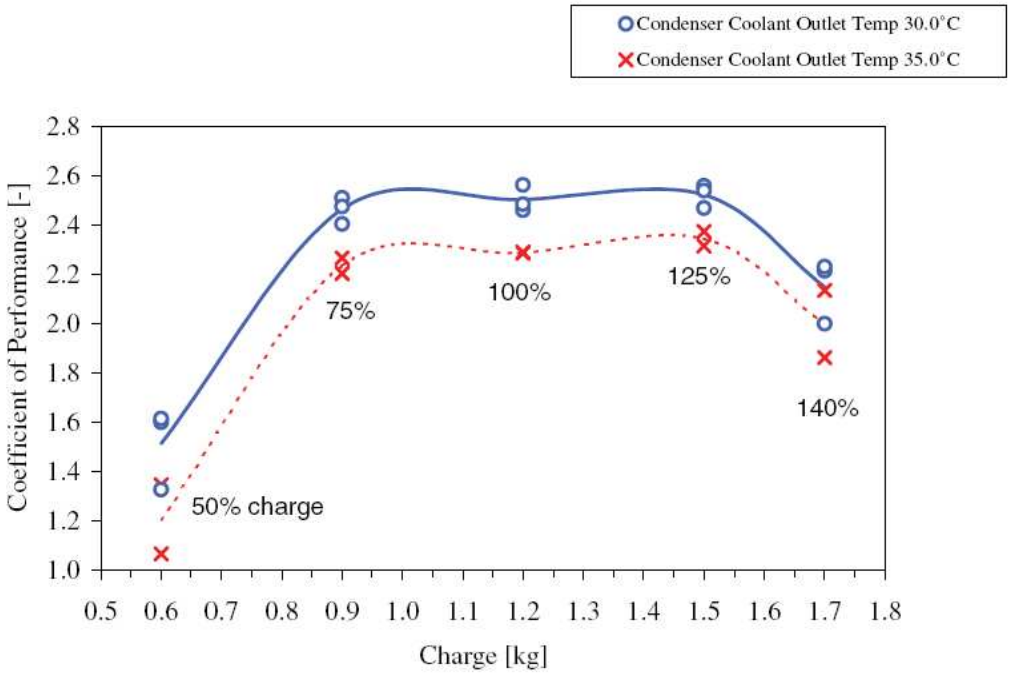

Figure 75: Experimental EER evolution with the charge levels for a water cooled reciprocating chiller [Grace 2000]

3.5.2 Condenser fouling on the air side

The fouling on the air side of the condenser leads to the reduction of the air flow and it has been simulated through the reduction of the air flow from the nominal flow rate (3 fans, 8 000 m^3/h per fan) following the fan characteristic for several levels of fouling.

The condenser fouling increases the resistance to the airflow: the operation point shifts for increased pressure drops decreasing the airflow.

It was not possible to obtain the real fan characteristic from the manufacturer. So the fan characteristic has been obtained from the rated point of operation. From the condenser geometrical data, the Wang

and Chen correlation for louvered fin (see chapter 2.4.2) allowed us to calculate the pressure drop of the fans: 150 Pa. With the hypothesis of a global fan efficiency of 0.45, the rating power absorbed by the fan is of 900 W. The calculated value corresponds to the catalogue value for the motor size. The rated point is then full defined. In order to build the characteristic, from several manufacturers catalogue curves, we defined a characteristic and an efficiency curve shape through the application of similarity criteria in the range of studied airflows, passing across the known rated point. The obtained fan characteristics are shown in Figure 76 with the operation point for different levels of fouling.

The fouling level is defined (as for the split system) as the increment of the pressure drop curve for the condenser and it is varied from 0 % to 100 % with the subsequent pressure and airflow changes (Table 20).

Table 20: Operation points of the fan for the simulated fouling levels

Increased pressure drop	Airflow (m^3/s)	New Pressure Drop (Pa)
0 %	2.22	150
25 %	2.05	160
50 %	1.93	169
75 %	1.83	177
100 %	1.74	185

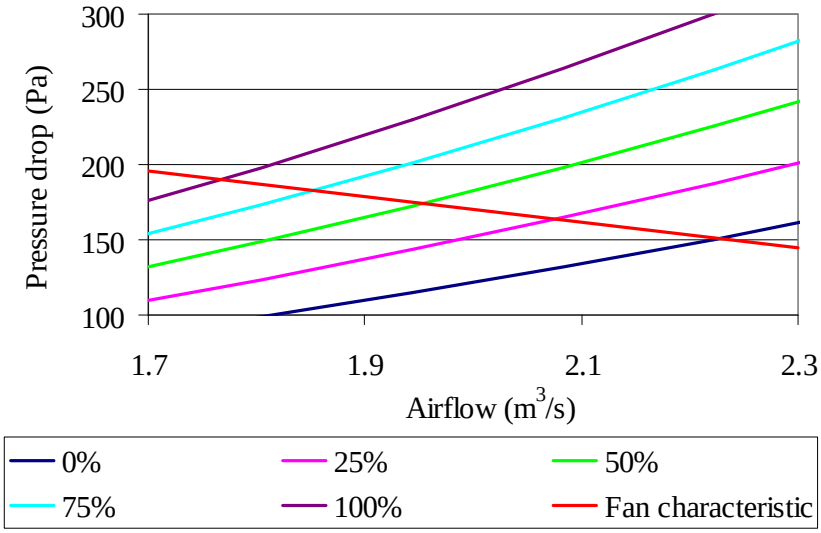

Figure 76: Fan characteristics and condenser pressure drop for different fouling levels

The reduction of the heat transfer at the condenser side due to the airflow reduction implies the modification of the thermodynamic cycle as in Figure 77. The major effects are on the upper part of the cycle and mainly on the condensing pressure and temperature.

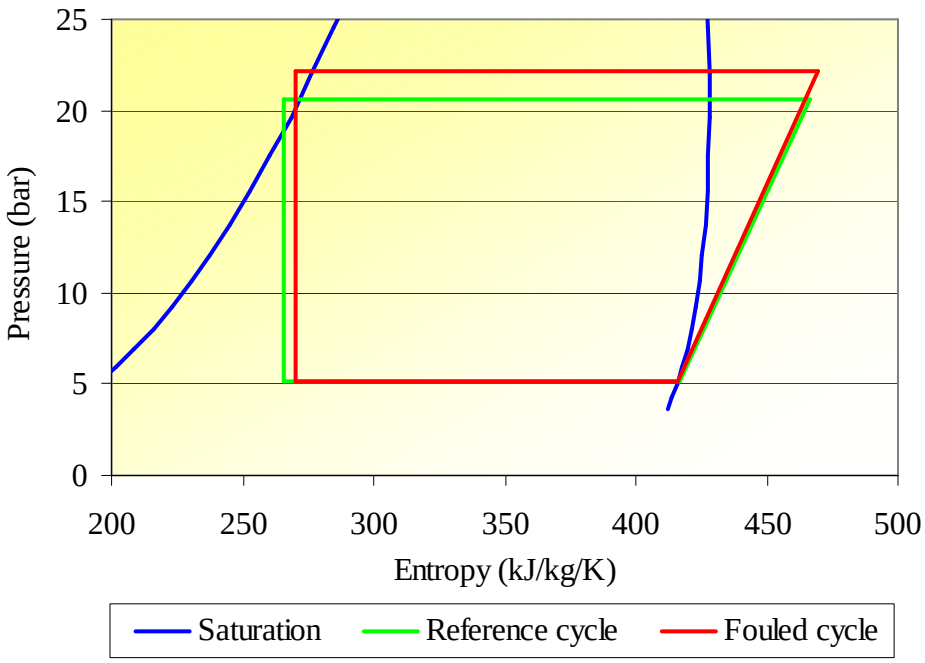

Figure 77: Effect on the thermodynamic R407C cycle of the chiller of the condenser fouling

The increased high pressure increases the compressor consumption, the low side remaining quite the same. The chiller capacity is not influenced except for lower temperatures where the capacity is slowly improved by an augmentation of the refrigerant flow. This is due to the valve range of operation that is able to compensate the higher pressure drop increasing the refrigerant flow for lower temperatures. It results in a higher impact on the performances at higher outdoor temperatures (Figure 78).

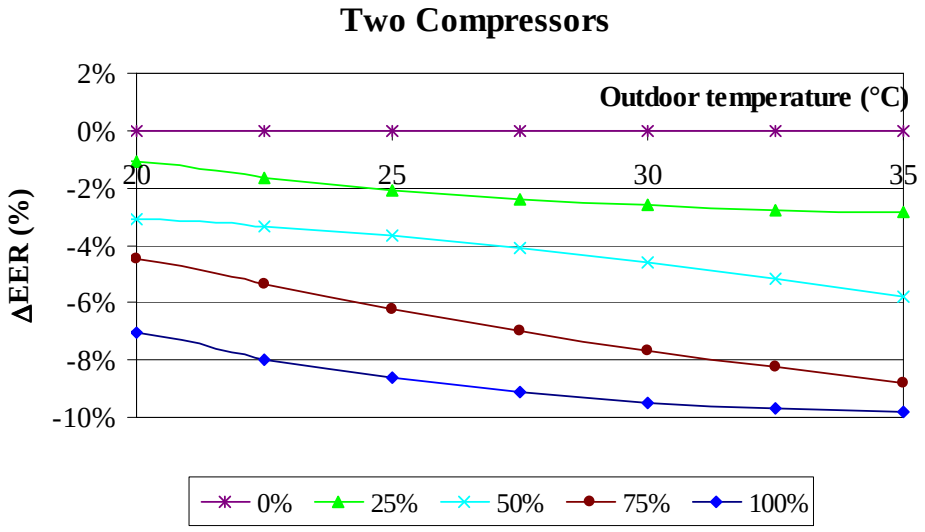

Figure 78: Effect on the efficiency for the tandem for increased condenser pressure drop

The reduction of the airflow has a slight effect on the performance for the one compressor operation (Figure 79) and in some cases manufacturers control the fans to operate at reduced speed (and reduced airflow) in order to save energy when balancing the overconsumption of the compressor with the savings at the fan motors for low loads.

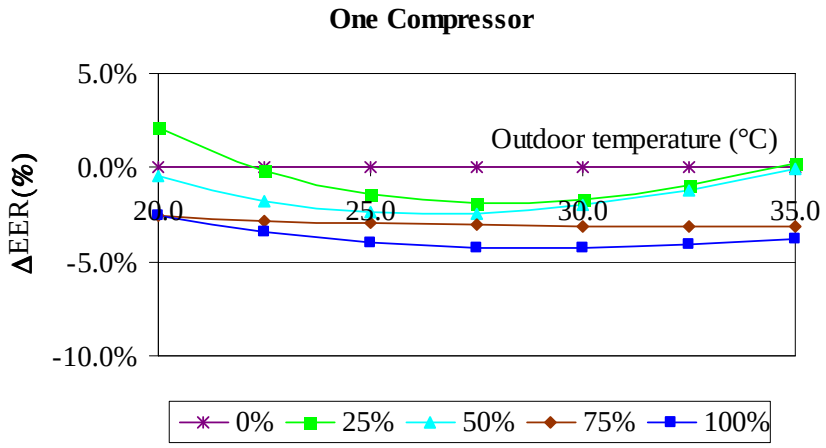

Figure 79: Effect on the efficiency for the one operating compressor for increased condenser pressure drop

For the investigated chiller different fan characteristics for different rotation speeds could be created from manufacturer catalogues (EBM-PAPST catalogue).

When the fan that initially operates at speed n_0 is set at new speed n_1, lower than n_0, it displaces its operation point from A to B of figure 80 and the pressure drop curve being the same, the airflow is reduced to q_0 to q_1.

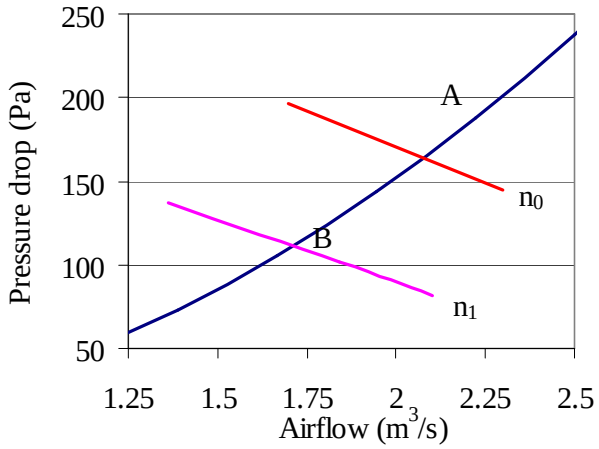

Figure 80: Operating points of fan at nominal (n_0) and lower speed (n_1)

The power absorbed by the fan is lower. If we consider the power reduction for the fan ΔP_{fan} and the compressor overconsumption ΔP_{compr} for the new operation point, they can be calculated as:

$$\Delta P_{fan}(n_1) = \alpha \cdot P_{fan}(n_0) \quad [46]$$

$$\Delta P_{comp}(q_1) = \beta \cdot P_{comp}(q_0) \quad [47]$$

Where α is the coefficient for fan power reduction, and β the coefficient for compressor overconsumption. The global energy savings are:

$$\Delta P_{global} = \Delta P_{fan}(n_1) \cdot N - \Delta P_{comp}(q_1) \quad [48]$$

Where N is the number of operating (identical) fans. We can assume α=40 %, from the manufacturer catalogues curves, and β=4 %, calculated from the previous simulations for a reduced airflow of 20 % at lower speed. Multiplied for the three operating fans, the energy savings amount is of 1.1 kW.

The comparison with the experimental data from Comstock [Comstock 2001], confirm the list of the chiller parameters more sensitive to this defect: mainly the increase of the high pressure, subcooling and the air temperature difference across the condenser.

3.5.3 Non-condensable accumulation in the refrigerant circuit

The presence of non-condensable gases in the chiller has been translated in the model by neutralising a part of the condenser surface available for the heat exchange. This means that the condenser area for refrigerant and air have been reduced with respect to the initial amount. The parameter has been varied between 0 % and 30 %. The volume occupied by the non-condensable gases is then considered constant for each test conditions: it is not physically true because the gases will expand or compress following the condenser pressure and the outdoor temperature. It is anyway very difficult to estimate the non–condensable truly occupied volumes as they are spread in the tubes length, between the refrigerant and the tube walls: the heat exchange is very complex.

The volume will be considered constant.

The global effect is very similar to the previous condenser fouling. It impacts on both operations with one and two compressors, increasing the absorbed power, the capacity remaining undisturbed for the one operating compressor and slowly decreases for the two operating compressors condition.

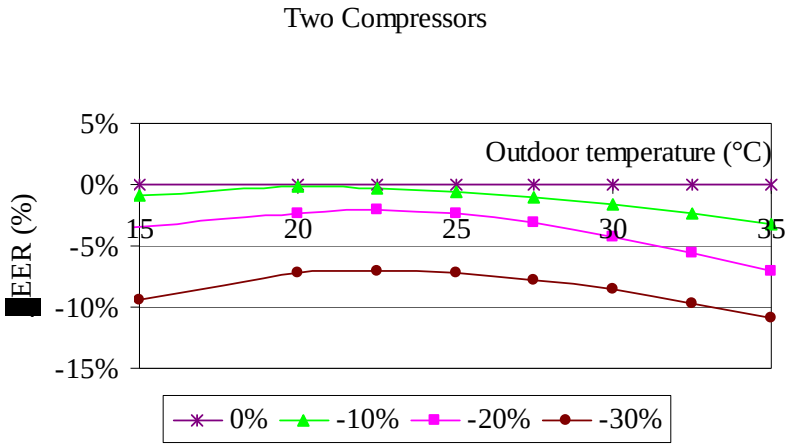

Figure 81: Efficiency variation with non-condensable in the condenser (two operating compressors)

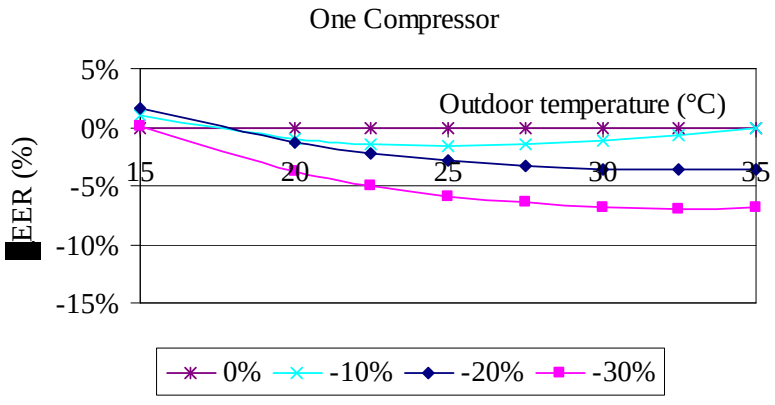

Figure 82: Efficiency variation with non-condensable in the condenser (one operating compressor)

During operation, most sensitive parameters are the same as in the case of the condenser fouling, except for the air temperature difference across the condenser.

The exchanged heat on the airside can be expressed as:

$$Q_{air} = \dot{m}_{air} \cdot c_{pair} (T_{o\_air} - T_{i\_air}) \quad [49]$$

While in the case of condenser fouling the reduced airflow ($\dot{m}$) leads to an increased temperature difference $(T_{o\_air} - T_{i\_air})$, in the case of non-condensables the air heat exchange has small changes with a small increased temperature difference, the most important impact is on the refrigerant side.

One simple approach for detecting the presence of non-condensables is to compare the measured high-side pressure with the saturation pressure at the condenser coil temperature. If the refrigerant charge is correct, then saturated conditions exist in the condenser. By comparing the saturation pressure to the actual high-side pressure, one can determine if there are any non-condensable gasses present in significant quantities in the refrigerant. Non-condensable gasses will raise the actual pressure above the saturation pressure. This method requires an accurate measurement of condensing refrigerant temperature so that the saturation pressure can be determined from a saturation pressure/temperature chart, and it requires an actual condenser pressure measurement.

3.5.4 Clogged expansion device

The effect of the clogging in the expansion valve reduces the cross section and so lowers the refrigerant flow. This defect has been introduced with a factor in the valve model that simulates the cross section restriction. The defect has been considered at two levels: 0.9 and 0.8 restriction area factors.

For the operation with only one compressor, the defect is not significant, although some variations were registered, due more to the convergence ranges than to a real change in the performance: in this case the valve is able to operate properly and still let pass the amount of fluid that ensures the normal operation of the chiller.

For the operation with the tandem, the performance is worsened: the refrigerant flow is reduced and this fact lowers subsequently the capacity of the chiller (Figure 83).

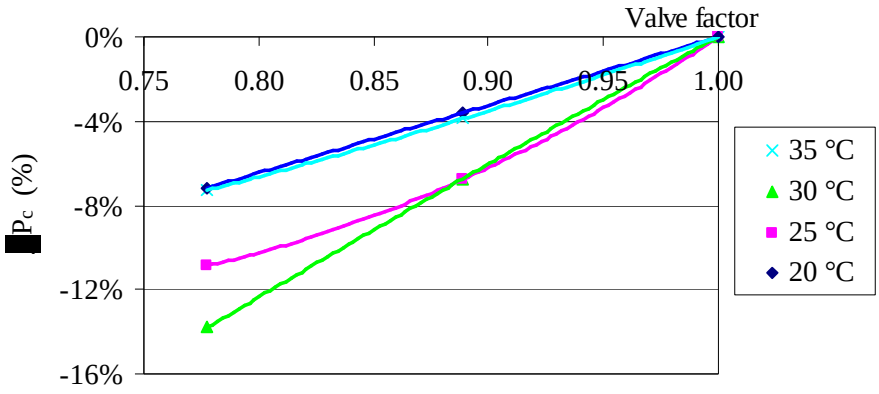

Figure 83: Normalised chiller capacity versus valve refrigerant flow factor

The reduced mass also leads to a reduction of the compressor power but the efficiency is reduced, the reduction of the capacity being higher.

The capacity variation due to the defect is linear with the outdoor temperature that is directly proportional to the refrigerant flow, while the absorbed power shows a quadratic evolution (Figure 84). This because the increased pressure difference leads to better performance at low temperatures, following the compressor isentropic efficiency shape (shown in Figure 63) and to a subsequent reduction of the input power at temperature lower than 20 °C.

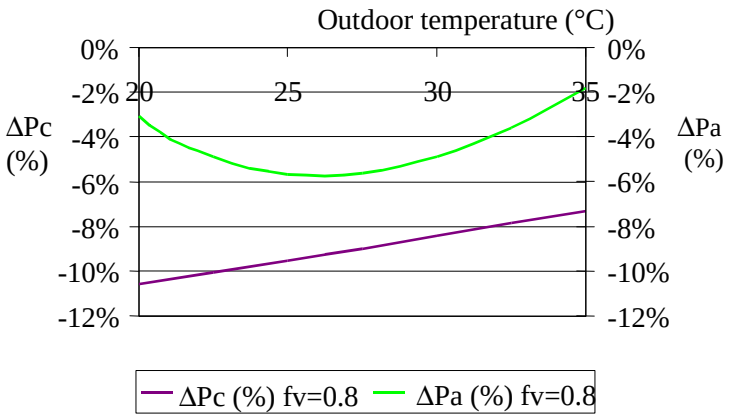

Figure 84: Influence of the clogged valve factor for different outdoor temperature values on the capacity (P_c) and the absorbed power (P_a)

If we look at the experimental data of Comstock this defect is very difficult to detect: the level was tested at only one level and the experimental parameters trends varied strongly with the conditions. Moreover the results show an increased consumption that we could not identify in our simulation for any condition. Unfortunately, it was not clear in the paper how the defective valve was represented and we can imagine that the "defective valve" considered is not defective in the meaning of clog. The main effects are on the superheat that is increased in order to increase the refrigerant flow until the limit of operation of the valve, and the low pressure that decreases.

The clogged valve problem cannot be corrected and it requires inexorably replacing the valve.

3.5.5 Defective compressor

Compressor defect is represented by a variation of the isentropic efficiency. The main source of degradation is the lubrication problems. The defect has been translated in a shift of the isentropic efficiency curve of the compressor of -10 %, -20 % and –30 %.

The effect of the defect is mainly visible on the absorbed power of the machine and it is quite independent of the outdoor temperature. It affects equally the operation with two (Figure 85) and one compressors.

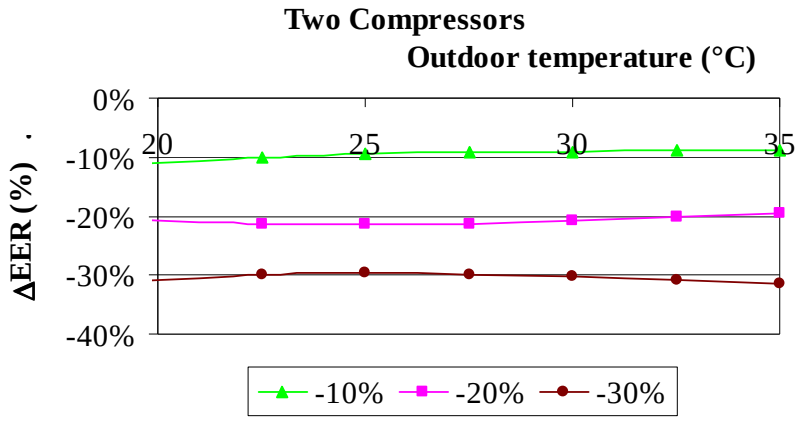

Figure 85: EER effect for worn compressor

The most sensitive parameter beside the absorbed power is the compressor discharge temperature that is increased with the lowering efficiency (Figure 86).

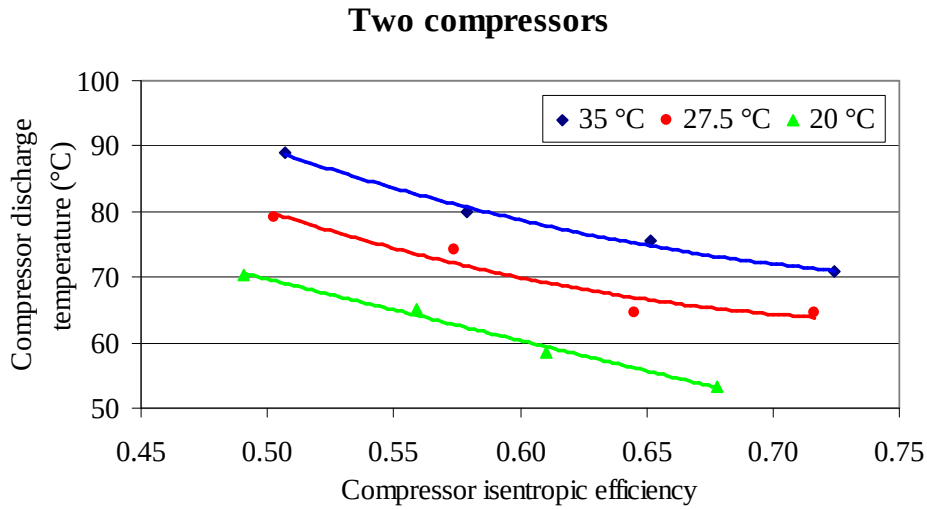

Figure 86: Discharge temperature for decreasing compressor efficiency at different outdoor temperatures

The problem is that this temperature increase can be locally very important and can burn the lubricant oil leading to a worsening of the problem. In general this defect leads very quickly to the failure of the system. The higher discharge temperature leads also to an increase of the temperature range of the condenser and to a higher air difference of temperature across the condenser but too small to be detected.

We could not compare our results with experimental data because the reviewed literature does not consider the compressor wearing except for reciprocating technology where the wearing is referred to the loss of volumetric efficiency. However, we could compare the method used and results obtained with the model developed by McIntosh and Mitchell [McIntosh 2000]: the authors used a chiller model to identify the characteristic quantities for several defects based on a centrifugal chiller model. The worn compressor was simulated as in our case by introducing a degradation factor in the isentropic efficiency model. The authors identified as the only characteristic parameter for the compressor defect detection the isentropic efficiency and the overall energy efficiency.

3.5.6 Evaporator fouling on the water side

The scaling on the waterside of the evaporator determines the reduction of the water flow due to the reduction of the hydraulic diameter and an additional thermal resistance on the plates due to the deposit.

The water flow is reduced by 14 % and 30 % of the nominal flow rate (7.4 kg/s).

It is also introduced a thermal resistance due to the fouling. The literature values showed experimental magnitude of fouling resistance after 6 000 min of 0.00003 m²K/W [Bansal 2000] and after 6 000 min of 0.00002 m²K/W [Kho 1997]. We kept the first precautionary value. The experimental data re also supported by the recommended fouling factors for PHE summarised in Panchal and Rabas [Panchal 1999] of 0.000018 m²K/W for soft water.

On the results, we were not able to observe differences on the chiller performances due to the scaling, as shown in the table for the outdoor temperature of 35 °C.

Table 21: Impact on the chiller performance of the evaporator fouling

Water flow (kg/s)	Water flow (%)	EER	ΔEER (%)
7.4	100%	2.78	0.0%
6.7	90%	2.78	-0.2%
5.2	70%	2.76	-0.9%
3.7	50%	2.80	0.6%

We can explain the absence of consequences with the heat exchange coefficient structure in the evaporator. The global heat exchanger is governed by the higher heat exchange resistance term as shown in the formula [36] also shown hereunder with the additional resistance due to scaling:

$$(UA)_{evaporator} = \frac{1}{R_{RF} + R_{water} + R_{scaling}} . A_{plates} = \frac{1}{\frac{1}{h_{RF}} . + \frac{1}{h_{water}} + R_{scaling}} . A_{plates} \quad [50]$$

R for resistance, h for conductivity, A_{plates} is the plates area.
In our case the higher resistance was the refrigerant one, the fouling one having a negligible impact on the global resistance (Figure 87). Although it may seem unlikely, the calculated refrigerant boiling resistance is in good agreement with the values found in the literature [Longo 2004].

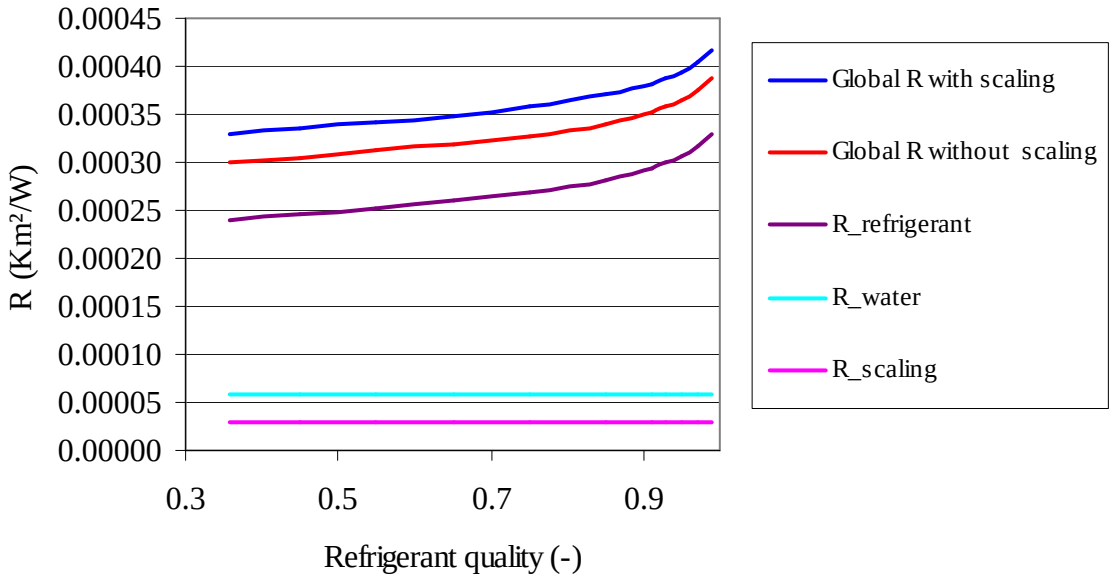

Figure 87: Evaporator heat exchange resistances with and without scaling

The reduction of the hydraulic diameter has a positive effect increasing the water velocity and increasing the heat exchange.

The only observable consequence for chilled water flow rate reduction is the increased temperature difference of the water.

The effect on the pump consumption is negligible and, if well sized, the pump consumption would decrease with the fouling.

The effects would be probably different if the evaporator was sized differently and the heat exchange coefficient on the refrigerant and water sides were closer than in our case: in that case a penalised water coefficient would probably have a more important impact on the exchange mechanism and on the performances.

The problem of the evaporator fouling should anyway be considered also on the rest of the distribution network. The terminal units are sized to work in a specific temperature range (in our case 7-12 °C at the full load) and for a fixed waterflow. The evaporator scaling would influence the final terminals, the sensitive and latent capacity ratio and the comfort aspects.

The uncertainty about the effects of this defect is also confirmed in the literature by the poor confidence in the patterns for the fault detection experimentally observed by Comstock et al. [Comstock 2002]: the authors could observe an increased consumption of the system and a reduced efficiency, but the sole parameter with a strong confidence trend was the water temperature difference as we have noticed as well.

3.6 Buildings seasonal performance with degradated chillers

3.6.1 Simulated building description

In order to examine the effect of the defects in a real context, we were able to model the chiller behaviour in three office building types. The first building is a large office building (15 000 m²) with open spaces. The second type is a smaller (5 000 *m²*) with closed offices. The third is a small building (2 000 m²) with separated offices as can be encountered in suburbs.

The building description is detailed in the annex 4.

All the buildings are considered to be equipped with a chilled water network with fancoils and a primary air system. The Consoclim [Consoclim 2002] model allowed us to obtain the hourly needs of cooling independently of the type of terminal used. Thus we consider only the sensible part of the cooling needs, the latent being strongly related to the terminal system type.

For the three buildings we have different needs and we sized the systems considering several identical chillers installed. The unitary capacity has been multiplied by a size factors that allows responding to the cooling demand using a reasonable number of chillers and with capacity magnitude in the range where four stages are commonly used (until 300 kW from Trane and Carrier catalogues). The sizing method used for each building is to simulate the building needs for the weather data suggested by the AICVF guide [AIC 1998] consisting in simulating four consecutive weeks with a hot day repeated. This method allows considering in the sizing method the inertia effect of the building during extremely hot season.

The buildings include several chillers as indicated in the table below for the two French locations Trappes and Nice with final installed single chiller capacity.

Table 22: Simulated office building installed capacities and sizing ratio (W/m²)

Building 1					
	Number of Chillers	Unitary rated capacity (kW)	Installed capacity (kW)	Cooled area (m²)	Sizing ratio (W/m²)
Trappes	4	250	1 000	14 111	71
Nice	6	280	1 680	14 111	119
Building 2					
	Number of Chillers	Unitary rated capacity (kW)	Installed capacity (kW)	Cooled area (m²)	Sizing ratio (W/m²)
Trappes	2	140	280	3 864	72
Nice	2	230	460	3 864	119
Building 3					
	Number of Chillers	Unitary rated capacity (kW)	Installed capacity (kW)	Cooled area (m²)	Sizing ratio (W/m²)
Trappes	1	160	160	1 542	105
Nice	1	210	210	1 542	138

The sizing ratios result to be coherent with the ratios used currently in reality for centralised system considered for Europe of 120 W/m² [EECCAC 2003].

3.6.2 Degradated chiller characterization in seasonal simulations

The previous set of simulations was necessary to characterise each defect behaviour with the changes in the temperatures of operation in order to introduce in the next simulation campaign a chiller model that operates as near as possible to the real performances.

A small programme under VBA allowed us to couple the needs of the buildings with the regulation of the stages of the chiller.

The cooling capacity and power at different indoor and outdoor conditions at full load are taken into account in building simulations using the following relation for cooling capacity (P_{c_fl}) and absorbed power (P_{a_fl}) at non rating conditions:

$$P_{c\_fl} = Pc_{rated}.(1+D_1(T_{i\_con}-T_{i\_con_{rated}})+D_2(T_{i\_eva}-T_{i\_eva\_rated}))$$ [51]

$$P_{a\_fl} = \frac{Pc}{EER_{rated}}(1+C_1DT+C_2DT^2)$$ [52]

$$DT=(\frac{T_{i\_con}}{T_{i\_con_{rated}}})-(\frac{T_{i\_eva}}{T_{i\_eva_{rated}}})$$ [53]

$$EER_{fl} = \frac{P_{c\_fl}}{P_{a\_fl}}$$ [54]

Where:

T_{i_con} inlet temperature at the condenser (°K)

T_{i_eva} inlet temperature at the evaporator (°K)

C_1, C_2, $D_1$and D_2 coefficients

rated = index for parameters defined or calculated at rating conditions (35 °C-7 °C)

The coefficients are calculated using a fit function for each defect at each considered level from the results of the previous model using the root mean square method.

The partial load behaviour EER_{pl} is modelled by a linear relation between EER_{pl} and the load rate (τ) with two coefficients k and q:

$$EER_{pl}=EER_{fl}.(k.\tau+q)$$ [55]

EER_{fl} is the efficiency ratio at full load calculated by the equation [54].
k and q are calculated in order to have a continuous partial load curve starting from the known efficiency corresponding to the stage 25 %, 50 %, 75 % and 100 % obtained by the first model.

When a single compressor is operating the behaviour is characterised differently by an efficiency model:

$$EER=EER_{fl}.\frac{\tau}{\tau+q}$$ [56]

With q=0.1.

Once the efficiency calculated, the cooling capacity is equal to the demand and the absorbed power is calculated:

$$P_a=\frac{P_f}{EER_{pl}}$$ [57]

The partial load behaviour can be represented by the curve of Figure 88 for rating conditions 35 °*C* outdoor temperature and 7 °*C*, leaving water temperature.

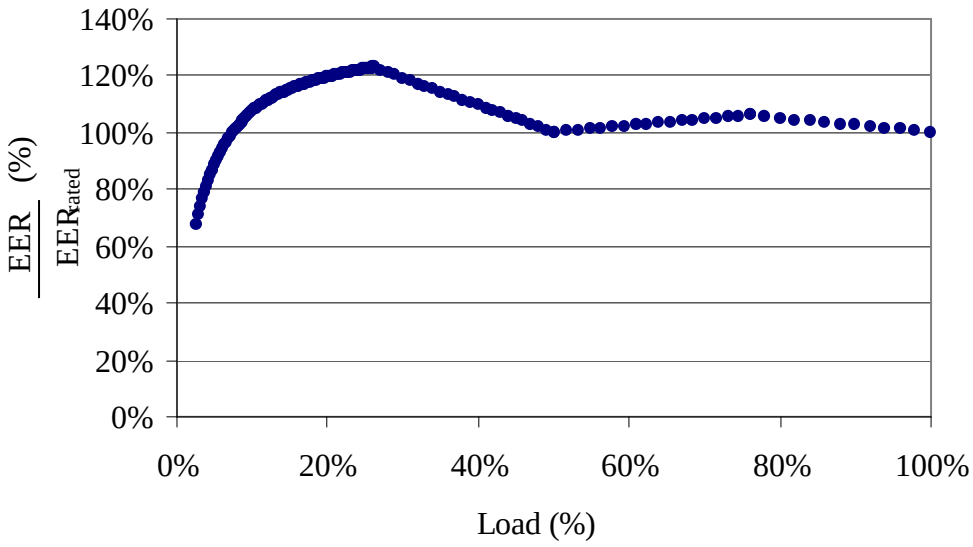

Figure 88: Chiller partial load behaviour

The shape of the partial load curve comes form experimental measured performances and the curve has been modelled in this way in order to best fit to the experimental data from Rivière [Rivière 2004].

3.6.3 Control strategies

The chiller is able to satisfy different load demands through an on/off cycling of the compressors.

Actually, the order of compressors start is random with the rule of not to switch off a compressor already in operation, in order to reduce the number of starts. The order of start and the capacity of each level are shown in Table 23.

Table 23: Compressors order of operation

		1	*2a*	*2b*	*3*	*4*
Circuit 1	Compressor 1	x	x	x	x	x
	Compressor 2		x		x	x
Circuit 2	Compressor 3			x	x	x
	Compressor 4					x
	$P_c/P_{c\ rated}$	25 %	51 %	50 %	75 %	100 %
	P_a/P_{arated}	21 %	42 %	50 %	71 %	100 %
	EER/EER_{rated}	119 %	119 %	100 %	106 %	100 %

For a load demand near 50 % two possibilities exist that are both used in order to have an equal time of wearing of the compressor on the two circuits independently of the efficiency of each level. But in this case, the system does not benefit of the performance enhancement due to the use of a single compressor on a single network (due to the oversized heat exchangers) as shown by the experimental values in the table.

In order to have a simpler model, we will consider the implemented regulation to use only the *2b* configuration for loads between 50 % and 75 % simulating the worst operation conditions.

For each building several chillers can be installed. The strategy of the use of the chillers cascade follows.

If we have x installed systems, the chillers are started one by one when the cooling need increases. For the hourly cooling demand N, x chillers operate at full load (P_{c_fl}), where x is the integer part of the ratio (N/P_{c_fl}). To satisfy the remaining cooling demand, one chiller operates at partial load τ activating the number of stages needed to satisfy it:

$$\tau = \frac{N - x.P_{fl}}{P_{fl}} \qquad [58]$$

The strategy scheme is summarised in Figure 89.

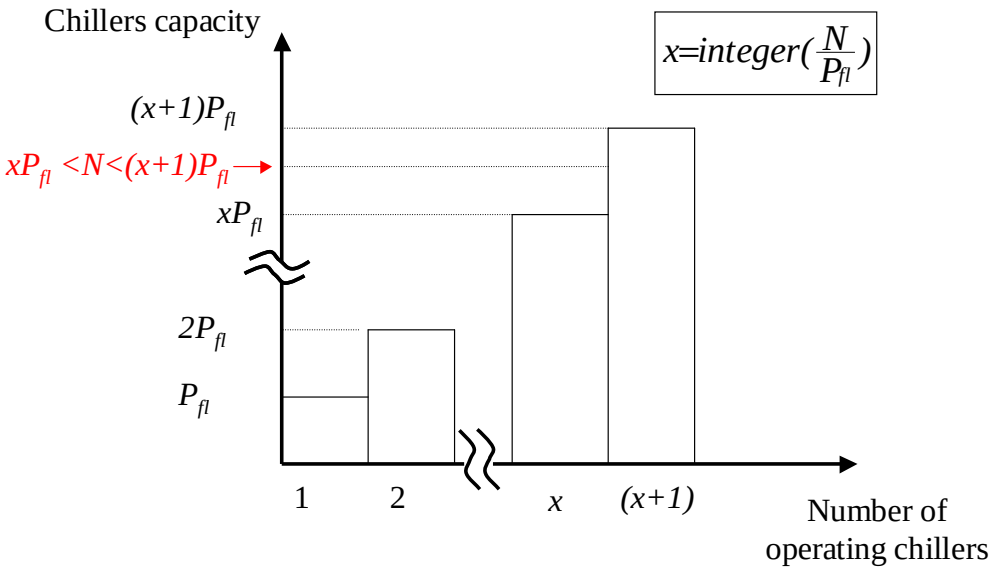

Figure 89: Scheme of the control of start of the chillers for the cooling load N

The different chillers are supposed to work on different water networks for large buildings justifying the chosen strategy for regulation. Actually, when more than one chiller is on the same network the strategy of load sharing can be different, chillers can be found working in parallel at a partial load that can be equally shared on the two systems.

3.7 Office buildings seasonal performance with defects

The results of the seasonal simulations allowed making some initial remarks.

The method used for the chiller sizing allowed guarantying the cooling demand in all degradated cases: in many cases the installed chiller number is higher than the number needed and some chillers can remain unused during all the cooling season. The main problems we could observe therefore are “overconsumption” problems, the comfort being always guaranteed.

The initially defect characterisation was based on a curve fit in a range of outdoor temperatures from 20 to 35 °C, but an abnormal behaviour was observed for some defects. In fact, if we look at the operating temperature of the chillers we can observe that operation takes place often for temperatures below of 20 °C: for example for office building 1 in Trappes more than 15 % of the time operation of the chillers is at temperatures below 18 °C (Figure 90). We had so to add a point at 15 °C to the previous simulation campaign in order to improve the accuracy of the model at low temperatures.

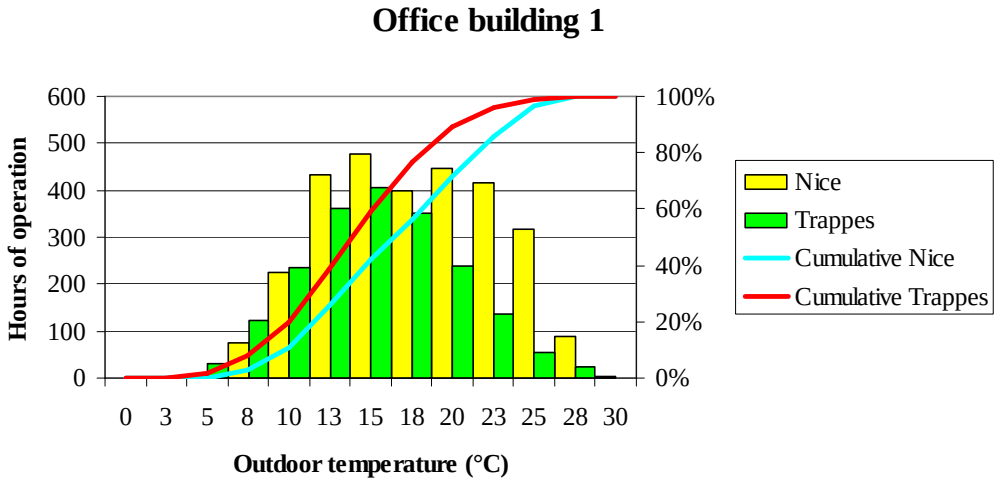

Figure 90: Distribution of the hours of operation of the chillers with the outdoor temperatures and their cumulative curve

We represent hereunder the results for the three buildings in a single graph for each defect.

The condenser fouling leads to overconsumption that is more important for Nice than for Trappes for all the simulated buildings: this because as we have seen before, condenser fouling is more penalizing at higher temperatures. The impact is more important for large buildings.

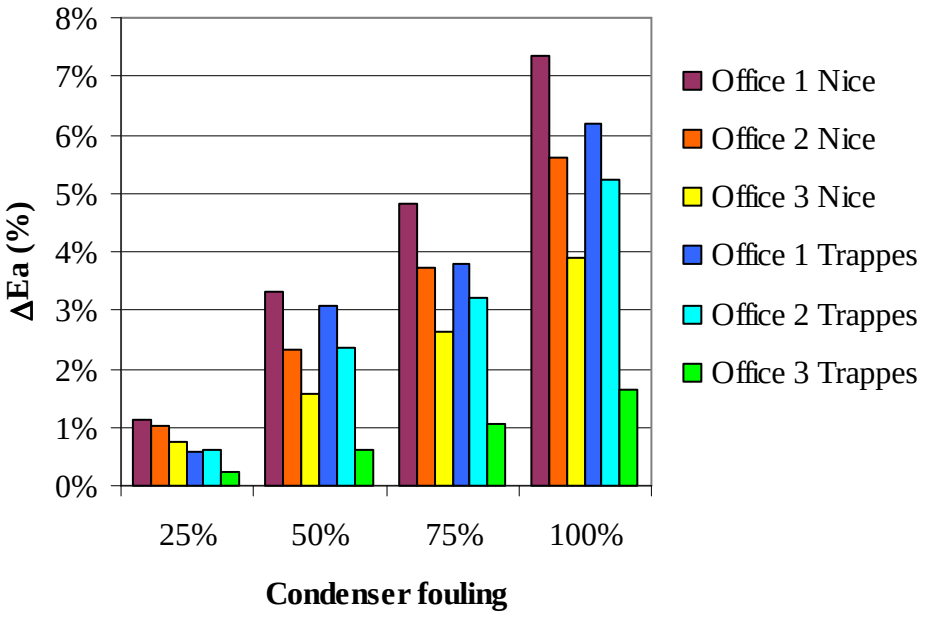

Figure 91: Condenser fouling effect on the seasonal consumption for the three office buildings and two analysed weather conditions

For the smaller building, the defect is quite negligible for Trappes but this is strongly related to the sizing method used to size the installed capacity: there is just one chiller installed that operates at partial load all along the cooling season. Because of the oversizing, the chiller works mainly at low stages of capacity as shown in the table below: the chiller seldom works with four compressors and most of the time the chiller operates at only one stage that is less sensitive to the condenser fouling as we saw in the previous chapter.

Table 24: Time distribution of the operating stages for Office 3

	Stage 1	Stage 2	Stage 3	Stage 4
Rate of hours of operation in Nice	54 %	35 %	10 %	1 %
Rate of hours of operation in Trappes	74 %	25 %	1 %	0 %

The presence of non-condensables has a very similar effect to the condenser fouling but in general for the three buildings the difference between the cold or hot climate is less important. This because the overconsumption is more sensitive to outdoor temperature and is larger for the low temperatures.

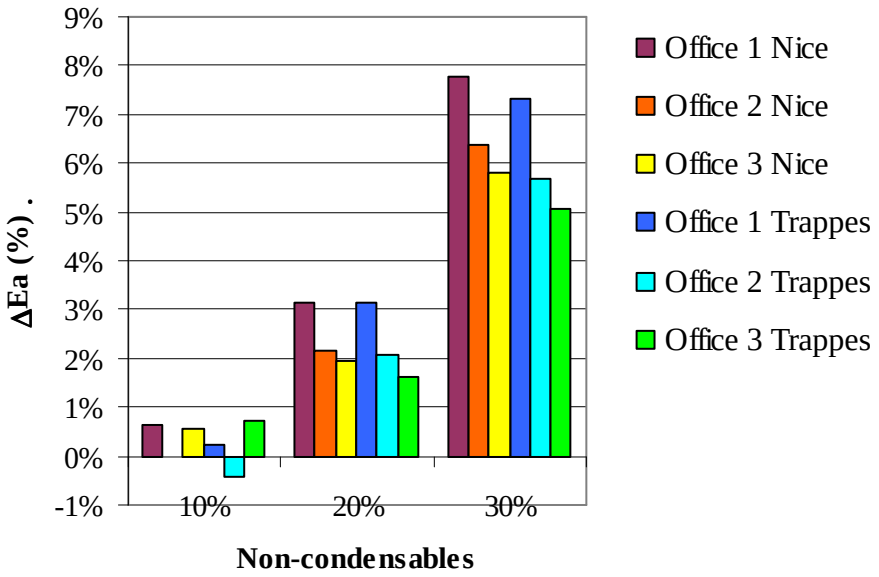

Figure 92: Condenser fouling effect on the seasonal consumption for the three office buildings and two analysed weather conditions

On the contrary, the clogged valve concerns more the operation in cold climates. The overconsumption and efficiency losses are however very limited with a magnitude of some % for the small office. For the office 1 and 2 the effect on the performance is important with seasonal performance lowered of 9 % in the worst case.

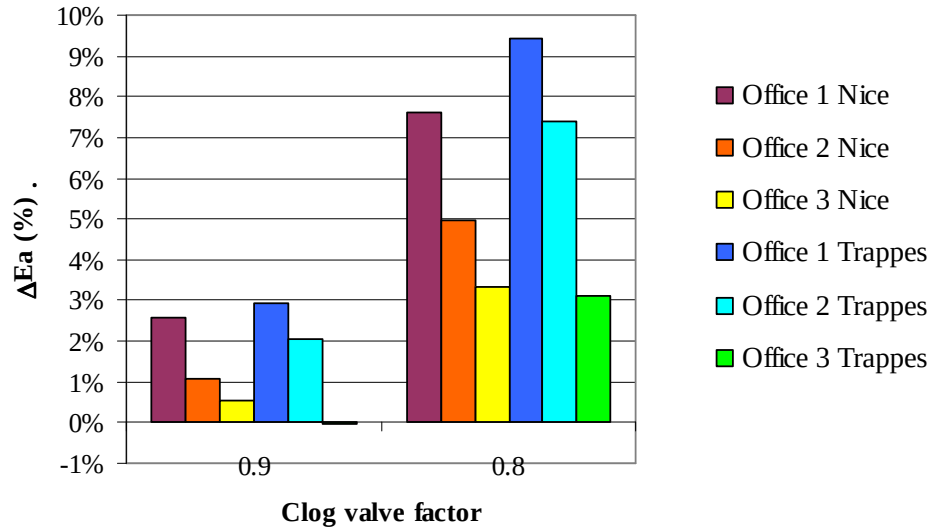

Figure 93: Clogged valve effect on the seasonal consumption for the three office buildings and two analysed weather conditions

The worn compressor has an equal effect on the seasonal performance that does not depend on the weather or partial load profile: results for all the buildings are very similar.

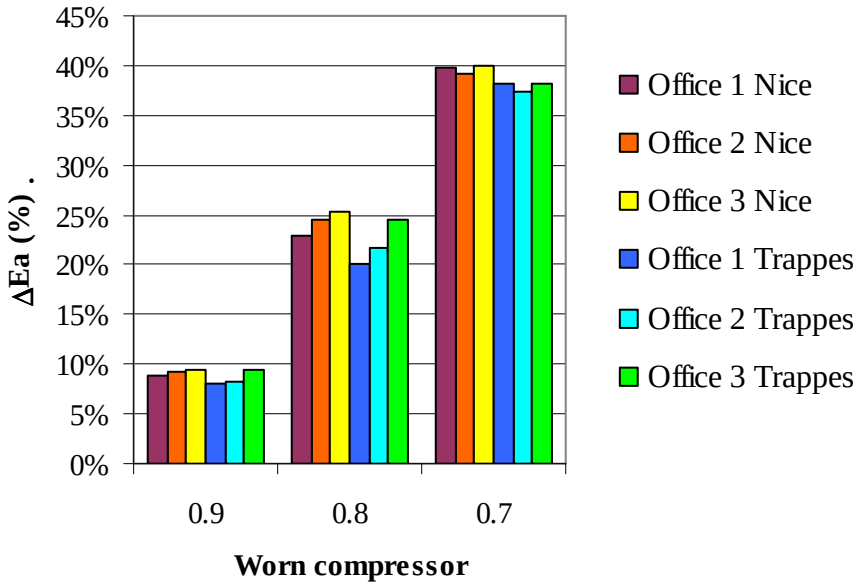

Figure 94: Condenser fouling effect on the seasonal consumption for the three office buildings and two analysed weather conditions

All the defects are in general more severe on office building 1: this is mainly due to the fact that the presence of several chillers working at full load makes them work at the point where the degradation is more important: four compressors operate with the lowest efficiency.

For the office building 2 only two chillers are installed: one of them seldom works (<2 % of the total operation time for Nice and 7 % for Trappes), while the second works at partial load, mostly using three stages.

Table 25: Time distribution of the operating stages for Office 2

	Stage 1	Stage 2	Stage 3	Stage 4
Rate of hours of operation in Nice	30 %	36 %	26 %	8 %
Rate of hours of operation in Trappes	25 %	34 %	27 %	13 %

The office building 3 has only one installed chiller that operates at very low partial load.

3.8 Conclusions for the chillers defect analysis

The chiller based systems stock is ageing and with age operation problems can arise that can lower the performances of the systems. These problems occur at the equipment level and can have impact on the cooling capacity and on the system consumption. An auditor or inspector should be able to target and detect the defects that are more severe and where the energy savings are larger.

A set of common defects has been simulated in order to understand their mechanism and consequences. The defects that have been shown to be the most frequent have been studied. We can summarize the consequences on the main chiller operation parameters in the table below.

Table 26: Trends of the main parameters and detection hints for the chillers defects

	P_c	P_a	*EER*	*LP*	*HP*	Subcooling	Superheat	Detection hints
Refrigerant leaks	⇓	⇓	⇓	⇓	⇓	⇓	⇔	Subcooling and superheat, techniques for leaks detection
Fouling of condenser	⇔	⇑	⇓	⇔	⇑	⇑	⇔	Air temperatures high pressures
Non-condensables	⇓ (⇑ for low T_{air})	⇑	⇓	⇔	⇑	⇔	⇔	Measurement of the condensing pressure
Clogged device	⇓	⇓	⇓	⇓	⇔	⇔	⇑	
Compressor efficiency reduction	⇔	⇑	⇓	⇔	⇔	⇔	⇔	Absorbed power

In the case of the chosen chiller the defect of evaporator scaling showed small impact on the performance and we did not analyse it anymore. Although the trends established in the table are in general agreement with the literature experimental data and seem to be applicable to different chillers, for the evaporator scaling more studies are necessary, putting the accent on the evaporator size and waterflow in order to understand in which conditions this defect becomes severe.

Although up to this point we have not considered several defect at the same time, just as an example, we developed one simulation where all the defects were present at the same time. Just to have an idea about what can happen when the chiller runs a long time without intervention, all the worst conditions are gathered on one case.

Table 27: Parameters variations for fully degradated conditions

2 compressors	*Pc* (kW)	*Pa* (kW)	*HP* (bar)	*BP* (bar)	Refrigerant flow (kg/s)	*EER*	Subcooling (°C)	Superheat (°C)
Rating conditions	81.5	29.6	20.6	5.1	0.53	2.8	0.5	2.8
Fully degradated	74.4	33.1	20.7	5.0	0.51	2.2	3.6	6.5
Δ(%)	-9.5%	10.6%	0.2%	-3.5%	-4.5%	-22.5%	-	-
1 compressors								
Rating conditions	42.1	12.5	16.9	5.2	0.27	3.4	1.4	3.9
Fully degradated	41.6	13.8	17.0	5.2	0.27	3.0	0.7	3.9
Δ(%)	-1.1%	9.4%	1.1%	0.0%	0.2%	-11.6%	-	-

In that case it will be impossible to define the occurring problem: several effects are added or compensated making any interpretation impossible. It is unlikely that an auditor can meet such a situation, but in that case the parameters in table 26 are not useful and all the observations possible on the machine components (liquid spy, fan consumptions etc.) are necessary to distinguish each defect.

The degradated seasonal simulations allowed us to highlight the effects of the defect with the partial load operations and with the climate zone. All the defects lead to an increase of the energy consumption; no impact on comfort has been observed, due to the oversized capacity installed that allows compensating any loss of capacity.

Chillers operating in hot climate are more sensitive to condenser fouling than in cold climate, the opposite happens for clogged valve. Non-condensables and worn compressor defects are weather neutral.

The fact to use a large number of chillers in cascade at full load instead of some chillers of higher capacity operating at partial load (or to use a different regulation strategy that would share the load equally between the chillers) increases the effects of the defect on the operation.

4 Model of time related defects and economic analysis of the action of correction

4.1 Find the best correction for energy and for money

The analysis of the defects already developed for the split and chiller systems can go further if we are able to translate the defect evolution into the quality of operation of the systems.

This is possible to relate the evolution of the defect with time. Time related defect scenarios allowed us to establish, from the owner point of view, the best intervention frequency taking into account several factors including the economic analysis that integrates the cost of the correction actions and the energy cost (with energy prices and cost references). So we add to our methodology of research a supplementary step as shown in the diagram below.

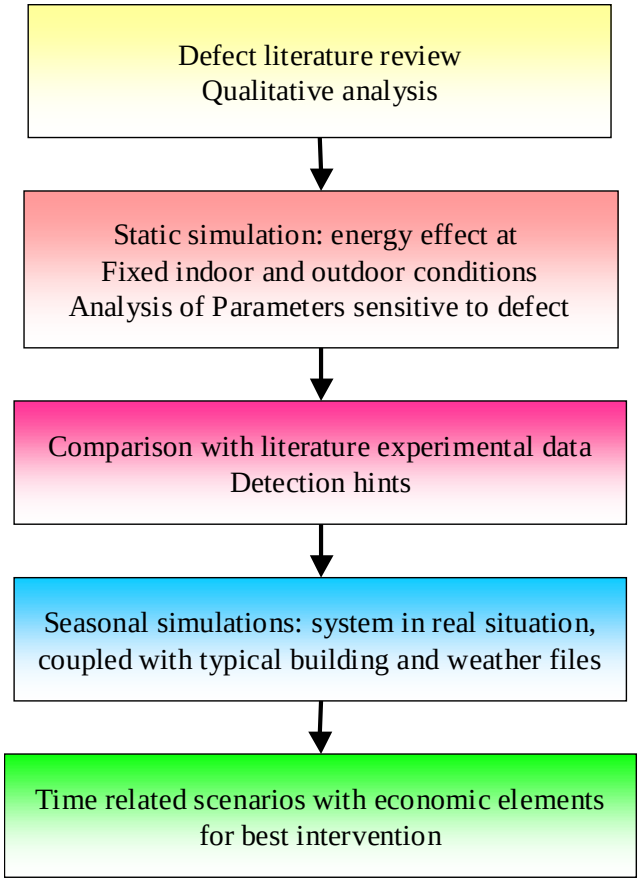

Figure 95: Research methodology steps

Not all the studied defects can be modelled with the time, because their appearance can be caused by human errors or by non-predictable events. This is the case for defects such as valve clogging or compressor wearing: they can appear after an intervention for maintenance, or because of local overheating that leads to burnt oil.

It is possible to produce time scenarios for the refrigerant leak and condenser fouling in both cases of (split and chiller) and to analyse the filter fouling development for the split system.

For refrigerant leaks, it was possible to developed different scenarios based on average leaks rate found in the literature although the leaks are probably not constant along the life of the system: they can occur from manufacturing defect, from bad installation, after a maintenance intervention (i.e. gasket replacement) etc.

Filter and condenser fouling are continuous phenomena that can be modelled with some assumptions and we based our model on existing literature models and experimental results.

4.2 A time related scenario for refrigerant leaks

A refrigerant leak is a phenomenon that, once started, evolves gradually and continuously emptying the system of its charge until repair or failure. It can occur at the time of the system installation due to an error of manufacturing or installation, or it can occur during the lifetime after maintenance activities. It should be kept in mind that we use average values of leaks and the perfect sealed system does not exist: all systems present, even if very low, refrigerant leak rates.

In order to take into account the refrigerant leak evolution, constant annual leak rates have been considered. The rates τ_0 are found in literature and the refrigerant charge m at the year n is then considered as:

$$m_n = m_{n-1} \cdot (1-\tau_0) = m_0 \cdot (1-\tau_0)^n \quad [59]$$

The global amount of refrigerant loss is then variable, leaks being related to the remaining charge. This because the leaks induce a reduction of the overall operation pressures of the machine and therefore a reduction of the amount of the leaks that are proportional to the pressure difference between the system and environment.

In the following paragraphs we present the leak effects for the building types considered in the seasonal simulation campaign. It should be taken into account all along the analysis that the refrigerant leaks impacts are strongly related to the initial sizing method applied to size the installed system capacity. For system strongly oversized, the leaks effect on the cooling capacity and then on the comfort can be negligible even for a large amount of refrigerant loss.

4.2.1 Case of a split system

We started considering a fixed leak rate of 5 % for split systems as estimated in Barrault and Clodic [Barrault 2007], the value being defined in that study from the discussion with the manufacturers and includes the leaks due to maintenance operations. Applying the law of leaks [59] we obtain the refrigerant charge reduction shown in figure over a mean lifetime of a split considered of 15 years [EERAC 1999].

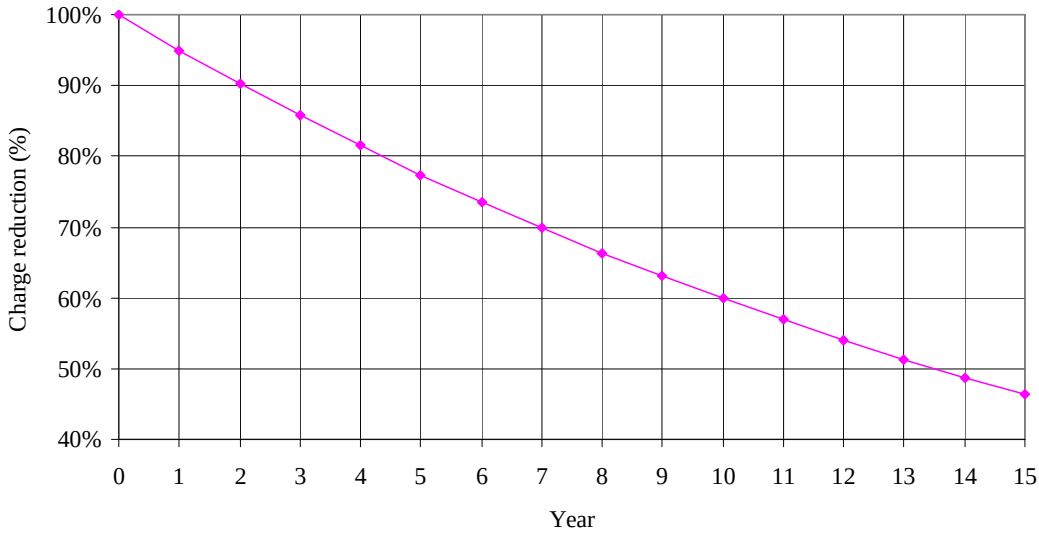

Figure 96: Charge evolution with an annual leak rate of 5 %

We could not develop a performance time scenario over all the lifetime of the system that would have lost at the end of its life more than 50 % of its initial charge. The Mark V model did not allow going further 22 % losses, that is why we consider a scenario of the performances on the capacity over 5 years. This limit may correspond to an implicit maintenance as well (see description hereunder).

In the Figure 97, the building performances evolution is represented versus time for an office building in Nice.

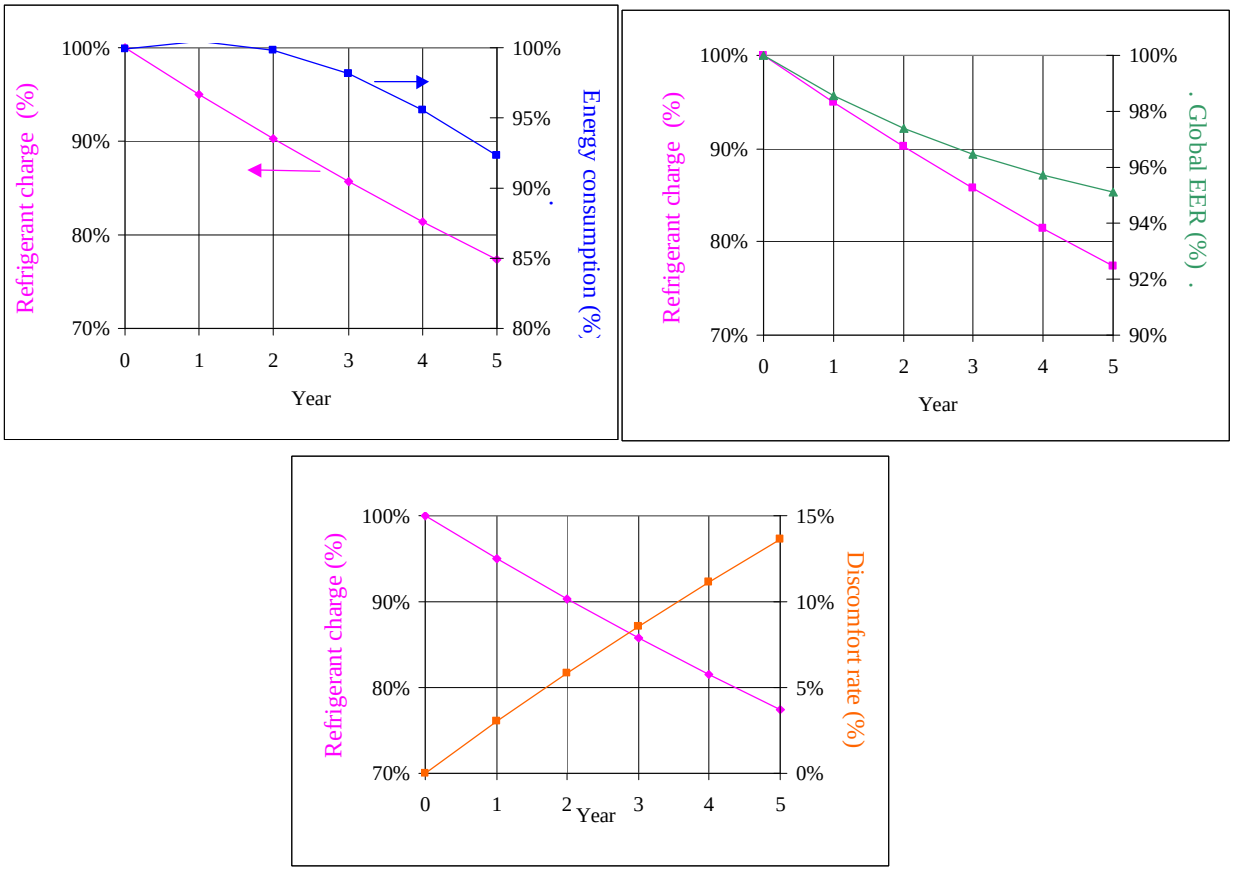

Figure 97: Refrigerant charge, capacity and comfort evolution for an office building in Nice

The pink curve represents the charge level evolution with time, the blue curve represents the consumption curve evolution, the green one the seasonal efficiency evolution, and the orange the comfort rate (hours of non respected setpoint higher than 1°C on the total air-conditioned hours $\frac{Nh(T_{indoor}>T_{setpoint}+1)}{Nh_{occupation}}$. The results for all the simulated buildings are shown in the annex 6.

In some cases (office building in Nice and house in both Trappes and Nice) the refrigerant charge reduction brings comfort problems accompanied by consumption reduction. In one case (case of office building in Trappes) the leaks lead to overconsumption with temperature setpoints always respected. The first case happens when the system is not strongly oversized and the capacity reduction due to the leaks brings the system to work at its limits. In the second case, even if the capacity is reduced, the oversized system is still able to produce enough cooling energy but with lower efficiency.

The impact on the operation is strong: the discomfort rate can be important especially for the hotter weather. The comfort problems are important both in Nice and Trappes with discomfort rates that reach 30 % in Nice and 12 % in Trappes.

The system operates longer for all the studied cases with time of operation increased by 20 % that would lead to a quicker wearing of the system.

4.2.2 Case of a chiller

As for the split system, we started from a leak rate of 10 % as proposed by Barrault and Clodic [Barrault 2007], value that was defined in the study from the discussion with the manufacturers and that includes the leaks due to maintenance operations. Also there, the amount of refrigerant leak is not considered constant, 10 % leaks being related to the remaining charge. Applying the leaks law [59] we obtain the refrigerant charge reduction shown in Figure 98 on a mean lifetime of a chiller considered of 15 years [EECCAC 2001].

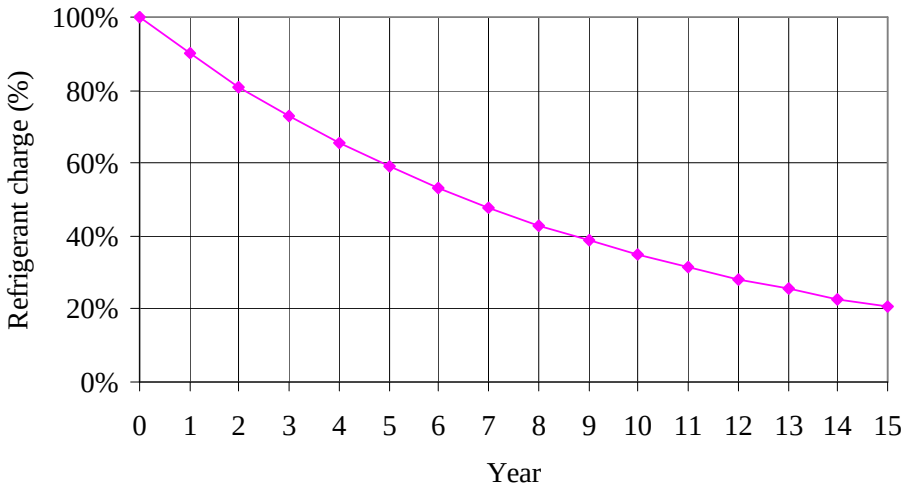

Figure 98: Refrigerant charge evolution with a yearly leak rate of 10 %

The curve of Figure 98 shows a mathematical model but actually the chiller would probably be out of service before reaching the 20 % charge left.

Because of the limits of the chiller model used for the simulations campaign at fixed temperatures conditions, we could not characterize charge losses lower than -15 %. In this range, thanks to the thermostatic expansion valve operation, the refrigerant leaks did not show major effects on the cooling capacity and efficiency. The following figure shows the evolution on the rated performances due to leaks until 20 % over two years operation. The rated point at 35 °C outdoor was the only condition we could model extensively [chapter 3.5.1].

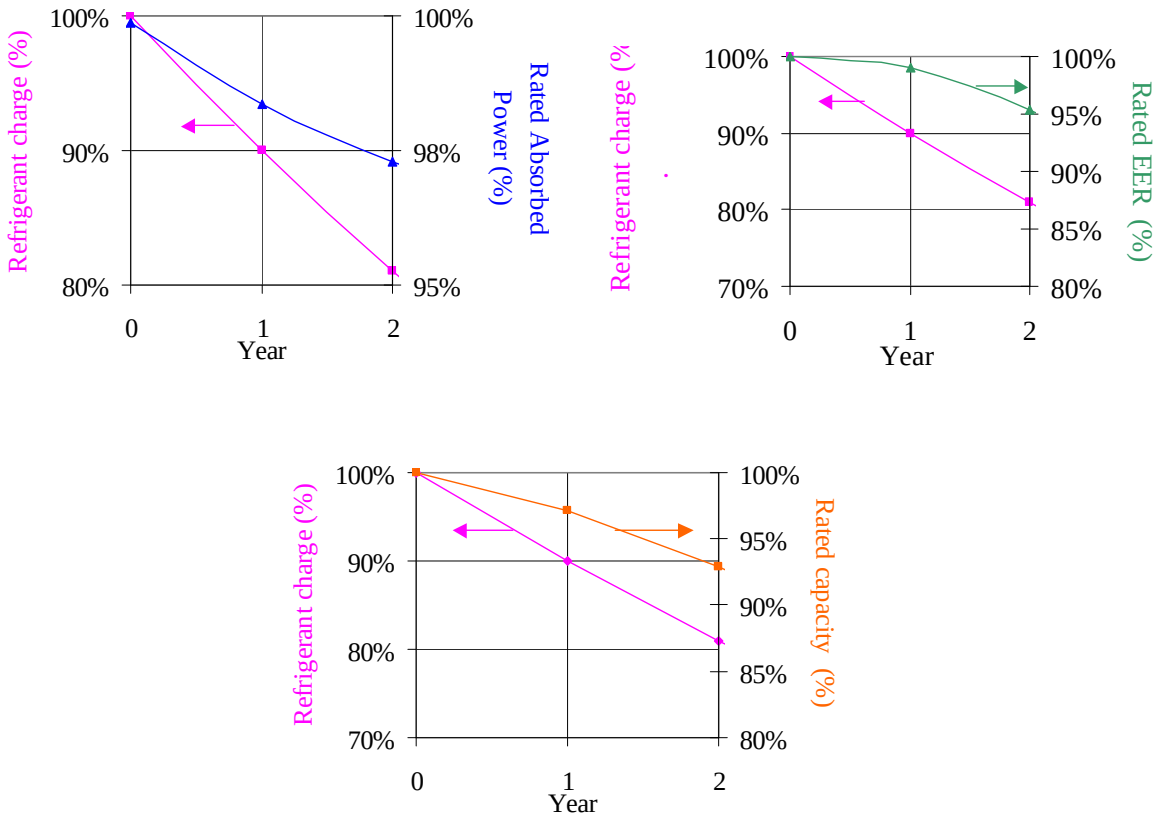

Figure 99: Refrigerant charge evolution with a yearly leak rate of 10 % for rating conditions over twot years

With the considered leaks rate, only two years would be enough to lose 20 % of the initial charge and reach the critical condition after which the valve cannot ensure proper operation and the performances stronger decrease.

The performance effects are mitigated by the valve operation with capacity reduction of 7 % and consumption reduction of 2 % (for a global efficiency effect of –4.6 %) for 19 % leaks after two years of operation.

4.2.3 The refrigerant refill

The refrigerant refill cannot be completely analysed as a cost effective action because although it reduces in general the energy costs, on the other hand, it leads to discomfort that cannot be translated as an economic term. Only part of the benefit is quantified.

The refrigerant recharge operation is a complex operation that requires qualified staff and, if performed following the best procedure, can take several hours even for the smaller systems.

The main steps are:

1) Empty the system and weigh the recovered charge with a precision balance
2) Fill the system with nitrogen
3) Search for leaks with the more suitable technique following the refrigerant used
4) Repair the leaks (if it can be repaired immediately, if not the system is stopped and some days can occur between the repair and the new put in service)
5) Refill the system with the charge recovered plus the charge compensation for the leaks, or with a complete new charge

The recovered charge cannot be always re-entered in the system, especially for refrigerant that result of the combination of two or several pure fluids. In this case, the leaks lead to a more important loss of

one of the components changing the global composition and changing therefore the refrigerant properties; only a refill with a new fluid ensures to use a correct fluid composition and to guarantee the system performance.

Depending on the required refrigerant, the prices can vary and fluctuate each year. Just for example, we could obtain for the refrigerant analysed in this work the following reference prices:

- R22: 9 €/kg
- R407C: 16 €/kg

The cost of the procedure will include the refrigerant cost, the labour cost, the equipment and displacement of the technician. The labour cost is estimated as 50 €/hour for a qualified technician. All the prices are considered excluding taxes. The global procedure costs for the procedure after 5 years of operation for the office and residential building are in annex*.

The results of the calculations suggest that to the use of a central system allows saving some money for the maintenance of the system, the refrigerant being confined in the centralised system while for several split system, the multiple refrigerant units make the maintenance cost higher, although the total refrigerant mass is lower. This is also due to the sizing criteria for the systems: the split systems are in general more oversized than chillers, leading to a larger amount of refrigerant and a large number of installed units. Different sizing criteria would choose a lower number of units with higher capacity. In this case, the seasonal efficiency would be penalised by the operation at lower load rates in the case of the split system (cf. Figure 37).

It should be highlighted also that, in the case of the chiller, the maintenance cost is shifted from the system to the terminal units, that do not contain refrigerant, and to the water network for which the maintenance is easier and cheaper. The global cost can be strongly reduced if the refrigerant refill is included in a periodic maintenance contract where the costs are negotiated and lowered because they cover several maintenance actions at the same time.

4.3 A time related scenario for condenser fouling

The condenser fouling evolution also can be modelled as a function of operation years because it can be considered as a continuous phenomenon that grows with the operation time of the system. Actually the following model is intended for continuous operation. We have to mention that it does not take into account the effect on the fouling of the continuous start and stop of the condenser fans. The on/off operation can decrease the fouling of the condenser because an amount of particles is held by the draught effect of the airflow, this particles fall on the floor when the fans stop, reducing the fouling rate. This aspect is very difficult to take into account and the model can be considered slightly worse than in reality. On the other hand, the chosen fouling particles do not take into account macro particles such as leaves, feathers or other debris that can stick on the condenser surface and increase the fouling.

4.3.1 Dynamic condenser fouling: Siegel's model

In order to represent dynamically the evolution of the fouling with time, we developed a fouling model for heat exchangers starting from the model developed by Siegel [Siegel 2002] and it has been adapted to our study in order to create a fan operation evolution during fouling.

In Siegel's dissertation we can find two models: for isothermal conditions and for non-isothermal conditions. Moreover the non-isothermal case is investigated in cooling mode without condensation and with condensation, the Siegel model being built to study the evaporator fouling.

In our case, we are interested in the condenser side, so with no water condensation and higher temperatures than in the evaporator. We use the isothermal model because the terms added to non-isothermal model are thermophoresis, for which aerosols are pushed away from hot objects, and diffusiophoresis, which is due to the gradient created by dehumidification. The Siegel model already showed negligible difference between the isothermal and the non-isothermal condition without condensation. In our case, we decided to neglect the thermal effects and consider only the isothermal collection model.

For the isothermal model the mechanisms of particle collection considered are: the impaction on the fin edges and on the tubes, the gravitational particles settling on the fins corrugation, the particle deposition due to turbulence, the Brownian deposition.

The single mechanism models are described hereunder. The geometrical data refer to the heat exchanger geometry as shown in the figure below for a wavy fin exchanger.

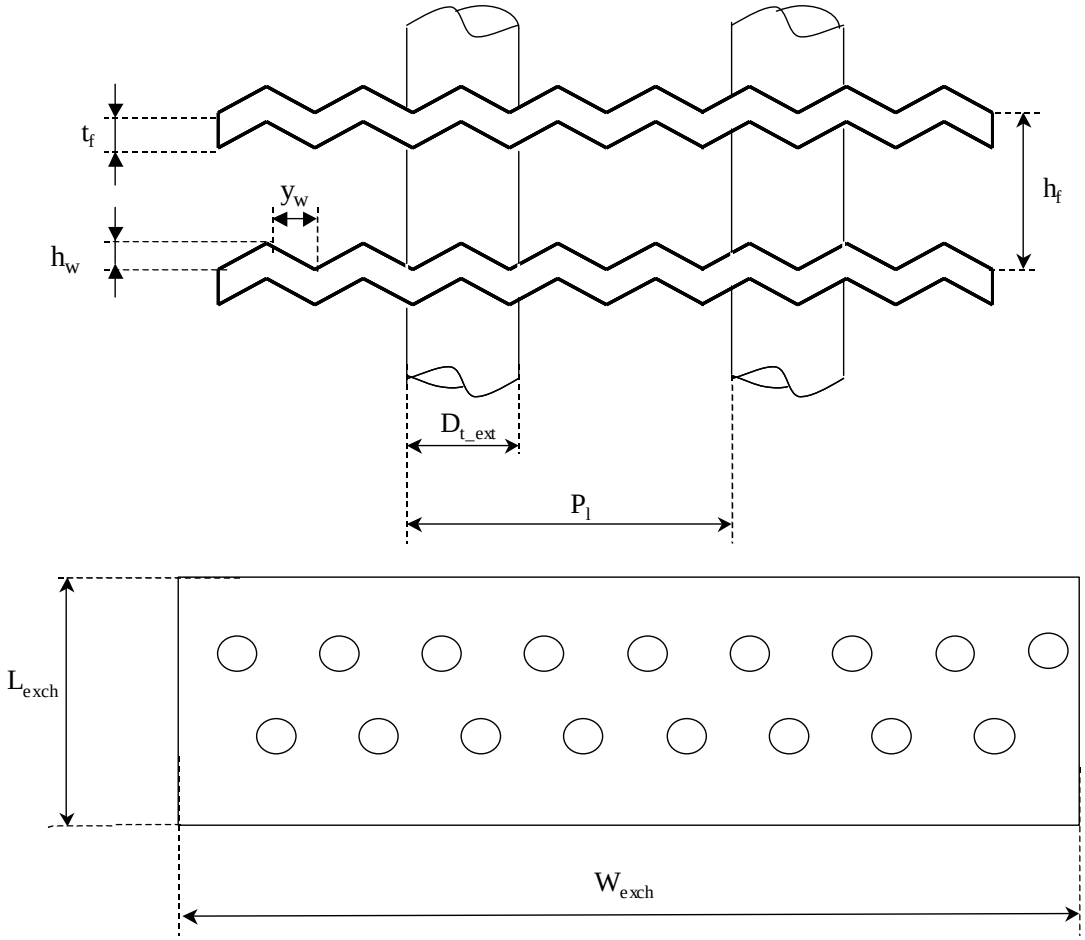

Figure 100: Geometric parameters of the heat exchanger

Deposition of leading edge of fins

For the deposition on leading edge of fins (P_{fin}) Siegel assumes that the fin edge is a blunt body and use Hinds analysis [Hinds 1999] for rectangular slit cascade impactors with a modification to account for the fraction of face area of the coil that is occupied by fin edges. This analysis assumes that the air approaching the fin edge makes a 90° bend (Figure 101).

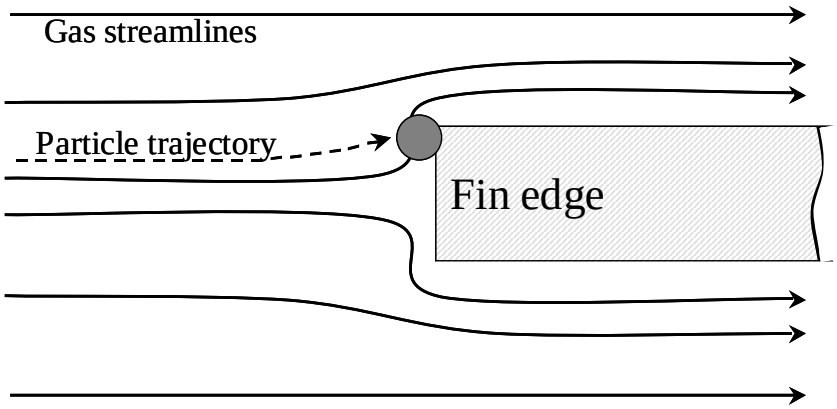

Figure 101: Particle deposition due to impaction on fin edges

All particles that impact on the surface are assumed to stick. The penetration fraction accounting only for losses because of impaction on fin edges, P_{fin}, is estimated as follows:

$$P_{fin}=1-(Stk_{eff,fin}\frac{\pi}{2}).\frac{t_f}{h_f}c_f \qquad [60]$$

Where $Stk_{eff,fin}=\frac{4C_c\rho_p d_p}{3C_D\rho_{air}t_f}$ is the particle Stokes number based on the duct air velocity and the fin thickness, corrected for particles having particle Reynolds numbers > 0.1, t_f is the fin thickness, h_f is fin pitch, and c_f is the corrugation factor. The corrugation factor takes into account the fact that a corrugated fin is longer than a straight fin and thus has more area for particle impaction. The corrugation factor is defined for wavy fins as $\sqrt{(h_w^2+y_w^2)/h_w^2}$ where h_w is the average height of the fin corrugations and y_w is the peak-to-trough corrugation width.

The term in brackets in equation [60] is limited to a maximum value of one to consider the deposition only for the fraction of particles that are directly in front of each fin.

Impaction on refrigerant tubes

Particles may also impact on the refrigerant tubes that run perpendicular to the airflow direction and the fins (Figure 102).

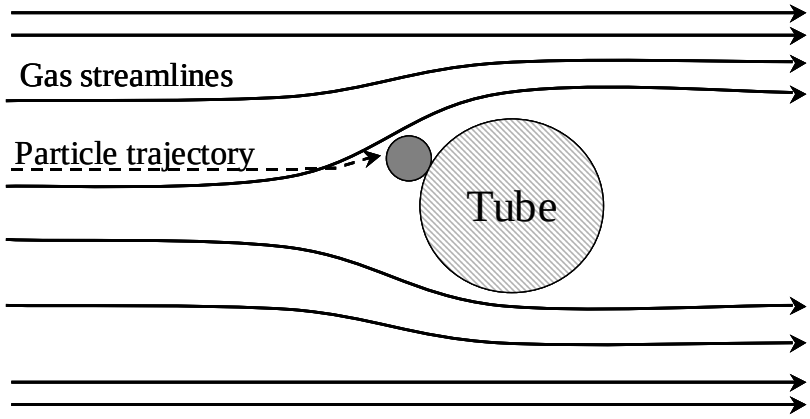

Figure 102: Particle deposition due impaction on tubes

There are several theoretical and experimental studies of particle impaction on tubes. An extension of the analysis of Israel and Rosner [Israel 1983] suggests the following formula for estimating penetration for flow past a network of tubes:

$$P_{tube}=(1-(1+1{,}25.\frac{1}{a}-0{,}014\frac{1}{a^2}+0{,}508.10^{-4}\frac{1}{a^3})^{-1}.\frac{D_{t\_ext}}{P_l}n_{offset})^{N_R} \qquad [61]$$

Where $a = (Stk_{eff,tube} - 1/8)$ where $Stk_{ef,ftube} = \frac{4C_c \rho_p d_p}{3C_D \rho_{air} D_{t\_ext}}$ is the particle Stokes number based on the air velocity in the heat exchanger and the tube diameter, N_R is the number of tube sets in the direction of flow, D_{t_ext} is the external refrigerant tube diameter, P_l is the longitudinal tube spacing, and n_{offset} is the number of offset tube rows in each tube set. The term in the innermost parenthesis is limited to a value of less than or equal to one and the $D_{t\_ext}/P_l\ n_{offset}$ factor is added to limit the deposition to particles in the volume of air directly in front of the tubes. The assumption that a given particle will not deposit if its Stokes number is less than 1/8 was first proposed by Taylor and has been verified by other researchers. Israel and Rosner report that single tube impaction deposition calculated with this formulation is good to 10 % root mean square (RMS) error for isolated horizontal tubes.

Gravitational settling on fin corrugations

In order to reduce the particle deposition on the fins, the heat exchangers are positioned with vertical fins. However, to increase heat transfer, manufacturers often corrugate fins. Large particles can deposit by gravitational settling on the corrugation ridges. The penetration fraction accounting for losses only from gravitational settling, P_G, is estimated as follows:

$$P_G = 1 - \left(\frac{V_s L_{exch}}{h_w U}\right) \cdot \frac{y_w}{h_f - t_{fin}} \qquad [62]$$

Where V_s is the particle settling velocity, L_{exch} is the heat exchanger depth in the direction of bulk airflow, h is the average height of the fin corrugations, U is the bulk air velocity in the heat exchanger, and y is the peak-to-trough corrugation width. The ratio in the parentheses is limited to a value of one. Particles are not assumed to be Stokesian for the calculation of V_s, for which this equation is used:

$$V_s = \sqrt{\frac{4.C_c.(\rho_p - \rho_{air})d_p.g}{3.C_D.\rho_{air}}} \qquad [63]$$

Where C_c is the Cunningham slip correction factor [Hinds 1999], ρ_p is the particle density, ρ_{air} is the air density, d_p is the particle diameter, g is acceleration due to gravity, and C_D is the coefficient of drag on the particle calculated assuming the particle is a sphere and using the formulation presented in Seinfeld and Pandis [Seinfeld 1998]. Because C_D is a function of particle Reynolds number, which is a function of V_s, an iterative scheme was used to determine V_s.

Deposition by air turbulence in fin channels

Air turbulence in the duct leading up to a heat exchanger can also induce deposition on heat-exchanger surfaces. The fluctuating components of velocity can impart an angled trajectory to particles as they enter the heat exchanger. If the particle has a sufficiently large relaxation time and a sufficient deviation in velocity direction from the bulk flow, it will impact on a fin and not penetrate the coil (Figure 103).

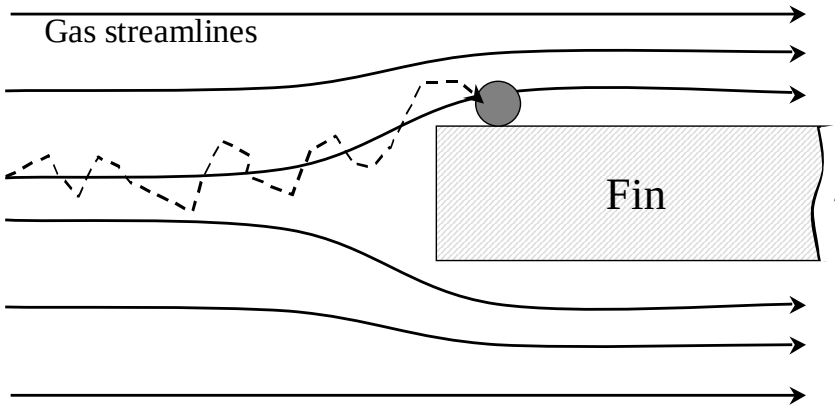

Figure 103: Particle deposition due to Brownian turbulence

Mathematically, Siegel estimates the penetration associated with losses owing to turbulent deposition as:

$$P_T = Prob\left(\frac{\tau_{imp}}{\tau_p} > 1\right) \quad [64]$$

Where τ_{imp} is the characteristic time for a particle to impact on the wall and τ_p is the particle relaxation time. The evaluation of the time of impacts and the probability distribution have been calculated through the Monte Carlo method on a large number of simulations.

Deposition by Brownian diffusion

Small particles are most likely to deposit by means of Brownian diffusion. The penetration fraction accounting for deposition only by Brownian diffusion is calculated assuming laminar flow in the heat exchanger core and follows the work of DeMarcus and Thomas [DeMarcus 1952] for channel flow:

$$P_D = 0{,}915.e^{(-1.885.\xi)} + 0{,}0592.e^{(-22.3.\xi)} + 0{,}0259.e^{(-152.\xi)} \quad [65]$$

Where:

$$\xi = 4\frac{Diff \cdot L_{exch}}{(h_f - t_f)^2 U} \quad [66]$$

Diff is the particle diffusion coefficient equal to $\frac{k_B T C_c}{3\mu d_p \pi}$), k_B is the Boltzmann constant, T is the air temperature, and μ is the dynamic viscosity of the air. The penetration fraction only considering particle loss by Brownian diffusion, P_D, is limited to lie between zero and one. Brownian diffusion was included in the model because it is the only possible significant deposition mechanism for submicron particles in this system (at least for the isothermal case). Nevertheless, due to the relatively short residence time in the system at typical velocities, particles of interest do not deposit significantly by Brownian diffusion.

Global particles deposition fraction

The model of Siegel is based on the overall deposition factor η of the heat exchanger that takes into account the previous deposition mechanisms, supposed independent:

$$\eta = 1 - P_{fin} P_{tub} P_G P_T P_D \quad [67]$$

P_{fin} = deposition of leading edge of fins

P_{tube} = impaction on refrigerant tubes

P_G = gravitational settling on fin corrugations

P_T = deposition by air turbulence in fin channels

P_D = deposition by Brownian diffusion

In our case, the last two mechanisms have been neglected: the turbulence deposition is important only for higher velocities (U>2 m/s) or fin spacing smaller than our case, the Brownian diffusion concerns only submicron particles (d_p<1 µm) that do not have significant impact in our study because of the poor mass amount in the considered air mass distribution. This was also confirmed by the values of the penetration factors by Siegel.

The Siegel's model has shown a good shape of the efficiency curve but generally underpredicts the mass deposition compared with the experimental results; however, the best fits are obtained for low velocities as in our case.

4.3.2 The hourly model of fouling

The overall deposition model has been used to simulate the fouling time for the heat exchanger, coupling the deposition mass with the fan curve, in order to obtain a dynamic simulation of the deposition mechanism coupled with the operation characteristic. The model uses a discrete mass distribution.

An hourly simulation has been developed. The scheme of the hourly steps of our model is shown in the figure and the main four steps explained in a few words.

1) Once entered the discrete mass distribution of the air, the deposition fraction relative to the different diameters is calculated as a function of the airflow

2) From the product of the deposition fraction and the mass distribution we obtain the distribution of the deposited mass and, adding the mass cumulated in the step before, the total amount of mass deposited on the heat exchanger

3) From the Siegel's curve of pressure increment versus deposited mass, we can obtain a new pressure drop at the initial airflow

4) From the fan characteristic, with the new pressure drop at the initial airflow, we obtain a new operation point and a new airflow

In the next loop, the airflow is changed, influencing the deposit fraction mechanism that is a function of the bulk air velocity.

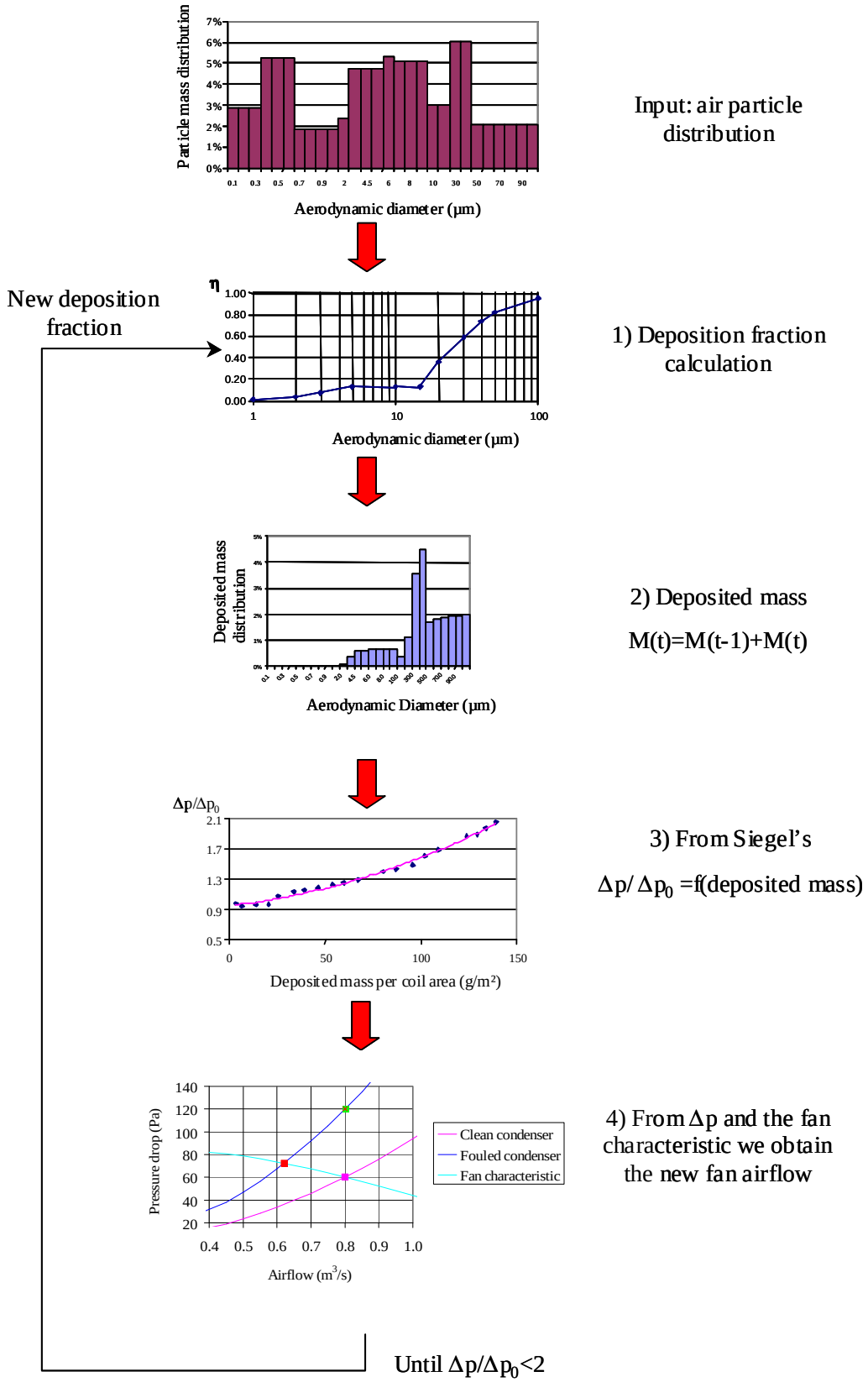

Figure 104: Detail of hourly calculations for the heat exchanger fouling model.

The more dust deposits on the heat exchanger, the more pressure drop is encountered by the fan that shifts its operation point following its operation curve. In order to couple these two mechanisms, the Siegel's curve of pressure drop relative to the initial pressure drop versus the deposited mass per coil surface has been used (in step 3).

The experimental curve by Siegel has been fitted with a quadratic law (Figure 105) as a function of the deposited mass (M_c) per coil area (A_c):

$$\frac{\Delta p}{\Delta p_0} = 4 \cdot 10^{-5} \left(\frac{M_c}{A_c}\right)^2 + 0.0025 \frac{M_c}{A_c} + 0.9575 \qquad [68]$$

With a $R^2 = 0.993$.

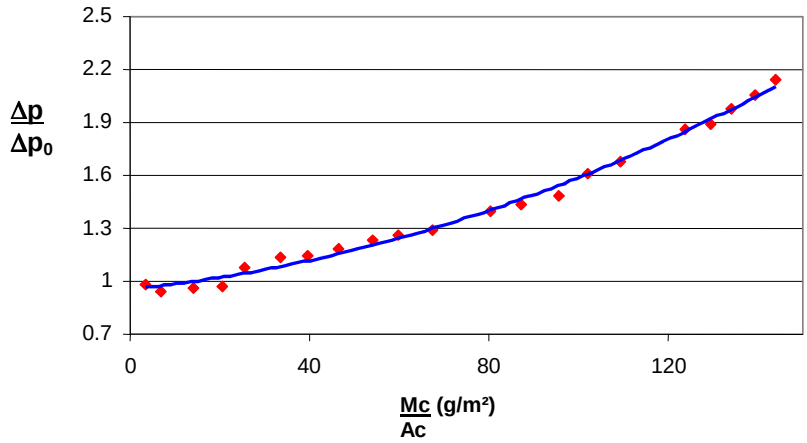

Figure 105: Normalized mass deposited versus relative pressure drop for 2.0 m/s air velocity (Siegel)

Although the curve by Siegel was obtained in specified conditions, we consider that the increment of pressure drop does not depend on the dust type, the fouling bringing the same pressure drop independently of the diameter of the particles introduced (that are supposed to have the same density), but just of their mass (Figure 106).

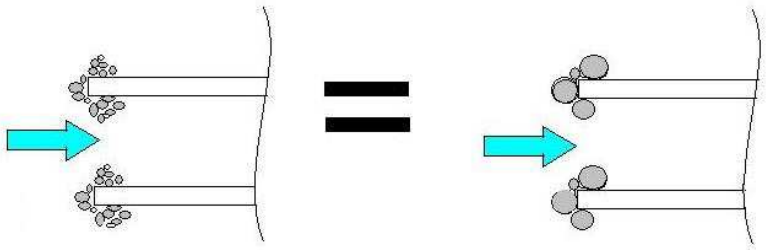

Figure 106: Fouling on the fins: we considered the fouling due to small particles equivalent to fouling due to larger particles

The condenser can be considered as a filter with very poor arrestance, where the main mechanisms of arrestance are due to fin and tubes impaction (Figure 107).

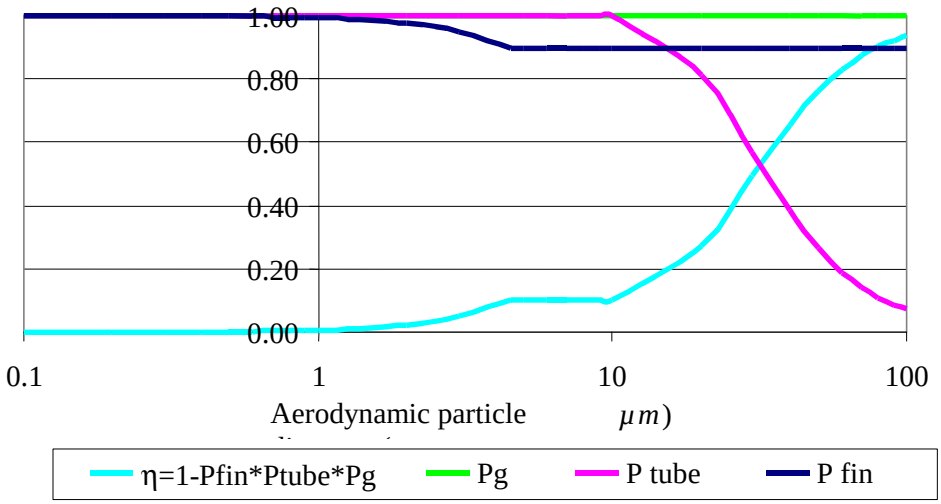

Figure 107: Deposition fraction of the heat exchanger as a function of the aerodynamic particle diameter

Several types of dust were considered: the American SAE (Society of Automotive Engineers) Coarse Dust, as used by Siegel in the experimental part of his work, an air particle mass distribution as described by Whitby [Whitby 1980], an air particle mass distribution as measured by Lestari et al. [Lestari 2003]. The details of the mass distributions are reported in annex 5. The dust was considered has having total atmospheric concentration of 0.1 mg/m^3 as encountered typically in urban zones.

The shape of the mass distribution strongly influences the results and corresponds to different environments. The SAE Coarse Dust is considered by Siegel as the dust that typically corresponds to the one that can be encountered on the evaporator. In our case we are interested in condenser side. The indoor and outdoor dusts in the air have similar particles but the indoor air is more contaminated by macro particles that come from furniture and textiles.

The Whitby distribution was largely used to represent the efficiency of filters and takes into account only fine particles with maximum diameter of 10 µm.

Finally, the Lestari distribution is based on more recent measurements in urban context: it revealed the presence of coarse particles with diameter around 20 µm that were already highlighted in other studies. The measurements were taken in urban zone (Chicago).

The Lestari values are also closer to the value of fine particles measured by the organisms in charge of the control of the air quality (in our case Airparif for Paris). If we look at the Airparif[3] data for fine particles, the average measured value of particles with diameters lower than 10 µm (*PM10*) and 2.5 µm (*PM2.5*) and the value for the three distributions are compared in the table below.

Table 28: Comparison between measured and literature particle mass concentration at 80 µg/m^3 (a) and 100 µg/m^3 (b) total mass per m^3 of air

	Average measurements in 2007 in Paris for Urban and Traffic zones	SAE		Whitby		Lestari	
		(a)	(b)	(a)	(b)	(a)	(b)
PM2.5 (µg/m^3)	20/33	3	4	55	70	**31**	**40**
PM10 (µg/m^3)	30/50	16	20	79	100	**58**	**70**

The Lestari's distribution seems to us the distribution more similar to the urban measured quantities, but we will simulate anyway the three distributions in order to highlight some facts.

[3]http://www.airparif.asso.fr/

4.3.3 Application to a split system with fouled condenser

The split condenser is a smooth finned heat exchanger. The fouling limit is defined, by Siegel, as the time for the condenser to foul enough to double its initial pressure drop at the initial airflow: from the fan characteristic (see chapter 2.4.2) the condenser fouling leads to a final fan operation point corresponding to an airflow of 0.61 m^3/s and a final pressure drop of 73 Pa, with a total deposited mass of 109 g.

In the model, the term due to gravitational settling of the deposition factor is not taken into account because the fins are plane. The three dust distributions lead to the fouling times represented in Table 29.

Table 29: Fouling times obtained for the different dust types

	Fouling time (hours)
Lestari distribution	1 717
SAE Coarse Dust	841
Whitby distribution	8 071

The model shows a lower fouling time for coarser dusts, as expected.

If we look at the deposited mass distribution (as for the SAE distribution in Figure 108) we can observe that quite all coarse particles are held back by the heat exchanger.

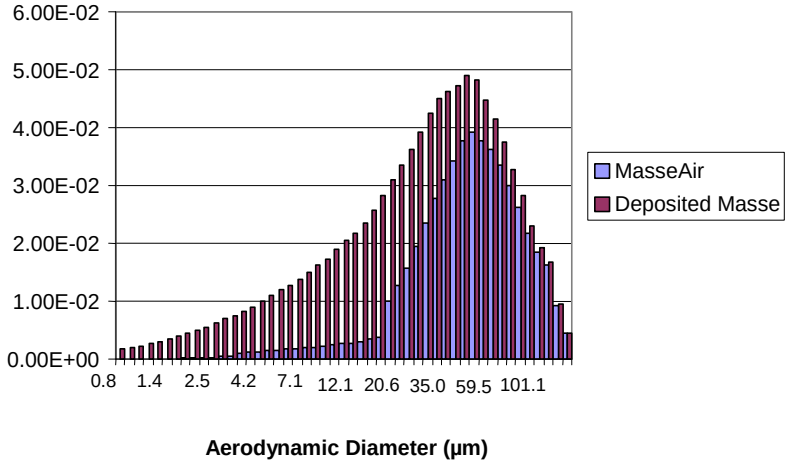

Figure 108: Mass distributions of air particles and deposited particles for SAE dust.

Including in maintenance actions the cleaning of the condenser, allows reducing the overconsumption of systems as indicated in the figure below (Figure 109), starting from a clean system.

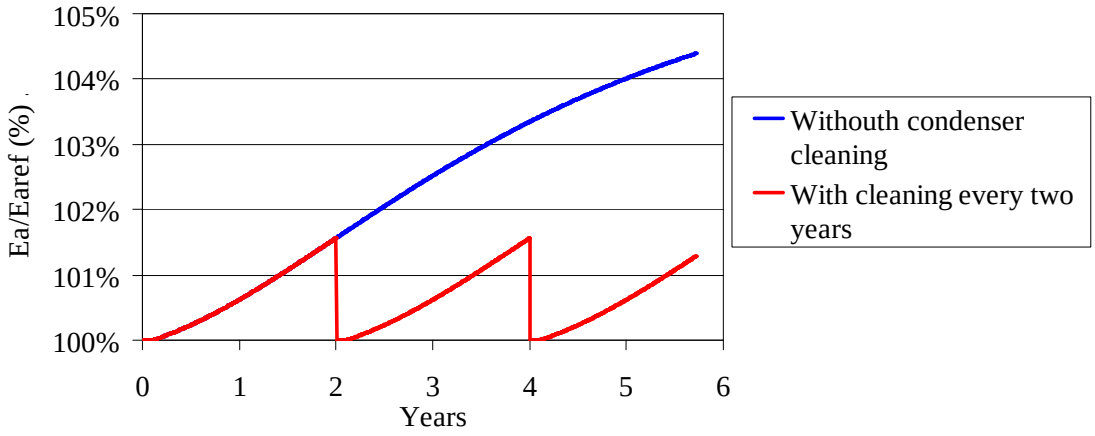

Figure 109: Overconsumption comparison with no cleaning and regular cleaning for an office building in Nice

The cost of condenser cleaning has been obtained from a service company specialised in heat exchanger maintenance with a patent of cleaning technique. The procedure consists in disassembling the upper part of the outdoor unit to access the heat exchanger, to brush it and then to clean it with under pressure spray (patented technique), finally to vacuum the residuals and reassemble the unit. The procedure takes about twenty minutes for a single outdoor unit treatment and it requires a low level trained staff. Most of the problems are encountered in the accessibility to the unit that are often put in higher locations difficult to reach. The average estimated cost for the procedure is 20 € (including taxes).

The benefit of the maintenance action for condenser fouling is given by the difference between the energy savings (*ES*) and the maintenance costs (*MC*) over *N* years:

$GS(N)= ES(N)-MC(N)$

The global cost of the action has been analysed in function of the frequency of the maintenance over several years of operation. The maintenance costs (*MC*) are an increasing function of the frequency of intervention (*f*):

$MC(€)=NU \cdot MC\_unit(€/unit) \cdot NI$

Where the number of interventions (*NI*) is the integer part of the ratio between the years and the frequency:

$$NI=integer(\frac{N}{f})$$

More frequent the intervention will be, higher the energy savings will be that are represented by the difference between the areas in the Figure 109 of the overconsumption without maintenance (blu curve) and the overconsumption with maintenance (for example the red curve with yearly cleaning *f*=1, with *N*=6 in the figure):

$$ES(\%)= \int_0^N \Delta E_a dt - (f-1)\int_0^{N/f} \Delta E_a dt$$

We pass from the relative overconsumption (%) to the total energy overconsumption by using the average hourly consumption for the reference case E_a.

$ES(kWh)=E_a \cdot ES(\%)$

We obtain the energy savings in term of money by multiplying for the electricity price:

$ES(€)=Energy\_cost(€/kWh) \cdot ES(kWh)$

An example of the evolution of the energy savings and maintenance cost with the frequency of condenser cleaning is shown in Figure 110. The point of intersection between the curves of the energy savings and maintenance cost indicates the frequency at which the global savings are zero; starting from the point of intersection the intervention becomes more and more interesting from the economic point of view.

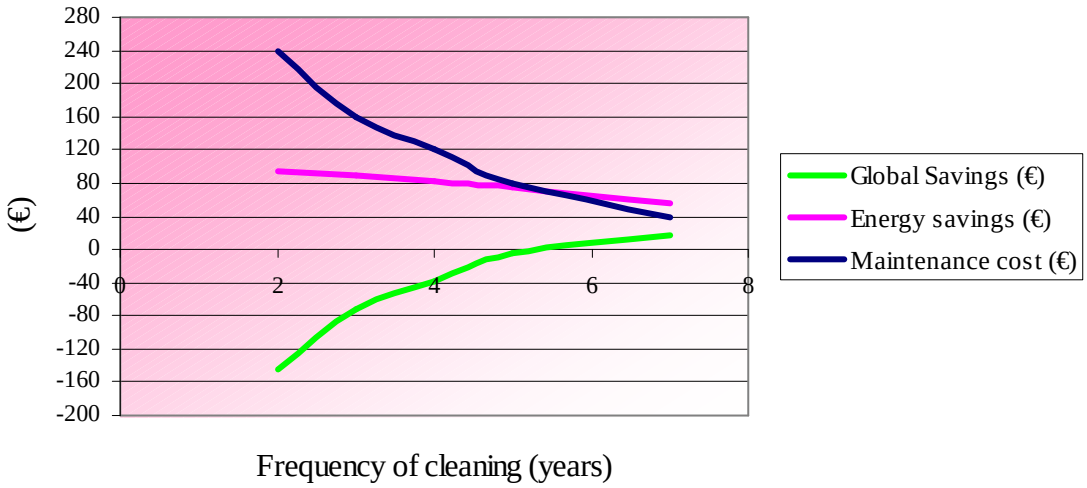

Figure 110: Maintenance cost, energy savings and global savings evolution with the frequency of maintenance for the house equipped with split in Nice

The fouling time chosen for economic estimation was the one for the Lestari distribution, 1717 *hours*. Over this period several intervention frequencies were applied. Depending on the building type and location, the times required for condenser fouling are given in Table 30.

Table 30: Condenser fouling times for the simulated buildings equipped with split systems

		Operation hours/year	Years
Office	Nice	300	6
	Trappes	150	12
House	Nice	130	13
	Trappes	114	14

Economically, the interest in condenser cleaning is strongly related to the electricity price. Sensitivity to electricity prices is illustrated comparing two countries with very different electricity market and price, Italy and France. Table 31 gives the prices (including taxes) from main electricity suppliers' prices lists (EDF and ENEL).

Table 31: Electricity prices including taxes for Italy and France

	Residential (€cents/kWh)	Business (€cents/kWh)
France	10.9	3.7
Italy	16.8	14.5

The calculations with Italy prices concern only the Nice case, the Trappes climate not corresponding to the Italian weather.

There is a difference in the price offer to residential and business customers from both energy suppliers. The global savings due to the different maintenance scheduling are shown in following tables.

The following tables display the result for the duration obtained in Table 30, which are different for each building and climate type.

Table 32: Savings for condenser cleaning scheduled at different interval, for office building in Italy and France

Office Nice				
Calculation over **6** years	France		Italy	
	Energy savings (€)	Global Savings (€)	Energy savings (€)	Global Savings (€)
Once per year	166	-2 234	660	-1740
Once every two years	134	-826	534	-426
Once every three years	99	-381	393	-87

Office Trappes		
Calculation over **12** years		
	Energy savings (€)	Global Savings (€)
Once per year	126	-3 834
Once every two years	117	-1 683
Once every three years	107	-973
Once every four years	95	-625
Once every six years	70	-290

The condenser cleaning seems not to be an interesting action at economic level for the office building both for Italy and France (global saving always negatives). The large number of installed condensers (24 for Nice and 18 for Trappes) makes the maintenance cost prevailing on the energy savings. In this case, to use when possible multi-split units would be an advantage, reducing the number of outdoor units to be cleaned. The very low electricity price for the French office building makes it difficult for the action to be cost effective.

For the residential case, a 20 € maintenance cleaning cost makes the cleaning operation cost effective at least once in the system life for hot climates where the energy savings are larger both for Italy and France. In Italy this action can be scheduled every 5 years to be cost effective.

Table 33: Savings for condenser cleaning scheduled at different interval, for a house in Italy and France

House Nice	France		Italy	
Calculation over **13** years				
	Energy savings (€)	Global Savings (€)	Energy savings (€)	Global Savings (€)
Once every two years	74	-166	114	-126
Once every three years	69	-91	106	-54
Once every four years	63	-57	98	-22
Once every five years	58	-22	89	9
Once every seven years	44	4	67	27

House Trappes		
Calculation over **14** years		
	Energy savings (€)	Global Savings (€)
Once every two years	7	-133
Once every three years	7	-73
Once every four years	6	-54
Once every five years	5	-35
Once every seven years	4	-16

4.3.4 Application to a chiller system with fouled condenser

The chiller condenser is a louvered finned heat exchanger. Although the louvers can represent a gravitational settling area for particles, it is very small and it has been neglected. The fouling limit is defined, by Siegel, as the time for the condenser to foul enough to double its initial pressure drop at the initial airflow: that leads to a finale operation point of the fan corresponding to an airflow of 1.71 m^3/s and a final pressure drop of 180 Pa, with a total deposited mass of 590 g.

Table 34: Fouling times obtained for the different dust types for the chiller condenser

	Fouling time (hours)
Lestari distribution	1 025
SAE Coarse Dust	487
Whitby distribution	4 501

Our assumption is that all the installed systems in the simulated buildings are used and the order of start is periodically changed in order to equalize the operation time of all chillers. So for a building with *N* installed systems, even if only *M (M<N)* systems would be used because of the oversizing of the installed capacity, all the *N* systems will be considered to operate.

The chiller cost maintenance is less certain: we analyse the sensitivity of the savings with the maintenance cost. The cost could be higher than considered in the previous case considering that the chiller condensers are bigger than the split ones. At the same time, the global time spent for cleaning is in a small part devoted to the cleaning operation and mainly for the preparation of the equipment. In general for the chiller case, the air cooled systems can be located on the roof or in other location that are easy to access, it can be needed to disassemble some covering part, while in some case they are directly accessible. When linked to other regular maintenance activities the cost of the cleaning can be negotiated. All these reasons made us varying the cost for one chiller condenser cleaning between 20 and 50 € (excluding taxes) for chiller.

The general results are shown as graphs in annex 9: the global savings are represented as a function of the intervention frequency for different unitary maintenance costs for the three simulated buildings, in the case of Nice and Trappes. Moreover two cases are considered:

- The cleaning is implemented since the installation of the system (starting from a clean condenser)
- The cleaning is scheduled for an existing system, supposed to be fully fouled

In the second case, the maintenance costs take into account the initial intervention; the energy savings are larger because the consumption without intervention is considered constant as the maximum overconsumption corresponding to the considered fouling limit.

Because of the high yearly operation times of the chillers, the condensers foul very quickly (about one year) except for building 1 for which the operation times are lower.

The calculations are performed for all simulated buildings over four years of operation, average period of duration of a maintenance contract. For the period after the fouling limit the overconsumption is considered constant.

Office building type 1

The total hours of chillers operation for a year is 2530 h for Nice, each of the 6 chillers are used for 422 h. For Trappes, the total operation time is 1609 h for 4 chillers that makes 402 h/chillers. Actually, designers tend to use less chillers with higher capacity than we chose; the number of installed chillers would be in reality lower with a high rate of operation, in order also to lower the chiller maintenance costs.

With these low rates of annual operation, the chillers will foul slowly: about two years and a half would be necessary to foul for both simulated locations (Figure 111).

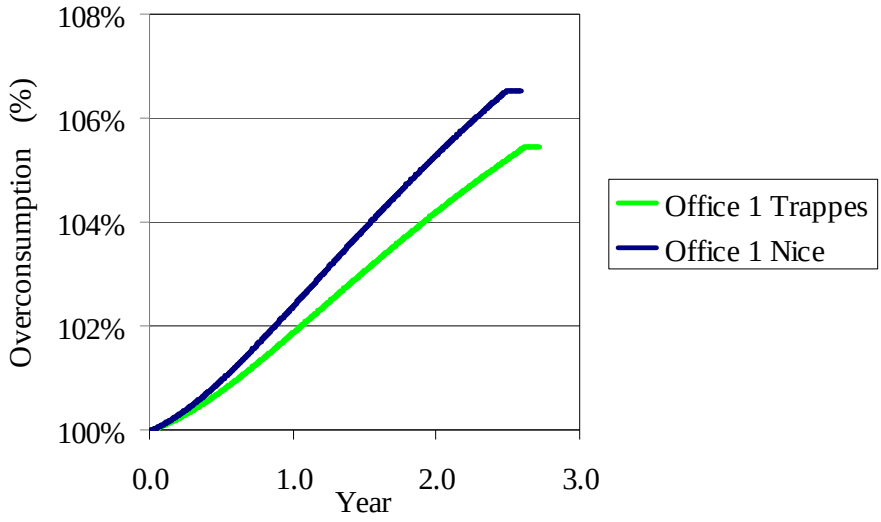

Figure 111: Overconsumption evolution with fouling and with maintenance for office 1 in Trappes

At the same time, the large number of installed units makes the maintenance cost very high.

The condenser cleaning allows saving energy amounts of table below.

Table 35: Energy savings (kWh) due to condenser cleaning over 4 years for office 1

	New		Existing	
Maintenance frequency (year)	Trappes	Nice	Trappes	Nice
0.5	2 241	4 152	4 313	7 705
1	460	842	3 913	6 923
2	302	545	3 279	5 734

The condenser cleaning has shown not to be a cost effective action for most French climate and electricity prices. At least one cleaning every three years is recommended for existing systems (cost effective since every three years cleaning for cost lower than 30 €/unit). For new systems it is difficult to make the action cost effective, the maintenance cost being more important than the savings in most French cases (Figure 152 annex 9). For the Italian energy price, the condenser cleaning appears to be cost effective in most cases with money saving until 800 € over the four years in the best case (Figure 154, annex 9).

Office building type 2

The office building 2 has two chillers installed both for the Nice and Trappes location. It corresponds to what is common in practice: using two chillers of medium capacity instead of one large chiller allows guarantying the cooling when one of the two chillers is put off for maintenance or if out of service. The chillers work 1 850 h in Nice that means 925 h/chiller and 1 230 h in Trappes that means 614 h/chiller.

The condensers foul in about a year for Nice and 1.7 years for Trappes. Behind the fouling limit, we made the hypothesis that the overconsumption is constant (red curve of Figure 112).

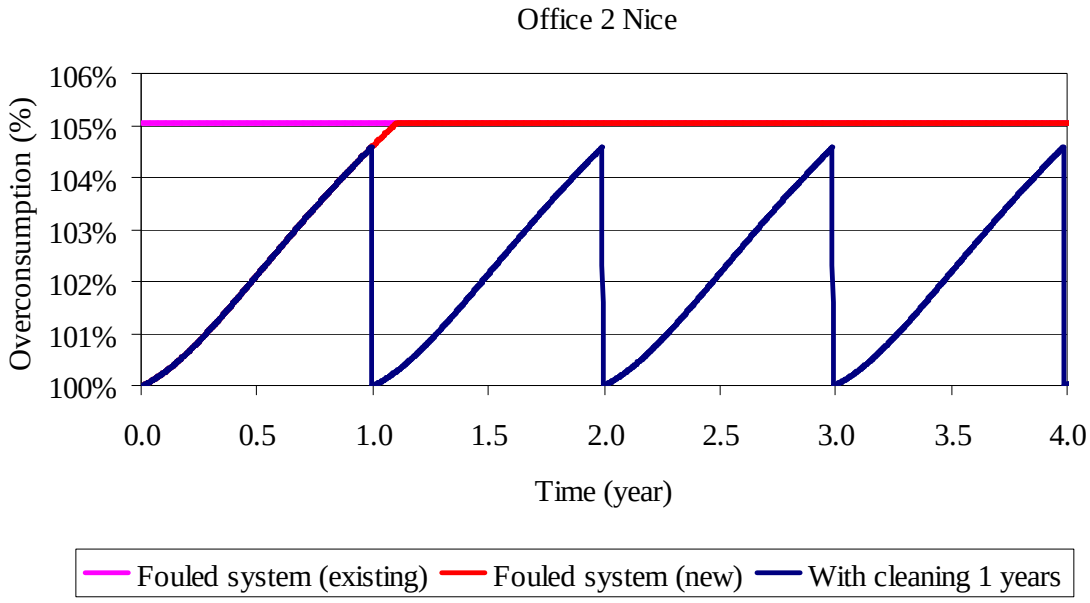

Figure 112: Overconsumption evolution with fouling and with maintenance for office 2 in Nice

The energy savings provided by condenser cleaning are given in the table below.

Table 36: Energy savings (kWh) due to condenser cleaning over 4 years for office 2

	New		Existing	
Maintenance frequency (year)	Trappes	Nice	Trappes	Nice
0.5	1 748	4 320	2 307	5 241
1	1 347	2 748	1 906	3 670
2	563	942	1 122	1 864
3	483	919	1 042	1 840

The condenser cleaning has shown not to be a cost effective action for French climate and electricity prices except for the lower maintenance cost for the lower maintenance frequency where the benefits are zero.

For the Italy electricity prices the cleaning operation shows benefits in quite all the conditions and maintenance cost (Figure 155 and Figure 156, annex 9); the curves have a wavy shape because of the

multiple crossing points of the maintenance and energy savings curves having different slopes (example in Figure 113).

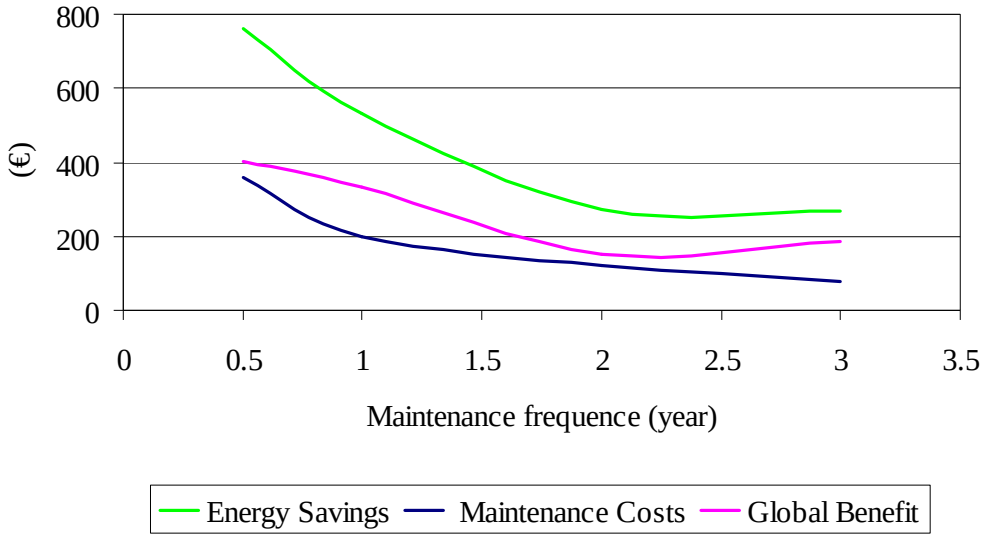

Figure 113: Costs balance for unitary maintenance cost of 20 € for Italy

Office building type 3
The building office 3 has only one chiller installed that covers the cooling demand. It operates most of time at partial load. Operation time per year is 847 h in Trappes and 1 421 h in Nice. It needs less than a year to reach the defined fouling limit in Nice, and 1.2 years for Trappes.

The condenser cleaning allows saving energy amounts of table below.

Table 37: Energy savings (kWh) due to condenser cleaning over 4 years for office 3

	New		Existing	
Maintenance frequency (year)	Trappes	Nice	Trappes	Nice
0.5	966	2 457	1 191	2 846
1	650	1 173	875	1 562
2	225	392	450	781
3	218	389	443	778

Also in this case, the condenser cleaning has shown not to be a cost effective action for French climate and electricity prices (Figure 158 and Figure 159 annex 9)

For the Italian case (Figure 160 and annex 9), for maintenance cost of 40 € per unit and less, quite all the cases lead to money savings. More frequent the cleaning is, larger are the savings, with a maximum of the global benefit curve corresponding to twice per year cleaning (corresponding to 0.5).

4.4 A time related scenario for filter fouling

For the split systems, the filter fouling represent a problem as already highlighted in chapter 2. It was possible to simulate the filter fouling evolution with the operation time thanks to existing literature models.

4.4.1 Dynamic filter fouling: Thomas model

In order to simulate a time scenario, we created a program capable of simulating the hourly fouling of a filter under VBA. The model is based on the filter collection model developed by Thomas et al. [Thomas 2001] with some modifications.

The model has been created originally to simulate fouling mechanism for HEPA filters. The main collection mechanisms considered are the interception (η_R) and diffusion (η_D). In our model we introduced the impaction collection mechanism (η_I) through model described by Landhal et al. [Landhal 1949] that is prevalent for low efficiency filter as in our case (*G2* filtration class).

The model takes into account the different fibres collection mechanisms as the sum of single mechanisms, considering them independent:

$$\eta_f = \eta_I + \eta_R + \eta_D \qquad [69]$$

The two main parameters of the filter model are the fibre diameter d_f and the filter packing density α_f, that represents the ratio between the volume occupied by fibres and the volume occupied by the filter. The efficiency depends on the size of the crossing particle d_p.

If a particle crosses the gas streamlines, due to its inertia and is collected on a fibre then it is said to be collected by impaction (Figure 114).

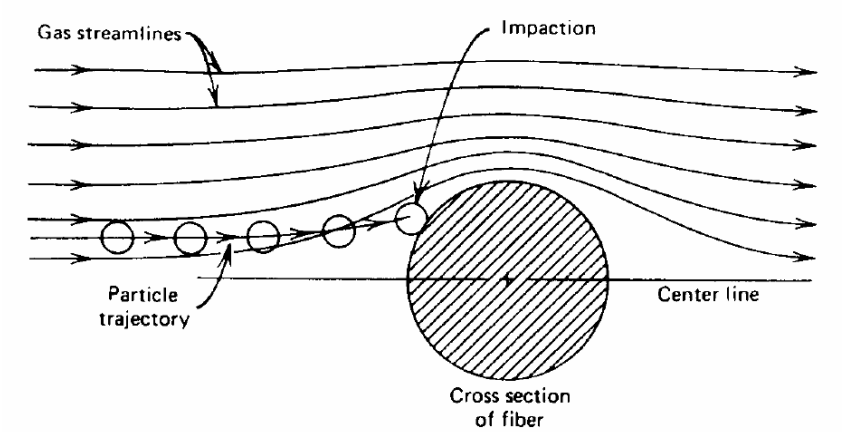

Figure 114: Impaction mechanism of particle collection (figure from http://www.unc.edu/courses/2007spring/envr/754/001/)

The impaction efficiency model from Landhal is:

$$\eta_I = \frac{Stk^3}{Stk^3 + 0{,}77Stk^2 + 0.22} \qquad [70]$$

Where the Stokes number ($Stk = \frac{d_p^2 \rho_p C_c U}{18 \mu_{air} d_f}$) represents the capacity of the particle to follow the stream in presence of an obstacle.

The particles are collected by interception if they collect on the fibre without deviating from the gas streamlines (Figure 115).

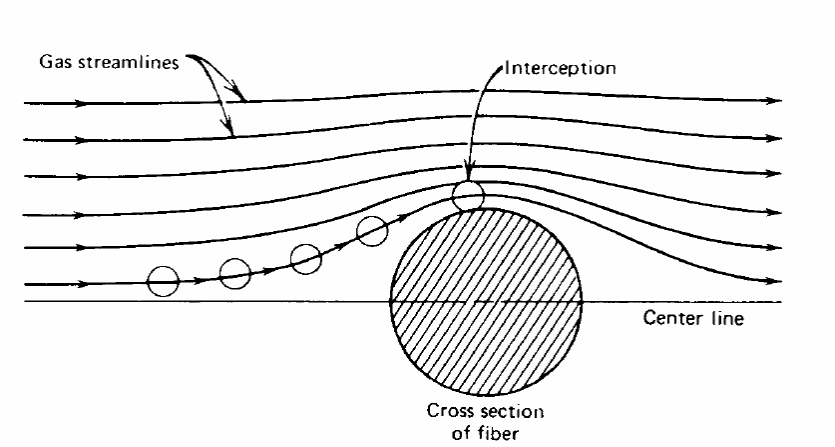

Figure 115: Interception mechanism of particle collection (figure from http://www.unc.edu/courses/2007spring/envr/754/001/)

Always according Lee and Liu, interception efficiency is given by:

$$\eta_R = 0.6 \frac{(1-\alpha_f)}{R} \frac{R^2}{(1+R)} \qquad [71]$$

Where R is the interception factor: $R = \frac{d_p}{d_f}$

Brownian motion causes small particles to dart about very quickly due to particle impact with gas molecules. As a result, the particle may touch the fibre if it happens to move in that direction as the gas streamline on which it is riding passes near the fibre surface (Figure 116).

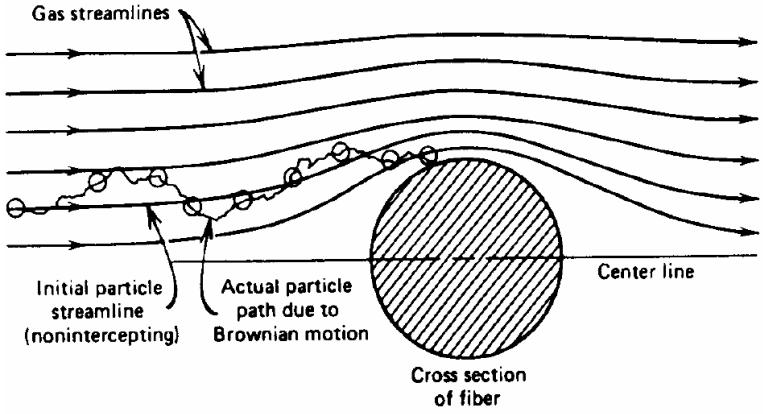

Figure 116: Diffusion (or Brownian) mechanism of particle collection (figure from http://www.unc.edu/courses/2007spring/envr/754/001/)

The diffusion term is from Lee and Liu [Lee 1982]; neglecting minor terms and simplifying the equation is:

$$\eta_D = 2.6 \left(\frac{1-\alpha_f}{Ku}\right)^{1/3} Pe^{-2/3} \qquad [72]$$

With the *Peclet* number:

$$Pe = \frac{U^* d_f}{Diff} \qquad [73]$$

Where *Diff* is the diffusion:

$$Diff = \frac{k_B T C_c}{3\pi\mu_{air} d_p} \quad [74]$$

And *Ku* the *Kuwabara* number:

$$Ku = -\frac{1}{2}\ln(\alpha_f) - \frac{3}{4} + \alpha_f + \frac{1}{4}\alpha_f^2 \quad [75]$$

For a low efficiency filter (high d_f and low α_f), the prevalent mechanism of fibre particle collection is the impaction as shown in the figure below.

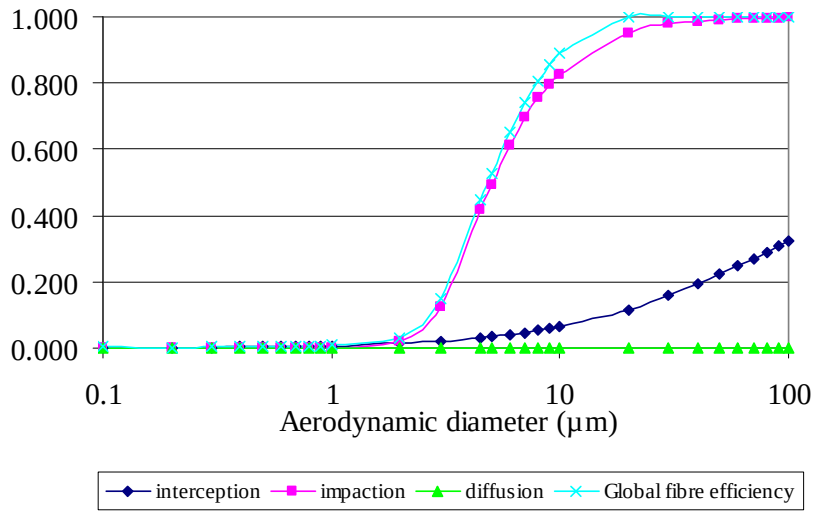

Figure 117: Efficiencies for different mechanism of impaction for a low efficiency filter

The pressure drop for the clean filter is:

$$\Delta p = F.\frac{4\mu_{air}\alpha_f UZ}{\pi d_f^{\,2}} \quad [76]$$

With *F* Davies's factor [Davies 1973]:

$$F = 16\pi\alpha_f^{\,1/2}(1+56\alpha_f^{\,3}) \quad [77]$$

For the fouled filter, the pressure drop is calculated as:

$$\Delta p = 64\mu UZ\left(\frac{\alpha_f}{d_f^2} + \frac{\alpha_p}{d_p^2}\right)^{1/2}\left(\frac{\alpha_f}{d_f} + \frac{\alpha_p}{d_p}\right)(1+56(\alpha_f+\alpha_p)^3) \quad [78]$$

Where α_p is the packing density of the collected particle and $\bar{d}_p$ the average diameter:

$$\bar{d}_p = \frac{\sum \alpha_i d_{pi}}{\sum \alpha_i} \quad [79]$$

We can observe that the additional pressure drop term is sensitive to the particle diameter and shows that fine particles having a more fouling effect than coarse particles.

The particles deposited on the filter form dendrites that participate to the particles collection and can be considered as new fibres. We consider then two terms for the collection mechanism: the fibre collection efficiency and the particle collection efficiency.

The global filter efficiencies for fibre E_f and particle E_p, following the Thomas model, finally take into account of the packing density through the formula:

$$E_f = 1 - exp\left(\frac{-4\alpha_f \eta_f Z}{\pi(1-\alpha_f-\alpha_p)d_p}\right) \quad [80]$$

$$E_p = 1 - exp\left(\frac{-4\alpha_p \eta_p Z}{\pi(1-\alpha_f-\alpha_p)d_p}\right) \quad [81]$$

The collected mass m_d by the filter is the sum of the collected mass by the fibres m_f and by the dendrites formed by the particles m_p:

$$m_d = m_f + m_p \quad [82]$$

$$m_f = \left(1 - \frac{\alpha_p}{1-\alpha_f}\right)\sum_i E_f \cdot m(d_{p_i}) \quad [83]$$

$$m_p = \left(\frac{\alpha_p}{1-\alpha_f}\right)\sum_i E_p \cdot m(d_{p_i}) \quad [84]$$

The program follows the diagram of Figure 118, with as input the filter characteristic d_f and α_f, the initial airflow and the air mass distribution as a function of the aerodynamic diameter of the particle. The air mass distributions simulated are discrete and are the same we used in the case of the condenser fouling [annex 5].

The fouling limit has been set for an airflow reduction of –36 %, as we could simulate in the Mark V simulation campaign.

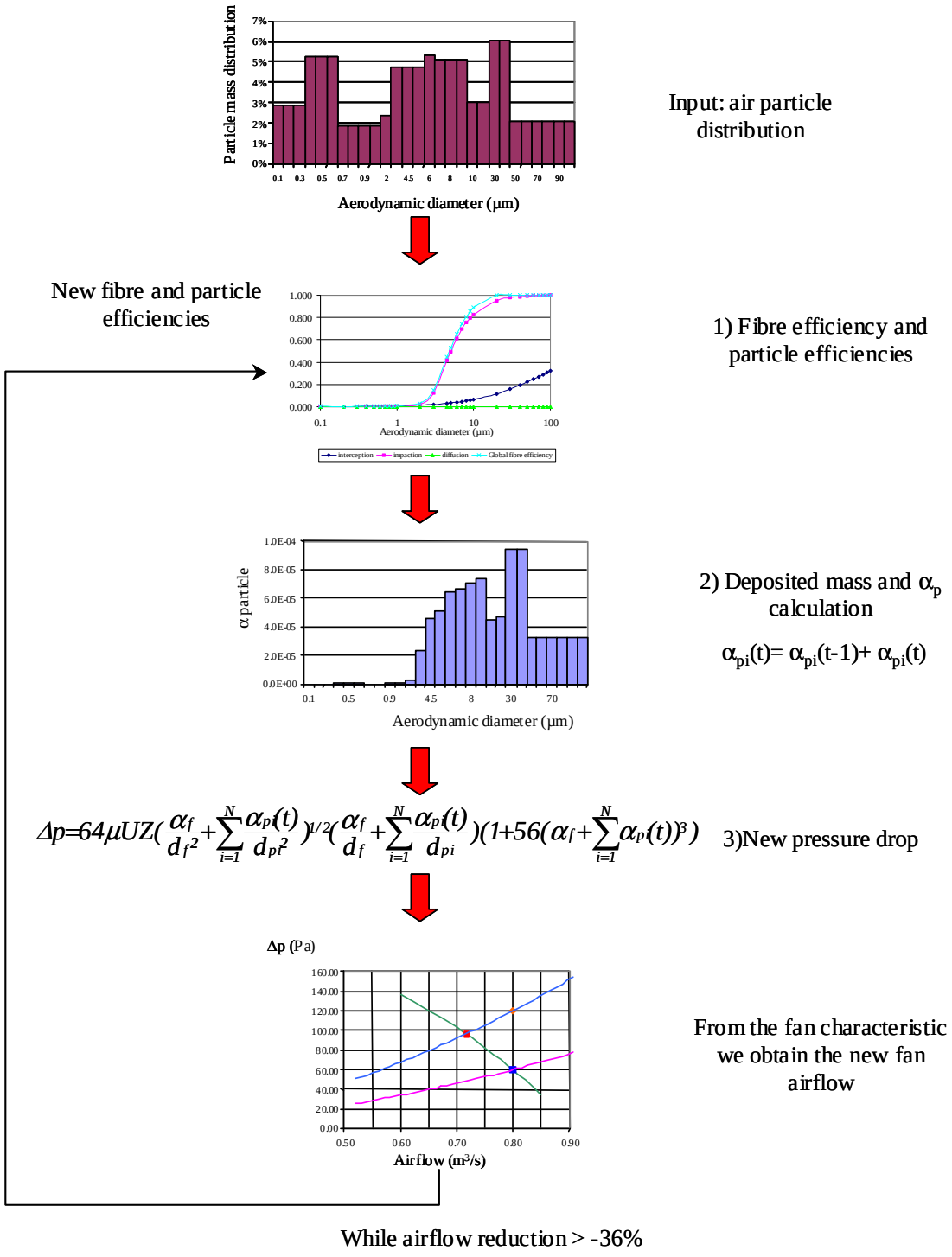

Figure 118: Scheme of the program for filter fouling

The formula has been originally created to model one single particle diameter fouling effects. Because of the large diameters range for the air mass distributions considered, the formula [78] is not really suitable to our case because the little average diameter of the collected particles make the time fouling too short to be physically representative. We modified as it follows in order to consider separately the contribution of each particle diameter:

$$\Delta p=64\mu UZ\left(\frac{\alpha_f}{d_f^2}+\sum_{i=1}^{N}\frac{\alpha_{pi}}{d_{pi}^2}\right)^{1/2}\left(\frac{\alpha_f}{d_f}+\sum_{i=1}^{N}\frac{\alpha_{pi}}{d_{pi}}\right)\left(1+56\left(\alpha_f+\sum_{i=1}^{N}\alpha_{pi}\right)^3\right) \qquad [85]$$

Before commenting the model results we have to make some observations about the model limits and hypothesis. The model does not take into account the on/off cycle of the unit that can influence the

particle collection, an amount of the particle deposited on the filter surface falling down when the draught air force is off. On the other side, in some case, split systems can ensure simple ventilation using the indoor unit fan without cooling function, the occupant accepting the simple cooling effect due to the airflow. In this case the use of the split becomes longer and the occupant can choose to use it in the mid season, increasing the fouling of the filter.

One last element should be considered that reduces the reliability of our model versus the reality: the presence of bypass. The filter casing, although initially conceived to force the total airflow to pass through the filter, presents in general some gaps that allow the air to bypass the filter. The amount of the bypass airflow is variable with the bypass shape, dimensions and it increases with the filter fouling, and has an important effect on the filter efficiency [Ward 2005]. This makes the filter efficiency decrease with the fouling that contrasts with the increasing collection efficiency due to the additional particle collection efficiency and increase the filter fouling time.

4.4.2 Fouling time for different air mass distribution and cleaning strategies

For the three air mass distributions, the model gave the fouling times shown in the table below.

Table 38: Fouling time, deposited masses and filter efficiencies from the filter fouling model

Dust distribution	Final α_p	Hours	Crossing mass (g)	Deposited mass (g)	Final filter efficiency
Whitby	6.94E-05	18	2.28	0.94	41 %
Lestari	1.15E-04	21	2.66	1.57	59 %
SAE Coarse	3.95E-04	50	6.35	5.38	85 %

We can observe that the filter fouls very quickly with fouling times between 18 and 50 hours. More the mass distribution is fine, more the filter fouls quickly with a lower efficiency, this because the more fouling particles are the finest although they are less arrested as shown by the total deposited mass.

Filter fouling has a minor impact on the energy efficiency as we saw in chapter 2.9.3 but its replacement or cleaning becomes important because of other consequences on the system operation such as the reduction of the superheat that allows liquid to enter into the compressor, or the decrease of the evaporating temperature, the increased latent heat removal and the ice formation on the evaporator for extreme fouling rate and low evaporating temperatures.

Actually, the filter replacement is scheduled differently following the manufacturers' indications: for some manufacturer it should be performed every two weeks, for some other monthly, or more if the space is dusty.

Following our seasonal simulations, for the office building, the splits units work at an average of three hours per day in Nice: the filters should be changed several times in a year, the best intervention frequency is shown by the yellow dots in the figure below for Nice and Trappes. Each filter cleaning is after twenty hours of operation from the Lestari mass distribution results (Table 38).

The operation time of the split is calculated as the sum of the hourly load rates calculated by the Consoclim model. As an example, an hourly load rate of 50 % is considered as the system worked half of an hour. The sum of the load rates of a day gives the daily operation time of the split.

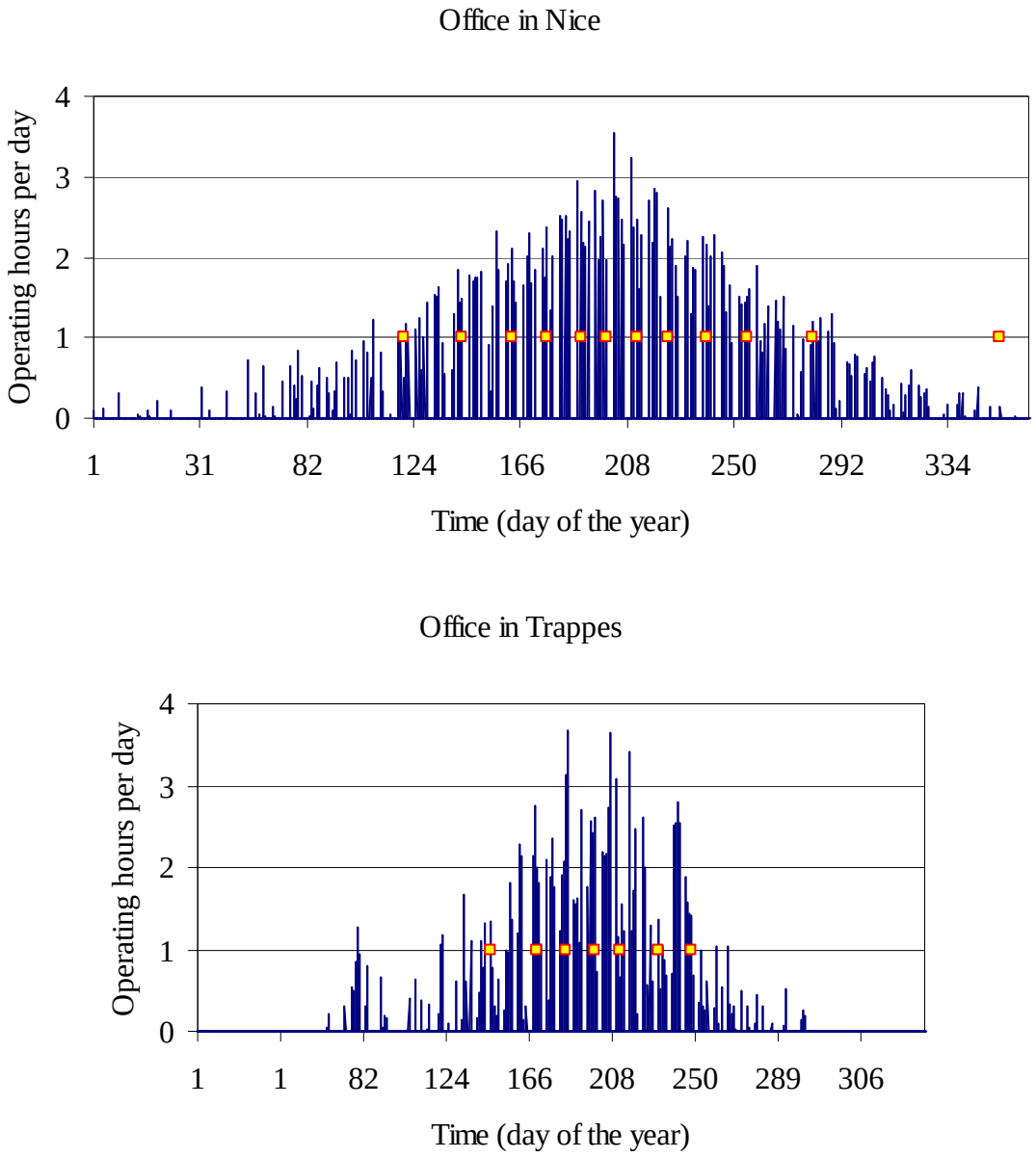

Figure 119: Operation hours per day of split and cleaning intervention (yellow dots) after 20 operation hours for a office building

The filter replacement or cleaning should be scheduled regularly in the hot season. The best method would be to install single counters for operating hours (at least on one split, the one supposed to work longer, that would be considered representative of the set) and to perform filter maintenance at regular interval such as it is done with car maintenance based on run kilometres.

However, we can estimate that the manufacturers' two weeks cleaning interval agrees with our results for office buildings: the intervention frequency established every twenty operating hours gives us an average interval between two interventions of fourteen days both for Nice and Trappes locations.

For the residential buildings things change: the operating hours per day are lower. The monthly cleaning interval seems more appropriate: the intervention frequency established every twenty operating hours give an average period between two interventions of twenty four days both for Nice and Trappes locations Figure 120.

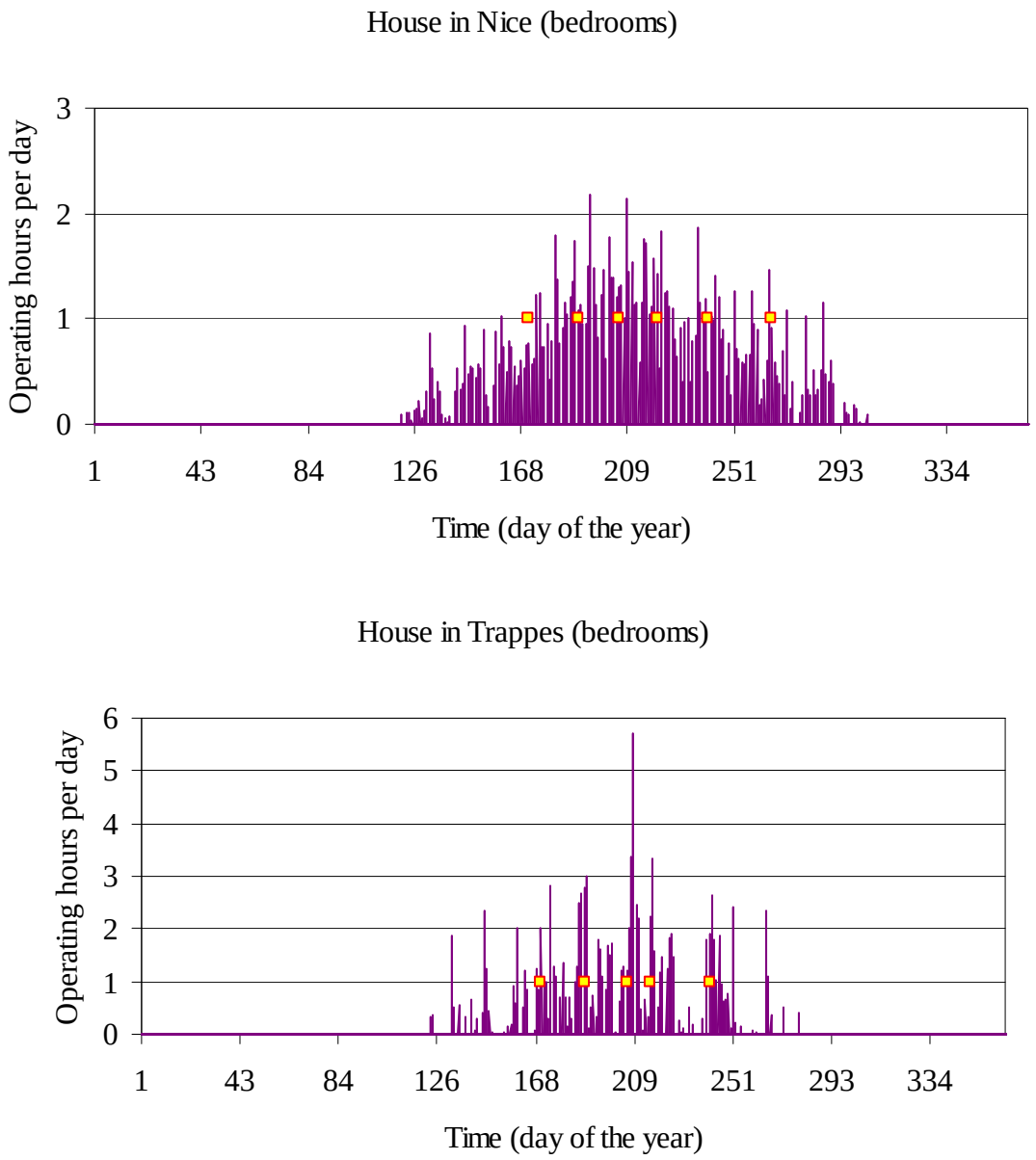

Figure 120: Operation hours per day of split and cleaning intervention (yellow dots) after 20 operation hours for a house building

4.4.3 Economic elements for filter replacement

The cost of the filter replacement is related to the filter type and in the case of the house; the owner would rather do it himself instead of paying someone. We could not perform energy savings calculations because we did not consider accurately enough the fan consumptions and, on the system side, we could not observe significant overconsumption for the fouled rate considered (see chapter 2.9.3).

We can however summarize some elements: the filter used in the split is a low efficiency air filter, it is often sold in rolls and afterwards cut to the desired dimensions, the filter does not need to be replaced but in most cases can be simply cleaned by vacuum or in same case washed; this cleaning does not restore back the filter performance as a new but improves it significantly. The unitary filter price, from some suppliers' catalogue, can be considered around 6 €. The operation of cleaning can take a quarter to half an hour if performed by a non-trained person and consists in disassembling the indoor unit, cleaning the other parts of the indoor unit (grills, water basket, etc.) and the filter (or replace it). The operation does not require expensive qualified staff.

4.5 Conclusions of the time scenarios of defects

The physics of the defects allowed us to create some time related model in order to observe the evolution of the defect with the operation of the air-conditioning system.

The refrigerant leaks represent a danger both for small air conditioners and chillers. The chillers show generally higher leaks rate. The simulation allowed us to determine a critical value for the system where the subcooling becomes zero and the performance is strongly degradated. For split systems with an average annual leaks rate of 5 %, the split can endure 5 years, before reaching this limit. Anyway the system can probably continue to work all along its lifetime without refill, the remaining charge after 15 years being about 50 %.

For chillers, the average leak rate is estimated to 10 %: it would be impossible to consider a lifetime of 15 years with such leak rate and periodic refill is necessary to ensure the chiller operation.

Condenser fouling can be avoided with periodic cleaning of the heat exchanger. Several techniques are available (with compressed air, water, specific product etc.). The cleaning can be a cost effective action when the maintenance cost is negotiated downwards, but in most French cases, the high maintenance cost and the low electricity cost make it not cost effective. The electricity cost is very decisive for the global cost and the higher electricity price of Italy makes the cleaning cost effective in most conditions.

Finally, filter cleaning is a key action for the air quality, the indoor comfort and the efficiency and lifetime duration of the system. Recommendations of manufacturers are to clean it regularly with intervals that depend on the manufacturer. The best intervention frequency should be related to the operation of the system: for a system that operates longer during the day, such as in the simulated offices, cleaning of the filter should be scheduled every fifteen days. For building with lower loads, such as residential, the monthly interval can be sufficient to ensure the cooling capacity and a longer life of the system.

General conclusions

Air conditioning is a key aspect in the energy scenario for energy savings and performance improvement. Several possibilities exist in order to reach better efficiency in existing systems by undertaking a set of actions aimed at keeping the system performance constant all along the system life. The maintenance activities are not anymore only based on availability and become a useful way to reach energy savings and to maintain the comfort level for the occupants.

For split and chiller systems the contexts are slightly different: the ranges of capacity are of a different order of magnitude, but in some contexts a choice can exist between the two systems.

The problem that such systems can meet all along their operation can be common to both systems (refrigerant leak, condenser fouling) or specific. While, for split systems, we can consider problems such as filter fouling, compressor sealing problems and additional pressure drop in the liquid line, for the chiller we will rather consider compressor lubrication problems, evaporator fouling, clogged valve and the presence of non-condensables in the condenser.

The use of models allowed us to analyse the systems in degradated conditions for several defect seriousness and various conditions of operation.

The first simulation campaign allowed us to define the impact on the system performance (cooling capacity, absorbed power end energy efficiency ratio) of each defect and to define the most sensitive system parameters that could allow detecting the problem.

The methodology of research for the defects impacts used simplified models in order to highlight the characteristics specific to each defect and to simulate a large range of defects. For the split systems, an existing model (ORNL heat Pump Model Mark V) has been used after tuning. For the chiller, an existing model developed by the Ecole des Mines de Paris has been tailored to respond to our objectives.

The preliminary results gave us the possibility to define specific parameters for each defect characterisation and to analyse performance evolution for several temperatures of operation.

The second simulation campaign showed the impact of the defect coupled with building types for two different climates taking into account partial load behaviour. In some cases, the trends shown in the first campaign are emphasised by the seasonal operation, in some other cases the partial load behaviour can hide or modify the effect on global consumption and on comfort inside the building.

On one side, the methodology chosen gave us the freedom to simulate a large range of values of defect level, on the other hand it required some assumptions: translation into the model cannot always represent all the physical consequences and the hypothesis that has been made leads in some case to overestimate, in some other to underestimate system performance. Generally speaking, the model is estimated suitable for simulating degradated conditions except for refrigerant leaks. For the used model, uncertainty exists about the calculation and the correlations for refrigerant charge calculation. Moreover it cannot simulate large ranges of charge conditions, because of the loss of validity of expansion device models when no subcooling occurs.

The consequences of a given defect are specific to the system and building chosen and cannot be generalised to all the air conditioning systems type existing in the stock, because of the specificity of the machine (component size, refrigerant fluid etc.), of the sizing method, of the control and of some building aspects in terms of setpoints and thermal characteristics.

Time-related models showed the evolution of the defects with the operation of the systems. A further step of validation of the theoretical model with experimental tests would be necessary: although the used models came from experimental works, the modifications made into the model for our purpose require further experimental data.

The economic aspects have been taken into account and the action of correction has been estimated in terms of cost effectiveness. Scenarios of refrigerant charge evolution have been calculated and this showed that, with the current average leak rate, both splits and chillers need regular inspection and refill in order to operate correctly and to guarantee comfort.

The model of condenser fouling made it possible to estimate the fouling time for the analysed systems. The fouling time is equivalent to six years in the worst case for the buildings equipped with split and less than a year in the worst chiller building case. In both cases, the regular cleaning showed benefit with a high electricity price (i.e. Italian). With low price it depends on the building and on the climate. The best frequency should be identified for each case.

For the split system, the model of filter fouling gave best cleaning frequencies consistent with the shortest manufacturers recommendations with two weeks average interval for office buildings. For residential building, the operation rate is lower and a monthly intervention is sufficient to guarantee at the evaporator a sufficient airflow and a good operating condition.

Globally, the results obtained can be useful for auditors and inspectors to give indicative energy savings values for the proposed correction actions. Some easy to use tools have been made available to calculate the fouling times for the condenser and the fouling times for the filters. Sensitive parameters and measurements trends have been identified as help for defect detection; they could be included in simple models the auditor can use to follow the performance of the installation without complex measurement instrumentation.

In future perspective, the same methodology of research could be applied to other air conditioning systems types based on other technologies, cooling and heating source and refrigerant fluids. Moreover, evaporator fouling can be analysed as another system defect in the same way we did for the condenser. Putting in sequence the filter and the heat exchanger fouling models would allow then identifying evaporator fouling times in the same direction of research explored by Siegel [Siegel 2002].

References

AIC 1998 « Calcul des charges de climatisation et conditionnement de l'air » AICVF Guide n°2 , R. Cadiergues (coordinator).

Arrêté du 7 mai 2007 « relatif au contrôle d'étanchéité des éléments assurant le confinement des fluides frigorigènes utilisés dans les équipements frigorifiques et climatiques », Journal Officiel De La République Française 8 mai 2007, Texte 63 sur 161.

ASHRAE 2005 « Interactive Web-based Owning aand Operating Cost Database » Fianle Report ASHRAE Project 1237-TRP.

Bailey Margaret B. 1998 "System Performance Characteristics of a Helical Rotary Screw Air-Cooled Chiller Operating Over a Range of Refrigerant Charge Conditions "ASHRAE Transactions, 1998, 4207.

Bansal B., Müller-Steinhagen H., Chen X. D. 2000 "Performance of plate heat exchangers during calcium sulphate fouling — investigation with an in-line filter" Chemical Engineering and Processing 39 pp507–519.

Barrault S., Clodic D. 2007 «Inventaire des fluides frigorigènes et de leurs émissions, France Année 2005 Document 1», ARMINES 70777.

Bott T. R., 1995 "Fouling of heat exchangers" New York: Elsevier, ISBN-10: 0444821864.

Breuker Mark S., Braun James E. 1999 "Evaluating the Performance of a Fault Detection and Diagnostic System for Vapor Compression Equipment", ASHRAE Transaction, 4269 (CH-99-18-2).

Breuker Mark S., Braun James E. 1998 "Common Faults and Their Impacts for Rooftop Air Conditioners", HVAC&R Research July Vol. 4, n°3 4268 (CH-99-18-1).

California energy Commission, 2005 "Residential Compliance Manual For California's 2005 Energy Efficiency Standards", Publication Number: CEC-400-2005-005-CMF.

CBAT v.1.3, « Bibliothèque de formules de calcul en aéraulique et thermique » CETIAT.

Chen B., Braun J. E. 2001 "Simple Rule-Based Methods for Fault Detection and Diagnostics Applied to Packaged Air Conditioners", ASHRAE Winter Meeting, AT-01-14-2, pages: 847-857.

Choi J., Kimb Y. 2004 "Influence of the expansion device on the performance of a heat pump using R407C under a range of charging conditions" International Journal of Refrigeration 27, pp. 378–384.

Climinfo 2005 « La climatisation en France en 2004 », Report, http://www.climinfo.fr.

Comstock M. C., Braun. J. E., Groll E.A. 2001 "The Sensitivity of Chiller Performance to Common Faults", AC-02-12-2 (4545), HVAC & R Research, Vol. 7, No. 3.

Comstock M. C., Braun J. E., Groll E. A. 2002 "A Survey of Common Faults for Chillers", ASHRAE Winter Meeting, AC-02-12-1, pages: 819-825.

Consoclim 2002 « Etude de la sensibilité et validation in situ de la méthode Consoclim : Rapport Final » Alessandrini J.M., Bolher A., Fleury E., Marchio D., Millet J.R., Roujol S., Stabat P..

Davies C.N. 1973 "Air Filtration" Academic Press London.

Dehausse R., 1974 « Cours de machines thermodynamiques », Ecole des Mines de Paris

DeMarcus, W., Thomas, J. W. 1952 "Theory of a diffusion battery" Oak Ridge National Laboratory ORNL-1413.

Dougherty B. P,. Filliben J. J., Avilés A. I. 2002 "Central Air Conditioner Test Procedure Public Workshop: A Technical Discussion on New Defaults for CCD, National Institute of Standards and Technology" http://www.eere.energy.gov/

ECODESIGN 2007 "Preparatory study on the environmental performance of residential room conditioning appliances-Draft report of Task 4 Technical Analysis of existing products" October .

EECCAC 2003 “Energy efficiency and Certification of Central Air Conditioners” final report, Study for the Directorate General Transportation-Energy of the Commission of the European Union, April.

EERAC 1999 "Energy Efficiency of Room Air-Conditioners" final report, Study for the Directorate General Transportation-Energy of the Commission of the European Union, May.

EN 14511-2:2004 “Air conditioners, liquid chilling packages and heat pumps with electrically driven compressors for space heating and cooling. Test conditions”

EN 779:2002 “Particulate air filters for general ventilation - Determination of the filtration performance”/NF EN 779 «Filtres à air de ventilation générale pour l'élimination des particules. - Détermination des performances de filtration. »

EPBD 2002 “Directive 2002/91/EC of the European Parliament and of the Council of 16 December 2002 on the energy performance of buildings” Official Journal L 001 , 04/01/2003 P. 0065 – 0071

Eurovent 2005 “Chiller Statistics 2005 – Total Sales Europe 2005” Eurovent Certification Company SCRL, Paris, France.

F-gas 2006, "Regulation (EC) No 842/2006 Of The European Parliament and of the Council of 17 May 2006 on certain fluorinated greenhouse gases” Official Journal of the European Union14.6.2006 L 161/1-3.

Fischer S. K., Rice, C. K. 1983 “The Oak Ridge Heat Pump Models: I. A Steady-State Computer Design Model for Air-to-Air Heat Pumps” ORNL/CON-80/R1.

Grace I.N., Datta D., Tassou S.A. 2005, “Sensitivity of refrigeration system performance to charge levels and parameters for on-line leak detection”, Applied Thermal Engineering 25 pp.557–566.

Haghighi-Khoshkhoo R., McCluskey F. M. J. 2007 “Air-Side Fouling of Compact Heat Exchangers for Discrete Particle Size Ranges", Heat Transfer Engineering , Volume 28, Number 1.

Hinds W. C. 1999 "Aerosol technology : Properties, behavior, and measurement of airborne particles" New York: Wiley.

Israel R. and Rosner D. E. 1983 "Use of a generalized stokes number to determine the aerodynamic capture efficiency of non-stokesian particles from a compessible gas-flow" Aerosol Sci. Technol. 2, 45-51.

Johansson A., Lundqvist P. 2001 “A method to estimate the circulated composition in refrigeration and heat pump using zeotropic refrigerant mixtures” International Journal of Refrigeration 24 pp.798-808.

Kho T., Zettler H. U., Müller-Steinhagen H., Hughes D. 1997 “Effect of flow distribution on scale formation in plate and frame heat exchangers” Trans IChemE, Vol 75, Part A, October, pp 635-640.

Kim N. H., Youn B., and Webb R. L. 1998"Heat Transfer and Friction Correlations for Plain Fin-and-Tube Heat Exchangers," 11th Int. Heat Transfer Conf., Kyongju, Korea, Vol. 6, pp. 209-213.

Kinab E., Fau A., Marchio D., Rivière P. 2007 « Model of a Reversible Heat Pump for Part Load Energy Based Optimization Design” Clima 2007 Proceedings.

Krarti M., Marchio D., Arditi I., Carretero C. 2001 “Guide technique d’audit énergétique des bâtiments” Mines de Paris.

Landahl H., Hermann K. 1949 “Sampling of liquid aerosols by wires, cylinders, and slides, and the efficiency of impaction of the droplets”, J. Colloid Interface Sci. 4 pp 103–136.

Lee K.W., Liu B.Y.H. 1982 “Theoretical study of aerosol filtration by fibrous filters”, Aerosol Sci. Technol. 1 pp 147–161.

Lestari, Puji , Oskouieb, Ali K, Noll Kenneth E. 2003 “Size distribution and dry deposition of particulate mass, sulfate and nitrate in an urban area” Atmospheric Environment 37, pp 2507–2516.

Longo G.A., Gasparella A., Sartori R. 2004 “Experimental heat transfer coefficients during refrigerant vaporisation and condensation inside herringbone-type plate heat exchangers with enhanced surfaces” International Journal of Heat and Mass Transfer 47 4125–4136.

McIntosh Ian B.D., Mitchell John W., Beckman William A. 1998 “Fault Detection and Diagnosis in Chillers—Part I: Model Development and Application”, HVAC&R RESEARCH 4395, VOL. 4, n°4.

Pak Bock Choon, Groll Eckhard A., Braun James E. 2005 “Impact of fouling in cleaning on plate fin and spine fin heat exchanger performance” ASHRAE Transaction Winter meeting, OR-05-1-3.

Panchal C.B., Rabas T.J. 1999 "Fouling Characteristics of Compact Heat Exchangers and Enhanced Tubes" International Conference on Compact Heat Exchangers and Enhancement Technology for the Process Industries, July 18 - 23, Alberta, Canada.

Parker D., Sherwin J., Raustad R., Shirey D. 1997 "Impact of Evaporator Coil Air Flow in Residential Air Conditioning Systems," ASHRAE Annual Meeting, Boston, BN-97-2-1.

Phelan J., Brandemuehl M.J., Krarti M. 1997 “In-situ performance Testing of Chillers for Energy Analysis”, ASHRAE Transaction, vol. 103, part 1, paper number 4040 (RP-827), pp. 290-302.

PrEN 1736 « Refrigerating systems and heat pumps - Flexible pipe elements, vibration isolators and expansion joints - Requirements, design and installation », February 2008 (Standard in preparation).

Refprop7 (REFerence fluid PROPerties), developed by the National Institute of Standards and Technology NIST.

Rice, C. K. 1991 “The ORNL Modulating Heat Pump Design Tool - Mark IV User's Guide”, Oak Ridge National Laboratory.

Rice, C. K. 1996 “ORNL Heat Pump Design Model: Description of Heat Pump Specification Data - Mark V, Version 95D - Update Notes”, Oak Ridge National Laboratory.

Rivière P. 2004 “Performances saisonnières des groupes de production d’eau glacée” Dissertation, Ecole Des Mines de Paris.

Seinfeld, J. H. and Pandis, S. N., 1998 "Atmospheric chemistry and physics : From air pollution to climate change" New York: Wiley.

Siegel, J. A. 2002 “Dissertation: Particulate Fouling of HVAC Heat Exchangers”, University of California, Berkeley Stylianou M. and Nikanpour D. 1996 “Performance monitoring, fault detection, and diagnosis of reciprocating chillers” ASHRAE Transactions 102(1): 699-706.

Thomas D. , Penicot P., Contal P., Leclerc D., Vendel. J. 2001 “Clogging of fibrous filters by solid aerosol particles. Experimental and modelling study” Chemical Engineering Science 56 3549–3561.

Wang C.C., Chang Y.J., Hsieh Y.J., Lin Y.T. 1996a “Sensible heat transfer characteristics of plate fin-and-tube heat exchangers having plane fins” Int. J. Refrigeration 19 4, pp. 223–230.

Wang, C. C., Chen P. Y., Jang J. Y. 1996b “Heat transfer and friction characteristics in convex louver fin and tube heat exchangers”. Experimental Heat Transfer, 9: 61-78.

Ward, M. and Siegel, J.A. 2005 “Modeling Filter Bypass: Impact on Filter Efficiency” ASHRAE Transactions. 111(2), 1091-1100.

Whitby K.T., Clark W.E., Marple V.A., Sverdrup G.M., Sem G.J., Willeke K., Liu B.Y.H. and Pui D.Y.H., 1975 "Characterisation of California aerosols — I. Size distributions of freeway aerosol" Atmospheric Environment 9, pp. 463–482.

Zivi S.M. 1964 “Estimation of Steady-State Steam Void-Fraction by Means of the Principle of Minimum Entropy Production.” Transactions ASME, J. of Heat Transfer Series C, 86: 247-52.

Annexes

Annex 1 - Characteristic of the simulated split in MarkV

Compressor data

Type of refrigerant	R22
Refrigerant superheat at the compressor shell inlet (°C)	6,9
Refrigerant subcooling at the condenser exit (°C)	5
Estimate of refrigerant saturation temperature at the compressor shell input (°C) Estimate of refrigerant saturation temperature at the compressor shell outlet (°C)	5 50
Total piston displacement of compressor (m^3)	$60{,}5 \cdot 10^{-6}$
Compressor shell heat loss rate: Absolute value (W) or As a fraction of compressor input power	 0,05
Compressor model that will be used	*Map based*
Selected compressor operating drive frequency (Hz)	50
Type of drive of base compressor	SWDIM
Type of drive of selected compressor	*SWDIM*
Nominal motor size for selected compressor (W)	2400
Nominal frequency for selected motor rating (Hz)	50
Nominal voltage for selected motor rating (Volts) - induction motors only -	400
Number of frequencies for which base compressor data curve fits are available	1
Base compressor displacement (m^3)	$60{,}5 \cdot 10^{-6}$
Base superheat at the compressor shell inlet (°C)	20
Motor size for base compressor (W)	2400
Nominal frequency for base motor rating (Hz)	50
Nominal voltage for base motor rating (Volts) - induction motors only -	400
Base compressor frequency value for which map data follow (Hz)	50
Nominal base compressor speed at given frequency (rpm)	2920
Base compressor motor voltage at given frequency (Volts) for which map data apply - induction motors only -	400
Performance curve data for specified base compressor frequency	*see Compressor Map fit model*

Evaporator data

Air temperature entering the indoor unit (°C)	27
Relative humidity of the air entering the indoor unit (%)	48
Operating frequency for indoor blower (Hz)	50
Nominal indoor blower frequency (Hz)	50
Nominal air flow rate (m^3/h)	1296
Only for ECM drives - nominal blower motor size (W)	-
Efficiency of fan only	0,45
Type of blower drive	SWDIM
External pressure drop of duct system - independent of specified air flow rate or fan speed (N/m^2) -	0
Frontal area of the coil (m^2)	0,5448
Number of refrigerant tube rows in the direction of air flow	2
Number of equivalent parallel refrigerant circuits in heat exchanger	3
Spacing of the refrigerant tubes in the direction of air flow (m)	0,0226
Spacing of the refrigerant tube passes perpendicular to the direction of air flow (m)	0,025
Total number of return bends in heat exchanger (all circuits)	9
Type of fin surface	*Louvered*
Fin pitch (fins/m)	556
Fin thickness (m)	0,00012

Outside diameter of the refrigerant tubes (m)	0,0095
Inside diameter of the refrigerant tubes (m)	0,0089
Thermal conductivity of the fins (W/m.°C)	204
Thermal conductivity of the tubes (W/m.°C)	384

Condenser data

Air temperature entering the outdoor unit (°C)	35
Relative humidity of the air entering the outdoor unit (%)	50
Operating frequency for outdoor fan (Hz)	50
Nominal outdoor fan frequency (Hz)	50
Nominal air flow rate (m^3/h)	2880
Only for ECM drives - nominal blower motor size (W)	-
Efficiency of fan only	0,45
Type of blower drive	SWDIM
Frontal area of the coil (m^2)	0,76
Number of refrigerant tube rows in the direction of air flow	2
Number of equivalent parallel refrigerant circuits in heat exchanger	4
Spacing of the refrigerant tubes in the direction of air flow (m)	0, 02165
Spacing of the refrigerant tube passes perpendicular to the direction of air flow (m)	0,025
Total number of return bends in heat exchanger (all circuits)	28
Type of fin surface	*Smooth*
Fin pitch (fins/m)	556
Fin thickness (m)	0,00012
Outside diameter of the refrigerant tubes (m)	0,0095
Inside diameter of the refrigerant tubes (m)	0,0089
Thermal conductivity of the fins (W/m.°C)	204
Thermal conductivity of the tubes (W/m.°C)	384

Refrigerant lines data

Rate of heat gain in the compressor suction line (W)	0
Rate of heat loss in the compressor discharge line (W)	0
Rate of heat loss in the liquid line (W)	0
Inside diameter of liquid line (m)	0,0085
Length of liquid line (m)	7
Inside diameter of vapor line between reversing valve and indoor coil (m)	0,0146
Length of vapor line between reversing valve and indoor coil (m)	7,5
Inside diameter of vapor line between reversing valve and outdoor coil (m)	0,0085
Length of vapor line between reversing valve and outdoor coil (m)	1
Inside diameter of line between reversing valve to compressor inlet (m)	0,0117
Length of line between reversing valve to compressor inlet (m)	0,75
Inside diameter of vapor line between compressor outlet to reversing valve (m)	0,0116
Length of line between compressor outlet to reversing valve (m)	0,75

Compressor data for *Map-based Model* to enter in the Mapfit programme

Base superheat at the compressor shell inlet (°C)						20
Base subcooling at the condenser exit (°C)						0
Power (kW)	Evaporating Temperature (°C) →					
Condensing Temperature (°C) ↓	-15	-10	-5	0	5	10
35	1,73	1,91	2,07	2,20	2,29	2,34
40	1,75	1,97	2,18	2,35	2,49	2,59
45	1,76	2,02	2,26	2,48	2,67	2,83
50	1,75	2,05	2,33	2,59	2,84	3,05
55	1,72	2,06	2,38	2,69	2,98	3,25
60	1,68	2,05	2,41	2,77	3,11	3,43
Mass Flow (g/s)	Evaporating Temperature (°C) →					
Condensing Temperature (°C) ↓	-15	-10	-5	0	5	10
35	24,7	31,92	40,14	49,42	59,87	71,57
40	22,85	29,97	38,08	47,24	57,56	69,11
45	20,93	27,94	35,92	44,95	55,12	66,51
50	18,97	25,85	33,69	42,57	52,57	63,78
55	16,99	23,72	31,41	40,12	49,93	60,94
60	15,02	21,59	29,10	37,62	47,23	58,01

Annex 2 - Details of simulated buildings equipped with splits

House

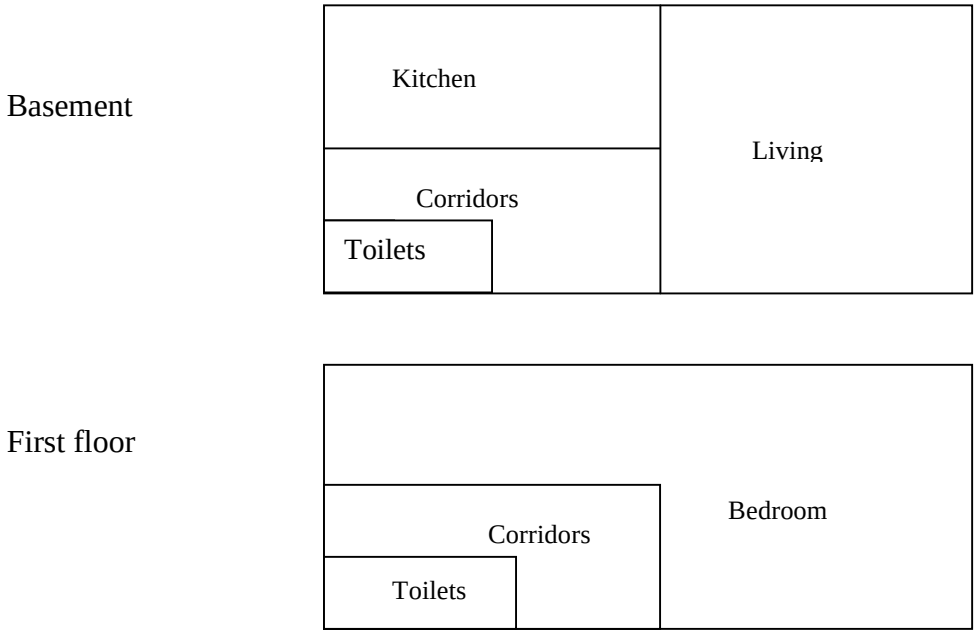

Figure 121: Plan of the floors of the simulated house

Table 39: Simulated house areas

Total area (m²)	127
Bathroom	9,5
Living room (air conditioned)	34
Kitchen	17
Bedrooms (air conditioned)	51
Corridors	25

Occupation scheduling

Living room occupation: 1 person / 9 m²

Bedrooms occupation: 1 person / 12 m²

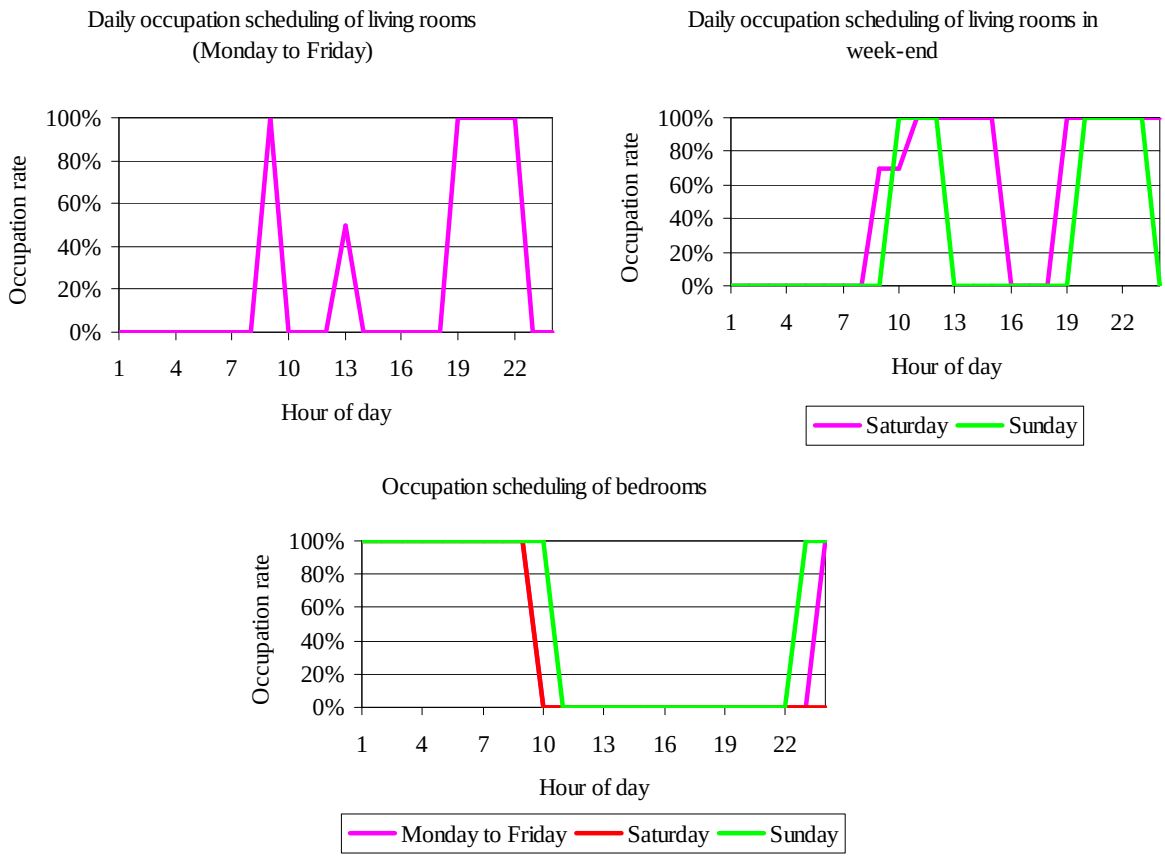

Figure 122: Daily occupation scheduling for the simulated house

Temperature setpoints

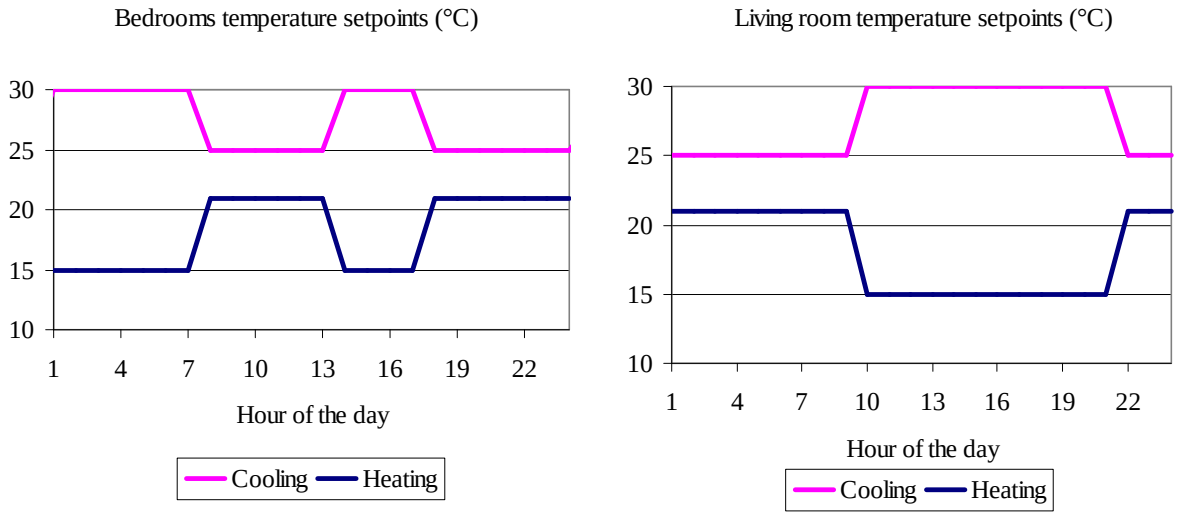

Figure 123: Daily temperature setpoints for the bedrooms and living room

Table 40: House thermal characteristics and cooling loads

Cooling loads		
	Bedrooms	Living room
Lighting	4 W/m²	15 W/m²
Electrical appliances	7 W/m²	10 W/m²
Thermal characteristic of the building		
Rooftop transmittance	0.6 W/m²/K	
Wall thermal transmittance	0.6 W/m²/K	
Windows transmittance	2.3 W/m²/K	

Office

The office building includes two storeys and five different thermal zones shown in the table below.

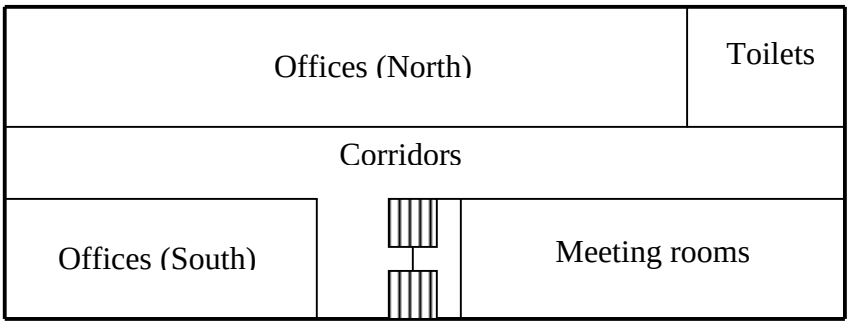

Figure 124: Office building typical storey plan

Table 41: Simulated office areas

Total area (m²)	1008
Toilets/service rooms	30
Offices A (South oriented)	180
Offices B (North oriented)	402
Meeting rooms (South oriented)	180
Corridors	216

Occupation scheduling

Offices occupation: 1 person / 12 m²

Meeting rooms occupation: 1 person / 3.5 m²

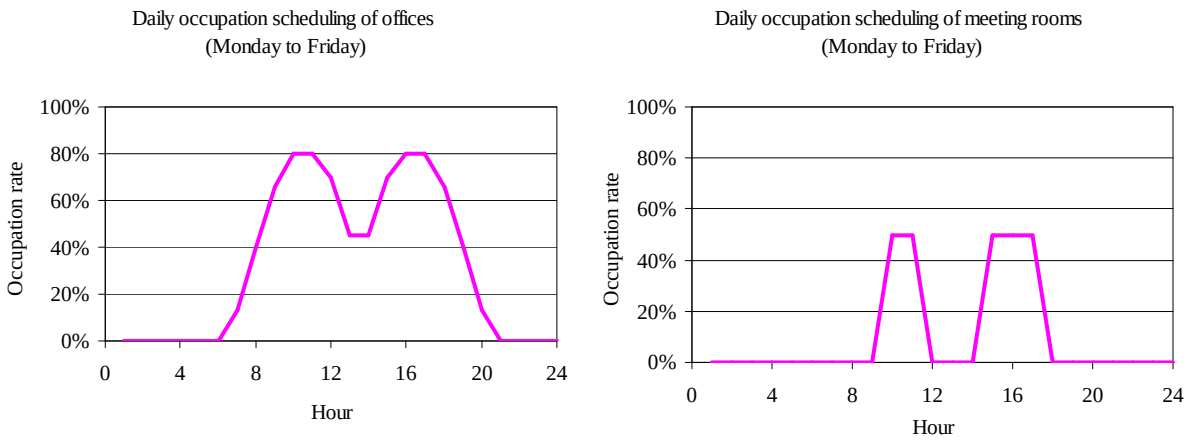

Figure 125: Daily occupation scheduling for offices and meeting rooms

Temperature setpoints

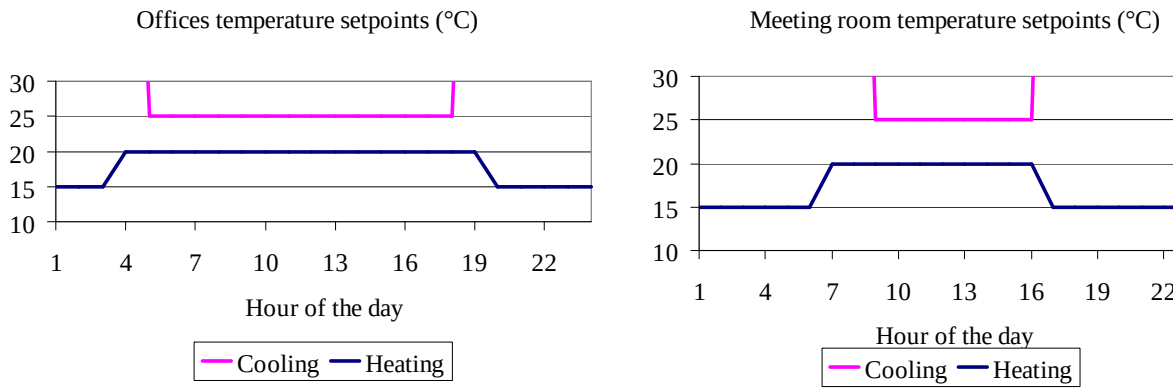

Figure 126: Daily temperature setpoints for the offices and meeting rooms

Table 42: Building thermal characteristics and cooling loads

Cooling loads	
Lighting	30 W/m²
Electrical appliances	15 W/m²
Thermal characteristic of the building	
Rooftop transmittance	0.5 W/m²/K
Wall thermal transmittance	1.3 W/m²/K
Windows transmittance	3.9 W/m²/K

Annex 3 - Seasonal results for house and buildings equipped with degradated splits

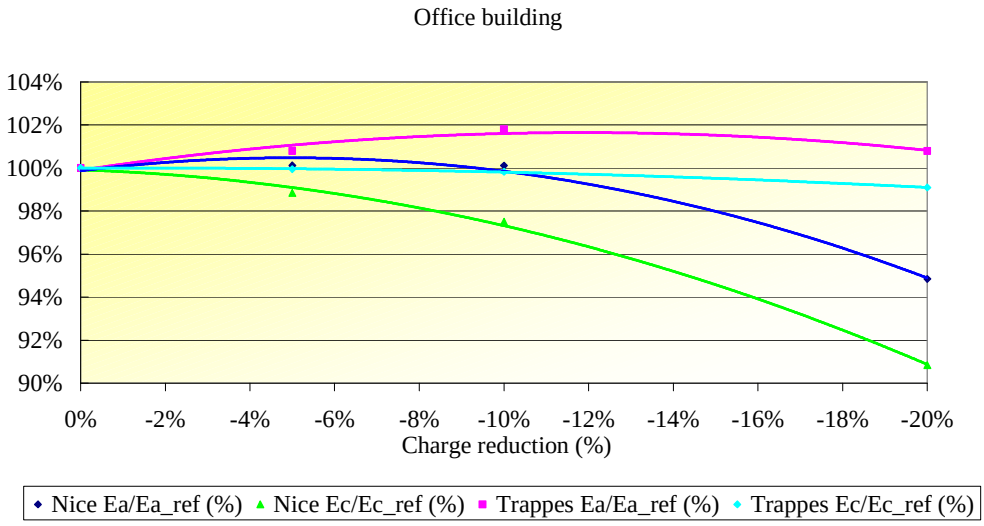

Figure 127: Effect on the cooling energy and the annual energy consumption for an office building in Nice and Trappes for reduced refrigerant charges.

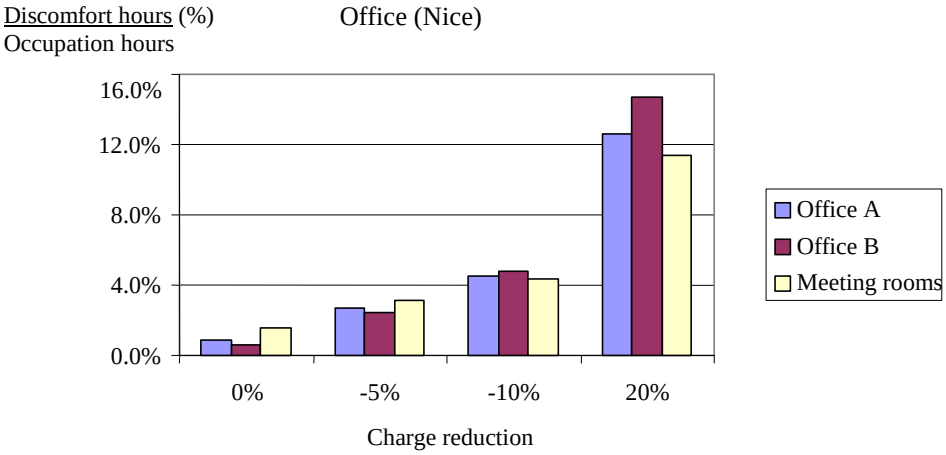

Figure 128: Subsequent discomfort for reduced refrigerant charges for an office building in Nice

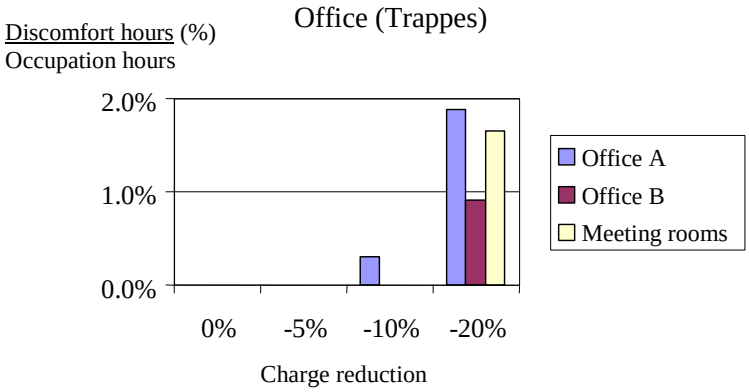

Figure 129: Subsequent discomfort for reduced refrigerant charges for an office building in Trappes

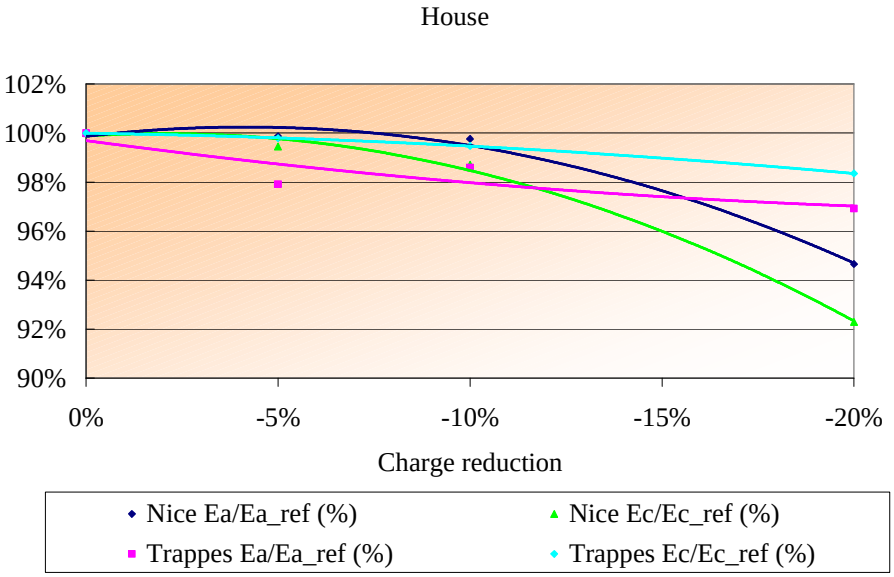

Figure 130: Effect on the cooling energy and the annual energy consumption for a house in Nice and Trappes for reduced refrigerant charges.

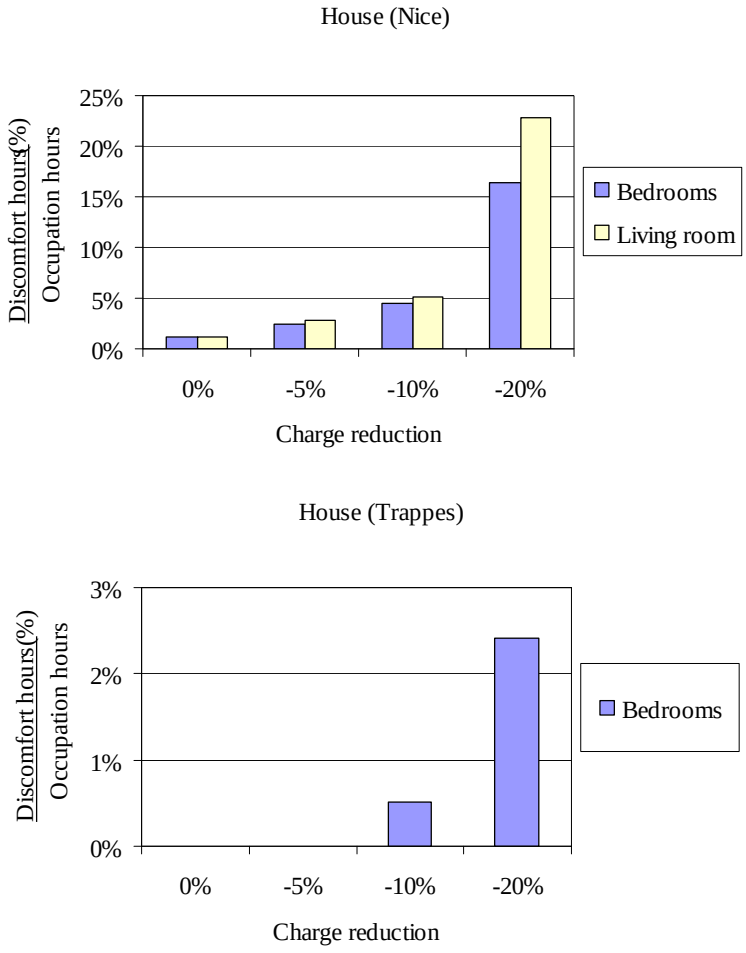

Figure 131: Subsequent discomfort for reduced refrigerant charges for a house in Nice and Trappes

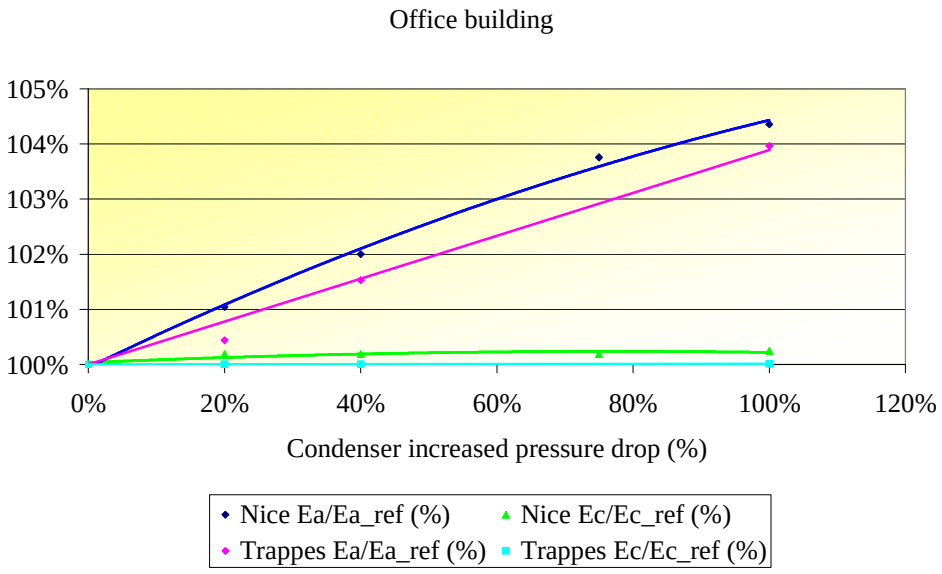

Figure 132: Effect on the cooling energy and the annual energy consumption for an office building in Nice and Trappes for condenser fouling.

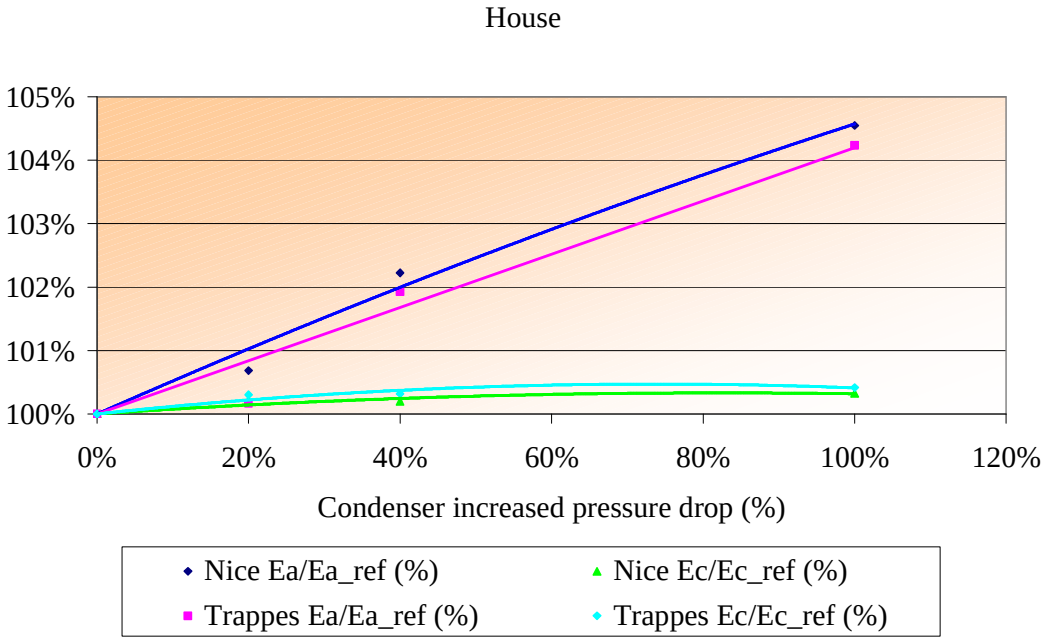

Figure 133: Effect on the cooling energy and the annual energy consumption for a house in Nice and Trappes for condenser fouling.

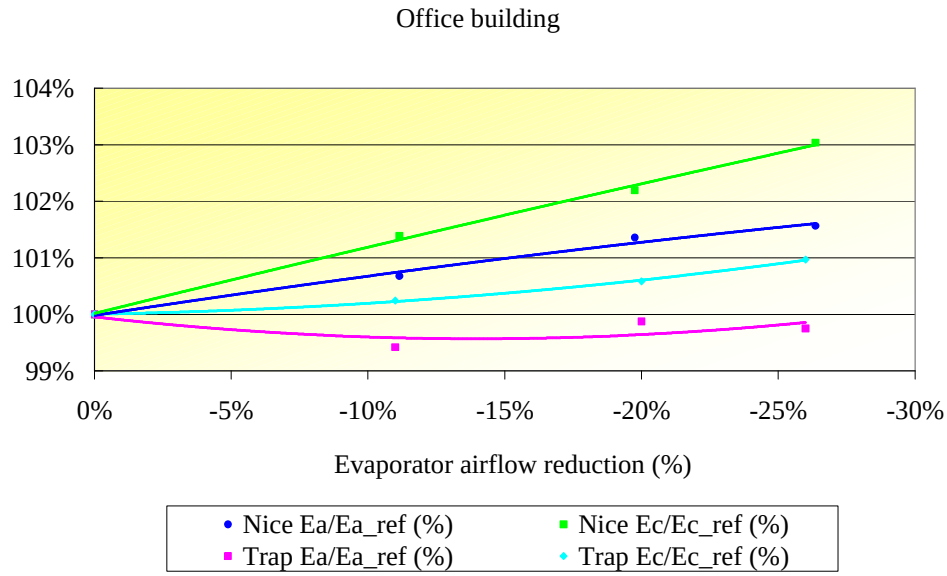

Figure 134: Effect on the cooling energy and the annual energy consumption for an office building in Nice and Trappes for filter fouling

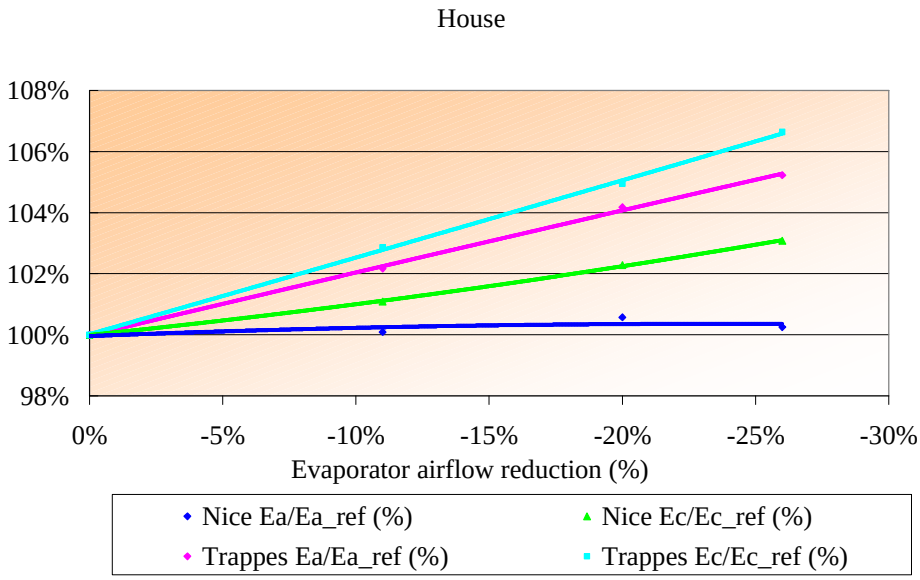

Figure 135: Effect on the cooling energy and the annual energy consumption for a house in Nice and Trappes for filter fouling

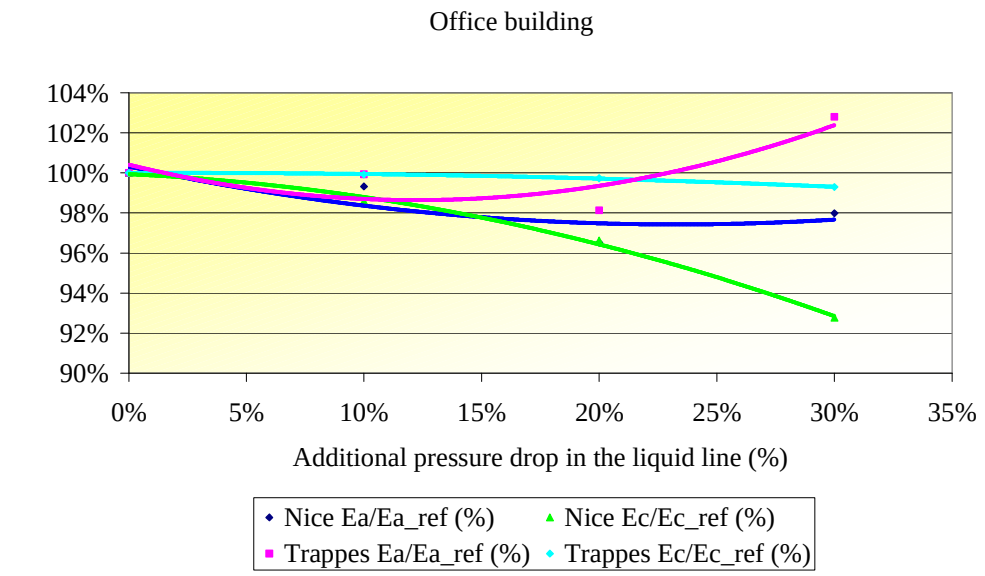

Figure 136: Effect on the cooling energy and the annual energy consumption for an office building in Nice and Trappes for additional pressure drop in the liquid line

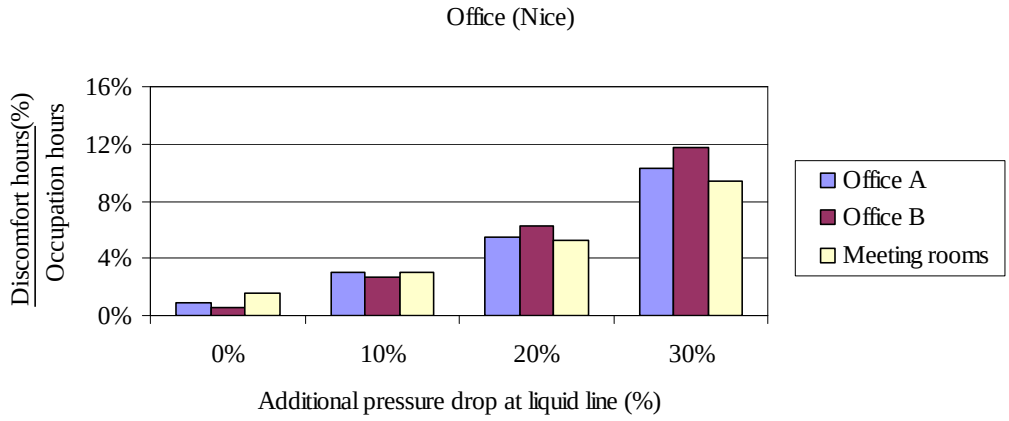

Figure 137: Subsequent discomfort for liquid line restriction for an office in Nice

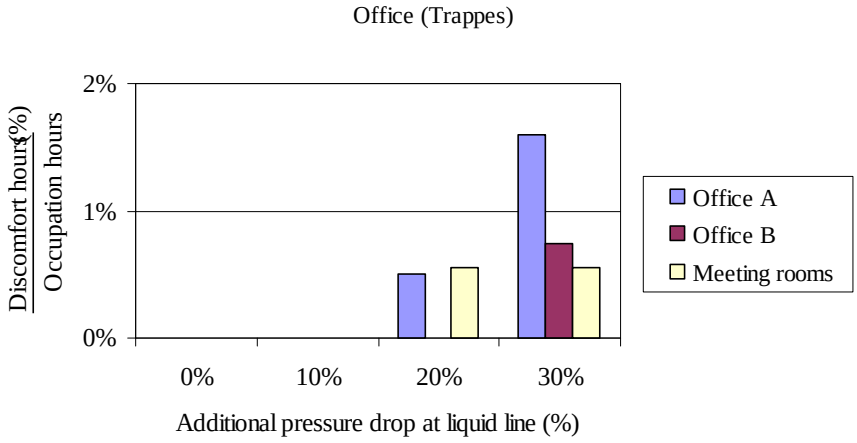

Figure 138: Subsequent discomfort for liquid line restriction for an office in Trappes

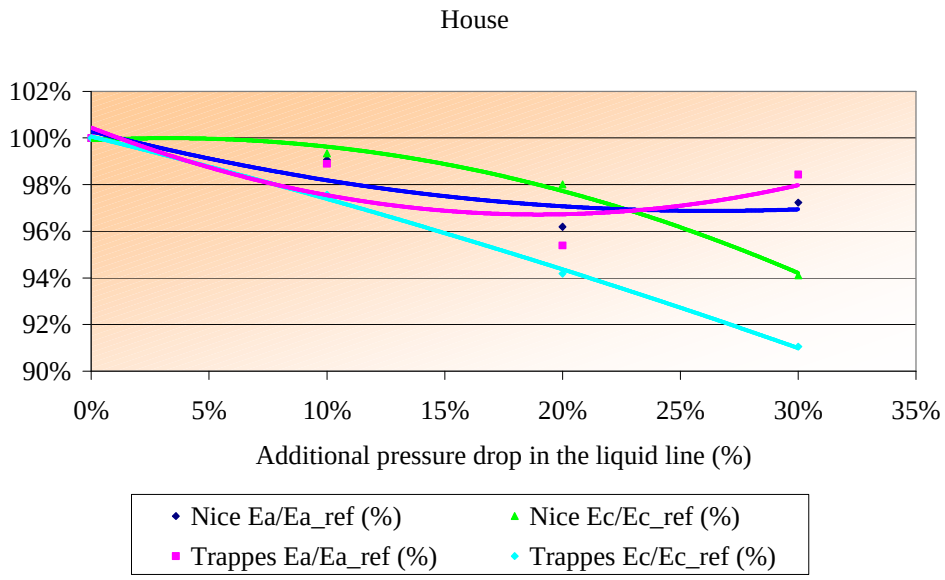

Figure 139: Effect on the cooling energy and the annual energy consumption for a house in Nice and Trappes for additional pressure drop in the liquid line

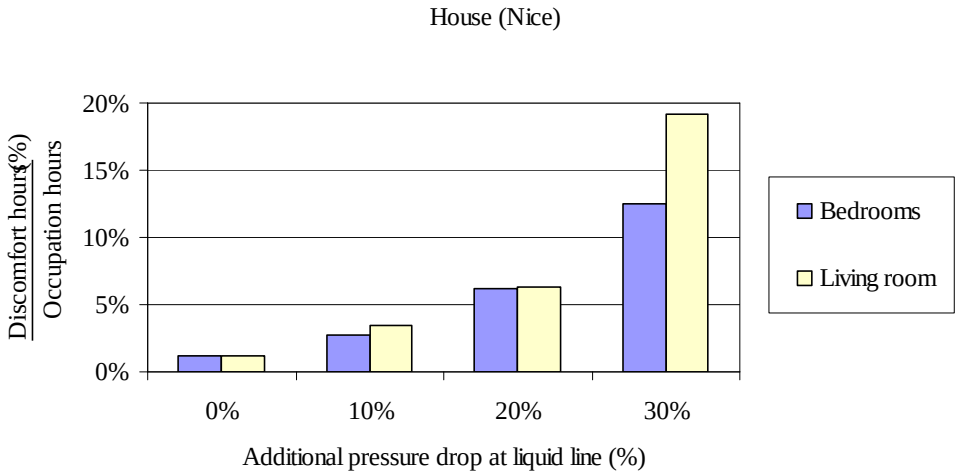

Figure 140: Subsequent discomfort for liquid line restriction for an house in Nice

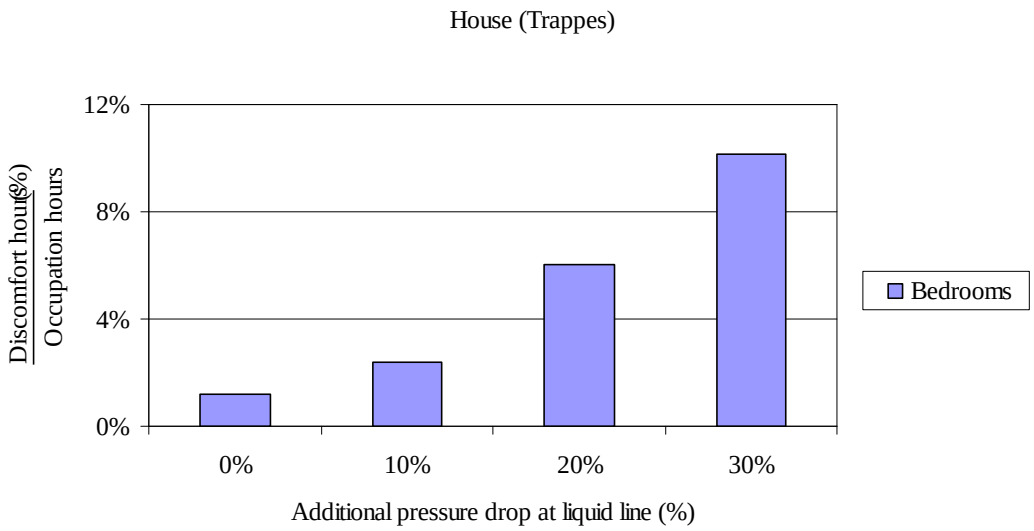

Figure 141: Subsequent discomfort for liquid line restriction for an house in Trappes

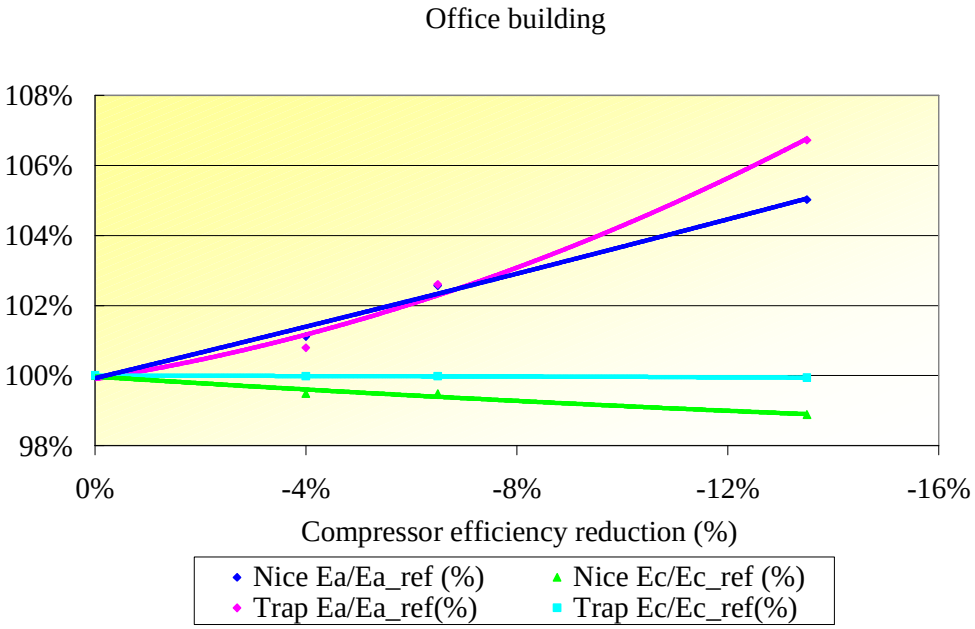

Figure 142: Effect on the cooling energy and the annual energy consumption for an office building in Nice and Trappes for compressor wearing

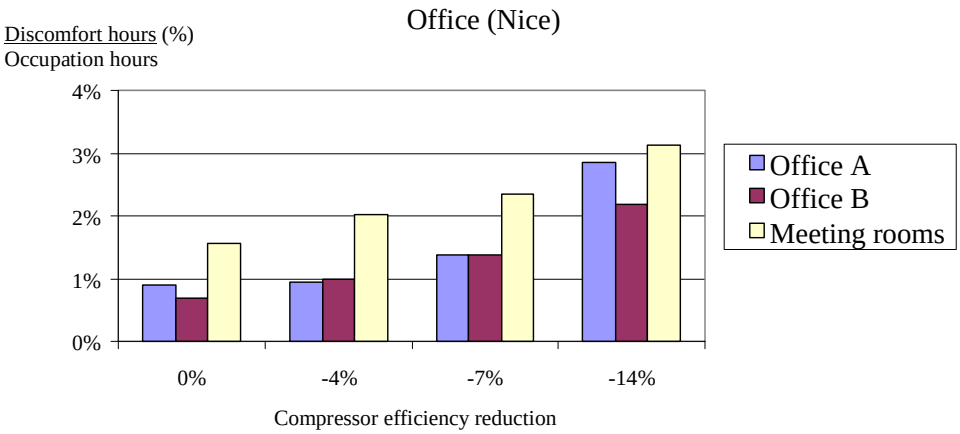

Figure 143: Subsequent discomfort for compressor wearing for an office in Nice

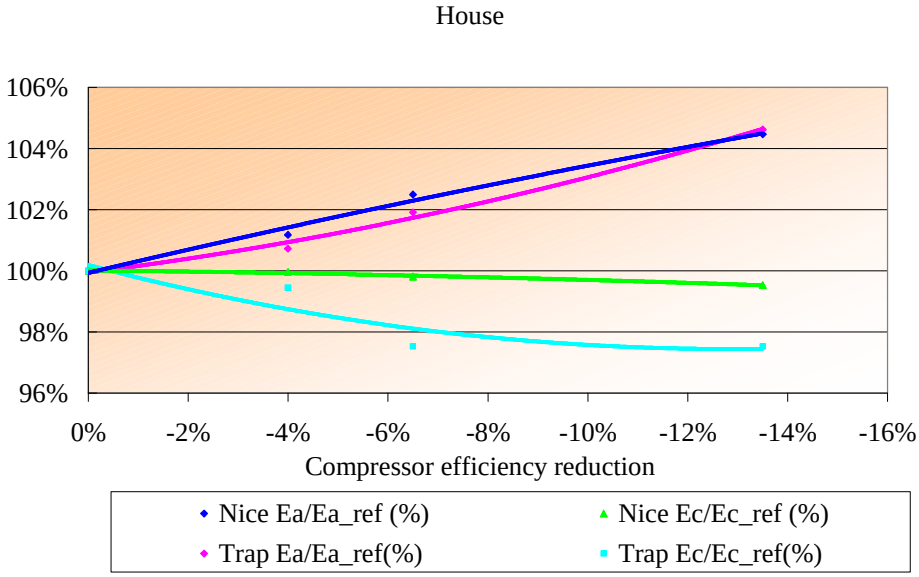

Figure 144: Effect on the cooling energy and the annual energy consumption for an office building in

Nice and Trappes for compressor wearing

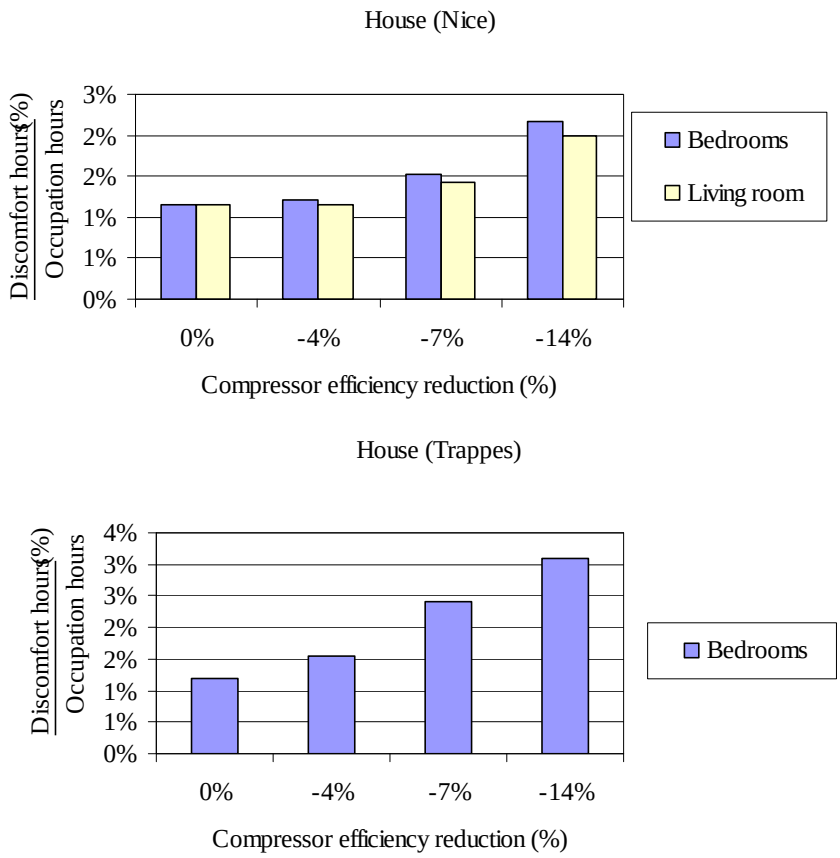

Figure 145: Subsequent discomfort for compressor wearing for a house in Nice

Annex 4 - Details of simulated building equipped with chillers

The occupation scheduling and the temperature setpoints are the same of the building described in the Annex 2.

Table 43: Simulated office areas

	Office 1	Office 2	Office 3
Corridors (m²)	1111	148	432
Office A (m²) North oriented	5928	1389	360
Office B (m²) South oriented	5870	1389	804
Meeting rooms (m²)	2371	1086	360
Toilets/Service rooms (m²)	1111	988	60
Total area (m²)	16391	5000	1584

Occupation scheduling

Offices occupation: 1 person / 12 m²

Meeting rooms occupation: 1 person / 3.5 m²

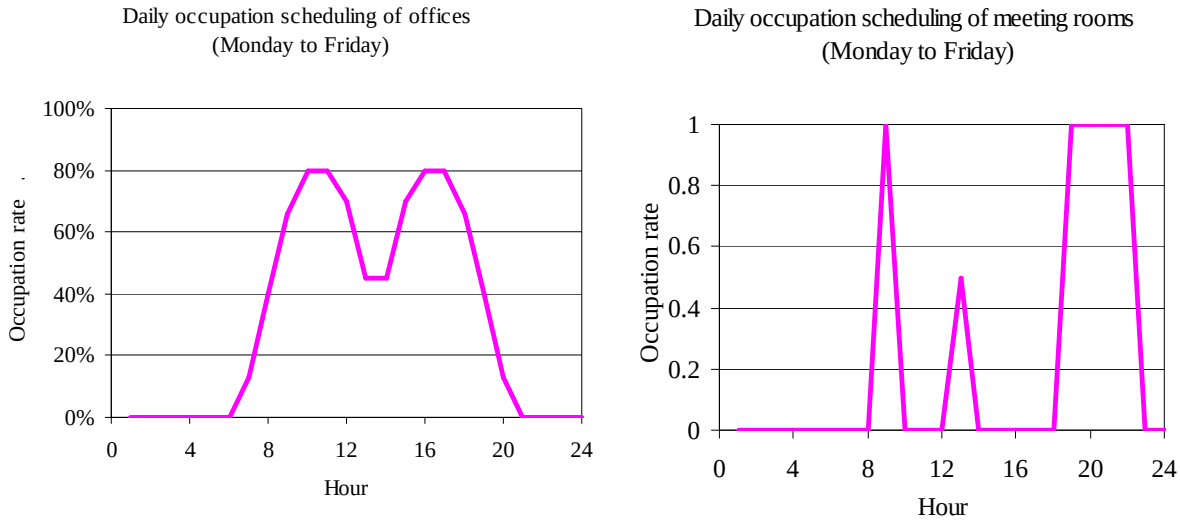

Figure 146: Daily occupation scheduling for offices and meeting rooms

Temperature setpoints

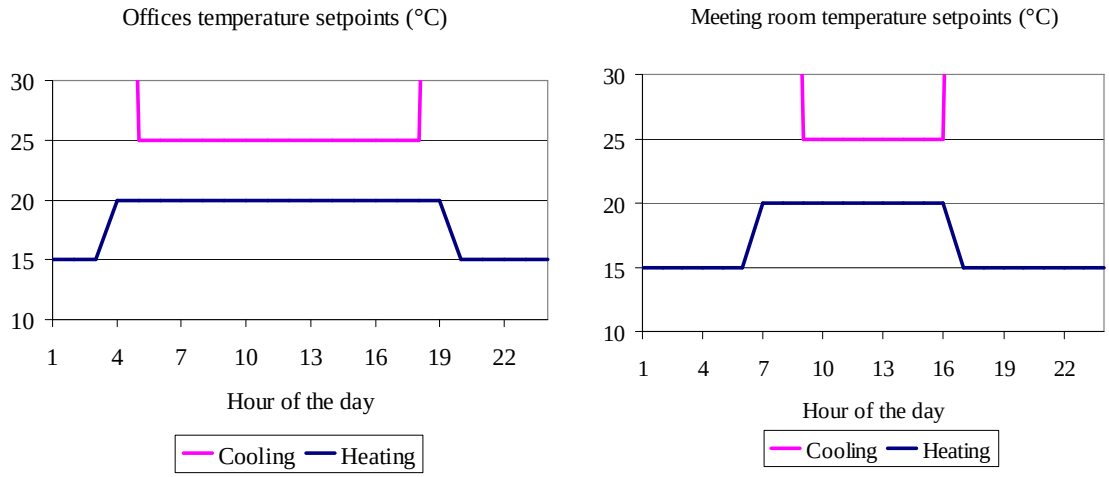

Figure 147: Daily temperature setpoints for the offices and meeting rooms

Table 44: Building thermal characteristics and cooling loads

Cooling loads	
Lighting	30 W/m²
Electrical appliances	15 W/m²
Thermal characteristic of the building	
Rooftop transmittance	0.5 W/m²/K
Wall thermal transmittance	1.3 W/m²/K
Windows transmittance	3.9 W/m²/K

Annex 5 - Air mass distributions

SAE Coarse Dust size distribution

Diameter (µm)	Diff Volume %
0.849	0.177
0.944	0.203
1.05	0.234
1.167	0.266
1.298	0.307
1.444	0.35
1.606	0.393
1.785	0.44
1.986	0.497
2.208	0.55
2.456	0.63
2.731	0.688
3.037	0.741
3.377	0.817
3.756	0.909
4.177	0.997
4.645	1.09
5.165	1.19
5.744	1.27
6.388	1.38
7.104	1.49
7.9	1.63
8.785	1.72
9.77	1.89
10.86	2.04
12.08	2.18
13.44	2.36
14.94	2.58
16.62	2.82
18.48	3.1
20.55	3.36
22.85	3.63
25.42	3.92
28.26	4.25
31.43	4.5
34.95	4.63
38.87	4.73
43.23	4.91
48.07	4.83
53.46	4.48
59.45	4.16
66.11	3.74
73.52	3.27
81.76	2.83
90.93	2.3
101.1	1.93
112.5	1.68
125.1	0.951
139.1	0.461

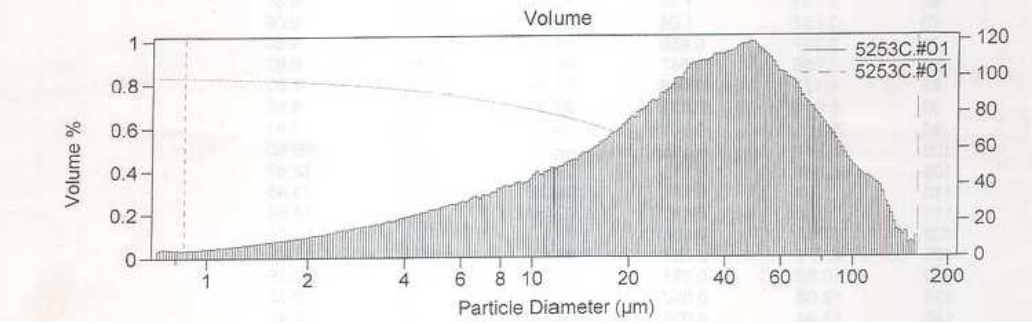

Air mass distribution, from Whitby diagram

Diameter (µm)	Diff Mass %
0.1	2.6
0.2	6.5
0.3	8
0.4	1
0.5	1
0.6	1
0.7	3
0.8	2
0.9	1
1	15
2	17
3	11
4	9
5	3
6	7
7	2
8	4
9	2
10	2
11	0

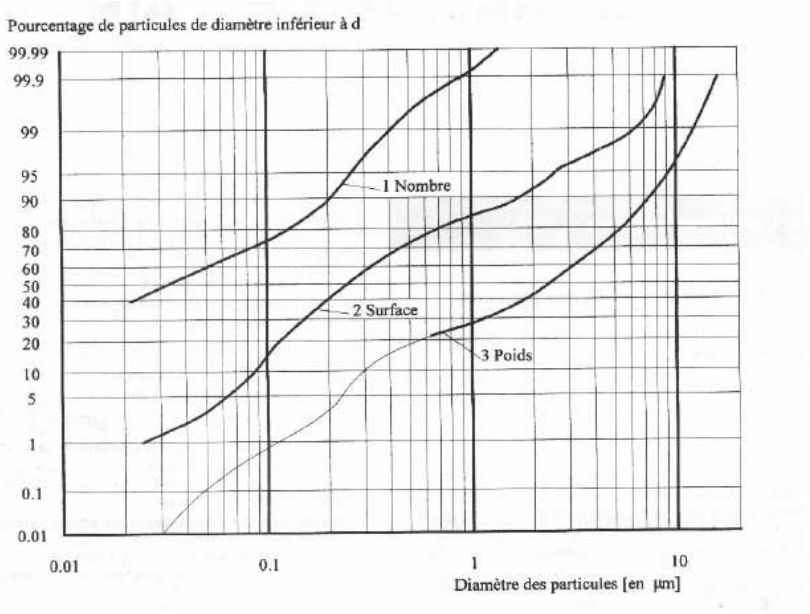

Average air mass distribution, from Lestari [Lestari 2003]

Diameter (µm)	Diff Mass %
0.1	2.85
0.2	2.85
0.3	2.85
0.4	5.23
0.5	5.23
0.6	5.23
0.7	1.90
0.8	1.90
0.9	1.90
1	1.90
2	2.38
3	4.75
4.5	4.75
5	4.75
6	5.32
7	5.13
8	5.13
9	5.13
10	3.04
20	3.04
30	6.08
40	6.08
50	2.09
60	2.09
70	2.09
80	2.09
90	2.09
100	2.09

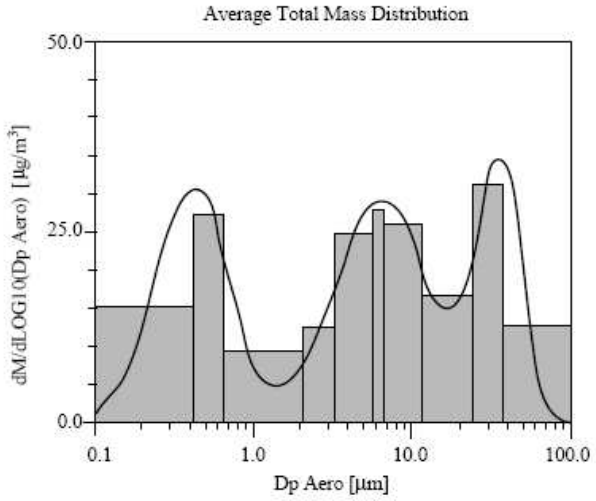

Annex 6 - Refrigerant leak evolution in buildings equipped with split systems

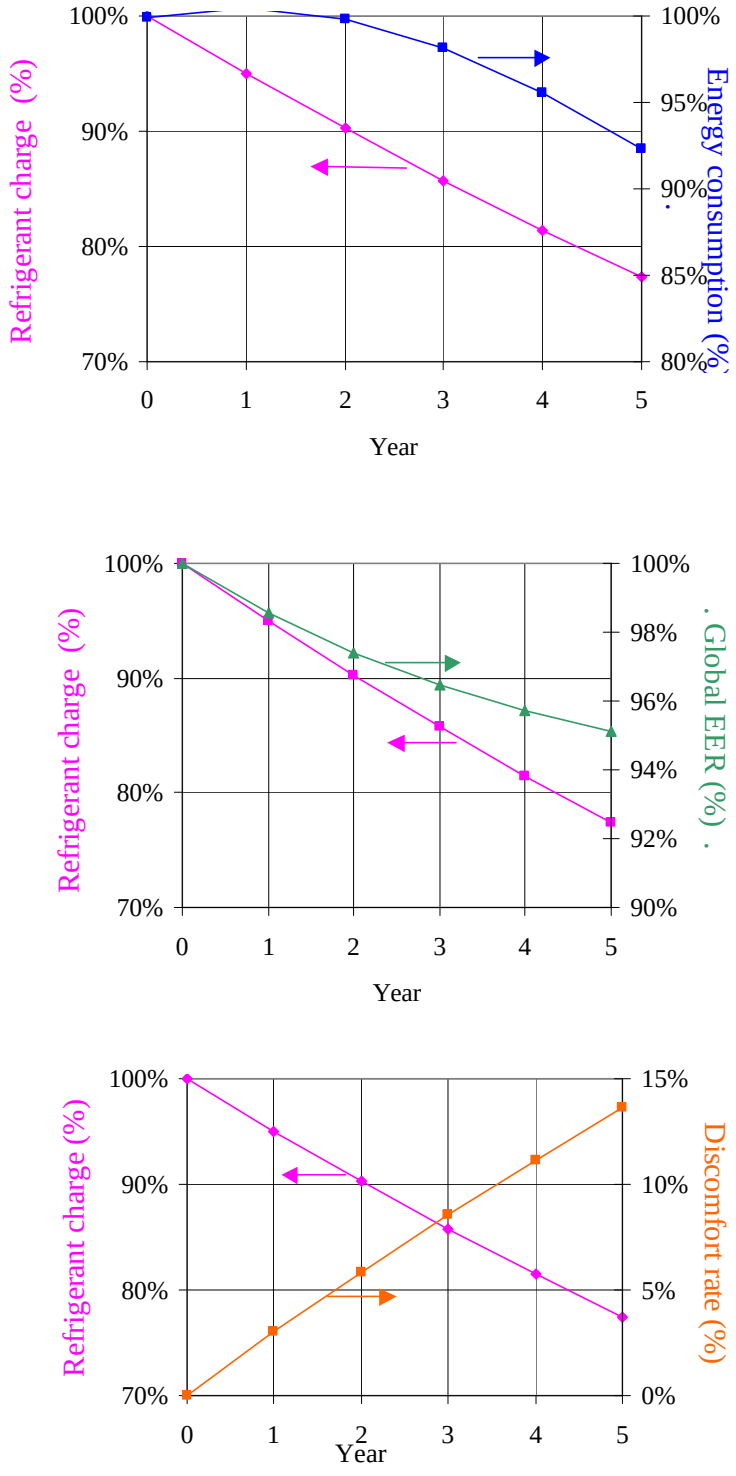

Figure 148: Refrigerant charge, capacity and comfort evolution for an office in Nice

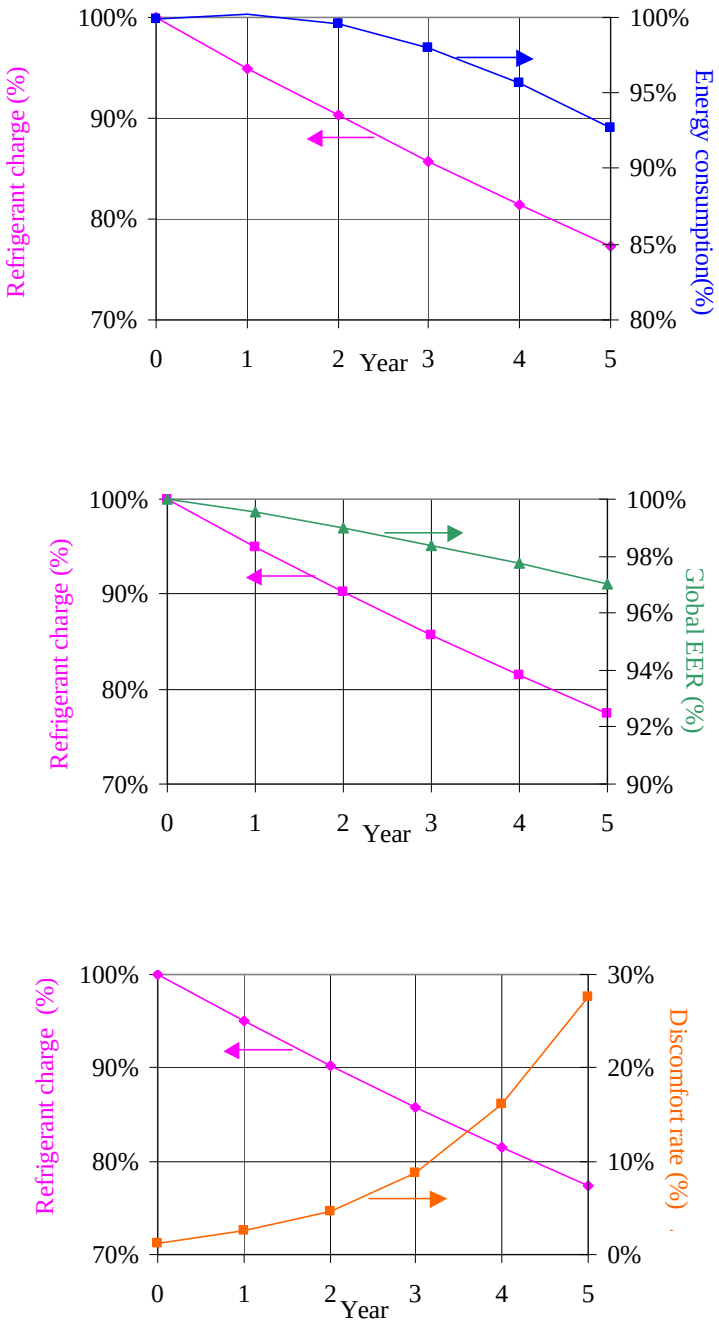

Figure 149: Refrigerant charge, capacity and comfort evolution for a house in Nice

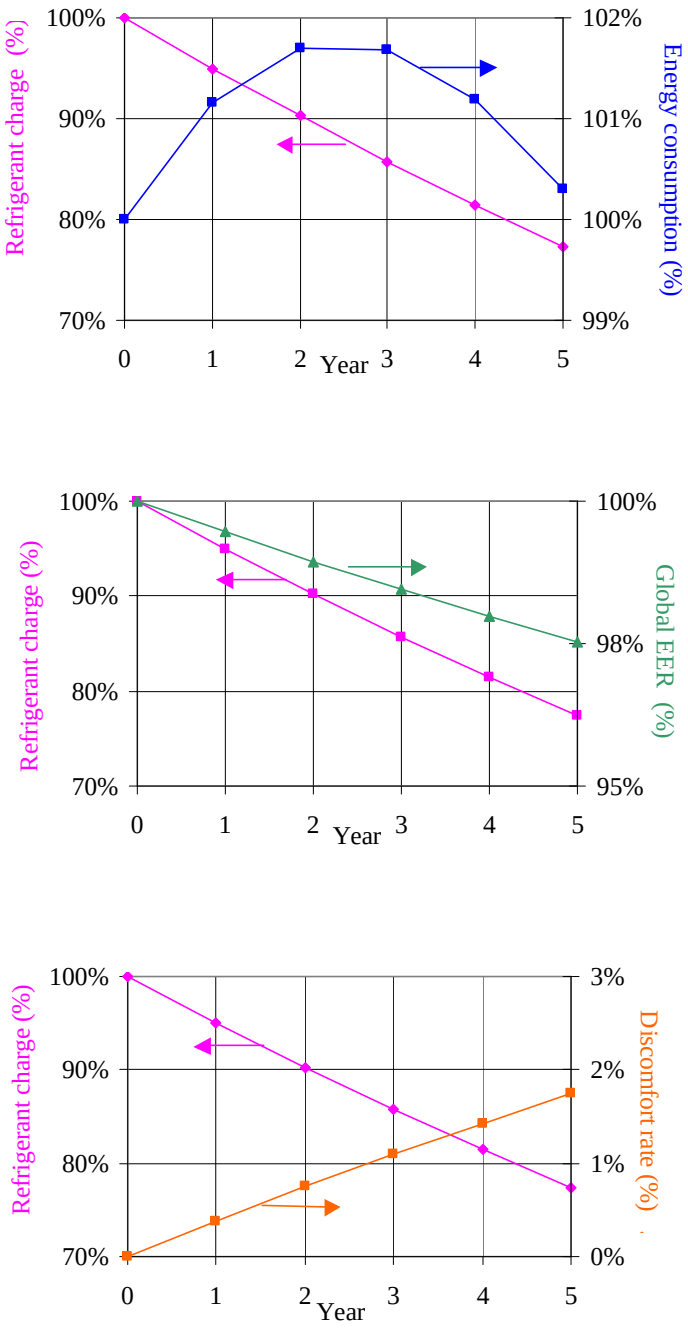

Figure 150: Refrigerant charge, capacity and comfort evolution for an office building in Trappes

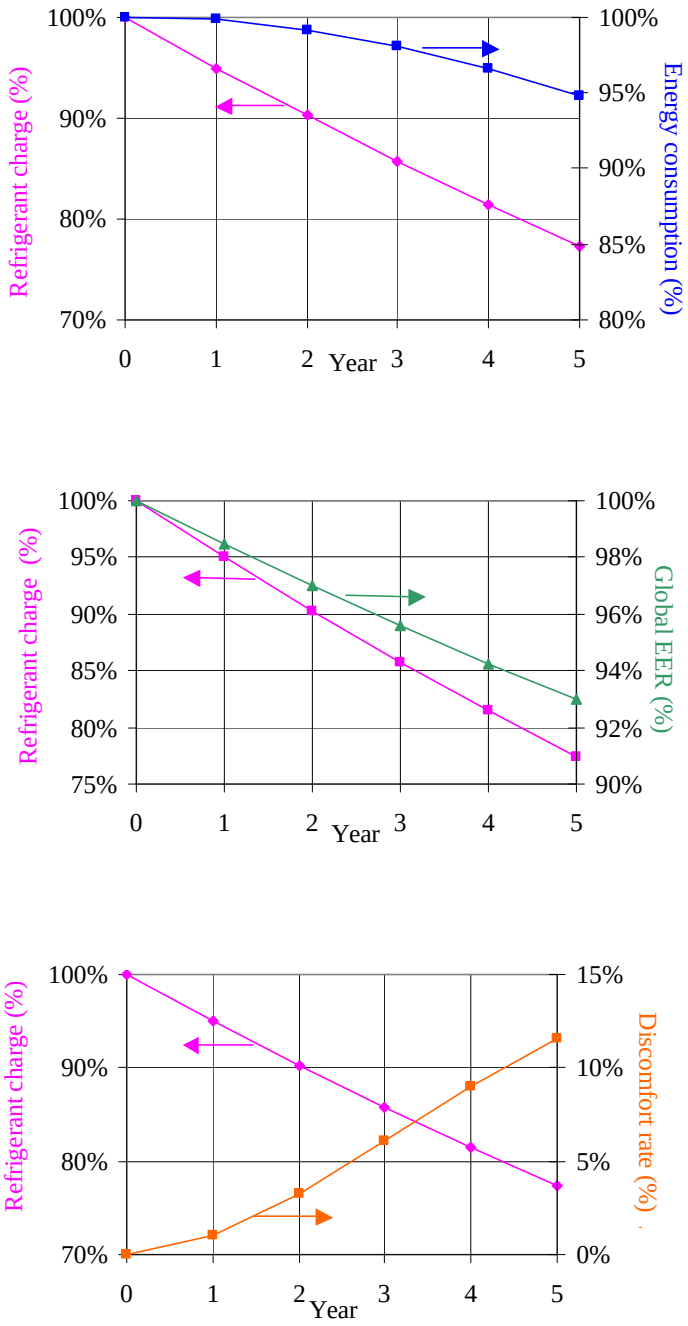

Figure 151: Refrigerant charge, capacity and comfort evolution for a house in Trappes

Annex 7 - Maintenance costs for charge refill for building equipped with split systems

Office building with splits	Nice	Trappes
Area (m²)	762	762
Number of units	24	18
Unitary capacity (kW)	8.7	8.7
Initial charge (kg)	67.2	50.4
Final charge (kg)	52.4	39.3
Refrigerant losses (kg)	14.8	11.1
Refrigerant cost (€)	133	100
Labour Hours (per unit)	2	2
Labour cost (€)	2400	1800
Displacement and material (€)	50	50
Total cost (€)	2583	1950
Cost per cooling capacity (€/kW)	12	12
Cost per cooled area (€/m²)	3.4	2.6

House	Nice	Trappes
Area (m²)	81	51
Number of units	2	1
Unitary capacity (kW)	8.7	3.3
Initial charge (kg)	5.6	2.8
Final charge (kg)	4.4	2.2
Refrigerant losses (kg)	1.2	0.6
Refrigerant cost (€)	11	6
Labour Hours (per unit)	2	2
Labour cost (€)	200	100
Deplacement and material (€)	50	50
Total cost (€)	261	156
Cost per cooling capacity (€/kW)	15	47
Cost per cooled area (€/m²)	3.2	3.0

Annex 8 - Maintenance costs for charge refill for building equipped with chiller systems

Office n°1	Nice	Trappes
Area (m²)	14111	14111
Number of units	10	6
Unitary capacity (kW)	170	160
Initial charge (kg)	498.7	281.6
Final charge (kg)	299.2	169.0
Refrigerant losses (kg)	199.5	112.6
Refrigerant cost (€)	3191	1802
Labour Hours (per unit)	5	5
Labour cost (€)	2500	1500
Deplacement and material (€)	50	50
Total cost (€)	5741	3352
Cost per cooling capacity (€/kW)	3.4	3.5
Cost per cooled area (€/m²)	0.4	0.2

Office n°2	Nice	Trappes
Area (m²)	3864	3864
Number of units	2	2
Unitary capacity (kW)	210	160
Initial charge (kg)	123.2	93.9
Final charge (kg)	73.9	56.3
Refrigerant losses (kg)	49.3	37.5
Refrigerant cost (€)	788	601
Labour Hours (per unit)	5	5
Labour cost (€)	500	500
Deplacement and material (€)	50	50
Total cost (€)	1338	1151
Cost per cooling capacity (€/kW)	3.2	3.6
Cost per cooled area (€/m²)	0.3	0.3

Office n°3	Nice	Trappes
Area (m²)	1524	1524
Number of units	1	1
Unitary capacity (kW)	160	210
Initial charge (kg)	46.9	61.6
Final charge (kg)	28.2	37.0
Refrigerant losses (kg)	18.8	24.6
Refrigerant cost (€)	300	394
Labour Hours (per unit)	5	5
Labour cost (€)	250	250
Displacement and material (€)	50	50
Total cost (€)	600	694
Cost per cooling capacity (€/kW)	3.8	3.3
Cost per cooled area (€/m²)	0.4	0.5

Annex 9 - Chiller savings for regular condenser cleaning

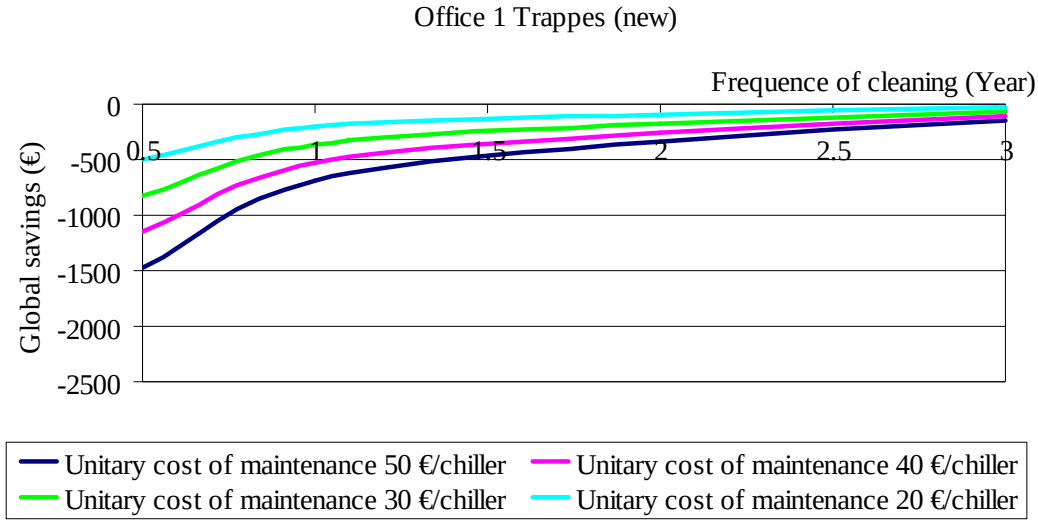

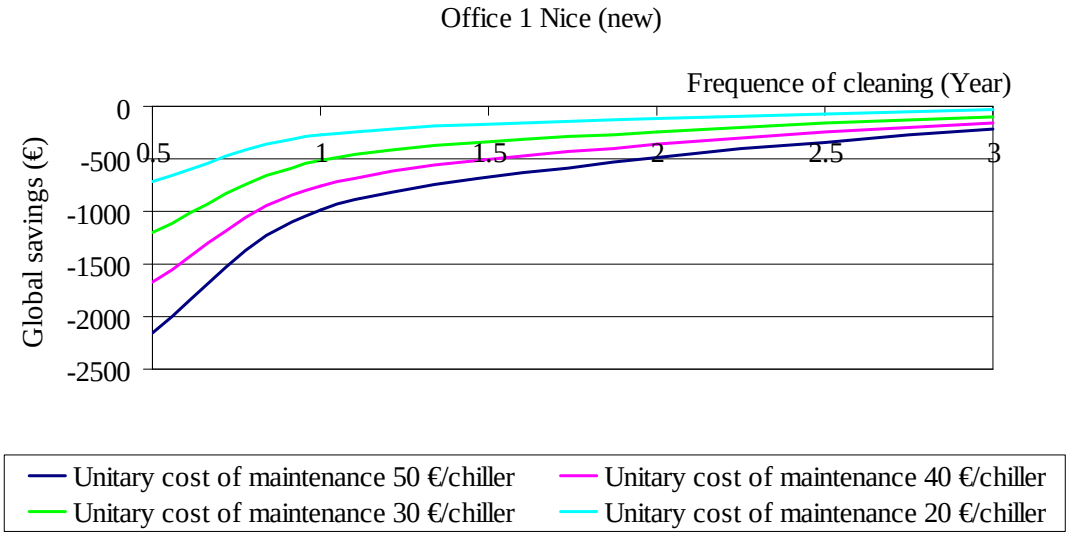

Figure 152: Global savings for regular condenser cleaning for office building 1 for a new (clean) system

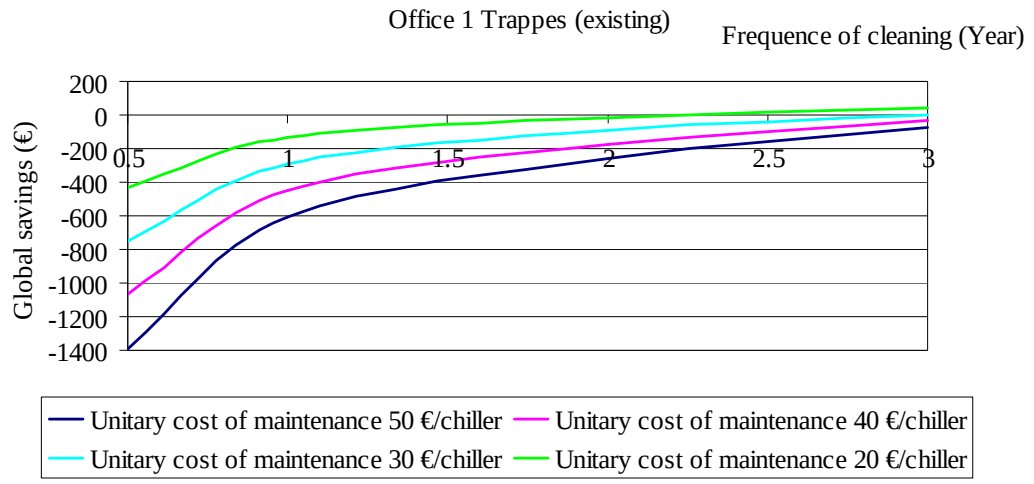

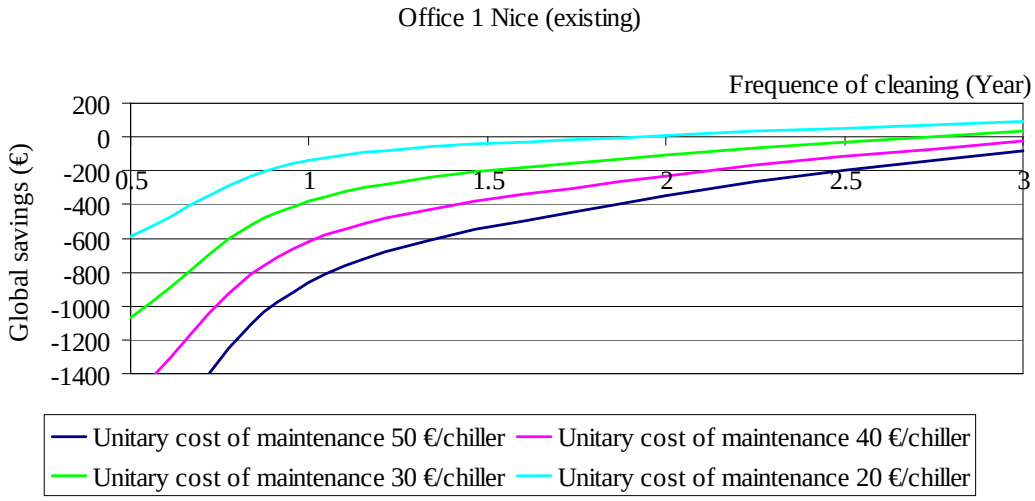

Figure 153: Global savings for regular condenser cleaning for office building 1 for an existing (fouled) system

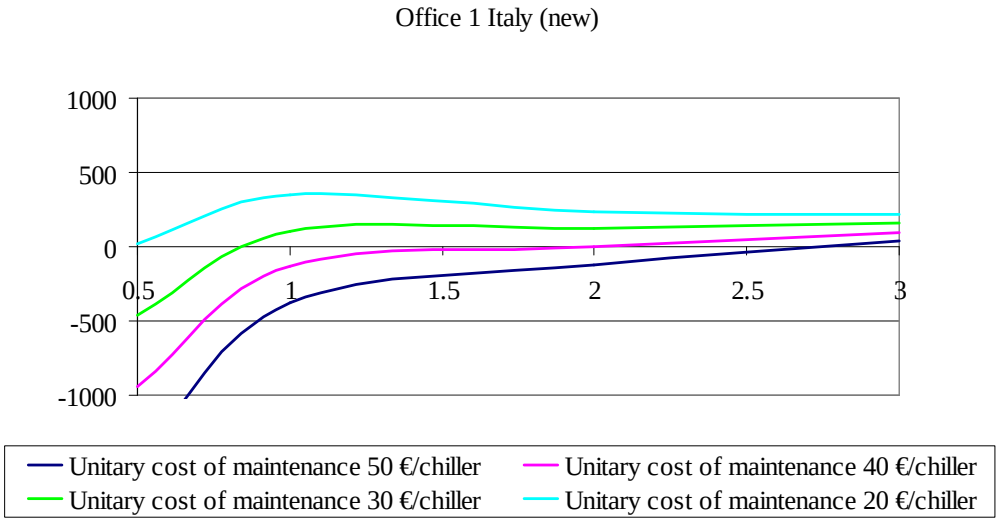

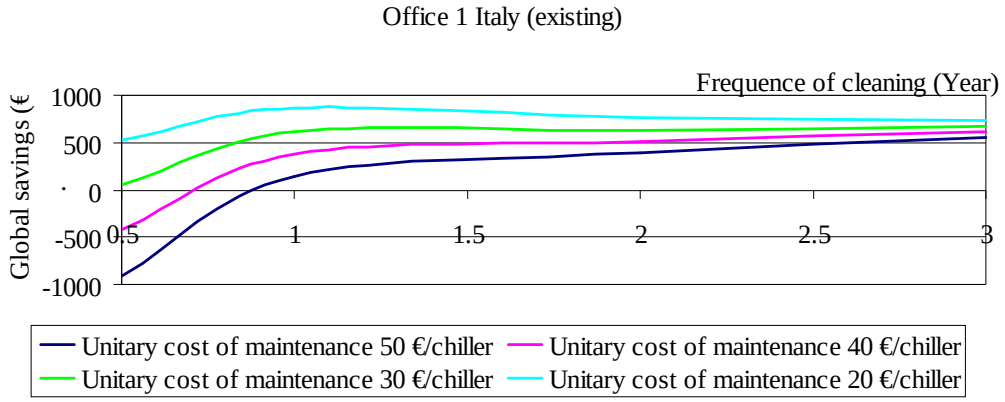

Figure 154: Global savings for regular condenser cleaning for office building 1 for a new (clean) and an existing (fouled) system with Italian electricity prices

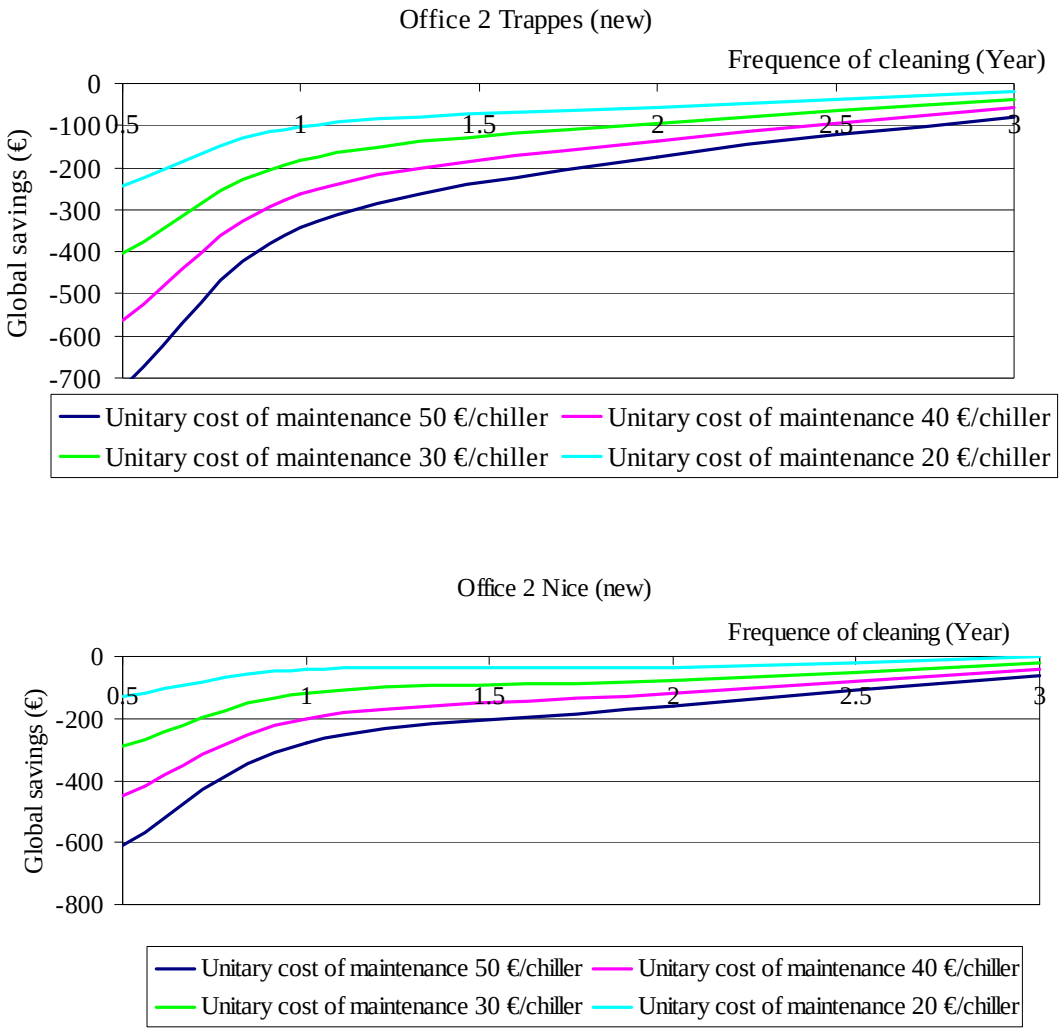

Figure 155: Global savings for regular condenser cleaning for office building 2 for a new (clean) system

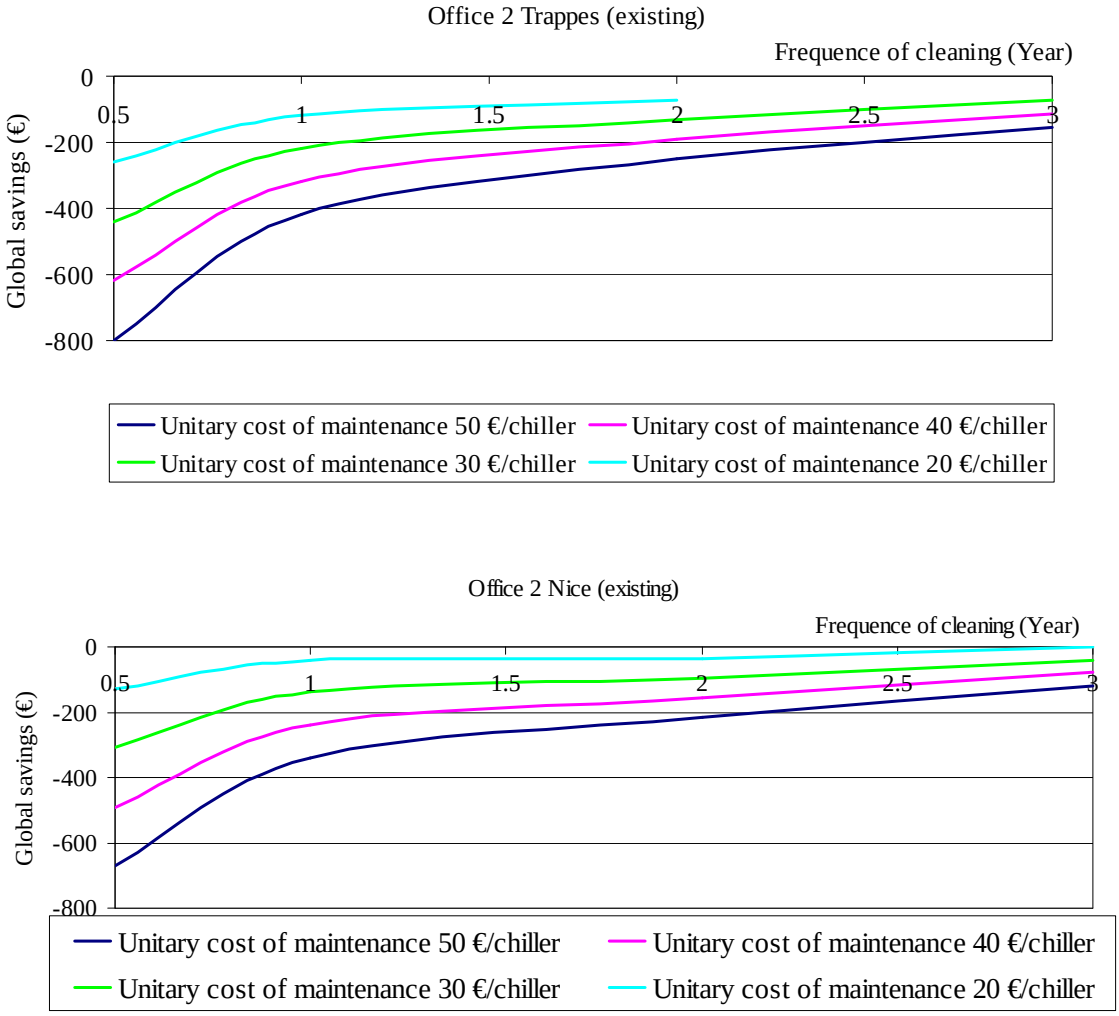

Figure 156: Global savings for regular condenser cleaning for office building 2 for an existing (fouled) system

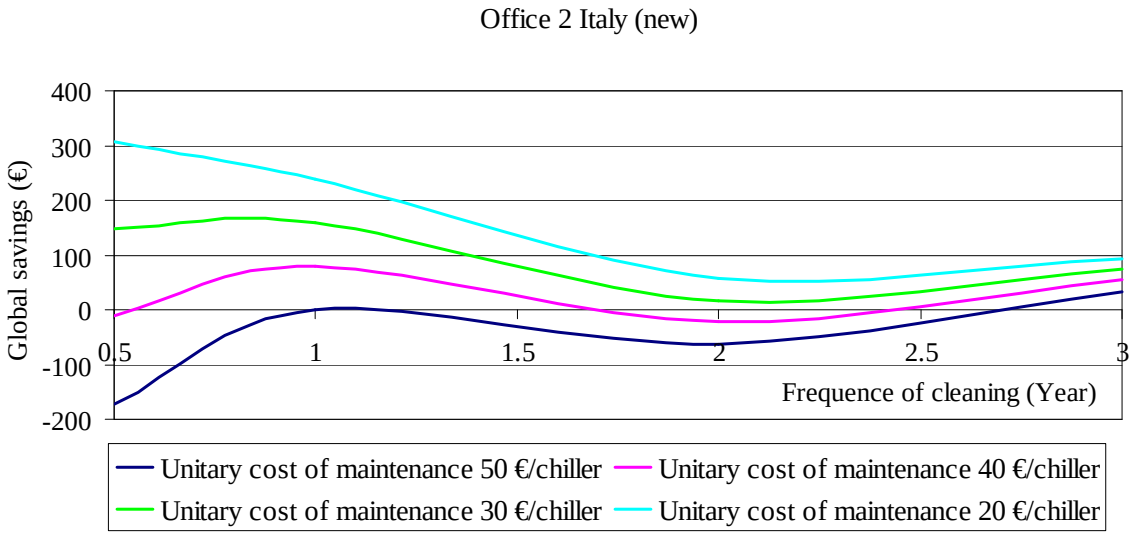

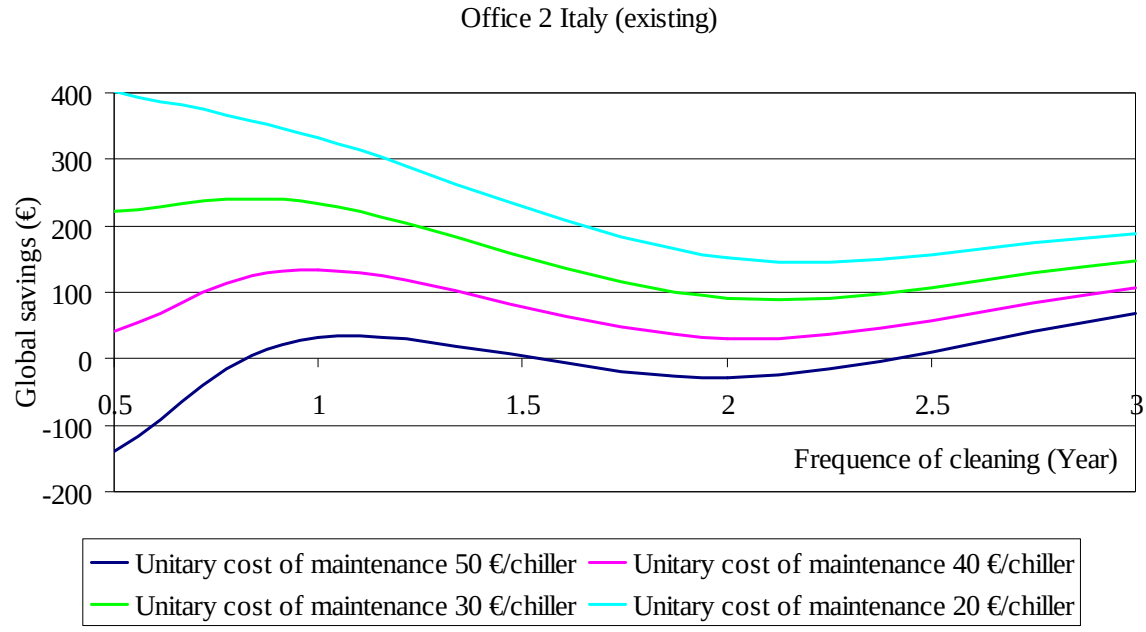

Figure 157: Global savings for regular condenser cleaning for office building 2 for a new (clean) and an existing (fouled) system with Italian electricity prices

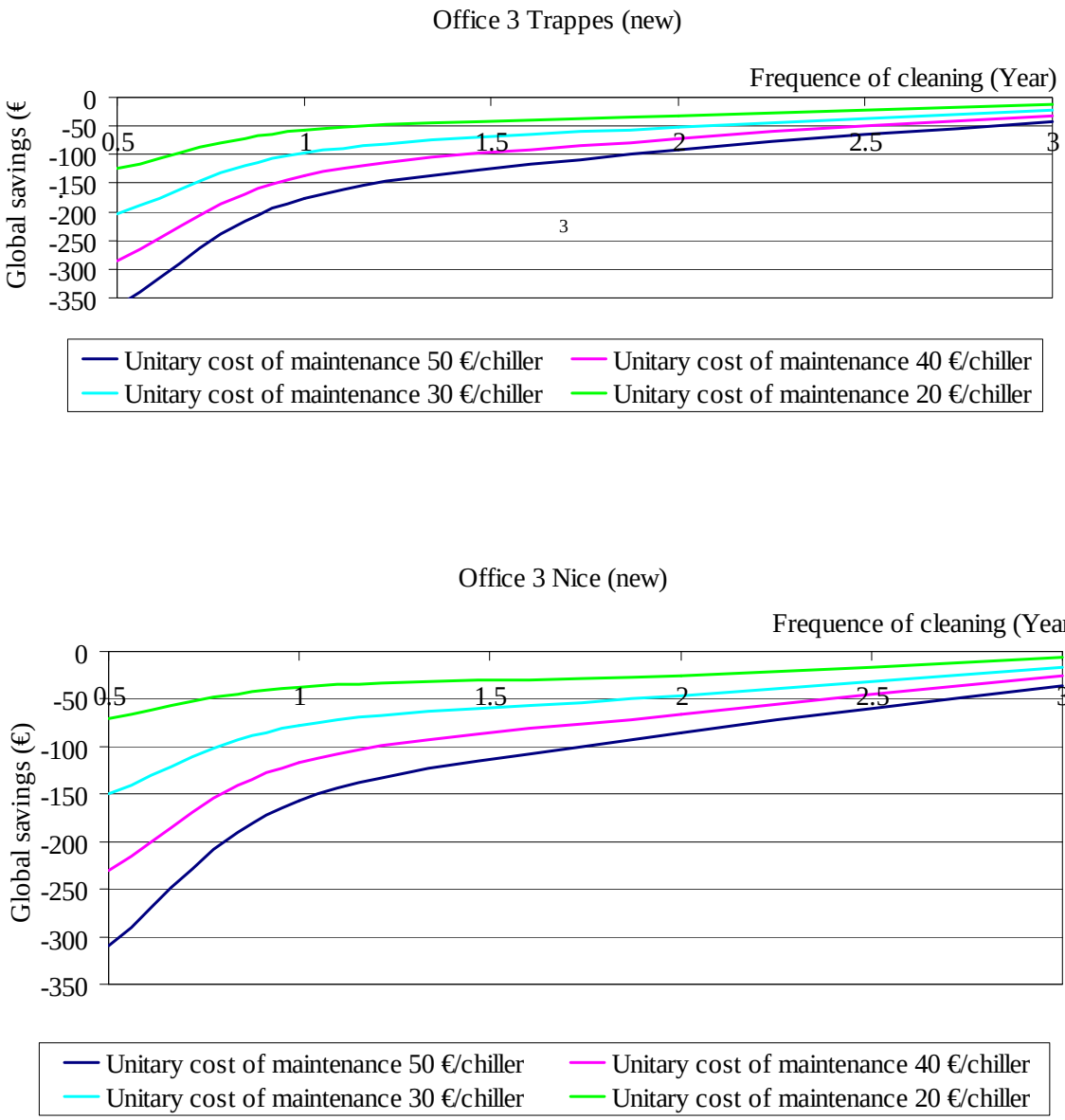

Figure 158: Global savings for regular condenser cleaning for office building 3 for a new (clean) system

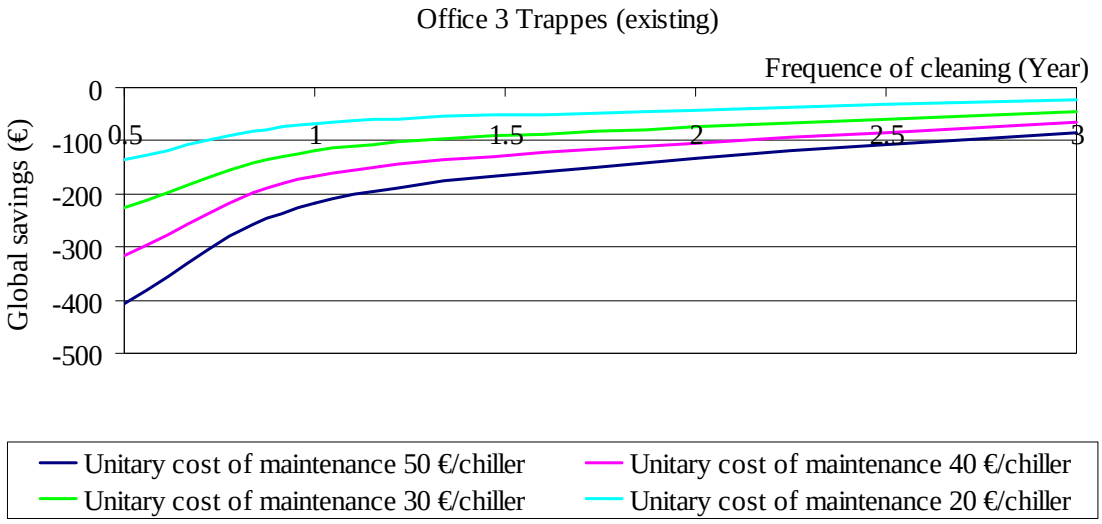

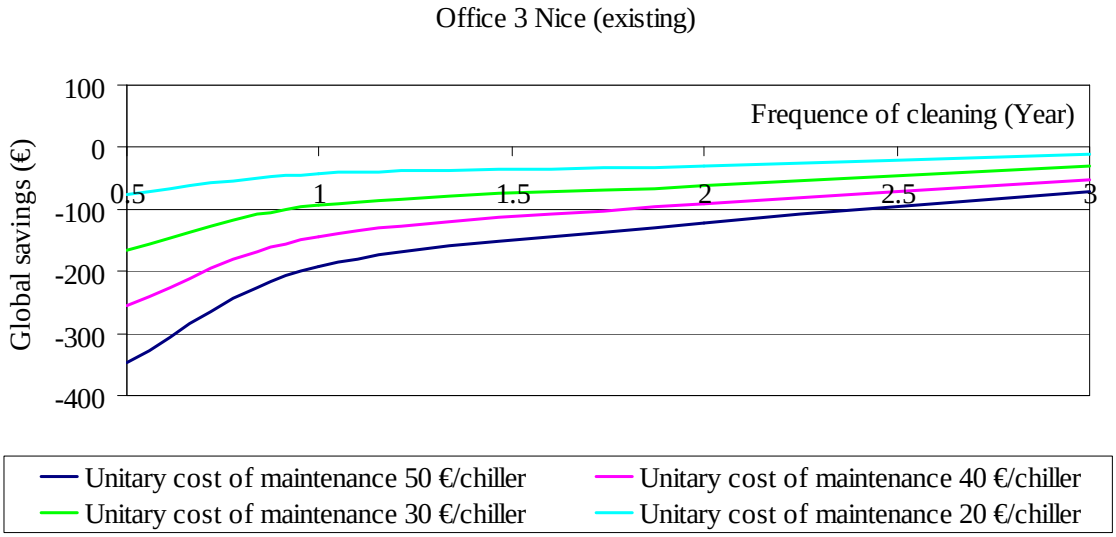

Figure 159: Global savings for regular condenser cleaning for office building 3 for an existing (fouled) system

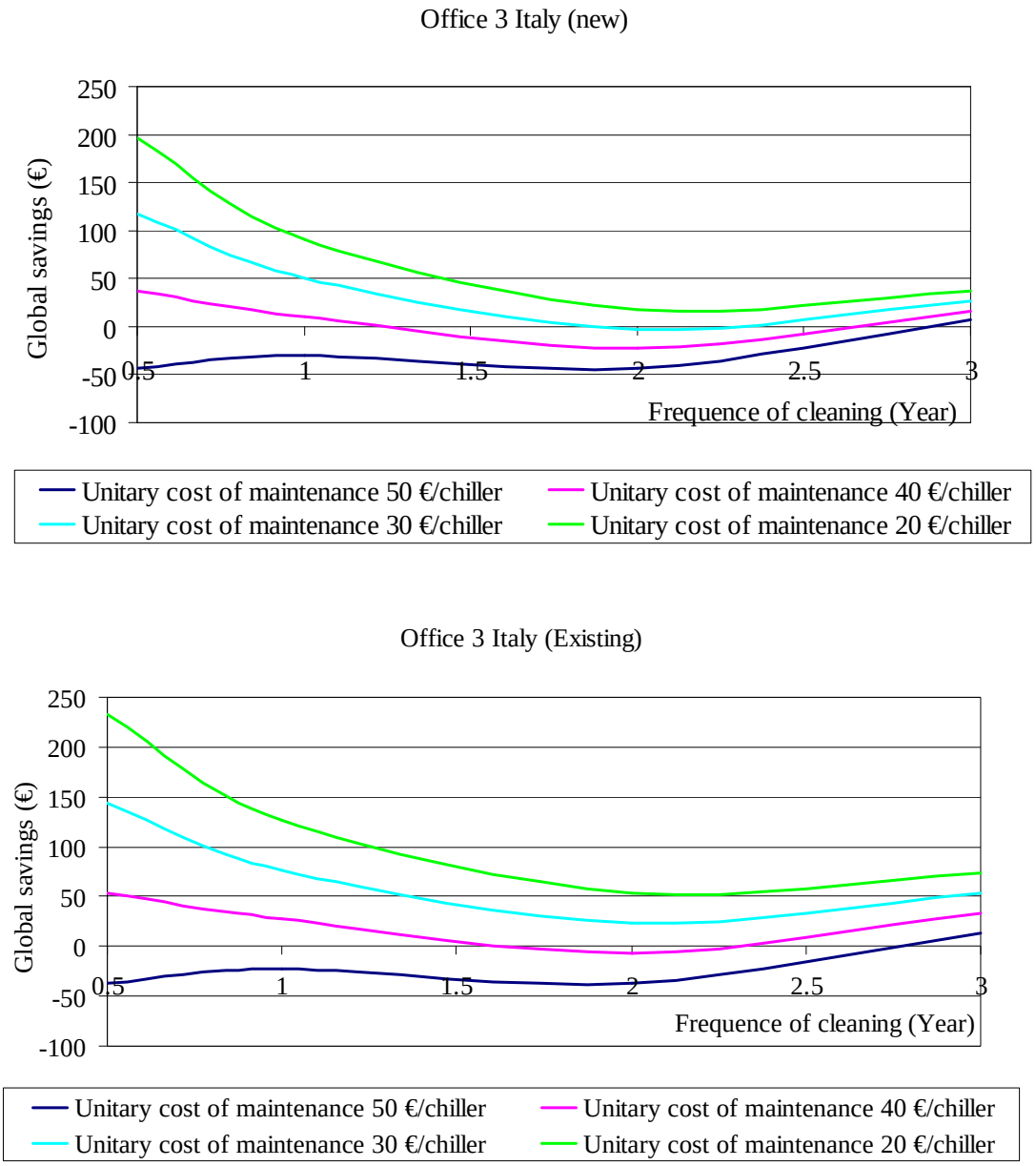

Figure 160: Global savings for regular condenser cleaning for office building 3 for a new (clean) and an existing (fouled) system with Italian electricity prices

ANALYSE ET SIMULATIONS DE DEFAUTS DES EQUIPEMENTS DE CLIMATISATION EN VUE D'UN AUDIT ENERGETIQUE

Résumé

La consommation due à climatisation est aujourd'hui un enjeu énergétique important. La Directive portant sur la Performance Energétique des Bâtiments s'intéresse aux systèmes de climatisation en prévoyant une inspection périodique afin d'évaluer le fonctionnement du système et ensuite à proposer des actions d'amélioration. Les méthodes pour la climatisation sont rares, parfois dérivées de celles pour le chauffage et pas optimisées. La thèse cherche à déterminer et quantifier les problèmes que les principaux systèmes de climatisation rencontrent pendant leur vie du point de vue technique. Il s'agit de savoir comment les détecter, quels sont les impacts énergétiques et les effets sur le confort.

Les technologies de climatisation sont nombreuses et diversifiées on a donc retenu deux types de système à analyser, les plus courants sur le marché européen : les climatiseurs split et les groupes de production d'eau glacée. Les défauts de fonctionnement les plus fréquents pour ces deux types de système ont été pris comme base.

Une préliminaire méthode d'analyse qualitative des défauts par représentation schématique en arbre de défaillance nous a permis de mieux comprendre la physique de chaque défaut. Ensuite une méthode quantitative de modélisation en conditions fixes de température nous a permis de définir les paramètres mesurables et les effets sur les performances. Pour nous rapprocher de la réalité une modélisation en conditions variables a été développée afin de quantifier les effets en terme de consommation et d'impact sur le confort dans des cas deux types de bâtiments placés dans des climats de référence. Enfin, une méthode temporelle a consistée à relier le niveau du défaut au temps afin d'observer la dégradation progressive et de pouvoir déterminer la fréquence optimale des actions de correction en termes d'énergie et de coût. On a pu ainsi obtenir une courbe de performance pluriannuelle avec ou sans action corrective ou préventive.

Mots clés : climatisation, audit, défaut de fonctionnement, split, groupe de production d'eau glacée

ANALYSIS AND SIMULATION OF DEFECTS OF OPERATION FOR AIR CONDITIONING AUDIT

Abstract

Nowadays the energy consumption due to air conditioning (AC) is a significant energy stake. The Directive on Energy Performance of Buildings wants to improve the air conditioning performance through the regular inspection of the system in order to assess how the system operates and to propose measures for improvement. Audit methods for air conditioning are rare, sometimes derived from those for heating and not optimised. The research wants to identify and quantify the problems that air conditioning systems meet all along their lifetime from a technical standpoint. The question is how to detect the operation problems and what are their energy impacts and effects on comfort.

The air conditioning technologies are many and two types of systems have been analysed, the widely present in the European market: the split air conditioners and chillers. The characteristics of the chosen systems are representative of system widely present in the stock. The most common defects for these two types of system have been taken as a base.

Firstly, a method of qualitative analysis of defects by a schematic representation of tree defects enabled us to better understand the physics of each defect. Then a quantitative method of modelling at fixed temperature conditions allowed us to define the sensitive parameters and measurable effects on performance. In order to be closer to reality, the systems have been modelled in variable conditions. The model takes into account part-load operation of the system and can quantify the effects in terms of seasonal consumption and impact on comfort in cases of French typical buildings located in climates of reference. Finally, a temporal method links the level of the defect to the operation time in order to observe the gradual deterioration and to determine the optimal frequency of corrective action in terms of energy and cost. We could thus obtain a multi-year performance curve with or without corrective action.

Key words: air conditioning, audit, defect of operation, split system, chiller

Laboratory:	Centre Energétique et Procédés - Ecole des Mines de Paris Paris : 60 Bd Saint-Michel - F-75272 Paris Cedex 06
Ph. D. dissertation by:	BORY Daniela
Discipline :	« Energétique » - Ecole des Mines de Paris